Qualitative structure-activity relationships of the major tyrocidines, cyclic decapeptides from Bacillus aneurinolyticus

by

Barbara Marianne Spathelf

B.Sc. (Hons.) Biochemistry

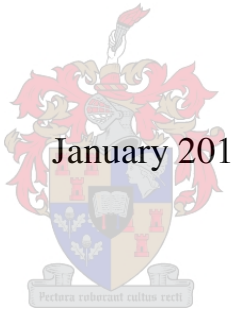

January 2010

Dissertation approved for the degree

Doctor of Philosophy (Biochemistry)

in the

Faculty of Science

at the

University of Stellenbosch

Supervisor: Prof. M. Rautenbach

Department of Biochemistry

University of Stellenbosch

Declaration

I, the undersigned, hereby declare that the work contained in this dissertation is my own original work and that I have not previously in its entirety or in part submitted it at any university for a degree.

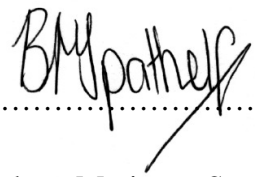

……. January 2010 ……

Barbara Marianne Spathelf Date

Summary

The need for alternative or supplementary treatments due to the global problem of microbial resistance towards conventional antimicrobials may be met by the development of novel drugs based on antimicrobial peptides. The antimicrobial peptides of interest to this study were the tyrocidines, cyclic decapeptides produced by *Bacillus aneurinolyticus*. Although these antimicrobial peptides were the first natural antibiotic to be discovered though a systematic search for antibacterial compounds, information regarding their bioactivity, structure-activity relationships, determinants of bioactivity and mode of action is limited. The aim of this study was to investigate the antibacterial and antiplasmodial activity, as well as to identify determinants of bioactivity modulation, of the natural tyrocidine library.

The study indicated that the tyrocidines exhibit significant activity toward Gram-positive bacteria, notably *Listeria monocytogenes*, and the intraerythocytic parasite, *Plasmodium falciparum*. Both the antilisterial and antiplasmodial activity was found to be highly dependent on peptide identity and self-assembly. The antilisterial activity of the tyrocidines was shown to be associated with increased self-assembly within a membrane-like environment, which suggested that formation of lytic complexes within the bacterial membrane may play a crucial role in tyrocidine activity. In contrast to the observations for antilisterial activity, the antiplasmodial activity of the tyrocidines was shown to be associated with reduced self-assembly within a membrane-like environment, which suggested that the antiplasmodial activity of the tyrocidines is mediated by a mechanism other than the formation of lytic complexes within the target cell membrane.

In addition to the influence of peptide identity and self-assembly, the bioactivity of the tyrocidines was found to be highly sensitive to environmental conditions, notably the presence of calcium. The antilisterial activity, as well as the mode of action, of the tyrocidines was also found to be highly sensitive to tyrocidine-Ca^{2+} complexation and the concomitant induction of higher-order structures. Tyrocidine-Ca^{2+} complexation was shown to greatly enhance antilisterial activity and change the mechanism of action from a predominantly membranolytic to an alternative, non-lytic mode of action.

The results of this investigation suggest that the alternative mode of tyrocidine activity may be related to complexation with Ca^{2+}. It is hypothesised that such complexation may either (1) promote tyrocidine-DNA complexation, and thus inhibition of transcription and/or replication; or (2) interfere with Ca^{2+} homeostasis, and thus influence vital cell functions.

Overall, it may be hypothesised that tyrocidine activity and mode of action is modulated by a critical play-off between self-assembly, cation-complexation and membrane-interaction. As these modulators of activity are highly dependent on tyrocidine sequence/structure, the wide variety of tyrocidines found in the natural complex may allow for optimal interaction with and activity toward a variety of microbes.

Opsomming

Die universele probleem van mikrobiese weerstand teen konvensionele antimikrobiese middels en die wêreld-wye noodsaaklikheid vir alternatiewe of bykomende behandeling mag deur die ontwikkeling van nuwe middels, gebasseer op antimikrobiese peptiede, vervul word. Die antimikrobiese peptiede van belang tot hierdie studie is die tirosidiene, sikliese dekapeptiede wat deur *Bacillus aneurinolyticus* geproduseer word. Informasie ten opsigte van die tirosidiene se bioaktiwiteit, struktuur-funksieverwantskap, determinante van bio-aktiwiteit en meganisme van aksie was beperk, alhoewel hierdie peptiede die eerste antimikrobiese peptiede was wat ontdek is deur ‘n sistematiese soektog vir antimikrobiese middels. Die doelwit van hierdie studie was die ondersoek van antibakteriële and antiplasmodiese aktiwiteit, sowel as om die determinante van bio-aktiwiteit modulering van die natuurlike tirosidienbiblioteek te ondersoek.

Hierdie studie het getoon dat die tirosidiene merkwaardige aktiwiteit teenoor Gram-positiewe bakterië, in besonder *Listeria monocytogenes* het, asook teenoor die intra-eritrositiese parasiet, *Plasmodium falciparum*. Daar is bevind dat beide die anti-listeriese en antiplasmodiese aktiwiteite hoogs afhanklik is van peptiedidentiteit en self-verpakking. Daar is gewys dat die antilisteriese aktiwiteit van die tirosidiene geassosieer is met verhoogde self-verpakking in ’n membraanagtige omgewing, wat ’n aanduiding is dat die vorming van litiese komplekse in die bakteriële membraan ’n kritiese rol in tirosidienaktiwiteit speel. Kontrasterend tot die waarnemings van antilisteriese aktiwiteit, is getoon dat die antiplasmodiese aktiwiteit van die tirosidiene geassosieer is met verlaagde self-verpakking in ’n membraanagtige omgewing. Dis ’n aanduiding dat die antiplasmodiese aktiwiteit van die tirosidiene gemediëer word deur ‘n ander meganisme en nie die vorming van litiese komplekse in die teikenselmembraan nie.

Bykomend tot die invloed van peptiedidentiteit en self-verpakking, is daar bevind dat die bioaktiwiteit van die tirosidiene hoogs sensitief is vir die omgewing, in besonder die teenwoordigheid van kalsium. Daar is ook bevind dat die antilisteriese aktiwiteit, sowel as die meganisme van aksie, van tirosidiene hoogs sensitief is vir tirosidien-Ca^{2+} kompleksvorming en die gevolglike induksie van of hoër-orde strukture. Daar is gewys

dat tirosidien-Ca^{2+} kompleksvorming die antilisteriese aktiwiteit drasties verhoog en dat die meganisme van aksie verander van ’n oorwegende membranolitiese meganisme na ’n alternatiewe nie-litiese meganisme van aksie.

Die resultate van hierdie ondersoek het aangedui dat die alternatiewe meganisme van aksie van tirosidienaktiwiteit moontlik verband kan hou met kompleksvorming met Ca^{2+}. Die hipotese is dat sodanige kompleksvorming moontlik of (1) tirosidien-DNA komplekvorming aanmoedig, en dus transkripsie en/of replikasie inhibibeer of (2) met Ca^{2+} homeostase inmeng, en sodoende lewensnoodsaaklike selfunksies beïnvloed.

Die algemene hipotese is dat tirosidienaktiwiteit en meganisme van aksie deur ’n kritiese spel tussen self-verpakking, katioonkompleksvorming en membraaninteraksie gemoduleer word. Die wye verskeidenheid van tirosidiene, wat in die natuurlike kompleks gevind word, kan moontlik toelaat vir die optimale interaksie met, en aktiwiteit teenoor ’n verskeidenheid van mikrobes, aangesien die aktiwiteitmoduleerders hoogs afhanklik is van tirosidien struktuur/volgorde.

Acknowledgements

I would like to acknowledge the contribution of the following persons:

- Prof. Marina Rautenbach, my supervisor, for her motivation, guidance and advise throughout this project and the preparation of this manuscript;

- Drs. Heinrich Hoppe (CSIR, Pretoria) and Ursula Wiehart (University of Cape Town), for *plasmodium* culturing and assistance with the activity determinations;

- Dr. Marietjie Stander (Central Analytical Facility, University of Stellenbosch), for the mass spectrometry;

- Dr. Ben Loos, (Central Analytical Facility, University of Stellenbosch), for assistance with the fluorescence microscopy;

- Drs. Raymond Sparrow and Stoyan Stoychev (CSIR, Pretoria), for assistance with the circular dichroism and fluorescence spectroscopy;

- Mrs. Gertrude Gerstner and Mr. Bertus Moolman (BIOPEP laboratory, Department of Biochemistry, University of Stellenbosch), for assistance and support;

- My co-workers, especially Mr. Gerald Penkler and Mr. Pierre Goosen, for support and invaluable discussions on all things biochemical;

- Christian, for providing the much needed distractions, endless patience and encouragement;

- My parents, for their love, their absolute belief in my abilities and moral support throughout the past 24 years.

Table of Contents

List of Abbreviations and Acronyms

ACN	Acetonitrile
AMP	Antimicrobial peptide
Arg	Arginine
A_S	Activity slope
Asn	Asparagine
Asp	Aspartic acid
B. aneurinolyticus	*Bacillus aneurinolyticus*
B. brevis	*Bacillus brevis*
BHI	Brain heart infusion
CD	Circular dichroism
CFU	Colony forming units
CID	Collision-induced dissociation
DOSY	Diffusion-ordered spectroscopy
E. coli	*Escherichia coli*
ESI	Electrospray ionisation
ESMS	Electrospray mass spectrometry
f	D-phenylalanine
F	Phenylalanine
Gln	Glutamine
Glu	Glutamic acid
GS	Gramicidin S
HC_{50}	Peptide concentration leading to 50 % haemolysis
HPLC	High performance liquid chromatography
IC_{50}	Peptide concentration leading to 50% inhibition
IC_F	Inhibition concentration factor
IC_{max}	Maximum inhibitory concentration
IC_{min}	Minimum inhibitory concentration
K	Lysine
L	Lipophilicity or Leucine

L. monocytogenes	*Listeria monocytogenes*
LAB	Lactic acid bacteria
LB	Luria broth
Leu	Leucine
LPS	Lipopolysaccaride
LTA	Lipoteichoic acid
Lys	Lysine
[M]	Molecular ion
M. luteus	*Micrococcus luteus*
M. tuberculosis	*Mycobacterium tuberculosis*
MALDI	matrix-assisted laser desorption/ionisation
MD	Molecular dynamic
MIC	Maximum inhibitory concentration
MOA	Mechanism of cction
MS	Mass spectrometry
MS-MS	Tandem mass spectrometry
m/z	Mass-to-charge ratio
N	Asparagine
NMR	Nuclear magnetic resonance
NOESY	Nuclear Overhauser effect spectroscopy
O	Ornithine
Orn	Ornithine
P	Proline
P. falciparum	*Plasmodium falciparum*
PBS	Phosphate buffered saline
Phc	Phenicidine
Phe	Phenylalanine
Pro	Proline
Q	Overall charge or glutamine
Q/L	Theoretical descriptor of amphipathicity
QSAR	Qualitative structure-activity relationship
RET	Resonance energy transfer

RMSD	Root mean square deviation
RP-HPLC	Reverse-phase high performance liquid chromatography
R_T	Retention time
SASA	Solvent-accessible surface area
SAV	Solvent-accessible volume
SCSA	Side-chain surface area
SEM	Standard error of the mean
SI	Selectivity index
T. brucei	*Trypanosoma brucei*
TFA	Trifluoroacetic acid
TFE	Trifluoroethanol
TOF-ESMS	Time-of-flight electrospray mass spectrometry
Tpc	Tryptocidine
Trc	Tyrocidine
TSB	Tryptone soy broth
UV	Ultraviolet
V	Valine
Val	Valine
W	Tryptophan
w	D-tryptophan
Y	Tyrosine

Preface

Microbial resistance towards conventional antimicrobials has become a global problem, necessitating the search for alternative antimicrobial compounds. The urgent need to find alternative or supplementary treatments for infections caused by various resistant microbes may be met by the development of novel drugs based on antimicrobial peptides and/or their analogues. A group of the first natural antibiotics to be discovered in the 1930's through a deliberate and systematic search for antibacterial compounds, namely the tyrocidines (cyclic antimicrobial decapeptides produced by *Bacillus aneurinolyticus*) may potentially be promising candidates as antimicrobials. However, the tyrocidines seem to be "the forgotten antibiotic group" and information regarding their bioactivity, structure-activity relationships, determinants of bioactivity and mode of action is limited.

This study was initiated to gain more knowledge of the tyrocidines and to explore their applicability as potential lead compounds for the development of bio-preservatives and novel drugs for the treatment of listeriosis, caused by *L. monocytogenes*, and malaria, caused by blood-borne parasites, such as *P. falciparum*. In order to develop therapeutic agents or bio-preservatives based on the tyrocidines, much insight regarding determinants of bioactivity, target interaction, and mechanism of action is required.

The goal of this study was therefore to elucidate the structural, physicochemical and environmental modulators of tyrocidine antimicrobial activity and selectivity. The objectives to meet this goal were:

1. The purification and analysis of tyrocidines from the tyrothricin complex of *Bacillus aneurinolyticus* (Chapter 2);
2. Spectrophotometric investigation of tyrocidine structure and self-assembly in an aqueous and membrane-mimetic environment (Chapter 3);
3. Structural investigation by homology modelling and physicochemical characterisation of the tyrocidines (Chapter 4);
4. Investigation of the antibacterial activity and structure-activity relationships of the tyrocidines towards selected bacterial strains, including the food-borne pathogen *Listeria monocytogenes* (Chapter 5);

5. Investigation of the influence of cations, specifically Ca^{2+}, on antilisterial activity (Chapter 6); and
6. Investigation of the antiplasmodial and haemolytic activity, structure-activity-selectivity relationships and modulation of the antiplasmodial activity of the tyrocidines (Chapter 7).

The chapters in this thesis were, to some extent, written as independent units so as to facilitate future publication. Although this led to some repetition, every attempt was made to keep this to a minimum.

Chapter 1

Literature Review

1.1 Introduction

Food-borne diseases have an extensive impact on both public health and economics worldwide, which calls for the development of more effective preventative measures and treatments for pathogens such as *Listeria*, *Campylobacter*, *E. coli* and *Salmonella* [1-5]. *L. monocytogenes,* the causative agent of listeriosis, is estimated to account for 28% of food-related deaths [1, 3]. *L. monocytogenes* has become a major concern due to the increased incidence of listeriosis, together with the emergence of resistance toward antibiotics and disinfectants [1, 2, 6-14]. In addition to the impact of food- and water-borne diseases on public health and world economy, diseases such as malaria and African sleeping sickness (trypanosomiasis), caused by blood-borne parasites such as *Plasmodium falciparum* and *Trypanosoma brucei*, are responsible for widespread morbidity and mortality [15-17], and yet are some of the most neglected diseases afflicting mankind. The endemic proportions of malaria and the rapid emergence of antibiotic-resistance in the causative parasite [15, 16, 18] is of great concern and requires the development of new treatments.

The above-mentioned diseases are part of the global problem of microbial resistance towards conventional antimicrobials, which necessitates the search for alternative antimicrobial compounds [19-21]. Since the adaptive mechanisms of microbes that lead to the development of resistance is largely dependent on the type and mechanism of action of the antibiotic [22, 23], an entirely new class of antibiotics needs to be developed [23, 24]. Desirable attributes of such a new class of antimicrobial agents include broad spectrum activity, selective toxicity, rapid killing and reduced likelihood of resistance development [23, 25, 26]. A class of compounds that display such attributes are the antimicrobial peptides.

Antimicrobial peptides represent an ancient and conserved part of innate immunity and are produced by all forms of life [19, 22, 24, 27-32]. Since the discovery of antimicrobial peptides, these compounds have received much research interest for the development of novel therapeutic and bio-preservative agents due to the growing

problem of microbial resistance to conventional antibiotics [19, 24, 26-29, 31, 33-35]. In general, antimicrobial peptides have been found to possess broad spectrum antimicrobial activity with targets such as Gram-positive and Gram-negative bacteria, fungi, parasites and virally-infected cells [19, 20, 22, 24, 34, 36, 37]. Despite the observed broad spectrum activity, the role of the cell membrane in peptide action, together with distinct differences between microbial cell membranes and those of multicellular plants and animals, allows for selective toxicity [31]. Furthermore, antimicrobial peptides differ from conventional antibiotics in so much as their rapid lytic mechanism of action prevents the development of resistant pathogenic mutants [30, 38]. The broad spectrum antimicrobial activity and mechanism of action implies that antimicrobial peptides may serve as invaluable templates for the development of novel antimicrobial agents [19, 22, 29, 31].

Antimicrobial peptides can be grouped into four broad categories based on their secondary structure: linear, α-helical peptides, linear peptides with an extended structure, looped structures and conformationally restrained β-sheet peptides (Figure 1) [20, 24, 26, 27, 29, 31, 34, 39].

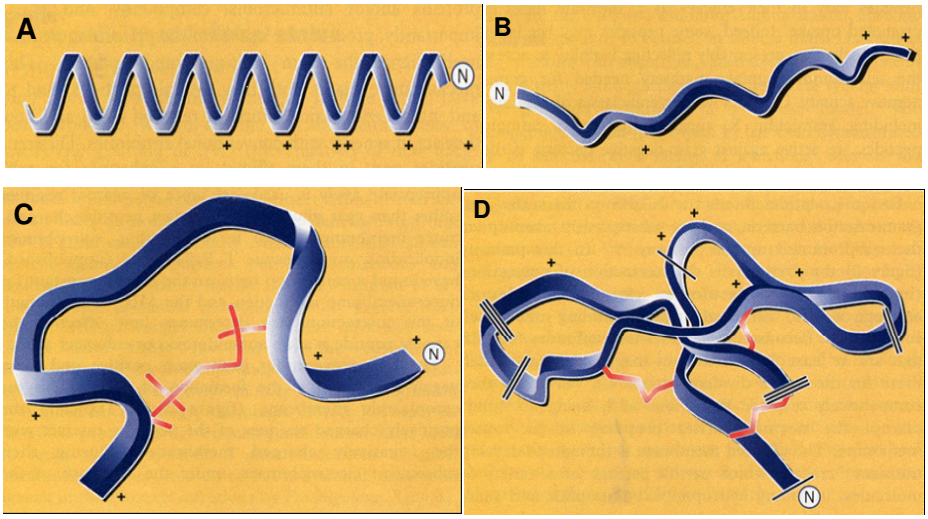

Figure 1 *Examples of the four major structural classes of antimicrobial peptides* [from [27]]. (A) α-helical cecropin-melitin hybrid; (B) extended coil indolicin; (C) loop bactenecin and (D) β-sheet human defensin-1 [27].

Tyrocidines, the antimicrobial peptides of interest to this project, together with the structurally related loloatins [40, 41], streptocidines [42, 43] and gramicidin S, comprise a family of antimicrobial β-sheet cyclic decapeptides, which adopt similar backbone conformations/molecular topologies [40-43]. The tyrocidines are found in tyrothricin, a secondary metabolite bactericidal complex produced by *Bacillus aneurinolyticus* [44,

45]. Tyrothricin was the "first natural antibiotic to be discovered though a deliberate and systematic search for antibacterial compounds" [44, 46] and is composed of two groups of peptides: the linear, neutral gramicidins and the cyclic, basic tyrocidines [47-49]. The primary structures of 28 tyrocidines have been determined [49] (Table 1).

Table 1 *Peptides from the tyrothricin complex of interest in this investigation*
The peptide sequences [from [49]] are given using conventional one letter abbreviations for amino acids, except that ornithine (Orn) is designated by O. Lower case abbreviations denote D-amino acid residues. The abundance of the tyrocidines is expressed relative to that of tyrocidine C. Peptides marked with * were named by our group; ** renamed from tyrocidine E

Number	Identity	Abbreviation	Sequence	Monoisotopic Mr	Abundance
1	Tyrocidine D*	TrcD	VOLfPYwNQY	1324.7	2.1
2	Tyrocidine D_1*	$TrcD_1$	VKLfPYwNQY	1338.7	1.7
3	-	-	VOLyPWwNQY	1363.7	<1
4	Tyrocidine E'*	TrcE'	VOLfPFyNQY	1285.7	<1
5	Tyrocidine E_1'*	$TrcE_1$'	VKLfPFyNQY	1299.7	<1
6	Tyrocidine C	TrcC	VOLfPWwNQY	1347.7	100
7	Tyrocidine C_1	$TrcC_1$	VKLfPWwNQY	1361.7	30
8	Tryptocidine C	TpcC	VOLfPWwNQW	1370.7	23
9	Tryptocidine C_1*	$TpcC_1$	VKLfPWwNQW	1384.7	2.3
10	Tyrocidine B'*	TrcB'	VOLfPFwNQY	1308.7	14
11	Tyrocidine B_1'*	$TrcB_1$'	VKLfPFwNQY	1322.7	5.8
12	Tyrocidine B	TrcB	VOLfPWfNQY	1308.7	109
13	Tyrocidine B_1	$TrcB_1$	VKLfPWfNQY	1322.7	44
14	Tryptocidine B	TpcB	VOLfPWfNQW	1331.7	26
15	Tryptocidine B_1*	$TpcB_1$	VKLfPWfNQW	1345.7	13
16	Tyrocidine A	TrcA	VOLfPFfNQY	1269.7	88
17	Tyrocidine A_1	$TrcA_1$	VKLfPFfNQY	1283.7	39
18	Tryptocidine A	TpcA	VOLfPFfNQW	1292.7	15
19	Phenycidine A**	PhcA	VOLfPFfNQF	1253.8	3.1
20	Tyrocidine E*	TrcE	VOLfPYfNQY	1285.7	2.2
21	Tyrocidine E_1*	$TrcE_1$	VKLfPYfNQY	1299.7	1.1
22	-	-	VOLfPF(?)NQY	1336.7	4.5
23	-	-	VKLfPF(?)NQY	1350.7	9.4
24	Phenycidine B*	PhcB	VOLfPWfNQF	1292.7	3.7
25	-	-	(L/I)OLfPWfNQY	1322.7	1.9
26	-	-	(L/I)KLfPWfNQY	1336.7	2.6
27	-	-	VOLfP(L/I)fNQY	1325.7	1.2
28	-	-	VKLfP(L/I)fNQY	1249.7	<1

The secondary structure of tyrocidine A has been shown to adopt an antiparallel β-pleated sheet structure [50, 51]. The most abundant tyrocidines have highly conserved amino acid sequences (*cyclo*[$f^1P^2X^3x^4N^5Q^6Y^7V^8X^9L^{10}$]), differing only by $Trp^{3,4}$/$Phe^{3,4}$ and Lys^9/Orn^9 mutations (the lower case abbreviations indicate D-amino acid residues). Upon its discovery, it was noted that tyrothricin, as well as the isolated tyrocidine fraction, exhibit marked bactericidal activity toward both Gram-positive and Gram-negative bacteria [44, 52]. In addition to the bactericidal activity, the tyrocidines have since been shown to possess activity toward the malarial parasite *P. falciparum* [37].

1.2 The mechanism of action of antimicrobial peptides

The antimicrobial activity of cationic peptides generally involves electrostatic and/or hydrophobic interaction with phospholipid cell membranes, followed by the integration of the antimicrobial peptide into the membrane, which leads to increased permeability, leakage of cellular components and/or depolarisation of the cell membrane [19, 20, 26, 29, 33, 34, 39, 53-56]. The most widely accepted models of peptide-induced membrane permeability include the barrel-stave [57], torroidal pore [58], carpet [59-61] and aggregate-channel [62] models (Figure 2) [20, 26, 39, 63-66]. In short, the barrel-stave model [57] proposes that antimicrobial peptides form barrel-like clusters, which line amphipathic pores without distorting the lipid bilayer; the carpet model [59, 60] suggests that the peptides cover the surface of the target membrane and, above a critical concentration, cause the integrity of the membrane to collapse, while below the this concentration pores, distorting the lipid bilayer, will form (personal communication Y. Shai) in a manner similar to the torroidal pore model [58]; and the aggregate-channel model [62] proposes that, once the peptides have inserted themselves into the membrane, they associate to form transient, unstructured aggregates that span the membrane [20, 65, 66].

Although the primary mechanism of antimicrobial peptide action is regarded to involve target membrane permeabilisation, there has been growing evidence of alternative/additional mechanisms [24, 26, 31, 33, 35, 63, 67, 68]. Some membrane active antimicrobial peptides, such as magainin 2 [69], PR-39 [70, 71], apidaecin [72], protegrin [73] and tachyplesin [74] can cross bacterial inner and outer membranes without inducing membrane lysis, which implies that these peptides may be able to

target intracellular molecules [20, 33, 53, 58, 63, 67, 75-79]. Indeed, antimicrobial peptides, such as pleurocidin [80], PR-39 [71], buforin II [81], and indolicidin [82], have been shown to be capable of inhibiting RNA and DNA synthesis, while antimicrobial peptides such as attacins [83] and pleurocidin [80] inhibit protein synthesis. Other peptides were found to interfere with metabolic processes of microbes, inducing selective transcription [84], inhibiting respiration [85], inhibition of enzymes [86-88] inhibiting cellular functions by binding to DNA and RNA [74, 81, 89], activation of autolysin [68] and altering cytoplasmic membrane septum formation [78, 82, 90, 91]. The membrane effects may therefore be a manner by which the peptides enter the cell to reach alternative targets rather than being related to the cytotoxic effect [33, 53, 92]. However, many antimicrobial peptides may possess more than one mode of action, acting on both the cell membrane and at internal sites [24, 26, 33, 63, 67, 93]. At high enough concentrations, most cationic antimicrobial peptides will lead to severe membrane perturbation, while other modes of action/targets may be affected at low peptide concentrations [63].

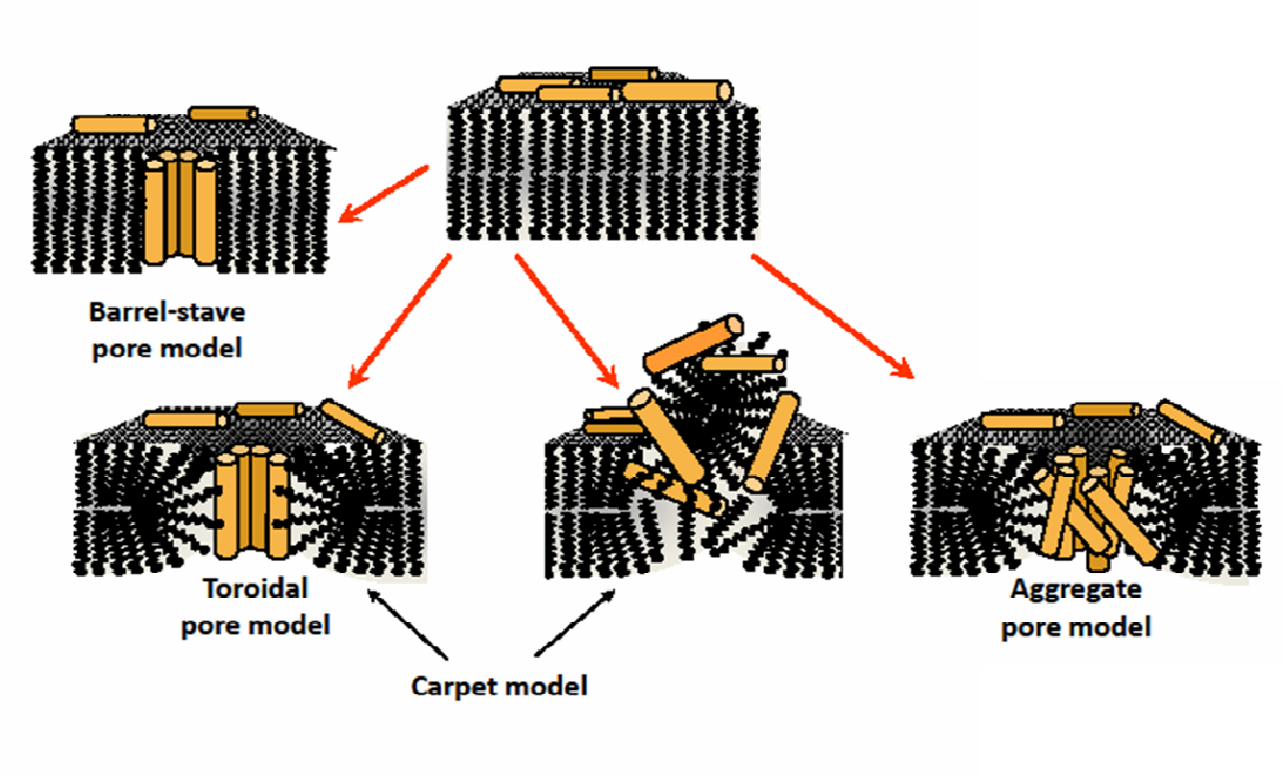

Figure 2 Cartoons of different models for the mechanism of action of α-helical cationic antimicrobial peptides. In all models the peptides associate with the membrane and adopt and an amphipathic α-helical structure (orange cylinders). Figure reproduced with permission from M. Rautenbach.

Valuable insight regarding the mechanism of action of the peptides in this study, the tyrocidines, was already gained during the discovery of their antibacterial activity [44]. Although the tyrocidines were found to induce lysis of target cells, lysis was shown to be a secondary process mediated by the autolytic enzymes of the target cell in response to a primary insult [44]. The bactericidal activity was suggested to be a result of inactivation of the glucose dehydrogenase system of the bacterial cell [44]. This is supported by the observation that the susceptibility of the target organism is related to their metabolic activity [44] and that the tyrocidines lead to the loss of oxygen uptake, acid production and reducing ability, indicating disruption of metabolic activity [52]. The tyrocidines have also been shown to form complexes with DNA in *B. brevis*, acting as a non-specific repressor by inhibiting transcription [94-96], which suggests that they may exert their antimicrobial action via a similar mechanism. Furthermore, the tyrocidines have been shown to inhibit β-galactosidase and acetylcholinesterase activity [97]. It is thus possible that the tyrocidines also act on an intracellular target or targets. Further, recent studies conducted by Rautenbach *et al.* (2007) [37] showed that the antiplasmodial activity of the tyrocidines is not a result of explicit lysis of infected erythrocytes but rather due to the inhibition of parasite development and life-cycle progression in erythrocytes, suggesting that the tyrocidines may also act by a non-membrane related mechanism of action. The possibility of membrane-related mechanism(s) of action should, however, not be dismissed as the tyrocidines have also been shown to perturb the barrier properties of dioleoylphosphatidylcholine model membranes [98], implying that disruption of membrane integrity may, under certain conditions, play a role in tyrocidine activity. Furthermore, research regarding gramicidin S (*cyclo*[VOLfPVOLfP]), a cyclic β-sheet decapeptide with high sequence identity with the tyrocidines, has indicated that interaction of this peptide with the outer and cell membrane of bacteria induces potassium leakage and destroys the structural integrity of the target membrane [99-101]. Alternative modes of action for GS, including inhibition of erythrocyte Ca^{2+}-ATPase [102], and *Escherichia coli* cytochrome *bd*-type quinol oxidase [103] have also been identified.

1.3 Modulation of antimicrobial peptide activity

Irrespective of the precise mechanism of action, the interaction of antimicrobial peptides with the target cell membrane is, at least initially, essential for activity [26, 33, 63, 68, 78, 104-106]. Activity is therefore modulated by the characteristics of both the peptide and the target cell [26, 34, 65, 93, 104, 105]. In addition to the role of peptide and target cell properties, environmental factors, such as ionic strength and pH may modulate the bioactivity of antimicrobial peptides [65, 107].

1.3.1 Physicochemical properties of the peptide that modulate bioactivity

Structural features of the peptides that influence their activity include conformation, charge distribution, amphipathicity, hydrophobicity and the relative size of the polar/nonpolar face [19, 20, 23, 26, 35, 64, 93, 104, 106-115]. These structural features may be related to different stages of a multi-step mechanism of action [108, 109, 116]. Initial electrostatic interaction with anionic outer membrane components will be modulated by peptide cationicity [26, 35, 108, 109, 115, 117], while peptide aggregation at the membrane surface and subsequent permeation into the membrane will be modulated by peptide amphipathicity and hydrophobicity [53, 108, 109, 115, 118-124]. In the case of an intracellular target, the peptide needs to cross the cell membrane of the target organism [38, 53], and the mode of interaction between antimicrobial peptides and target cell membranes will therefore be a major determinant of activity and selectivity [27]. The activity of antimicrobial peptides may thus be modulated by altering parameters that are required/dictate the type and/or efficacy of interactions involved in the crucial association of the peptide with the target cell membrane.

Information regarding the structure-activity relationships of the tyrocidines is limited, especially with regard to antibacterial activity. However, the high structural similarity (50% sequence homology and about 100% backbone homology) between gramicidin S and the tyrocidines suggests that these peptides are likely to have similar effects on the membranes with which they interact and may share similar structure-activity relationships. Research involving gramicidin S has indicated that the presence of both hydrophobic and basic residues, a defined secondary (β-sheet) structure, amphipathic character and a minimal ring size are essential features for antimicrobial activity [99,

106, 125-128]. In general, enhanced haemolytic activity is associated with increased amphipathicity, increased hydrophobicity, and the presence of a large hydrophobic face [93, 125, 127, 129]. Enhanced antibacterial activity is associated with reduced amphipathicity and increased hydrophobicity [125, 127]. Although high amphipathicity and hydrophobicity is not desirable, optimal amphipathicity and hydrophobicity for antimicrobial activity exist, with such optima being species specific [106, 127].

As noted for gramicidin S, cyclic conformation is important for the antibacterial activity of the tyrocidines [130, 131]. Furthermore, D-Phe^4 and Gln^6 have been identified as potential targets for substitution for improved antibacterial activity and reduced haemolytic activity of tyrocidine A [131, 132]. Substitution of the D-Phe^4 residue by negatively charged D-Glu or D-Asp leads to a loss of antibacterial activity [131], while substitution by cationic D-Orn, D-Lys or D-Arg, leads to improved therapeutic indices, largely due to reduced haemolytic activity [131, 132]. Substitution of Gln^6 by cationic Orn, Lys or Arg also leads to greatly improved therapeutic indices, although this is largely due to significantly enhanced antibacterial activity and moderately reduced haemolytic activity [132]. The enhanced selectivities upon introduction of a cation residue in positions 4 or 6 were attributed to preferential interaction with anionic phospholipids of bacterial cell membranes relative to interaction with zwitterionic phospholipids in eukaryotic cell membranes [131, 132]. Previous investigation of the antiplasmodial activity of the tyrocidines by Rautenbach *et al.* (2007) [37] found a strong correlation between the antiplasmodial activity of the tyrocidines and increased apparent hydrophobicity and reduced side-chain surface area.

In addition to the direct modulating effect of the abovementioned biophysical properties, these peptide features may also have an indirect influence on activity and selectivity by modulating peptide aggregation/self-assembly. The amphipathic nature of antimicrobial peptides poses a problem for solubility in an aqueous environment, especially for structurally rigid β-sheet peptides [26, 67], which may overcome this solubility issue by the formation of multimeric complexes [26, 67]. The tendency/ability of antimicrobial peptides to form aggregates/self-assemblies/supramolecular complexes are related to their primary structure, conformation, general topology, amphipathicity and hydrophobicity [93, 105, 109, 118, 133]. The potential for an equilibrium between monomeric peptides and peptide aggregates in aqueous solution may impact membrane

interaction and/or transport across biological barriers [54, 65, 118]. Aggregation/self-assembly in solution may influence the extent of peptide insertion and disruption of membrane integrity, decreasing activity [107, 133, 134], whereas multimer formation following initial membrane interaction has been suggested to play a key role in the cytolytic activity of β-sheet peptides [19, 26, 54, 64].

The tyrocidines have been found to undergo extensive, stable aggregation/self-assembly in aqueous solution [130, 135-139]. Such aggregation/self-assembly was hypothesised to be driven by hydrophobic side-chain interactions [130, 135, 136, 138] as it was observed to be highly dependent on amino acid sequence, conformation as dictated by the ring-structure and proper spatial orientation of the amino acid residues [130, 135, 139].

1.3.2 Target cell properties that modulate bioactivity

Interpreting the correlations between the biophysical properties and antimicrobial activity of the peptides requires consideration of the structure of the cell wall and cell membrane of the target cell [93]. Features of the target cell that affect interaction with cationic antimicrobial peptides include membrane lipid composition and the presence of sterols [26, 104], electrochemical potential [29], and metabolic state [77]. Gram-positive bacteria have a thick peptidoglycan layer that surround the cell membrane, whereas the cell membranes of Gram-negative bacteria are surrounded by a peptidoglycan layer as well as an outer membrane composed mainly of lipids, proteins and lipopolysaccaride (LPS). The peptides need to pass through these surrounding layers in order to reach the cytoplasmic membrane. The presence of anionic phospholipids, a highly negative electrochemical gradient and the absence of cholesterol promote membrane-peptide interaction [29]. The high anionic phospholipid content (mainly phosphatidylglycerol), the high electrical-potential gradient and the lack of cholesterol in bacterial membrane therefore provides the basis for antimicrobial peptide selectivity [25, 26, 29, 33, 140]. Gramicidin S has been shown to associate more strongly with anionic lipid membranes whereas cholesterol inhibits its lytic action [99]. Although membrane interaction is generally regarded as being non-specific interaction with the phospholipids [141, 142], other membrane targets such as membrane-bound proteins/enzymes [143], lipopolysaccaride (LPS) [144-147], lipoteichoic acid (LTA) [148], and lipid II [149, 150] have been suggested [26, 33, 97, 103, 144, 151-154].

1.3.3 Environmental modulators of bioactivity

In addition to the role of peptide and target cell properties in activity modulation, environmental conditions are known to influence antimicrobial peptide activity and selectivity [19, 20, 31, 32, 65, 68, 107]. Many antimicrobial peptides, such as defensins [155-157], dermaseptin [107], lactoferrin [158], bactenecins [85] and nisin [154] lose their antibacterial activity under physiological salt and serum conditions [19, 32, 68]. The activity of most antimicrobial peptides is reduced by the presence of cations such as Na^+, Mg^{2+} and Ca^{2+} [19, 85, 154-160]. The antimicrobial activities of mouse β-defensin [155], insect defensin A [156], and dermaseptin S4 derivatives [107] are inhibited by Na^+ and divalent cations (Ca^{2+} and Mg^{2+}) have been found to reduce the activity of human neutrophil defensins [157], lactoferrin [158], bactenecins [85] and nisin [154]. The inhibition of antimicrobial peptide activity by cations may be due to either increased aggregation induced by cations [156, 161], which would decrease the number of "active" peptide, or inhibition of membrane-binding, probably by shielding electrostatic interaction between the peptide and the target membrane [107, 154, 156]. As tyrocidine aggregation/self-assembly is highly dependent on solvent composition and the presence of salt [136, 138], the bioactivity of the tyrocidines is likely to be affected by serum and/or food components.

1.4 Potential application of antimicrobial peptides

The broad spectrum antimicrobial activity, rapid mechanism of action and low propensity for resistance development suggest that antimicrobial peptides may serve as invaluable templates for the development of novel therapeutic agents for bacterial and parasitic infections [19, 22, 24, 25, 27, 29-32, 34, 36, 39, 162]. Antimicrobial peptides that are currently in clinical, albeit topical, use include the polymyxin, bacitracin, tyrothricin and gramicidin S [27-29, 32, 62]. The applications of antimicrobial peptides, including ones currently undergoing clinical trials, are summarised in Table 2. However, the susceptibility to proteolysis, toxicity, immunogenicity, bioavailability, unknown toxicology and pharmacokinetics of antimicrobial peptides may limit their therapeutic applicability [20, 32, 34, 39, 162].

In order to develop novel therapeutic agents or bio-preservatives based on antimicrobial peptides, much insight regarding determinants of bioactivity and mechanism of action is

required. An understanding of the structure-function relationships and mechanism of action may allow for the development of more efficacious molecules with reduced toxicity [26, 108, 125, 127]. The development of novel therapeutic also requires consideration of several technical difficulties and safety considerations, such as sensitivity to physiologically relevant ionic strength and serum conditions, toxicity and selectivity; susceptibility to proteolysis; delivery; high production costs; distribution and clearance; and immunogenicity [20, 22, 26, 27, 29, 31, 162, 163].

Table 2 *Summary of AMP clinical applications and status* [22, 32, 164]

Compound	Parent AMP	Application and status	Company
	Polymyxin	Wound creams, eye and ear drops (In clinical use)	Generic
	Gramicidin S	Wound creams, eye and ear drops (In clinical use)	Generic
	Bacitracin	Wound creams, eye and ear drops (In clinical use)	Generic
	Tyrothricin	Throat lozenges (in clinical use)	Generic
Omiganin	Indolicidin	Topical prevention of catheter-related blood-stream infections (Completed phase III trial)	Migenix, Vancouver, BC
MBI	Indolicidin	Topical treatment for acne (Phase III trial)	Microbiologix, Vancouver, BC
P113	Histatins	Mouth rinse for oral candidiasis (Passed phase II trial)	Demegen, PA, USA
hLF-11	Human lactoferrin	Systemic antifungal (Completed phase I trials)	AM-Pharma Holding, BV
	Nisin	Anti-ulcer drug	Applied Microbiology
		Intravaginal contraceptive and microbicide	Astra Merck
XMP.629	BPI	Topical treatment for acne (Failed phase III trial)	Xoma, Berkeley, CA
Neuprex	BPI	Pareteral treatment of pediatric meningococcemia (Failed phase III trials)	Xoma, Berkeley, CA
Iseganan	Protegrin	Mouth rinse for stomatitis (Failed phase III trials)	Intrabiotics, CA, USA
Pexiganan	Magainin 2	Topical treatment of diabetic foot ulcers (Failed Phase III trials)	Genaera, PA, USA

The broad spectrum antimicrobial activity of the tyrocidines implies that they may be promising templates for alternative treatments for infections caused by various resistant pathogens. The tyrocidines are, however, also haemolytic and exhibit toxicity toward certain human cell lines *in vitro* [37, 52]. Investigation of tyrocidine structure-activity-

toxicity relationships, mode of action and sensitivity to physiologically relevant ionic strength and serum conditions may thus provide insight regarding their applicability as potential lead compounds for development of bio-preservatives and novel drugs for the treatment of listeriosis and blood-borne parasites, such as *P. falciparum*.

1.5 References

[1] D.G. White, S. Zhao, S. Simjee, D.D. Wagner, P.F. McDermott, Antimicrobial resistance of foodborne pathogens, Microb. Infect. 4 (2002) 405–412.

[2] R.V. Tauxe, Emerging foodborne pathogens, Int. J. Food Microbiol. 78 (2002) 31-41.

[3] M. Gandhi, M.L. Chikindas, *Listeria*: A foodborne pathogen that knows how to survive, Int. J. Food. Microbiol. 113 (2007) 1-15.

[4] J. Cleveland, T.J. Montville, I.F. Nes, M.L. Chikindas, Bacteriocins: safe, natural antimicrobials for food preservation, Int. J. Food Microbiol. 71 (2001) 1-20.

[5] J.M. Farber, P.I. Peterkin, *Listeria monocytogenes*, a food-borne pathogen, Microbiol. Rev. 55 (1991) 476-511.

[6] M. Teuber, Spread of antibiotic resistance with food-borne pathogens, Cell Mol. Life Sci. 56 (1999) 755–763.

[7] C. Poyart-Salmeron, C. Carlier, P. Trieu-Cuot, P. Courvalin, A.-L. Courtieu, Transferable plasmid-mediated antibiotic resistance in *Listeria monocytogenes* The Lancet 335 (1990) 1422-1426

[8] E. Charpentier, P. Courvalin, Antibiotic Resistance in *Listeria* spp., Antimicrob. Agents Chemother. 43 (1999) 2103–2108.

[9] E. Charpentier, G. Gerbaud, C. Jacquet, J. Rocourt, P. Courvalin, Incidence of antibiotic resistance in *Listeria* species, J. Infect. Dis. 172 (1995) 277–281.

[10] M.A. Prazak, E.A. Murano, I. Mercado, G.R. Acuff, Antimicrobial resistance of *Listeria monocytogenes* isolated from various cabbage farms and packing sheds in Texas, J. Food Prot. 65 (2002) 1796-1799.

[11] C. Mauro, P. Domenico, D.O. Vincenzo, V. Alberto, I. Adriana, Antimicrobial susceptibility of *Listeria monocytogenes* isolated from food and food-processing environment, Ann. Fac. Medic. Vet. di Parma XXVII (2007) 157-164.

[12] L. Mereghetti, R. Quentin, N. Marquet-van der Mee, A. Audurier, Low sensitivity of *Listeria monocytogenes* to quaternary ammonium compounds, Appl. Environ. Microbiol. 66 (2000) 5083–5086.

[13] J. Lunden, T. Autio, A. Markkula, S. Hellstrom, H. Korkeala, Adaptive and cross-adaptive responses of persistent and non-persistent *Listeria*

monocytogenes strains to disinfectants, Int. J. Food Microbiol. 82 (2003) 265–272.

[14] N. Romanova, S. Favrin, M.W. Griffiths, Sensitivity of *Listeria monocytogenes* to sanitizers used in the meat processing industry, Appl. Environ. Microbiol. 68 (2002) 6405–6409.

[15] C. Guinovart, M.M. Navia, M. Tanner, P.L. Alonso, Malaria: burden of disease, Curr. Mol. Med. 6 (2006) 137-140.

[16] P. Newton, N. White, Malaria: new developments in treatment and prevention, Annu. Rev. Med. 50 (1999).

[17] E.L. Korenromp, Malaria incidence estimates at country level for the year 2004–proposed estimates and draft report, Geneva, Roll Back Malaria, World Health Organization, 2004.

[18] C. Wongsrichanalai, A.L. Pickard, W.H. Wernsdorfer, S.R. Meshnick, Epidemiology of drug-resistant malaria, Lancet Infect. Dis. 2 (2002) 209-218.

[19] P.M. Hwang, H.J. Vogel, Structure-function relationships of antimicrobial peptides, Cell Biol. 76 (1998) 235-246.

[20] W. Van 't Hof, E.C. Veerman, E.J. Helmerhorst, A.V. Amerongen, Antimicrobial peptides: properties and applicability, Biol. Chem. 382 (2001) 597-619.

[21] R.A. Bonomo, Multiple antibiotic–resistant bacteria in long-term-care facilities: An emerging problem in the practice of infectious diseases, Clin. Infect. Dis. 31 (2000) 1414–1422.

[22] H. Jenssen, P. Hamill, R.E.W. Hancock, Peptide Antimicrobial Agents, Clin. Microbiol. Rev. 19 (2006) 491–511.

[23] M. Stark, L.P. Liu, C.M. Deber, Cationic hydrophobic peptides with antimicrobial activity, Antimicrob. Agents Chemother. 46 (2002) 3585-3590.

[24] R.E. Hancock, A. Patrzykat, Clinical development of cationic antimicrobial peptides: from natural to novel antibiotics, Curr. Drug Targets Infect. Disord. 2 (2002) 79-83.

[25] K. Matsuzaki, Why and how are peptide–lipid interactions utilized for self defence?, Biochem. Soc. Trans. 29 (2001) 598-601.

[26] N.Y. Yount, M.R. Yeaman, Immunocontinuum: perspectives in antimicrobial peptide mechanisms of action and resistance, Protein Pept. Lett. 12 (2005) 49-67.

[27] R.E.W. Hancock, Peptide antibiotics, The Lancet 349 (1997) 418-422.

[28] R.W. Jack, Jung, G. , Natural peptides with antimicrobial activity, Chimia 52 (1998) 48-55.

[29] R.E. Hancock, R. Lehrer, Cationic peptides: a new source of antibiotics, Trends Biotechnol. 16 (1998) 82-88.

[30] M. Zasloff, Reconstructing one of nature's designs, TiPS 21 (2000) 236-238.

[31] M. Zasloff, Antimicrobial peptides of multicellular organisms, Nature 415 (2002) 389-395.

[32] A.K. Marr, W.J. Gooderham, R.E.W. Hancock, Antibacterial peptides for therapeutic use: obstacles and realistic outlook, Curr. Opin. Pharmacol. 6 (2006) 468-472.

[33] R.M. Epand, H.J. Vogel, Diversity of antimicrobial peptides and their mechanisms of action, Biochim. Biophys. Acta 1462 (1999) 11-28.

[34] K.H. Lee, Development of short antimicrobial peptides derived from host defense peptides or by combinatorial libraries, Curr. Pharm. Des. 8 (2002) 795-813.

[35] O. Toke, Antimicrobial peptides: new candidates in the fight against bacterial infections, Biopolymers (Pept. Sci.) 80 (2005) 717-735.

[36] J. Vizioli, M. Salzet, Antimicrobial peptides versus parasitic infections?, Trends Parasitol 18 (2002) 475-476.

[37] M. Rautenbach, N.M. Vlok, M. Stander, H.C. Hoppe, Inhibition of malaria parasite blood stages by tyrocidines, membrane-active cyclic peptide antibiotics from *Bacillus brevis*, Biochim. Biophys. Acta - Biomembranes 1768 (2007) 1488–1497.

[38] H. Zhao, Mode of Action of Antimicrobial Peptides, Faculty of Medicine, University of Helsinki, Helsinki, 2003.

[39] A.R. Koczulla, R. Bals, Antimicrobial peptides: current status and therapeutic potential, Drugs 63 (2003) 389-406.

[40] J. Gerard, P. Haden, M.T. Kelly, R.J. Andersen, Loloatin B, a cyclic decapeptide antibiotic produced in culture by a tropical marine bacterium, Tetrahedron Letters 37 (1996) 7201-7204.

[41] J. Gerard, P. Haden, M.T. Kelly, R.J. Andersen, Loloatins A-D, cyclic decapeptide antibiotics produced in culture by a tropical marine bacterium, J. Nat. Prod. 62 (1999) 80-85.

[42] K. Gebhardt, R. Pukall, H.-P. Fiedler, Streptocidins A-D, novel cyclic decapeptide antibiotics produced by *Streptomyces* sp. Tu 6071. I. Taxonomy, Fermentation, Isolation and Biological Activities, Journal of Antibiotics 54 (2001) 428-433.

[43] A. Holtzel, R.W. Jack, G.J. Nicholson, G. Jung, K. Gebhardt, H.-P. Fiedler, R.D. Sussmuth, Streptocidins A-D, novel cyclic decapeptide antibiotics produced by *Streptomyces* sp. Tu 6071. II. Structure Elucidation, Journal of Antibiotics 54 (2001) 434-440.

[44] R.J. Dubos, Studies on a bactericidal agent extracted from a soil bacillus. I. Preparation of the agent. Its activity in vitro, J. Exp. Med. 70 (1939) 1-10.

[45] R.J. Dubos, Studies on a bactericidal agent extracted from a soil bacillus. II. Protective effect of the bactericidal agent against experimental Pneumococcus infections in mice, J. Exp. Med. 70 (1939) 11-17.

[46] H.L. Van Epps, Rene Dubos: unearthing antibiotics, J. Exp. Med. 203 (2006) 259.

[47] R.D. Hotchkiss, R.J. Dubos, The isolation of bactericidal substances from cultures of *Bacillus brevis*, J. Biol. Chem. (1941) 155-162.

[48] R.D. Hotchkiss, The chemical nature of gramicidin and tyrocidine, J. Biol. Chem. (1941) 171-185.

[49] X.-J. Tang, P. Thibault, R.K. Boyd, Characterisation of the tyrocidine and gramicidin fractions of the tyrothricin complex from *Bacillus brevis* using liquid chromatography and mass spectrometry, Int. J. Mass Spectrom. Ion Process. 122 (1992) 153-179.

[50] W.A. Gibbons, C.F. Beyer, J. Dadok, R.F. Sprecher, H.R. Wyssbrod, Studies of individual amino acid residues of the decapeptide tyrocidine A by proton double-resonance difference spectroscopy in the correlation mode, Biochemistry 14 (1975) 420-429.

[51] M.C. Kuo, W.A. Gibbons, Nuclear Overhauser effect and cross-relaxation rate determinations of dihedral and transannular interproton distances in the decapeptide tyrocidine A, Biophys. J. 32 (1980) 807-836.

[52] R.J. Dubos, R.D. Hotchkiss, The production of bactericidal substances by aerobic sporulating bacilli, J. Exp. Med. 73 (1941) 629-640.

[53] M. Wu, E. Maier, R. Benz, R.E. Hancock, Mechanism of interaction of different classes of cationic antimicrobial peptides with planar bilayers and with the cytoplasmic membrane of Escherichia coli, Biochemistry 38 (1999) 7235-7242.

[54] Y. Shai, Mode of action of membrane active antimicrobial peptides, Biopolymers (Pept. Sci.) 66 (2002) 236-248.

[55] H. Kamimori, J. Blazyk, M.-I. Aguilar, Lipid membrane-binding properties of tryptophan analogues of linear amphipathic beta-sheet cationic antimicrobial peptides using surface plasmon resonance, Biol. Pharm. Bull. 28 (2005) 148-150.

[56] L.-P. Liu, C.M. Deber, Anionic phospholipids modulate peptide insertion into membranes, Biochemistry 36 (1997) 5476-5482.

[57] G. Boheim, Statistical analysis of alamethicin channels in black lipid membranes, J. Membr. Biol. 19 (1974) 277-303.

[58] K. Matsuzaki, O. Murase, N. Fujii, K. Miyajima, . An antimicrobal peptide, magainin 2, induced rapid flip-flop of phospholipids coupled with pore formation and peptide translocation, Biochemistry 35 (1996) 11361-11368.

[59] Y. Pouny, D. Rapaport, A. Mor, P. Nicolas, Y. Shai, Interaction of antimicrobial dermaseptin and its fluorescently labeled analogues with phospholipid membranes., Biochemistry 31 (1992) 12416-12423.

[60] Y. Shai, Mechanism of the binding, insertion and destabilization of phospholipid bilayer membranes by alpha-helical antimicrobial and cell non-selective membrane-lytic peptides Biochim. Biophys. Acta - Biomembranes 1462 (1999) 55-70.

[61] N. Papo, Y. Shai, Exploring peptide membrane interaction using surface plasmon resonance: Differentiation between pore formation versus membrane disruption by lytic peptides, Biochemistry 42 (2003) 458-466.

[62] R.E. Hancock, D.S. Chapple, Peptide antibiotics, Antimicrob. Agents Chemother. 43 (1999) 1317-1323.

[63] R.E. Hancock, A. Rozek, Role of membranes in the activities of antimicrobial cationic peptides, FEMS Microbiol. Lett. 206 (2002) 143-149.

[64] Y. Shai, From innate immunity to *de-novo* designed antimicrobial peptides, Curr. Pharm. Des. 8 (2002) 715-725.

[65] B. Bechinger, K. Lohner, Detergent-like actions of linear amphipathic cationic antimicrobial peptides, Biochim. Biophys. Acta 1758 (2006) 1529–1539.

[66] R. Jelinek, S. Kolusheva, Membrane interactions of host-defense peptides studied in model systems, Curr. Protein Pept. Sci. 6 (2005) 103-114.

[67] N.Y. Yount, A.S. Bayer, Y.Q. Xiong, M.R. Yeaman, Advances in antimicrobial peptide immunobiology, Biopolymers (Pept. Sci.) 84 (2006) 435–458.

[68] D. Andreu, L. Rivas, Animal antimicrobial peptides: an overview, Biopolymers (Pept. Sci.) 47 (1998) 415-433.

[69] K. Matsuzaki, O. Murase, N. Fujii, K. Miyajima, Translocation of a channel-forming antimicrobial peptide, magainin 2, across lipid bilayers by forming a pore, Biochemistry 34 (1995) 6521-6526.

[70] Y.R. Chan, R.L. Gallo, PR-39, a syndecan-inducing antimicrobial peptide, binds and affects p130Cas J. Biol. Chem. 273 (1998) 28978-28985.

[71] H.G. Boman, B. Agerberth, A. Boman, Mechanisms of action on *Escherichia coli* of cecropin P1 and PR-39, two antimicribial peptides from pig intestine, Infect. Immun. 61 (1993) 2978-2984.

[72] M. Castle, A. Nazarian, S.S. Yi, P. Tempst, Lethal effects of apidaecin on *Escherichia coli* involve sequential molecular interactions with diverse targets, J. Biol. Chem. 274 (1999) 32555-32564.

[73] M.E. Mongoni, A. Aumelas, C. P., L. Chiche, E. Despaux, G. Grassy, B. Callas, A. Chavanieu, Change in membrane premebility induced by protegrin 1: implication of disulphide bridges for pore formation, FEBS Lett. 383 (1996).

[74] A. Yonesawa, J. Kuwahara, N. Fujii, Y. Sugiura, Binding of tachyplesin I to DNA revealed by footprinting analysis, Biochemistry 31 (1992) 2998-3004.

[75] R. Gennaro, M. Zanetti, M. Benincasa, E. Podda, M. Miani, Pro-rich antimicrobial peptides from animals: structure, biological functions and mechanism of action, Curr. Pharm. Des. 8 (2002) 763-778.

[76] A. Scheller, J. Oehlke, B. Wiesner, M. Dathe, E. Krause, M. Beyermann, M. Melzig, M. Bienert, Structural requirements for cellular uptake of alpha-helical amphipathic peptides J. Pept. Sci. 5 (1999) 185-194.

[77] J.F. Liang, S.C. Kim, Not only the nature of peptide but also the characteristics of cell membrane determine the antimicrobial mechanism of a peptide, J. Pept. Res. 53 (1999) 518-522.

[78] K.A. Brogden, Antimicrobial peptides: pore formers or metabolic inhibitors in bacteria?, Nature Rev. Microbiol. 3 (2005) 238-250.

[79] K. Matsuzaki, O. Murase, K. Miyajima, Kinetics of pore formation by an antimicrobial peptide, magainin 2, in phospholipid bilayers, Biochemistry 34 (1995) 12553-12559.

[80] A. Patrzykat, C.L. Friedrich, L. Zhang, V. Mendoza, R.E.W. Hancock, Sublethal concentrations of pleurocidin-derived antimicrobial peptides inhibit macromolecular synthesis in *Escherichia coli*, Antimicrob. Agents Chemother. 46 (2002) 605–614

[81] C.B. Park, H.S. Kim, S.C. Kim, Mechanisms of action of the antimicrobial peptide buforin II: buforin II kills microorganisms by penetrating the cell membrane and inhibiting cellular functions, Biochem. Biophys. Res. Commun. 244 (1998) 253-257.

[82] C. Subbalakshmi, N. Sitaram, Mechanisms of action of indolicin, FEMS Microbiol. Lett. 160 (1998) 91-96.

[83] A. Carlsson, P. Engström, E.T. Palva, H. Bennich, Attacin, an antibacterial protein from *Hyalophora cecropia*, inhibits synthesis of outer membrane proteins in *Escherichia coli* by interfering with omp gene transcription, Infect. Immun. 59 (1999) 3040 – 3045.

[84] J. Oh, Y. Cajal, E.M. Skowronska, S. Belkin, J. Chen, T.K. Van Dyk, R.M. Sasse, M.K. Jain, Cationic peptide antimicrobials induce selective transcription of micF and osmY in *Escherichia coli*, Biochim. Biophys. Acta 1463 (2000) 43 – 54.

[85] B. Skerlavaj, D. Romeo, R. Gennaro, Rapid membrane permeabilization and inhibition of vital functions of Gram-negative bacteria by bactenecins, Infect. Immun. 58 (1990).

[86] M. Nishikata, T. Kanehira, H. Oh, H. Tani, M. Tazki, Y. Kuboki, Salivary histatin as an inhibitor of a protease produced by the oral bacterium *Bacteroides gingivalis* Biochem. Biophys. Res. Commun. 174 (1991) 625-630.

[87] M.A. Couto, S.S. Harwig, R.I. Lehrer, Selective inhibition of microbial serine proteases by eNAP-2, an antimicrobial peptide from equine neutrophils, Infect. Immun. 61 (1993) 2991-2994.

[88] L. Otvos, Interaction between heat shock proteins and antimicrobial peptides, Biochemistry 39 (2000).

[89] A. Bateman, A. Singh, L.F. Congote, S. Solomon, The effect of HP-1 and related neutrophil granule peptides on DNA synthesis in HL60 cells. Regul Pept. , Regul. Pept. 35 (1991) 135–143.

[90] R.A. Salomon, R.N. Farias, Microcin 25, a novel antimicrobial peptide produced by *Escherichia coli*, J. Bacteriol. 174 (1992) 7428-7435.

[91] J. Shi, Antibacterial activity of a synthetic peptide (PR-26) derived from PR-39, a proline-arginine-rich neutrophil antimicrobial peptide, Antimicrob. Agents Chemother. 40 (1996) 115-121.

[92] D. Gidalevitz, Y. Ishitsuka, A.S. Muresan, O. Konovalov, A.J. Waring, R.I. Lehrer, K.Y. Lee, Interaction of antimicrobial peptide protegrin with biomembranes, Proc Natl Acad Sci U S A 100 (2003) 6302-6307.

[93] M. Jelokhani-Niaraki, E.J. Prenner, L.H. Kondejewski, C.M. Kay, R.N. McElhaney, R.S. Hodges, Conformation and other biophysical properties of cyclic antimicrobial peptides in aqueous solutions, J. Pept. Res. 58 (2001) 293-306.

[94] A. Bohg, H. Ristow, DNA-supercoiling is affected in vitro by the peptide antibiotics tyrocidine and gramicidin, Eur. J. Biochem. 160 (1986) 587-591.

[95] A. Bohg, H. Ristow, Tyrocidine-induced modulation of the DNA conformation in *Bacillus brevis*, Eur. J. Biochem. 170 (1987) 253-258.

[96] T. Chakraborty, J. Hansen, B. Schazschneider, H. Ristow, The DNA-tyrocidine complex and its dissociation in the presence of gramicidin D, Eur. J. Biochem. 90 (1978) 261-270.

[97] J.-P. Changeux, A. Ryter, W. Leuzinger, P. Barrand, T. Podleski, On the association of tyrocidine with acetylcholinesterases, Proc. Nat. Acad. Sci. 62 (1969) 986-993.

[98] F.J. Aranda, B. De Kruijff, Interrelationships between tyrocidine and gramicidin A' in their interaction with phospholipids in model membranes, Biochim. Biophys. Acta - Biomembranes 937 (1988) 195-203.

[99] E.J. Prenner, R.N. Lewis, R.N. McElhaney, The interaction of the antimicrobial peptide gramicidin S with lipid bilayer model and biological membranes, Biochim. Biophys. Acta 1462 (1999) 201-221.

[100] T. Katsu, H. Kobayashi, Y. Fujita, Mode of action of gramicidin S on *Escherichia coli* membrane, Biochim. Biophys. Acta 860 (1986) 608-619.

[101] E. Staudegger, E.J. Prenner, M. Kriechbaum, G. Degovics, R.N. Lewis, R.N. McElhaney, K. Lohner, X-ray studies on the interaction of the antimicrobial peptide gramicidin S with microbial lipid extracts: evidence for cubic phase formation, Biochim. Biophys. Acta 1468 (2000) 213-230.

[102] R.O. Iglesias, A.F. Rega, Gramicidin S inhibition of the Ca^{2+}-ATPase of human red blood cells, Biochim. Biophys. Acta 905 (1987) 383-389.

[103] T. Mogi, H. Ui, K. Shiomi, S. Omura, K. Kita, Gramicidin S identified as a potent inhibitor for cytochrome *bd*-type quinol oxidase, FEBS Lett. 582 (2008) 2299-2302.

[104] M. Jelokhani-Niaraki, E.J. Prenner, C.M. Kay, R.N. McElhaney, R.S. Hodges, Conformation and interaction of the cyclic cationic antimicrobial peptides in lipid bilayers, J. Pept. Res. 60 (2002) 23-36.

[105] S. Rotem, I. Radzishevsky, A. Mor, Physicochemical properties that enhance discriminative antibacterial activity of short dermaseptin derivatives, Antimicrob. Agents Chemother. 50 (2006) 2666-2672.

[106] L.H. Kondejewski, D.L. Lee, M. Jelokhani-Niaraki, S.W. Farmer, R.E. Hancock, R.S. Hodges, Optimization of microbial specificity in cyclic peptides by modulation of hydrophobicity within a defined structural framework, J. Biol. Chem. 277 (2002) 67-74.

[107] T. Rydlo, S. Rotem, A. Mor, Antibacterial properties of dermaseptin S4 derivatives under extreme incubation conditions, Antimicrob. Agents Chemother. 50 (2006) 490–497.

[108] V. Frecer, QSAR analysis of antimicrobial and haemolytic effects of cyclic cationic antimicrobial peptides derived from protegrin-1, Bioorg. Med. Chem. 14 (2006) 6065-6074.

[109] V. Frecer, B. Ho, J.L. Ding, *De novo* design of potent antimicrobial peptides, Antimicrob. Agents Chemother. 48 (2004) 3349-3357.

[110] A. Mor, K. Hani, P. Nicolas, The vertebrate peptide antibiotics dermaseptins have overlapping structural features but target specific microorganisms, J. Biol. Chem. 269 (1994) 31635-31641.

[111] M.B. Strom, B.E. Haug, O. Rekdal, M.L. Skar, W. Stensen, J.S. Svendsen, Important structural features of 15-residue lactoferricin derivatives and methods for improvement of antimicrobial activity, Biochem. Cell Biol. 80 (2002) 65-74.

[112] M. Dathe, J. Meyer, M. Beyermann, B. Maul, C. Hoischen, M. Bienert, General aspects of peptide selectivity towards lipid bilayers and cell membranes studied by variation of the structural parameters of amphipathic helical model peptides, Biochim. Biophys. Acta 1558 (2002) 171-186.

[113] M. Dathe, H. Nikolenko, J. Klose, M. Bienert, Cyclization increases the antimicrobial activity and selectivity of arginine- and tryptophan-containing hexapeptides, Biochemistry 43 (2004) 9140-9150.

[114] M. Dathe, T. Wieprecht, H. Nikolenko, L. Handel, W.L. Maloy, D.L. MacDonald, M. Beyermann, M. Bienert, Hydrophobicity, hydrophobic moment and angle subtended by charged residues modulate antibacterial and haemolytic activity of amphipathic helical peptides, FEBS Lett. 403 (1997) 208-212.

[115] A. Giangaspero, L. Sandri, A. Tossi, Amphipathic alpha helical antimicrobial peptides, Eur. J. Biochem. 268 (2001) 5589-5600.

[116] L. Zhang, P. Dhillon, H. Yan, S. Farmer, R.E.W. Hancock, Interactions of bacterial cationic peptide antibiotics with outer and cytoplasmic membranes of *Pseudomonas aeruginosa* Antimicrob. Agents Chemother. 44 (2000).

[117] M. Dathe, M. Schumann, T. Wieprecht, A. Winkler, M. Beyermann, E. Krause, K. Matsuzaki, O. Murase, M. Bienert, Peptide helicity and membrane surface charge modulate the balance of electrostatic and hydrophobic interactions with lipid bilayers and biological membranes, Biochemistry 35 (1996) 12612-12622.

[118] E. Guerrero, J.M. Saugar, K. Matsuzaki, L. Rivas, Role of positional hydrophobicity in the leishmanicidal activity of magainin 2, Antimicrob. Agents Chemother. 48 (2004) 2980-2986.

[119] Z. Oren, Y. Shai, Selective lysis of bacteria but not mammalian cells by diastereomers of melittin: structure–function study, Biochemistry 36 (1997) 1826-1835.

[120] K. Matsuzaki, Magainins as paradigm for the mode of action of pore forming polypeptides, Biochem. Biophys. Acta 1376 (1998) 391-400.

[121] S. Ludtke, K. He, W. Heller, T. Harroun, L. Yang, H. Huang, Membrane pores induced by magainin, Biochemistry 35 (1996) 13723-13728.

[122] B. Christensen, J. Fink, R.B. Merrifield, D. Mauzerall, Channel-forming properties of cecropins and related model compounds incorporated into planar lipid membranes, Proc. Natl. Acad. Sci. USA 85 (1988) 5072-5076.

[123] W.C. Wimley, S.H. White, Membrane partitioning: distinguishing bilayer effects from the hydrophobic effect, Biochemistry 32 (1993) 6307-6312.

[124] A. Ladokhin, S. White, Folding of amphipathic alpha-helices on membranes: energetics of helix formation by melittin, J. Mol. Biol. 285 (1998) 1363-1369.

[125] C. McInnes, L.H. Kondejewski, R.S. Hodges, B.D. Sykes, Development of the structural basis for antimicrobial and hemolytic activities of peptides based on gramicidin S and design of novel analogs using NMR spectroscopy, J. Biol. Chem. 275 (2000) 14287-14294.

[126] L.H. Kondejewski, S.W. Farmer, D.S. Wishart, C.M. Kay, R.E. Hancock, R.S. Hodges, Modulation of structure and antibacterial and hemolytic activity by ring size in cyclic gramicidin S analogs, J. Biol. Chem. 271 (1996) 25261-25268.

[127] L.H. Kondejewski, M. Jelokhani-Niaraki, S.W. Farmer, B. Lix, C.M. Kay, B.D. Sykes, R.E. Hancock, R.S. Hodges, Dissociation of antimicrobial and hemolytic activities in cyclic peptide diastereomers by systematic alterations in amphipathicity, J. Biol. Chem. 274 (1999) 13181-13192.

[128] E.J. Prenner, R.N. Lewis, K.C. Neuman, S.M. Gruner, L.H. Kondejewski, R.S. Hodges, R.N. McElhaney, Nonlamellar phases induced by the interaction of gramicidin S with lipid bilayers. A possible relationship to membrane-disrupting activity, Biochemistry 36 (1997) 7906-7916.

[129] M. Jelokhani-Niaraki, L.H. Kondejewski, S.W. Farmer, R.E.W. Hancock, C.M. Kay, R.S. Hodges, Diastereoisomeric analogues of gramicidin S: structure, biological activity and interaction with lipid bilayers, Biochem. J. 349 (2000) 747-755.

[130] M.A. Ruttenberg, T.P. King, L.C. Craig, The use of the tyrocidines for the study of conformation and aggregation behavior, J. Am. Chem. Soc. 87 (1965) 4196-4198.

[131] R.M. Kohli, C.T. Walsh, M.D. Burkart, Biomimetic synthesis and optimization of cyclic peptide antibiotics, Nature 418 (2002) 658-661.

[132] C. Qin, X. Zhong, X. Bu, N.L.J. Ng, Z. Guo, Dissociation of antibacterial and hemolytic activities of an amphipathic peptide antibiotic, J. Med. Chem. 46 (2003) 4830-4833.

[133] A. Scaloni, M. Dalla Serra, P. Amodeo, L. Mannina, R.M. Vitale, A.L. Segre, O. Cruciani, F. Lodovichetti, M.L. Greco, A. Fiore, M. Gallo, C. D'Ambrosio, M. Coraiola, G. Menestrina, A. Graniti, V. Fogliano, Structure, conformation and

biological activity of a novel lipodepsipeptide from *Pseudomonas corrugata*: cormycin A, Biochem. J. 384 (2004) 25-36.

[134] E. Glukhov, M. Stark, L.L. Burrows, C.M. Deber, Basis for selectivity of cationic antimicrobial peptides for bacterial versus mammalian membranes, J. Biol. Chem. 280 (2005) 33960–33967.

[135] M.A. Ruttenberg, T.P. King, L.C. Craig, The chemistry of tyrocidine. VII. Studies on association behavior and implications regarding conformation, Biochemistry 5 (1966) 2857-2863.

[136] S. Laiken, M. Printz, L.C. Craig, Circular dichroism of the tyrocidines and gramicidin S-A, J. Biol. Chem. 244 (1969) 4454-4457.

[137] S.L. Laiken, M.P. Printz, L.C. Craig, Studies on the mode of self-assembly of tyrocidine B, Biochem. Biophys. Res. Commun. 43 (1971) 595-600.

[138] H.H. Paradies, Aggregation of tyrocidine in aqueous solutions, Biochem. Biophys. Res. Commun. 88 (1979) 810-817.

[139] R.C. Williams, D.A. Yphantis, L.C. Craig, Noncovalent association of tyrocidine B, Biochemistry 11 (1972) 70-77.

[140] H. Zhao, P.K. Kinnunen, Binding of the antimicrobial peptide temporin L to liposomes assessed by Trp fluorescence, J. Biol. Chem. 277 (2002) 25170-25177.

[141] D. Wade, A. Boman, B. Wahlin, C.M. Drain, D. Andreu, H.G. Boman, R.B. Merrifeld, All-D amino acid-containing channel-forming antibiotic peptides, Proc. Natl. Acad. Sci. USA 87 (1990) 4761-4765.

[142] R. Bessalle, A. Kapitkovsky, A. Gorea, I. Shalit, M. Fridkin, All-D-magainin: chirality, antimicrobial activity and proteolytic resistance, FEBS Lett. 274 (1990) 151-155.

[143] N.I.F. Gallagher, M. Sailer, W.P. Niemczura, T. Nakashima, M.E. Stiles, J.C. Vederas, Three-dimensional structure of leucocin A in trifluoroethanol and dodecylphosphocholine micelles: spatial location of residues critical for biological activity in type IIa bacteriocins from lactic acid bacteria, Biochemistry 36 (1997) 15062-15072.

[144] K. Matsuzaki, K. Sugishita, K. Miyajima, Interactions of an antimicrobial peptide, magainin 2, with lipopolysaccharide-containing liposomes as a model for outer membranes of gram-negative bacteria, FEBS Lett. 449 (1999) 221-224.

[145] K.L. Piers, R.E. Hancock, The interaction of a recombinant cecropin/melittin hybrid peptide with the outer membrane of Pseudomonas aeruginosa, Mol Microbiol 12 (1994) 951-958.

[146] E.A. Macias, F. Rana, J. Blazyk, M.C. Modrzakowski, Bactericidal activity of magainin 2: use of lipopolysaccharide mutants Can. J. Microbiol. 36 (1990) 582-584.

[147] F. Rana, C.M. Sultana, J. Blazyk, Interaction between *Salmonella typhimurium* lipopolysaccharide and the antimicrobial peptide, magainin 2 amide FEBS Lett. (1990) 464-467.

[148] M.G. Scott, M.R. Gold, R.E. Hancock, Interaction of cationic peptides with lipoteichoic acid and gram-positive bacteria, Infect. Immun. 67 (1999) 6445-6453.

[149] H. Brotz, G. Bierbaum, K. Leopold, P.E. Reynolds, H.G. Sahl, The lantibiotic mersacidin inhibits peptidoglycan synthesis by targeting lipid II Antimicrob. Agents Chemother. 42 (1998) 154-160.

[150] R. Bauer, L.M. Dicks, Mode of action of lipid II-targeting lantibiotics, Int. J. Food Microbiol. 101 (2005) 201-216.

[151] E. Breukink, P. Ganz, B. de Kruijff, J. Seelig, Binding of nisin Z to bilayer vesicles as determined with isothermal titration calorimetry, Biochemistry 39 (2000) 10247-10254.

[152] Y. Hirakura, S. Koabyashi, K. Matsuzaki, Specific interactions of the antimicrobial peptide cyclic β-sheet tachyplesin I with lipopolysaccharides, Biochim. Biophys. Acta. 1562 (2002) 32-36.

[153] P. Fehlbaum, P. Bulet, S. Chernysh, J.P. Briand, J.P. Roussel, L. Letellier, C. Hetru, J.A. Hoffmann, Structure-activity analysis of thanatin, a 21-residue inducible insect defense peptide with sequence homology to frog skin antimicrobial peptides, Proc Natl Acad Sci U S A 93 (1996) 1221-1225.

[154] T.J. Montville, Y. Chen, Mechanistic action of pediocin and nisin: recent progress and unresolved questions, Appl. Microbiol. Biotechnol. 50 (1998) 511-519.

[155] R. Bals, M.J. Goldman, J.M. Wilson, Mouse beta-Defensin 1 is a salt-sensitive antimicrobial peptide present in epithelia of the lung and urogenital tract, Infect. Immun. 66 (1998) 1225-1232.

[156] S. Cociancich, A. Ghazi, C. Hetru, J.A. Hoffmann, L. Letellier, Insect defensin, an inducible antibacterial peptide, forms voltage-dependent channels in *Micrococcus luteus*, J. Biol. Chem. 268 (1993) 19239-19245.

[157] R.I. Lehrer, T. Ganz, D. Szklarek, M.E. Selsted, Modulation of the *in vitro* candidacidal activity of human neutrophil defensins by target cell metabolism and divalent cations, J. Clin. Invest. 81 (1988) 1829-1835.

[158] K. Yamauchi, K. Tomita, T.J. Giehl, R.T. Ellison, Antibacterial activity of lactoferrin and a pepsin-derived lactoferrin peptide fragment, Infect. Immun. 61 (1993) 719-728.

[159] W.F. Broekaert, F.R.G. Terras, B.P.A. Cammue, R.W. Osborn, Plant defensins: Novel antimicrobial peptides as components of the host defense system, Plant Physiol. 108 (1995) 1353-1358.

[160] D.M.E. Bowdish, D.J. Davidson, Y.E. Lau, K. Lee, M.G. Scott, R.E.W. Hancock, Impact of LL-37 on anti-infective immunity, J. Leukoc. Biol. 77 (2005) 451-459.

[161] R. Urrutia, R.A. Cruciani, J.L. Barker, B. Kachar, Spontaneous polymerization of the antibiotic peptide magainin 2, FEBS Lett. 247 (1989) 17-21.

[162] J. Bradshaw, Cationic antimicrobial peptides : issues for potential clinical use, BioDrugs 17 (2003) 233-240.

[163] M. Rautenbach, J.W. Hastings, Cationic peptides with antimicrobial activity - the new generation of antibiotics?, Chimica Oggi (1999) 81-89.

[164] Y.J. Gordon, E.G. Romanowski, A.M. McDermott, A review of antimicrobial peptides and their therapeutic potential as anti-infective drugs, Curr. Eye Res. 30 (2005) 505-515.

Chapter 2

Purification and analyses of cyclic decapeptides from the tyrothricin complex

2.1 Introduction

Investigation of the structure, biological activity and structure-function relationships of the tyrocidines and analogues from the tyrothricin complex requires highly purified fractions. Because of the high analogy of the cyclic peptides in the tyrothricin complex, it required the design of a purification protocol and the subsequent analyses of the obtained fractions in order to ascertain purity and confirm the identity of the peptide(s) present in each fraction. Various techniques are available for the isolation, purification and analysis of peptides, most notably high-performance liquid chromatography (HPLC) and mass spectrometry (MS). HPLC has the advantage of being both a purification and analytical tool, which can be used to assess purity. MS provides an indication of purity, allows the determination of accurate molecular mass and can be used to determine primary sequence. These techniques do, however, have certain limitations and should ideally be used in combination in order to deduce purity and confirm identity.

When designing a protocol for the purification of individual peptides from a complex mixture, advantage should be taken of the differences in their physicochemical properties, such as charge, mass and hydrophobicity. Reverse-phase HPLC (RP-HPLC), which separates compounds based on their differential interaction with a hydrophobic stationary phase in the presence of a polar mobile phase, is one of the most powerful techniques for the separation of biomolecules, including peptides. Two characteristics of antimicrobial peptides that may impede their purification by RP-HPLC include small differences in hydrophobicity and amphipathic character. Careful consideration of factors that influence RP-HPLC resolution, such as matrix, column dimensions, eluant compositions, the gradient

profile and temperature, is required in order to separate and purify individual peptides from a mixture of peptides that have similar hydrophobicities. The amphipathic character of antimicrobial peptides often results in aggregate/complex formation, especially between the more hydrophobic peptides. Eluant compositions, method temperature and peptide concentration need to be optimised in order to limit such aggregation.

Mass spectrometry is a powerful technique for the determination of purity, accurate molecular mass and sequence information. Time-of-flight electrospray mass spectrometry (TOF-ESMS) is commonly used in the analyses of peptides due to its high sensitivity, high mass accuracy and ability to generate and observe multiply charged species. TOF-ESMS allows for the identification of specific molecular masses in a sample, but does not distinguish between different molecules with the same molecular mass. Tandem mass spectrometry (MS-MS) can be used to sequence peptides, thus allowing discrimination between peptides with identical molecular masses. The most common MS-MS technique involves a triple quadrupole combined with electrospray ionisation (ESI), due to its high sensitivity and reasonable fragmentation information. The collision-induced dissociation (CID) of peptides in ESI-MS results in two classes of fragment ions. Fragments that retain their charge on the N-terminal and are cleaved at the C-terminal form fragment types a_n, b_n, or c_n, whereas the fragments that retain their charge on the C-terminal and are cleaved at the N-terminal form fragment types x_n, y_n or z_n (Figure 1) [1, 2]. Peptides commonly dissociate to yield the b_n and y_n product ion series [3]. Determining the primary sequence of cyclic peptides using MS-MS is, however, more complicated than that of linear peptides due to the variety of possible ring openings that the peptide can undergo prior to fragmentation.

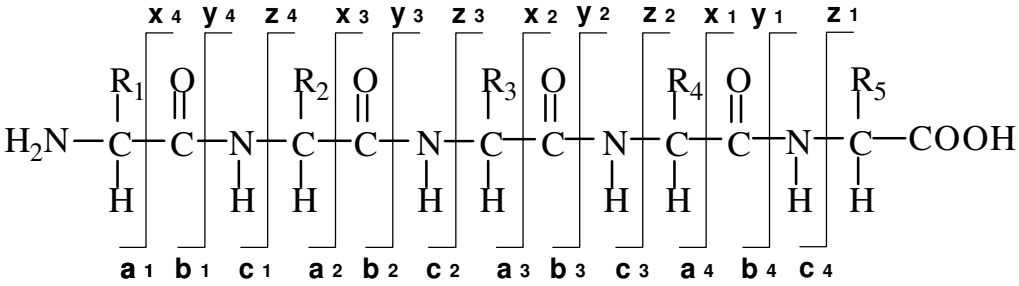

Peptide backbone product ions

a 1 $H_2\overset{+}{N}{=}CHR_1$

b 1 $H_2N{-}CHR_1{-}C{\equiv}O^+$

c" 1 $H_2N{-}CHR_1{-}\overset{O}{\overset{\|}{C}}{-}NH_3^+$

a 2 $H_2N{-}CHR_1{-}\overset{O}{\overset{\|}{C}}{-}\overset{+}{N}H{=}CHR_2$

z 1 $R_5HC{=}\overset{+}{C}OOH$

y" 1 $H_3\overset{+}{N}{-}CHR_5{-}COOH$

x 1 $O^+{\equiv}C{-}NH{-}CHR_5{-}COOH$

z 2 $R_4HC{-}\overset{O}{\overset{\|}{C}}{-}NH{-}CHR_5{=}\overset{+}{C}OOH$

Side-chain ions

d-ions

$a_2 + H \xrightarrow{-R_{2a} \text{ or } R_{2b}} d_2$

immonium ions (i-ions)

mass of residue - (CO + H)

v-ions

$y_2 + 2H \xrightarrow{-R_4H} v_2$

w-ions

$z_2 + H \xrightarrow{-R_{4a} \text{ or } R_{4b}} w_2$

Figure 1 *Fragmentation patterns of a peptide during mass spectrometry*
The possible peptide backbone cleavage sites, and resulting fragment ions, are illustrated. The nomenclature of the fragment ions and side-chain ions follows that of Roepstorff and Fohlmann [1], as revised by Biemann and Martin [2]. (Figure reproduced with permission from M. Rautenbach)

2.1.1 Peptides of interest to this study

The antimicrobial peptides of interest to this study are the tyrocidines, cyclic decapeptides found in the fermentation broth of *Bacillus brevis* [4, 5]. The tyrocidines are found in a complex mixture of peptides, known as tyrothricin, which is composed of the cyclic, basic tyrocidines and the linear, neutral gramicidins [4, 5]. The tyrocidines and related peptides have very high sequence identity, with limited conservative amino acid substitutions (Table 1), and therefore have very similar physicochemical characteristics, which complicate the purification of the individual peptides.

Table 1 *Peptides from the tyrothricin complex of interest in this investigation*
The peptide sequences are given using conventional one letter abbreviations for amino acids, except that ornithine (Orn) is designated by O. Lower case abbreviations denote D-amino acid residues. The monoisotopic Mr were calculated as the sum of the molecular weights of the constituent amino acids.

Identity	Abbreviation	Sequence	Monoisotopic Mr
Major natural tyrocidines			
Tyrocidine A	TrcA	*Cyclo*-(VOLfPFfNQY)	1269.70
Tyrocidine A_1	$TrcA_1$	*Cyclo*-(VKLfPFfNQY)	1283.70
Tyrocidine B	TrcB	*Cyclo*-(VOLfPWfNQY)	1308.70
Tyrocidine B_1	$TrcB_1$	*Cyclo*-(VKLfPWfNQY)	1322.70
Tyrocidine C	TrcC	*Cyclo*-(VOLfPWwNQY)	1347.70
Tyrocidine C_1	$TrcC_1$	*Cyclo*-(VKLfPWwNQY)	1361.70
Minor natural tyrocidines			
Tyrocidine B`	TrcB’	*Cyclo*-(VOLfPFwNQY)	1308.70
Tyrocidine B_1`	$TrcB_1$’	*Cyclo*-(VKLfPFwNQY)	1322.70
Tryptocidine B	TpcB	*Cyclo*-(VOLfPWfNQW)	1331.70
Tryptocidine C	TpcC	*Cyclo*-(VOLfPWwNQW)	1370.70
Gramicidin S	GS	*Cyclo*-(VOLfPVOLfP)	1140.70

The tyrocidines were categorised into two groups based on their prevalence in the tyrocidine complex. Tyrocidines A, A_1, B, B_1, C and C_1 are the most prevalent [5] and referred to as the major tyrocidines, whereas the less prevalent tyrocidines B` and $B_1$` (named in this study) and tryptocidines B and C [5] are designated as the minor tyrocidines.

2.2 Materials

The tyrothricin and gramicidin S was supplied by Sigma (St. Louis, USA). The diethyl ether and acetone were supplied by Saarchem (Krugersdorp, RSA). Acetonitrile (ACN1) (HPLC-grade, far UV cut-off) and trifluoroacetic acid (TFA, >98%) was supplied by Romill Ltd. (Cambridge, UK) and Sigma-Aldrich (St. Louis, USA), respectively. Waters-Millipore (Milford, USA) supplied the Nova-Pak® C_{18} (5µm particle size, 60Å pore size, 150mm X 3.9mm) reverse-phase analytical column and the Nova-Pak® C18 (6µm particle size, 60Å pore size, 7.8mm X 300mm) semi-preparative HPLC column. Analytical grade water was prepared by filtering water from a reverse osmosis plant through a Millipore Milli-Q® water purification system (Milford, USA).

2.3 Methods

2.3.1 Purification of the tyrocidines

The tyrocidines were isolated from the tyrothricin complex from *Bacillus aneurinolyticus*, commercially obtained from Sigma (St Louis, USA), by organic extraction, as described by Hotchkiss and Dubos (1941) [4] with some modifications. Briefly, the tyrothricin in dry powder form (300 mg) was washed three times with equal volumes ether/acetone (1:1, v/v) and the insoluble fraction/precipitate containing the tyrocidines was collected by centrifugation and dried under vacuum. The crude tyrocidine complex (obtained from the fractionation) was dissolved in acetonitrile/water (1:1, *v/v*) (20 mg/mL) and purified by semi-preparative reverse-phase high performance liquid chromatography (RP-HPLC), using a Nova-Pak® C_{18} (6µm particle size, 60Å pore size, 7.8mm X 300mm) semi-preparative HPLC column. The chromatographic system, composed of two Waters 510 pumps, Waters model 440 detector and a WISP 712 auto-sampler, was controlled by a MAXIMA software control system and the separation monitored at 254nm. A solvent gradient of decreasing polarity, using eluant A (0.1% TFA in water) and eluant B (10% A in 90% acetonitrile), at a flow rate of 3 mL/min was created and run at 35°C (Table 2) [6, 7]. For the semi-preparative RP-HPLC, 100 µL of the crude tyrocidine mixture (20 mg/mL in acetonitrile/water, 1:1, *v/v*) was injected per run. Those fractions of which insufficient separation was observed on the semi-preparative column were further purified on a reverse-

phase analytical C_{18} Nova-Pak® column (5µm particle size, 60Å pore size, 150mm X 3.9mm), using the same solvents and gradient program (Table 2) as for the semi-preparative purifications, but with a flow rate of 1 mL/min. For purification using the analytical C_{18} column, 50 µL of the peptide solution (2 mg/mL in acetonitrile/water, 1:1, *v/v*) was injected per run.

Table 2 *HPLC gradient program used for the purification and analyses*
Eluant A was 0.1% TFA in water; eluant B was 10% A in acetonitrile. The gradient profile was defined by the Waters gradient control curve type.

Time (min)	% eluant A	% eluant B	Curve type
0.0	50	50	
0.5/1.0[1]	50	50	6 (linear)
23.0	20	80	5 (curve)
24.0	0	100	6 (linear)
26.0	0	100	6 (linear)
28.0	-	-	-
30.0	50	50	6 (linear)
35.0	50	50	6 (linear)

[1] 0.5 min for semi-preparative RP-HPLC, 1.0 min for analytical RP-HPLC

2.3.2 Analysis of the purified tyrocidines

The collected fractions were subjected to analytical RP-HPLC, time-of-flight electrospray mass spectrometry (TOF-ESMS), and tandem mass spectroscopy (MS-MS) in order to determine the degree of purity of each fraction and to identify the purified product. The same column and conditions as for purification on the analytical RP-HPLC column were employed for the analytical RP-HPLC analyses (Table 2). Peptide concentrations used for the analytical RP-HPLC analysis were optimised to limit peptide aggregation, and 20 µL injection volumes were used. TOF-ESMS and MS-MS analyses were performed using a Waters Q-TOF Ultima mass spectrometer fitted with an electrospray ionisation source. For TOF-ESMS, 10 µL of each peptide sample (10 µg/mL in acetonitrile/water, 1:1, v/v) was injected into the ESMS and subjected to a capillary voltage of 3.5 kV. The source temperature and cone voltage was set at 100 ºC and 35 V, respectively. The data was collected in positive mode by scanning the first mass analyser (MS_1) through m/z = 100–1999. MS–MS analyses were performed by injecting 30 µL of peptide sample (10 µg/mL in acetonitrile/ water, 1:1, *v/v*) into the mass spectrometer and subjecting the selected

molecular species to decomposition at a collision energy of 40 eV. Data was collected in MS_2 through *m/z* = 100-1999.

2.4 Results and Discussion

Organic extraction of the tyrothricin complex yielded 200 mg (67% yield) of the crude tyrocidine complex, which corresponds to the expected yield as tyrothricin is composed of gramicidins and tyrocidines in a ratio of approximately 40:60 [4].

Table 3 *Summary of the purification data*
The HPLC retention times of the tyrocidines were obtained from the analytical HPLC chromatograms of the purified tyrocidines. The observed monoisotopic Mr were calculated from TOF-ESMS spectra. The expected monoisotopic Mr were calculated as the sum of the molecular weights of the constituent amino acids. The percentage purity was calculated from analytical HPLC analyses at 254 nm of the purified tyrocidines. The percentage yield was calculated as the percentage of the mass of the crude tyrocidine complex (200 mg) obtained from organic extraction.

Identity	HPLC R_T (min)	Monoisotopic Mr Observed (Expected)	% Purity	% Yield (Yield, mg)
Major natural tyrocidines				
TrcA	11.81	1269.70 (1269.70)	> 95%	5.8 (11.6)
$TrcA_1$	11.33	1283.71 (1283.70)	> 95%	2.3 (4.5)
TrcB	9.48	1308.71 (1308.70)	> 95%	9.4 (18.8)
$TrcB_1$	9.24	1322.71 (1322.70)	> 95%	4.6 (9.1)
TrcC	8.31	1347.71 (1347.70)	> 95%	13.6 (27.1)
$TrcC_1$	7.90	1361.75 (1361.70)	> 95%	6.1 (12.2)
Minor natural tyrocidines				
TrcB'	8.98	1308.70 (1308.70)	94%	0.2 (0.4)
$TrcB_1$'	9.72	1322.70 (1322.70)	> 95%	0.4 (0.7)
TpcB	11.33	1331.65 (1331.70)	59%[1]	2.1 (4.2)
TpcC	9.63	1370.67 (1370.70)	73%[1]	0.8 (1.6)
GS	12.05	1140.72 (1140.70)	>95%	-

[1] Purity estimated from ESMS signals

During the first round of semi-preparative C_{18}-RP-HPLC, the crude tyrocidine complex (Figure 2) was divided into six fractions. Analytical C_{18}-RP-HPLC and TOF-ESMS analyses of fraction I indicated the presence of purified (>95%) tyrocidine C_1, with a RP-HPLC retention time (R_T) of 7.90 minutes (Figure 3A). TOF-ESMS spectra indicated the singly (*m/z* = 1362.75) and doubly (*m/z* = 681.89) charged molecular ion, as well as the singly (*m/z* = 1384.74) and doubly (*m/z* = 692.88) charged sodium adduct of $TrcC_1$ (Figure 3B). Fraction II contained purified (>95%) tyrocidine C, with a R_T 8.31 minutes (Figure 4A). The TOF-ESMS spectra of tyrocidine C indicated the singly (*m/z* = 1348.71) and doubly (*m/z* = 674.87) charged molecular ions, as well as the singly charged sodium adduct (*m/z* = 1370.74) (Figure 4B).

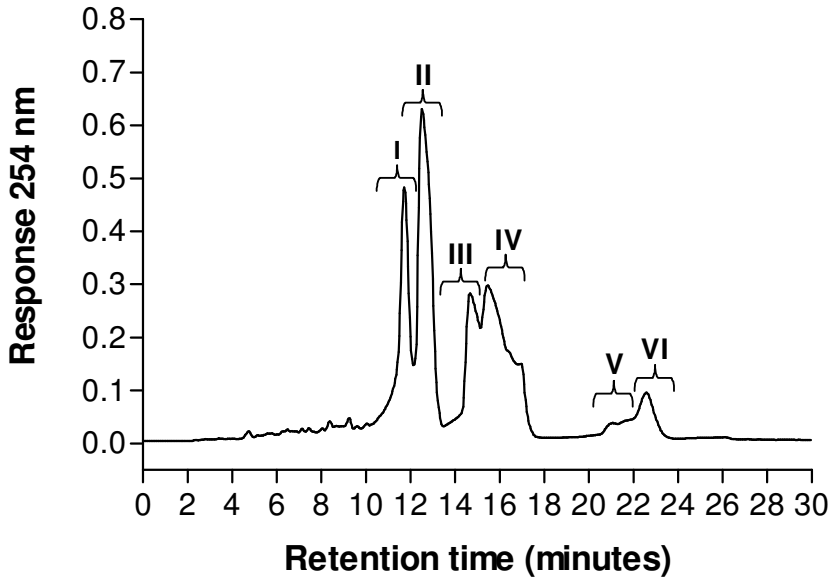

Figure 2 *Semi-preparative RP-HPLC chromatogram of the tyrocidine mixture*
Semi-preparative C_{18}-RP-HPLC chromatogram indicating the six fractions (fractions I to VI) isolated during the first round of semi-preparative RP-HPLC purification.

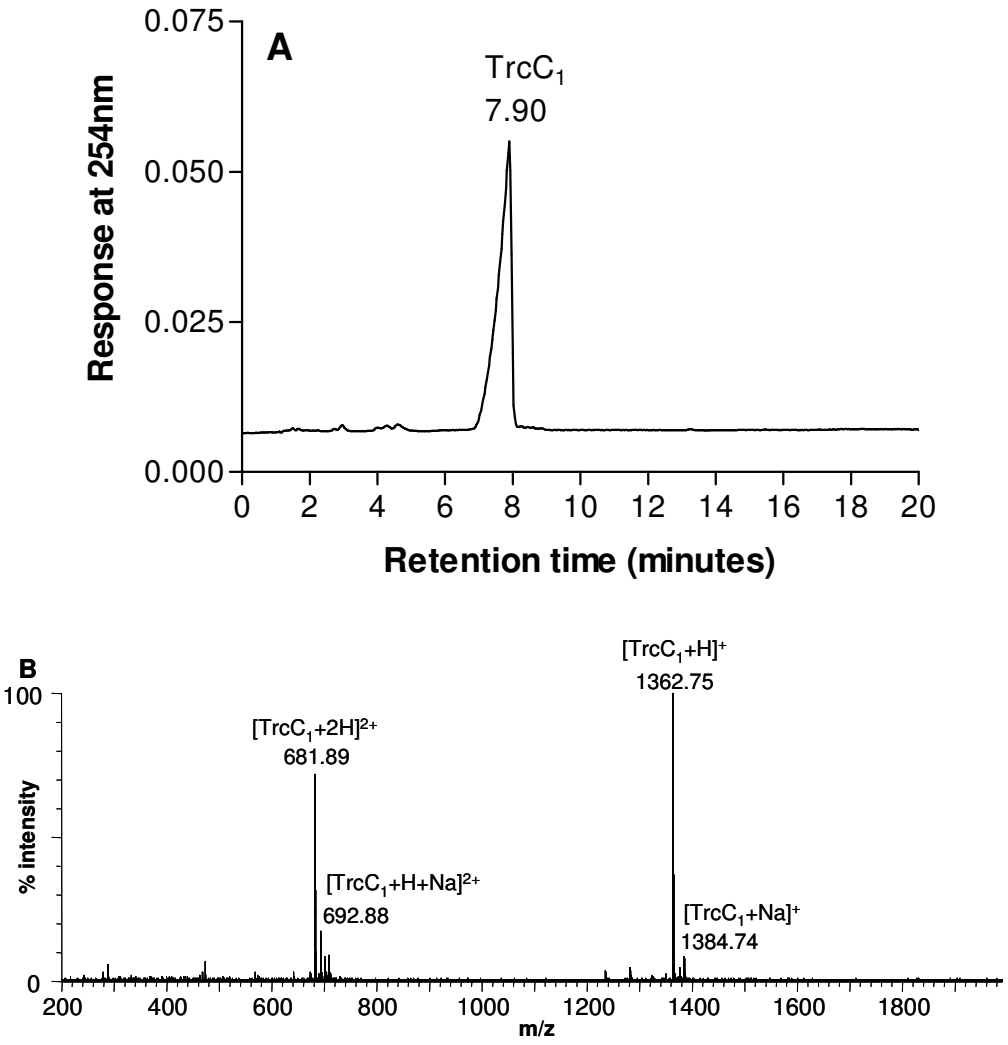

Figure 3 *Analytical RP-HPLC and TOF-ESMS analysis of purified tyrocidine C_1*
A: Analytic C_{18}-RP-HPLC chromatogram of purified tyrocidine C_1 at 500 µg/mL (20 µL injection volume), indicating peptide identity and elution time (in minutes). *B:* TOF-ESMS spectrum of purified tyrocidine C_1, indicating the monoisotopic peaks and *m/z* ratios of the singly charged molecular ion ($[M+H]^+$), singly charged sodium adduct ($[M+Na]^+$), the doubly charged molecular ion ($[M+2H]^{2+}$) and the doubly charged sodium adduct ($[M+H+Na]^{2+}$).

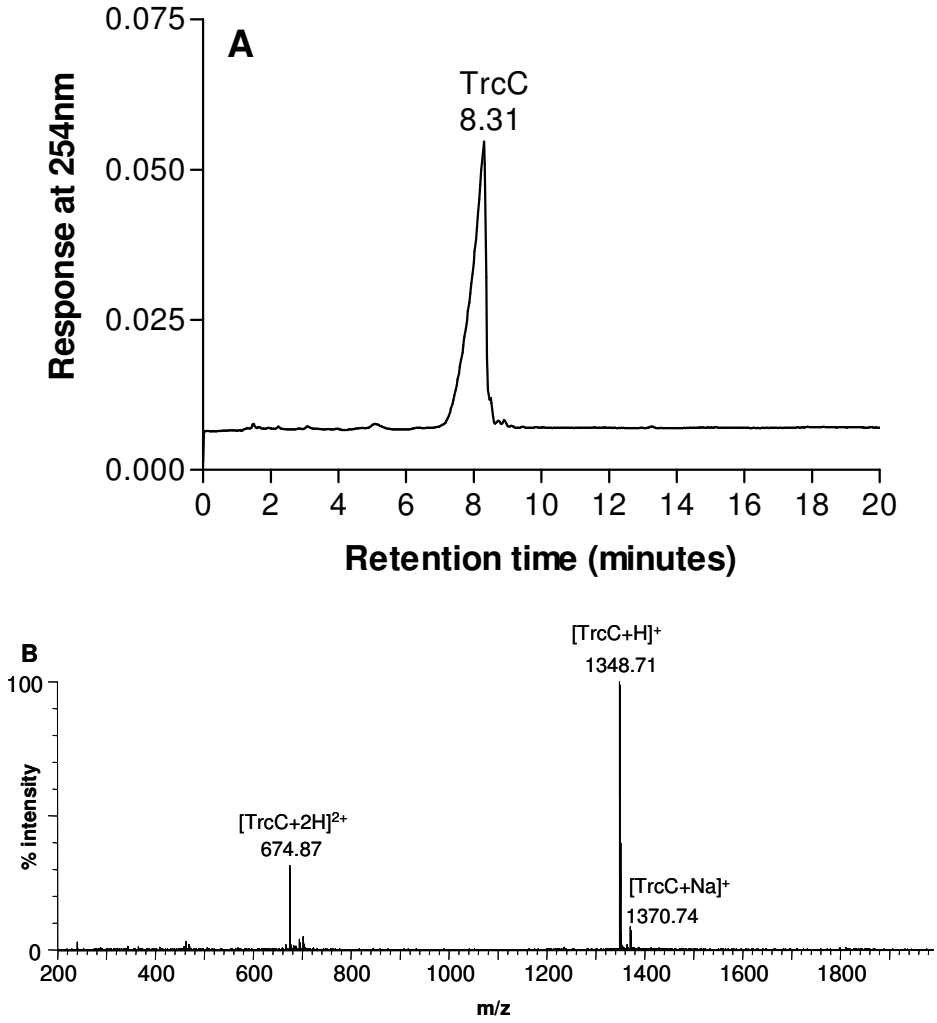

Figure 4 *Analytical RP-HPLC and TOF-ESMS analysis of purified tyrocidine C*
A: Analytic C_{18}-RP-HPLC chromatogram of purified tyrocidine C at 500 µg/mL (20 µL injection volume), indicating peptide identity and elution time (in minutes). *B:* TOF-ESMS spectrum of purified tyrocidine C, indicating the monoisotopic peaks and *m/z* ratios of the singly charged molecular ion ($[M+H]^+$), singly charged sodium adduct ($[M+Na]^+$), and the doubly charged molecular ion ($[M+2H]^{2+}$).

Fraction III was found to contain a mixture of $TrcB_1$, $TrcB_1$`, TrcB and TrcB`; fraction IV contained $TrcB_1$`, TrcB, TrcB` and TpcC; fraction V contained $TrcA_1$ and TrcA; and fraction VI contained TrcA, $TrcA_1$ and TpcB. These fractions were thus subjected to a second round of semi-preparative C_{18}-RP-HPLC. Tyrocidine B_1, with a R_T of 9.24 minutes, was successfully purified (>95%) from fraction III (Figure 5A). The TOF-ESMS spectra of tyrocidine B_1 indicated the singly (*m/z* = 1323.71) and doubly (*m/z* = 662.37) charged molecular ion, as well as the singly charged sodium adduct (*m/z* = 1345.71) (Figure 5B).

Tyrocidine B (R_T = 9.48 minutes) was successfully purified (>95%) from fraction IV (Figure 6A) and the TOF-ESMS spectra of tyrocidine B indicated the singly (*m/z* = 1309.71) and doubly (*m/z* = 655.37) charged molecular ion, as well as the singly charged sodium adduct (*m/z* = 1331.72) (Figure 6B).

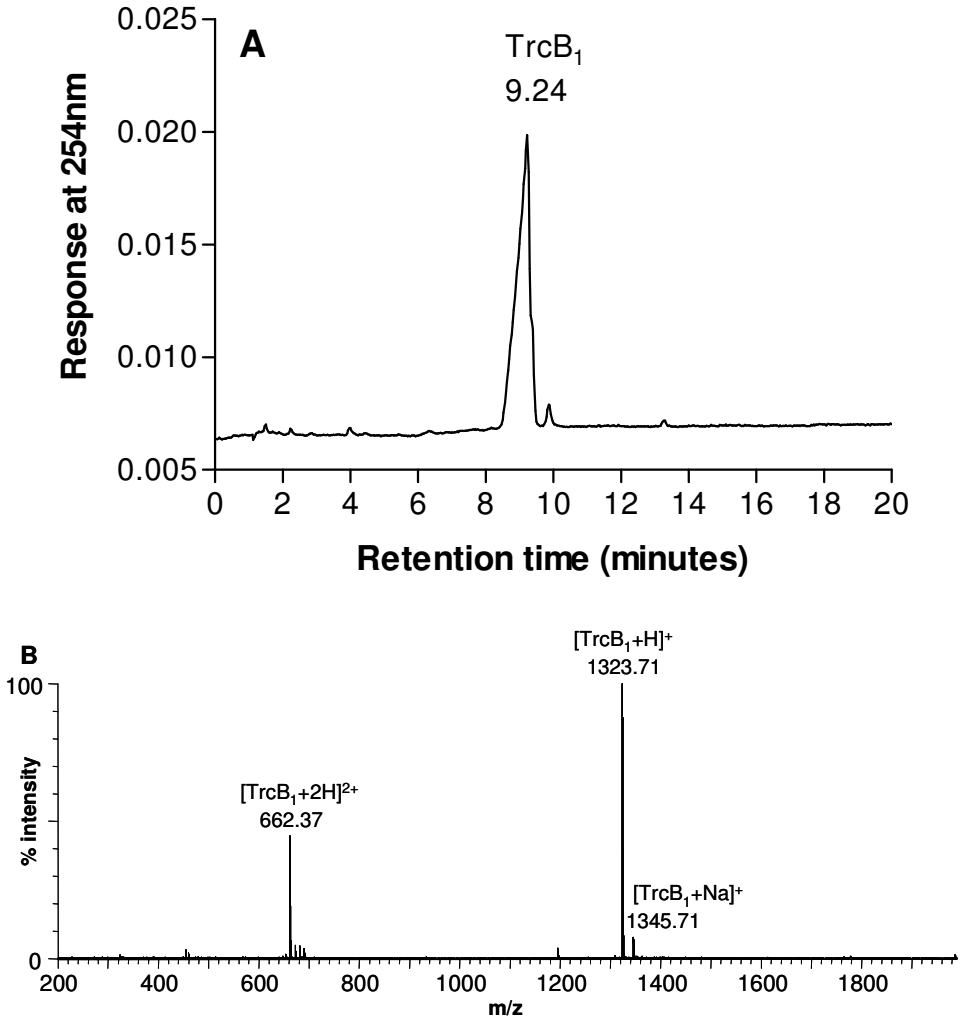

Figure 5 *Analytical RP-HPLC and TOF-ESMS analysis of purified tyrocidine B_1*
A: Analytic C_{18}-RP-HPLC chromatogram of purified tyrocidine B_1 at 200 µg/mL (20 µL injection volume), indicating peptide identity and elution time (in minutes). *B:* TOF-ESMS spectrum of purified tyrocidine B_1, indicating the monoisotopic peaks and *m/z* ratios of the singly charged molecular ion ($[M+H]^+$), singly charged sodium adduct ($[M+Na]^+$), and the doubly charged molecular ion ($[M+2H]^{2+}$).

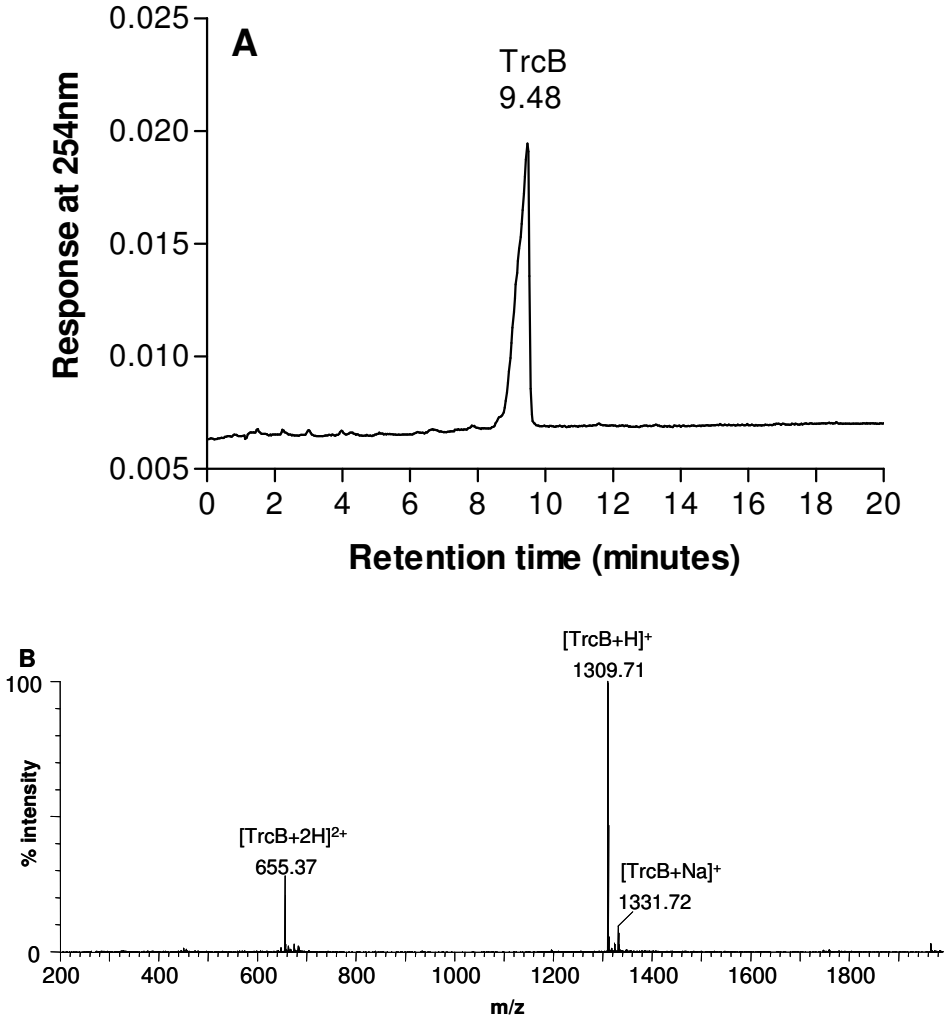

Figure 6 *Analytical RP-HPLC and TOF-ESMS analysis of purified tyrocidine B*
A: Analytic C_{18}-RP-HPLC chromatogram of purified tyrocidine B at 200 µg/mL (20 µL injection volume), indicating peptide identity and elution time (in minutes). *B:* TOF-ESMS spectrum of purified tyrocidine B, indicating the monoisotopic peaks and *m/z* ratios of the singly charged molecular ion ($[M+H]^+$), singly charged sodium adduct ($[M+Na]^+$), and the doubly charged molecular ion ($[M+2H]^{2+}$).

Tyrocidine B`, $TrcB_1$`, TrcA, $TrcA_1$, TpcB and TpcC, could not be successfully purified by semi-preparative C_{18}-RP-HPLC. The semi-preparative fractions containing these peptides were therefore further purified using an analytical C_{18}-reverse phase column. Tyrocidine B` (R_T = 8.98 minutes), was successfully purified (94%), and the TOF-ESMS spectrum

indicated the singly (*m/z* = 1309.70) and doubly (*m/z* = 655.36) charged molecular ion, as well as the singly charged sodium adduct (*m/z* = 1331.71) (Figure 7). Tyrocidine B_1` (R_T = 9.72 minutes) was successfully purified (>95%), and the TOF-ESMS spectrum indicated the singly (*m/z* = 1323.70) and doubly (*m/z* = 662.37) charged molecular ion, as well as the singly (*m/z* = 1345.71) and doubly (*m/z* = 673.37) charged sodium adduct (Figure 8).

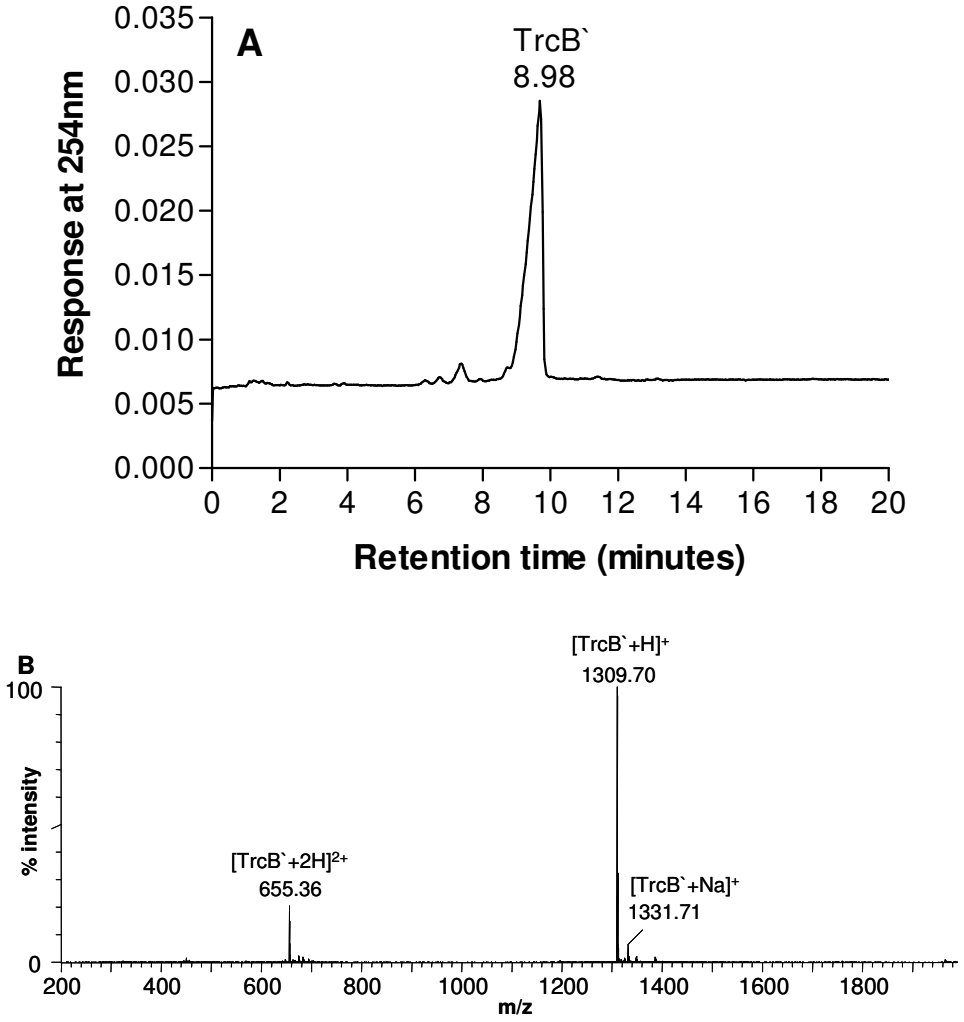

Figure 7 *Analytical RP-HPLC and TOF-ESMS analysis of purified tyrocidine B`*
A: Analytic C_{18}-RP-HPLC chromatogram of purified tyrocidine B` at 200 µg/mL (20 µL injection volume), indicating peptide identity and elution time (in minutes). *B:* TOF-ESMS spectrum of purified tyrocidine B`, indicating the monoisotopic peaks and *m/z* ratios of the singly charged molecular ion ($[M+H]^+$), singly charged sodium adduct ($[M+Na]^+$), and the doubly charged molecular ion ($[M+2H]^{2+}$).

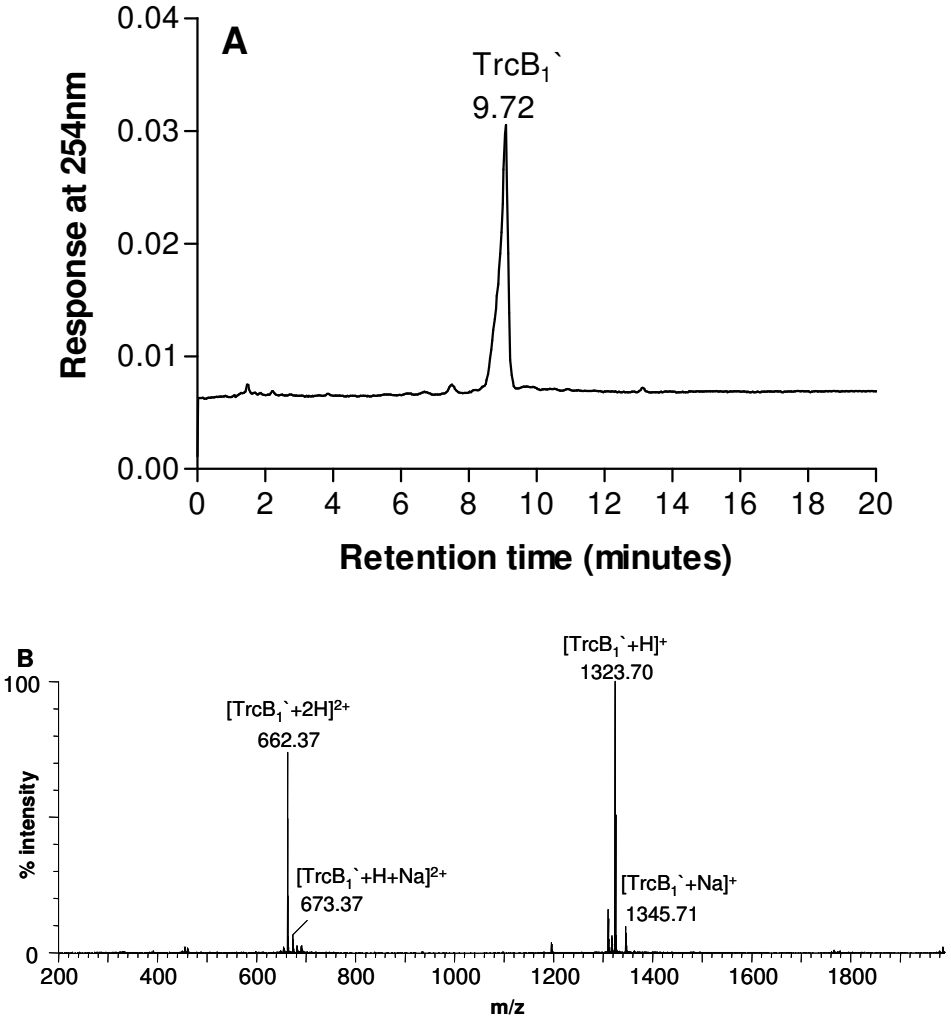

Figure 8 *Analytical RP-HPLC and TOF-ESMS analysis of purified tyrocidine B_1`*
A: Analytic C_{18}-RP-HPLC chromatogram of purified tyrocidine B_1` at 200 µg/mL (20 µL injection volume), indicating peptide identity and elution time (in minutes). *B:* TOF-ESMS spectrum of purified tyrocidine $B_1$`, indicating the monoisotopic peaks and *m/z* ratios of the singly charged molecular ion ($[M+H]^+$), singly charged sodium adduct ($[M+Na]^+$), the doubly charged molecular ion ($[M+2H]^{2+}$) and the doubly charged sodium adduct ($[M+H+Na]^{2+}$).

Difficulty was encountered in the purification of tyrocidines A and A_1, with each round of purification still showing multiple peaks in analytical RP-HPLC analysis even though TOF-ESMS analysis indicated purity (Figures 9 and 10). The observed multiple peaks may be ascribed to aggregate formation due to the more hydrophobic nature of these peptides. Such

aggregation may be reduced if purification and subsequent analyses are performed at sufficiently low concentrations (100 µg/mL). Tyrocidine A_1, with a retention time of 11.33 minutes, was successfully purified (>95%), and the TOF-ESMS spectrum indicated the singly (*m/z* = 1284.71) and doubly (*m/z* = 642.87) charged molecular ion, as well as the singly (*m/z* = 1306.72) and doubly (*m/z* = 653.87) charged sodium adduct (Figure 9). Tyrocidine A (R_T = 11.81 minutes) was successfully purified (>95%), and the TOF-ESMS spectrum indicated the singly (*m/z* = 1270.70) and doubly (*m/z* = 635.87) charged molecular ion, as well as the singly charged sodium adduct (*m/z* = 292.71) (Figure 10).

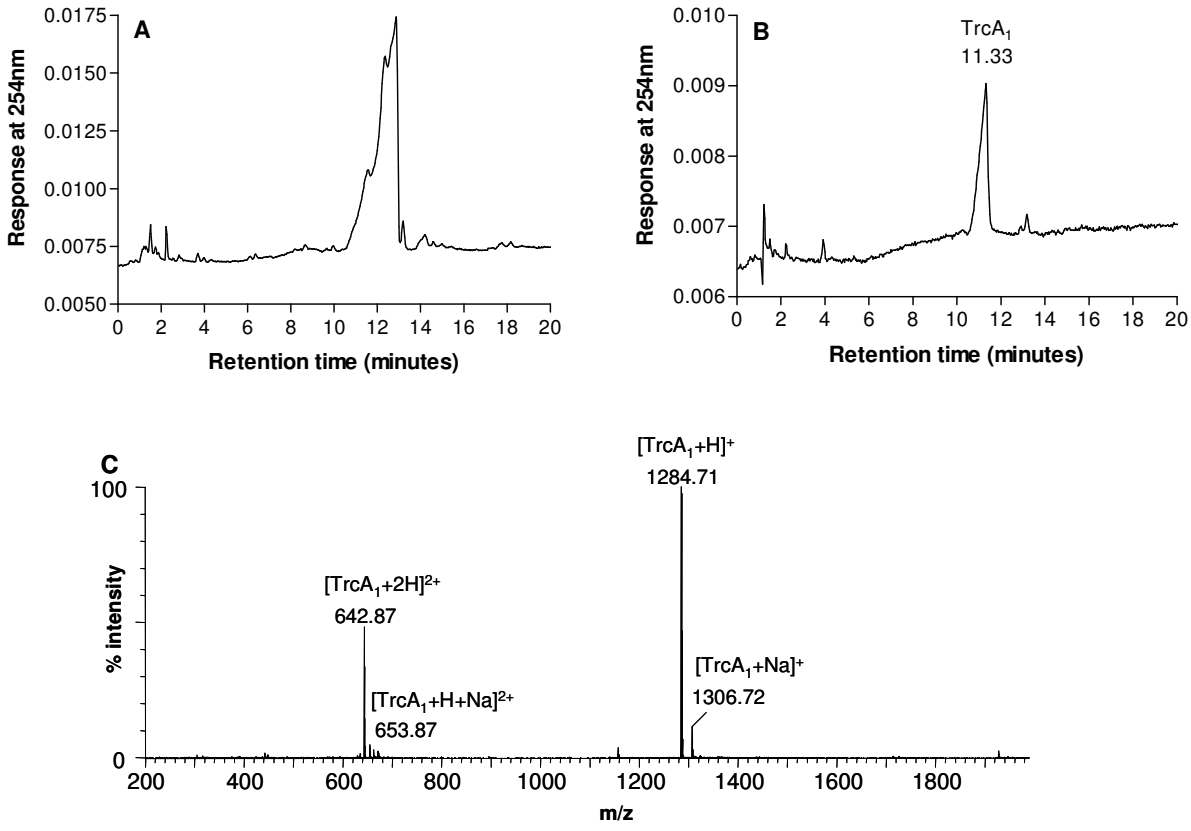

Figure 9 *Analytical RP-HPLC and TOF-ESMS analysis of purified tyrocidine A_1*
A: Analytic C_{18}-RP-HPLC chromatogram of purified tyrocidine A_1 at 1 mg/mL. *B:* Analytic C_{18}-RP-HPLC chromatogram of purified tyrocidine A_1 at 100 µg/mL, indicating peptide identity and elution time (in minutes). 20 µL injections were used. *C:* TOF-ESMS spectrum of purified tyrocidine A_1, indicating the monoisotopic peaks and *m/z* ratios of the singly charged molecular ion ($[M+H]^+$), singly charged sodium adduct ($[M+Na]^+$), the doubly charged molecular ion ($[M+2H]^{2+}$) and the doubly charged sodium adduct ($[M+H+Na]^{2+}$).

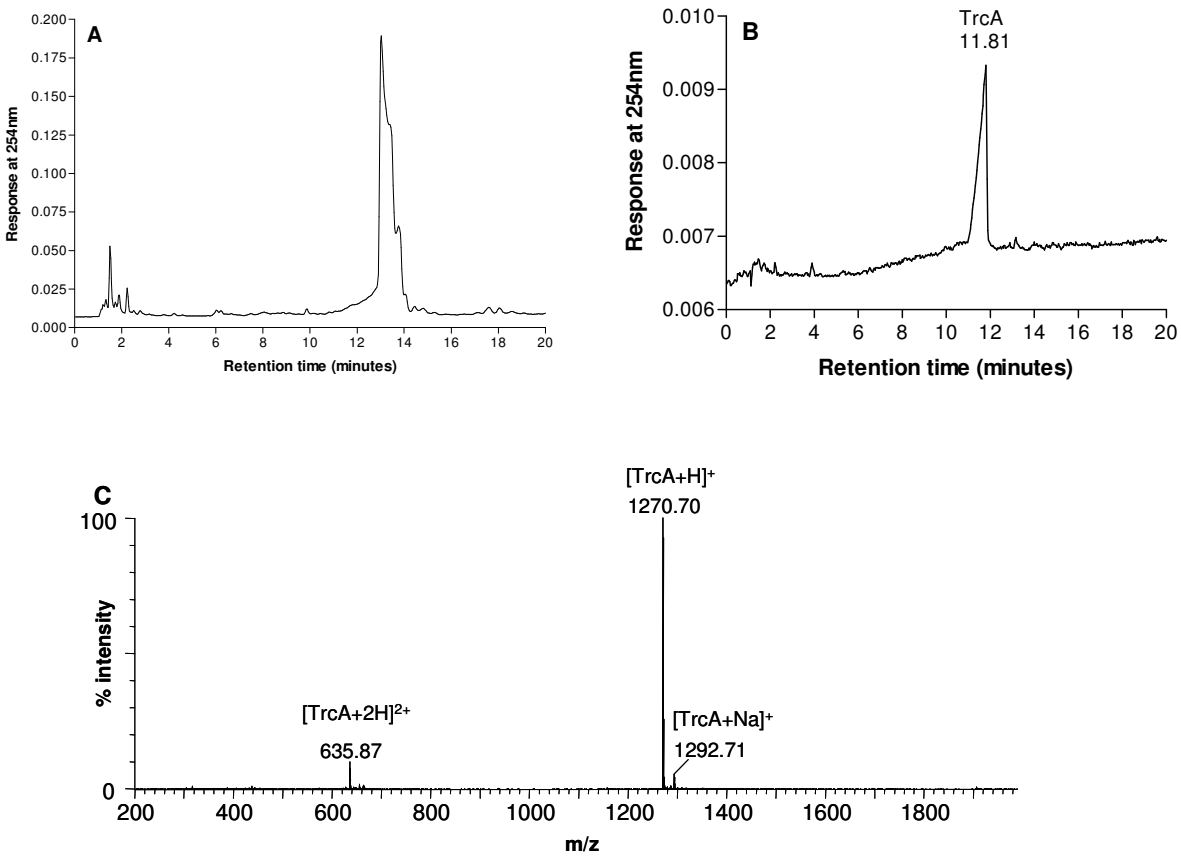

Figure 10 *Analytical RP-HPLC and TOF-ESMS analysis of purified tyrocidine A*
A: Analytic C_{18}-RP-HPLC chromatogram of purified tyrocidine A at 1 mg/mL. *B:* Analytic C_{18}-RP-HPLC chromatogram of purified tyrocidine A at 100 µg/mL, indicating peptide identity and elution time (in minutes). 20 µL injections were used. *C:* TOF-ESMS spectrum of purified tyrocidine A, indicating the monoisotopic peaks and *m/z* ratios of the singly charged molecular ion ($[M+H]^+$), singly charged sodium adduct ($[M+Na]^+$), and the doubly charged molecular ion ($[M+2H]^{2+}$).

The purification of the minor tryptocidines (TpcB and TpcC) could not be accomplished for, regardless of the number of purifications done, TpcB co-eluted with tyrocidine A (Figure 11), and TpcC co-eluted with a tyrocidine with Mr of 1336.69 (LKLfPWfNQY [5]) (Figure 12). Such co-elution may be due to association/formation of complexes between these tyrocidines.

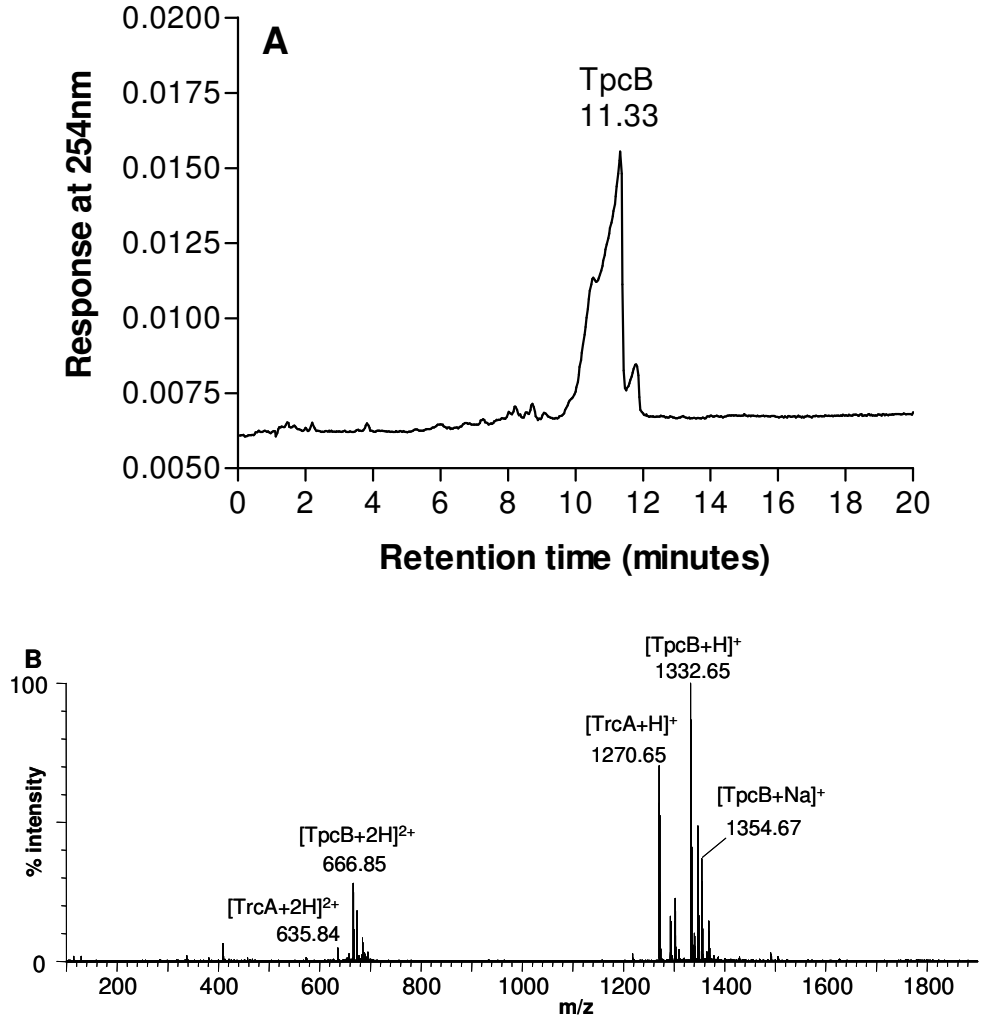

Figure 11 *Analytical RP-HPLC and TOF-ESMS analysis of purified tryptocidine B* *A:* Analytic C_{18}-RP-HPLC chromatogram of tryptocidine B at 200 µg/mL (20 µL injection volume), indicating peptide identity, elution time (in minutes), and contaminating peaks. *B:* TOF-ESMS spectrum of tryptocidine B, indicating the monoisotopic peaks and *m/z* ratios of the singly charged molecular ions ($[M+H]^+$), singly charged sodium adducts ($[M+Na]^+$), and the doubly charged molecular ions ($[M+2H]^{2+}$).

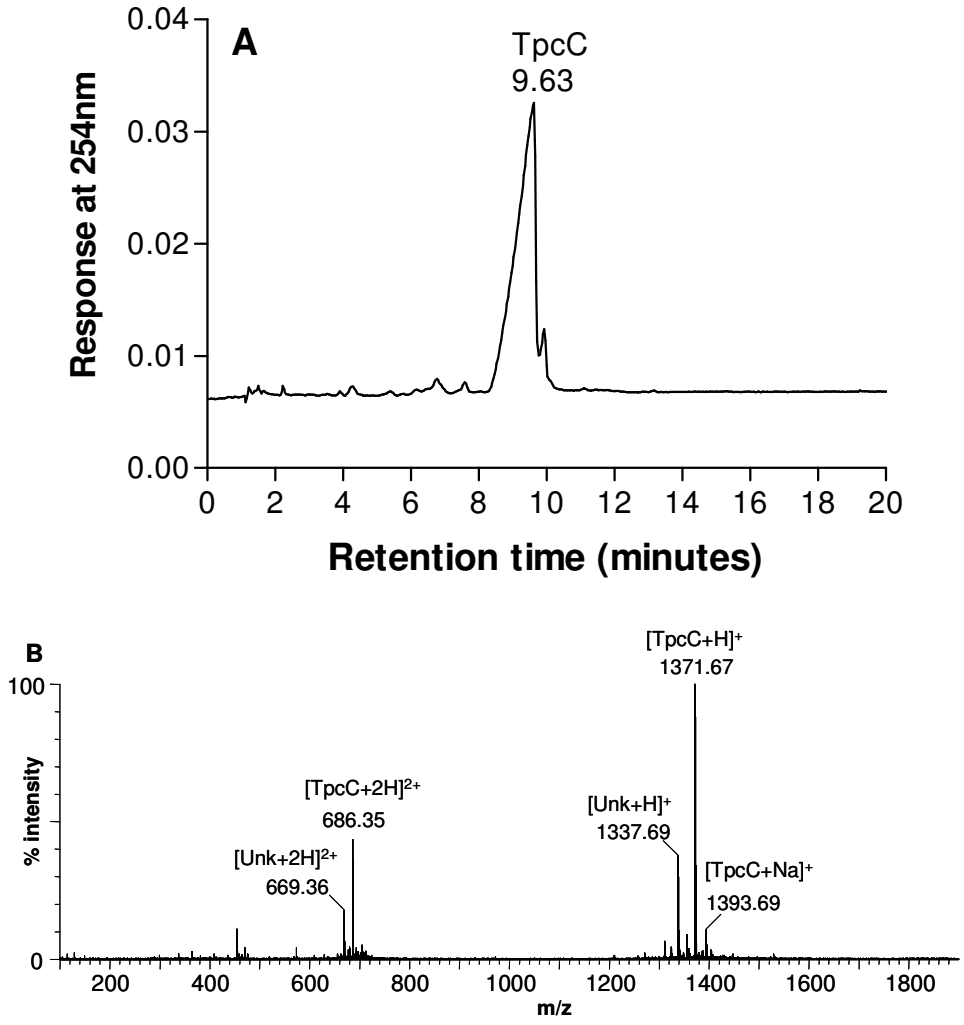

Figure 12 *Analytical RP-HPLC and TOF-ESMS analysis of purified tryptocidine C* *A:* Analytic C_{18}-RP-HPLC chromatogram of tryptocidine C at 200 µg/mL (20 µL injection volume), indicating peptide identity, elution time (in minutes), and contaminating peaks. *B:* TOF-ESMS spectrum of tryptocidine C, indicating the monoisotopic peaks and *m/z* ratios of the singly charged molecular ions ($[M+H]^+$), singly charged sodium adducts ($[M+Na]^+$), and the doubly charged molecular ions ($[M+2H]^{2+}$).

In addition to analytical RP-HPLC and TOF-ESMS, MS-MS analyses were performed on the purified tyrocidines to confirm their chemical integrity and amino acid sequence. MS-MS analysis of cyclic peptides requires initial ring-opening to yield a linear product. All the natural tyrocidines in this investigation preferentially opened between the D-Phe[1]

and Pro^2 residues, with Pro^2 forming the N-terminus (Table 4, Figure 13). Such ring-cleavage is consistent with observations that peptide bonds flanking a proline residue are particularly susceptible to cleavage [8, 9]. In some cases, ring-openings between Val^8 and Orn^9/Lys^9 (Table 4; Figure 13) were also observed. For all the natural tyrocidines, fragments formed from the D-Phe^1-Pro^2 ring-opened structure included the complete b_2 to b_9 series (Table 4), with some of these fragments having lost ammonia ($-NH_3$). This loss is consistent with previous observations of fragments that contain a lysine, asparagine and/or glutamine residue(s) [10]. Some a-ions were also observed, which is consistent with the observation that b-ions are susceptible to further degradation [5, 10]. The a_2 ion of the D-Phe^1-Pro^2 ring-opened structure was also observed for all the peptides. (*See supplementary tables SI-1 – SI-10 for fragment assignments and sequences.*) These results (summarised in Table 4) are consistent with previous research by Tang *et al.* (1992), which indicated initial ring-openings between D-Phe^1-Pro^2 and Val^8-Orn^9/Lys^9, and predominant formation of b-ion, and some a-ion, fragments [5].

The two minor tyrocidines, TrcB` and $B_1$`, have identical molecular weights to the major TrcB (Mr = 1308.70) and B_1 (Mr = 1322.70), respectively. These peptides can thus not be distinguished based on TOF-ESMS analysis. However, the b_2 and a_2 ions of these peptides have different sequences and MS-MS analysis allowed us to distinguish between TrcB and TrcB` as well as between $TrcB_1$ and $TrcB_1$`. The MS-MS spectra of TrcB and $TrcB_1$ indicated fragments with *m/z* = 284 and 256, which correspond to the b_2 and a_2 ions with sequence Pro^2-Trp^3. The MS-MS spectra of TrcB` and $TrcB_1$` indicated fragments with *m/z* = 245 and 217, which correspond to the b_2 and a_2 ions with sequence Pro^2-Phe^3.

In addition to the b- and a-ion fragments, internal fragments were identified. Tyrocidines A, A_1, B and B_1 formed three internal fragments, which could have originated from either of the initial ring-openings (Table 4), assigned as $N^5Q^6Y^7$, N^5Q^6 and $F^4N^5Q^6$. Tyrocidines B`, $B_1$`, C and C_1 formed two of these internal fragments, assigned as $N^5Q^6Y^7$, and N^5Q^6, but did not form the related $W^4N^5Q^6$ fragment. This suggests that the peptide bond between Phe^3/Trp^3 and D-Phe^4 (TrcA, A_1, B and B_1) is more labile or more exposed than the peptide bond between Phe^3/Trp^3 and D-Trp^4 (Trc C, C_1, B` and $B_1$`). Tryptocidine B formed three

internal fragments, which could have originated from any of the three initial ring-openings (Table 4), assigned as $N^5Q^6W^7$, N^5Q^6 and $F^4N^5Q^6$. Tryptocidine C formed two of these internal fragments, assigned as $N^5Q^6W^7$ and N^5Q^6, but did not form the related $W^4N^5Q^6$ fragment, which further supports the hypothesis that the Trp^3-D-Phe^4 bond (TpcB) is more labile or more exposed than the Trp^3-D-Trp^4 bond (TpcC).

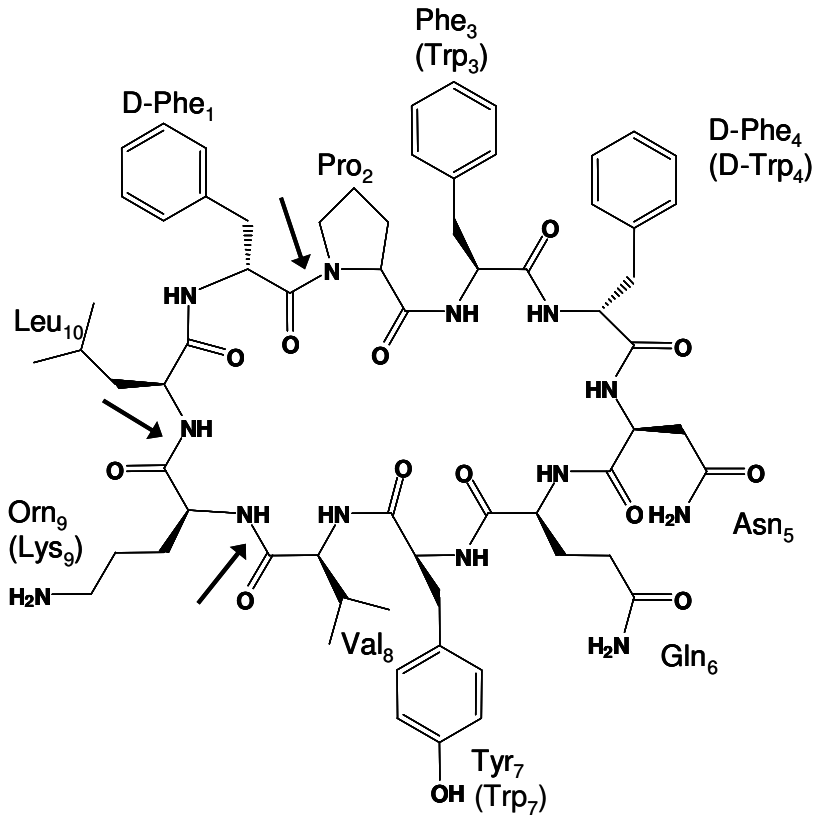

Figure 13 *The primary structure of the tyrocidine A*
The amino acid abbreviations in brackets indicated the variable amino acid identities in the other tyrocidines (refer to Table 1). The numbering of the peptide chain is based on the biological synthesis sequence. The arrows indicate peptide bonds (D-Phe^1-Pro^2; Val^8-Orn^9; and Orn^9-Leu^{10}) preferentially broken during initial ring-opening in MS-MS analysis.

Table 4 *Summary of the MSMS data of the natural tyrocidines*

The predominant fragment ions formed from the linear product of Phe[1]-Pro[2] and Val[8]-Orn[9]/Lys[9] ring-openings, as well as the internal fragment ions, are given. *See supplementary tables SI-1 – SI-10 for fragment assignments and sequences.*

	Phe_1-Pro_2	**Val_8-Orn_9/Lys_9**	**Internal fragments**
TrcA	$b_2 - b_9$; a_2	b_1	$N^5Q^6Y^7$; N^5Q^6; $F^4N^5Q^6$
$TrcA_1$	$b_2 - b_9$; a_2; a_3; y_1	b_6	$N^5Q^6Y^7$; N^5Q^6; $F^4N^5Q^6$
TrcB	$b_2 - b_9$; a_2	-	$N^5Q^6Y^7$; N^5Q^6; $F^4N^5Q^6$; W^3
$TrcB_1$	$b_2 - b_9$; a_2	-	$N^5Q^6Y^7$; N^5Q^6; $F^4N^5Q^6$
TrcC	$b_2 - b_9$; a_2	b_6	$N^5Q^6Y^7$; N^5Q^6
$TrcC_1$	$b_2 - b_9$; a_2	-	$N^5Q^6Y^7$; N^5Q^6
TrcB`	$b_1 - b_9$; a_2; y_2	b_1, b_6	$N^5Q^6Y^7$; N^5Q^6
$TrcB_1$`	$b_1 - b_9$; a_2	-	$N^5Q^6Y^7$; $N^5Q^6W^3$
TpcB	$b_2 - b_9$; a_2	b_6	$N^5Q^6Y^7$; N^5Q^6; $F^4N^5Q^6$
TpcC	$b_2 - b_9$; a_2	-	$N^5Q^6Y^7$; N^5Q^6

2.5 Conclusions

Our group developed and optimised a RP-HPLC purification methodology [6, 7], which allowed purification of the six major tyrocidines (TrcA, A_1, B, B_1 C and C_1) and two minor (TrcB` and $B_1$`) tyrocidines and partial purification of two analogous tryptocidines. The identity, purity and chemical integrity were confirmed by analytical RP-HPLC, TOF-ESMS and MS-MS analyses. In order to purify additional minor tyrocidine-like peptides, such as TpcB and TpcC, the purification methodology requires further refinement/development. However, this is the first reported study in which eight tyrocidines were purified to >95% purity from the natural tyrothricin complex in milligram quantities. The successful purification allowed investigation of the physicochemical character (Chapters 3 and 4) and bioactivity (Chapters 5-7) of the eight purified tyrocidines.

2.6 References

[1] P. Roepstorff, J.J. Fohlmann, Biomed. Env. Mass Spectrom. 11 (1984) 601.

[2] K. Biemann, Biomed. Env. Mass Spectrom. 16 (1988) 99-111.

[3] K. Vekey, Mass Spectrom. Rev. 14 (1995) 195-225.

[4] R.D. Hotchkiss, R.J. Dubos, The isolation of bactericidal substances from cultures of *Bacillus brevis*, J. Biol. Chem. (1941) 155-162.

[5] X.-J. Tang, P. Thibault, R.K. Boyd, Characterisation of the tyrocidine and gramicidin fractions of the tyrothricin complex from *Bacillus brevis* using liquid chromatography and mass spectrometry, Int. J. Mass Spectrom. Ion Process. 122 (1992) 153-179.

[6] M. Rautenbach, N.M. Vlok, M. Stander, H.C. Hoppe, Inhibition of malaria parasite blood stages by tyrocidines, membrane-active cyclic peptide antibiotics from *Bacillus brevis*, Biochim. Biophys. Acta - Biomembranes 1768 (2007) 1488–1497.

[7] H.A. Eyeghe-Bikong, B.M. Spathelf, M. Rautenbach, C_{18}-based HPLC purification protocols for the analysis and purification of fourteen peptides from the tyrothricin complex, 2009 (Personal communication).

[8] B.L. Schwartz, M.M. Bursey, Biol. Mass Spectrom. 21 (1992) 92-96.

[9] J.A. Loo, C.C. Edmonds, R.D. Smith, Anal. Chem. 65 (1993) 425-438.

[10] D.F. Hunt, J.R. Yates, J. Shabanowitz, S. Winston, C.R. Hauer, Protein sequencing by tandem mass spectrometry, Proc. Natl. Acad. Sci. 83 (1986) 6233-6237.

2.7 Supplementary information

Table SI-1 *Summary of fragment assignment of the product ions generated by CID of tyrocidine A $[M+H]^+$*

m/z observed	Proposed ring opening	Proposed fragment type	m/z calculated	Sequence
1270.67	Phe^1-Pro^2	$[trcA]^+$	1270.66	$P^2F^3F^4N^5Q^6Y^7V^8O^9L^{10}F^1$
1253.66	Phe^1-Pro^2	trcA $-NH_3$	1253.66	$P^2F^3F^4N^5Q^6Y^7V^8O^9L^{10}F^1$
1243.70	Phe^1-Pro^2	trcA -CO	1242.65	$P^2F^3F^4N^5Q^6Y^7V^8O^9L^{10}F^1$
1105.60	Phe^1-Pro^2	b_9 $-NH_3$	1105.56	$P^2F^3F^4N^5Q^6Y^7V^8O^9L^{10}$
1010.54	Phe^1-Pro^2	b_8	1010.51	$P^2F^3F^4N^5Q^6Y^7V^8O^9$
896.45	Phe^1-Pro^2	b_7	896.43	$P^2F^3F^4N^5Q^6Y^7V^8$
879.42	Phe^1-Pro^2	b_7 $-NH_3$	879.42	$P^2F^3F^4N^5Q^6Y^7V^8$
797.35	Phe^1-Pro^2	b_6	797.36	$P^2F^3F^4N^5Q^6Y^7$
780.35	Phe^1-Pro^2	b_6 $-NH_3$	780.36	$P^2F^3F^4N^5Q^6Y^7$
634.31	Phe^1-Pro^2	b_5	634.30	$P^2F^3F^4N^5Q^6$
617.29	Phe^1-Pro^2	b_5 $-NH_3$	617.29	$P^2F^3F^4N^5Q^6$
506.25	Phe^1-Pro^2	b_4	506.24	$P^2F^3F^4N^5$
406.18	any	Internal fragment	406.17	$N^5Q^6Y^7$
392.21	Phe^1-Pro^2	b_3	392.20	$P^2F^3F^4$
390.18	any	Internal fragment	390.18	$F^4N^5Q^6$
245.14	Phe^1-Pro^2	b_2	245.13	P^2F^3
243.15	any	Internal fragment	243.11	N^5Q^6
217.14	Phe^1-Pro^2	a_2	217.12	P^2F^3
115.09	Val^8-Orn^9	b_1	115.09	O^9

Table SI-2 *Summary of fragment assignment of the product ions generated by CID of tyrocidine A_1 $[M+H]^+$*

m/z observed	Proposed ring opening	Proposed fragment type	m/z calculated	Sequence
1284.69	Phe^1-Pro^2	$[trcA_1]^+$	1284.68	$P^2F^3F^4N^5Q^6Y^7V^8K^9L^{10}F^1$
1267.67	Phe^1-Pro^2	$trcA_1$ -NH_3	1267.67	$P^2F^3F^4N^5Q^6Y^7V^8K^9L^{10}F^1$
1137.63	Phe^1-Pro^2	b_9	1137.61	$P^2F^3F^4N^5Q^6Y^7V^8K^9L^{10}$
1120.62	Phe^1-Pro^2	b_9 -NH_3	1120.63	$P^2F^3F^4N^5Q^6Y^7V^8K^9L^{10}$
1024.54	Phe^1-Pro^2	b_8	1024.53	$P^2F^3F^4N^5Q^6Y^7V^8K^9$
896.46	Phe^1-Pro^2	b_7	896.43	$P^2F^3F^4N^5Q^6Y^7V^8$
879.42	Phe^1-Pro^2	b_7 -NH_3	879.42	$P^2F^3F^4N^5Q^6Y^7V^8$
797.36	Phe^1-Pro^2	b_6	797.36	$P^2F^3F^4N^5Q^6Y^7$
780.36	Phe^1-Pro^2	b_6 -NH_3	780.36	$P^2F^3F^4N^5Q^6Y^7$
764.33	Val^8-Lys^9	b_6 -NH_3	763.44	$K^9L^{10}F^1P^2F^3F^4$
634.31	Phe^1-Pro^2	b_5	634.30	$P^2F^3F^4N^5Q^6$
617.29	Phe^1-Pro^2	b_5 -NH_3	617.29	$P^2F^3F^4N^5Q^6$
506.25	Phe^1-Pro^2	b_4	506.24	$P^2F^3F^4N^5$
489.23	Phe^1-Pro^2	b_4 -NH_3	489.23	$P^2F^3F^4N^5$
406.18	any	Internal fragment	406.17	$N^5Q^6Y^7$
392.21	Phe^1-Pro^2	b_3	392.20	$P^2F^3F^4$
390.19	any	Internal fragment	390.18	$F^4N^5Q^6$
364.20	Phe^1-Pro^2	a_3	364.19	$P^2F^3F^4$
245.14	Phe^1-Pro^2	b_2	245.13	P^2F^3
243.15	any	Internal fragment	243.11	N^5Q^6
217.14	Phe^1-Pro^2	a_2	217.12	P^2F^3
120.09	any	Internal fragment -CO	120.07	F^1 or F^3 or F^4

Table SI-3 *Summary of fragment assignment of the product ions generated by CID of tyrocidine B $[M+H]^+$*

m/z observed	Proposed ring opening	Proposed fragment type	m/z calculated	Sequence
1309.69	Phe^1-Pro^2	$[trcB]^+$	1309.67	$P^2W^3F^4N^5Q^6Y^7V^8O^9L^{10}F^1$
1292.68	Phe^1-Pro^2	trcB $-NH_3$	1292.67	$P^2W^3F^4N^5Q^6Y^7V^8O^9L^{10}F^1$
1281.70	Phe^1-Pro^2	trcB –CO	1281.66	$P^2W^3F^4N^5Q^6Y^7V^8O^9L^{10}F^1$
1144.62	Phe^1-Pro^2	b_9 $-NH_3$	1145.60	$P^2W^3F^4N^5Q^6Y^7V^8O^9L^{10}$
1049.53	Phe^1-Pro^2	b_8	1049.52	$P^2W^3F^4N^5Q^6Y^7V^8O^9$
935.47	Phe^1-Pro^2	b_7	935.44	$P^2W^3F^4N^5Q^6Y^7V^8$
836.37	Phe^1-Pro^2	b_6	836.37	$P^2W^3F^4N^5Q^6Y^7$
819.37	Phe^1-Pro^2	b_6 $-NH_3$	819.37	$P^2W^3F^4N^5Q^6Y^7$
673.33	Phe^1-Pro^2	b_5	673.31	$P^2W^3F^4N^5Q^6$
545.27	Phe^1-Pro^2	b_4	545.25	$P^2W^3F^4N^5$
431.22	Phe^1-Pro^2	b_3	431.21	$P^2W^3F^4$
406.18	any	Internal fragment	406.17	$N^5Q^6Y^7$
390.19	any	Internal fragment	390.18	$F^4N^5Q^6$
284.14	Phe^1-Pro^2	b_2	284.14	P^2W^3
256.15	Phe^1-Pro^2	a_2	256.13	P^2W^3
243.12	any	Internal fragment	243.11	N^5Q^6
159.10	any	Internal fragment -CO	159.08	W^3

Table SI-4 *Summary of fragment assignment of the product ions generated by CID of tyrocidine B_1 $[M+H]^+$*

m/z observed	Proposed ring opening	Proposed fragment type	m/z calculated	Sequence
1323.72	Phe^1-Pro^2	$[trcB_1]^+$	1323.69	$P^2W^3F^4N^5Q^6Y^7V^8K^9L^{10}F^1$
1307.69	Phe^1-Pro^2	$trcB_1$ -NH_3	1306.68	$P^2W^3F^4N^5Q^6Y^7V^8K^9L^{10}F^1$
1296.70	Phe^1-Pro^2	$trcB_1$ -CO	1295.68	$P^2W^3F^4N^5Q^6Y^7V^8K^9L^{10}F^1$
1176.62	Phe^1-Pro^2	b_9	1176.62	$P^2W^3F^4N^5Q^6Y^7V^8K^9L^{10}$
1159.61	Phe^1-Pro^2	b_9 –NH_3	1159.61	$P^2W^3F^4N^5Q^6Y^7V^8K^9L^{10}$
1063.56	Phe^1-Pro^2	b_8	1063.54	$P^2W^3F^4N^5Q^6Y^7V^8K^9$
935.44	Phe^1-Pro^2	b_7	935.44	$P^2W^3F^4N^5Q^6Y^7V^8$
918.45	Phe^1-Pro^2	b_7 –NH_3	918.43	$P^2W^3F^4N^5Q^6Y^7V^8$
836.37	Phe^1-Pro^2	b_6	836.37	$P^2W^3F^4N^5Q^6Y^7$
819.36	Phe^1-Pro^2	b_6 –NH_3	819.37	$P^2W^3F^4N^5Q^6Y^7$
673.33	Phe^1-Pro^2	b_5	673.31	$P^2W^3F^4N^5Q^6$
545.26	Phe^1-Pro^2	b_4	545.25	$P^2W^3F^4N^5$
431.22	Phe^1-Pro^2	b_3	431.21	$P^2W^3F^4$
406.18	any	Internal fragment	406.17	$N^5Q^6Y^7$
390.19	any	Internal fragment	390.18	$F^4N^5Q^6$
284.15	Phe^1-Pro^2	b_2	284.14	P^2W^3
256.15	Phe^1-Pro^2	a_2	256.13	P^2W^3
243.12	any	Internal fragment	243.11	N^5Q^6

Table SI-5 *Summary of fragment assignment of the product ions generated by CID of tyrocidine C $[M+H]^+$*

m/z observed	Proposed ring opening	Proposed fragment type	m/z calculated	Sequence
1348.63	Phe^1-Pro^2	$[trcC]^+$	1348.68	$P^2W^3W^4N^5Q^6Y^7V^8O^9L^{10}F^1$
1331.62	Phe^1-Pro^2	trcC $-NH_3$	1331.68	$P^2W^3W^4N^5Q^6Y^7V^8O^9L^{10}F^1$
1184.61	Phe^1-Pro^2	b_9 $-NH_3$	1184.61	$P^2W^3W^4N^5Q^6Y^7V^8O^9L^{10}$
1088.51	Phe^1-Pro^2	b_8	1088.53	$P^2W^3W^4N^5Q^6Y^7V^8O^9$
957.41	Phe^1-Pro^2	b_7 $-NH_3$	957.45	$P^2W^3W^4N^5Q^6Y^7V^8$
875.38	Phe^1-Pro^2	b_6	875.38	$P^2W^3W^4N^5Q^6Y^7$
844.43	Val^8-Orn^9	b_6	844.45	$O^9L^{10}F^1P^2W^3W^4$
712.31	Phe^1-Pro^2	b_5	712.32	$P^2W^3W^4N^5Q^6$
584.25	Phe^1-Pro^2	b_4	584.26	$P^2W^3W^4N^5$
470.21	Phe^1-Pro^2	b_3	470.22	$P^2W^3W^4$
406.17	any	Internal fragment	406.17	$N^5Q^6Y^7$
284.14	Phe^1-Pro^2	b_2	284.14	P^2W^3
256.14	Phe^1-Pro^2	a_2	256.13	P^2W^3
243.10	any	Internal fragment	243.11	N^5Q^6

Table SI-6 *Summary of fragment assignment of the product ions generated by CID of tyrocidine C_1 $[M+H]^+$*

m/z observed	Proposed ring opening	Proposed fragment type	m/z calculated	Sequence
1362.73	Phe^1-Pro^2	$[trcC_1]^+$	1362.7	$P^2W^3W^4N^5Q^6Y^7V^8K^9L^{10}F^1$
1345.72	Phe^1-Pro^2	$trcC_1$ -NH_3	1345.69	$P^2W^3W^4N^5Q^6Y^7V^8K^9L^{10}F^1$
1198.65	Phe^1-Pro^2	b_9 -NH_3	1198.62	$P^2W^3W^4N^5Q^6Y^7V^8K^9L^{10}$
1102.58	Phe^1-Pro^2	b_8	1102.55	$P^2W^3W^4N^5Q^6Y^7V^8K^9$
974.49	Phe^1-Pro^2	b_7	974.45	$P^2W^3W^4N^5Q^6Y^7V^8$
858.51	Phe^1-Pro^2	b_6 -NH_3	858.38	$P^2W^3W^4N^5Q^6Y^7$
712.33	Phe^1-Pro^2	b_5	712.32	$P^2W^3W^4N^5Q^6$
584.29	Phe^1-Pro^2	b_4	584.26	$P^2W^3W^4N^5$
470.23	Phe^1-Pro^2	b_3	470.22	$P^2W^3W^4$
406.19	any	Internal fragment	406.17	$N^5Q^6Y^7$
284.15	Phe^1-Pro^2	b_2	284.14	P^2W^3
256.10	Phe^1-Pro^2	a_2	256.13	P^2W^3
243.10	any	Internal fragment	243.11	N^5Q^6

Table SI-7 *Summary of fragment assignment of the product ions generated by CID of tyrocidine B` $[M+H]^+$*

m/z observed	Proposed ring opening	Proposed fragment type	m/z calculated	Sequence
1309.68	Phe^1-Pro^2	$[trcB`]^+$	1309.67	$P^2F^3W^4N^5Q^6Y^7V^8O^9L^{10}F^1$
1292.67	Phe^1-Pro^2	$trcB`-NH_3$	1292.67	$P^2F^3W^4N^5Q^6Y^7V^8O^9L^{10}F^1$
1281.70	Phe^1-Pro^2	trcB` -CO	1281.66	$P^2F^3W^4N^5Q^6Y^7V^8O^9L^{10}F^1$
1144.61	Phe^1-Pro^2	b_9 $-NH_3$	1145.60	$P^2F^3W^4N^5Q^6Y^7V^8O^9L^{10}$
1049.54	Phe^1-Pro^2	b_8	1049.52	$P^2F^3W^4N^5Q^6Y^7V^8O^9$
935.45	Phe^1-Pro^2	b_7	935.44	$P^2F^3W^4N^5Q^6Y^7V^8$
918.42	Phe^1-Pro^2	b_7 $-NH_3$	918.43	$P^2F^3W^4N^5Q^6Y^7V^8$
836.37	Phe^1-Pro^2	b_6	836.37	$P^2F^3W^4N^5Q^6Y^7$
788.39	Val^8-Orn^9	b_6 $-NH_3$	788.43	$O^9L^{10}F^1P^2F^3W^4$
673.32	Phe^1-Pro^2	b_5	673.31	$P^2F^3W^4N^5Q^6$
545.26	Phe^1-Pro^2	b_4	545.25	$P^2F^3W^4N^5$
431.21	Phe^1-Pro^2	b_3	431.21	$P^2F^3W^4$
406.18	any	Internal fragment	406.17	$N^5Q^6Y^7$
261.17	Phe^1-Pro^2	y_2	261.16	$L^{10}F^1$
245.13	Phe^1-Pro^2	b_2	245.13	P^2F^3
243.14	any	Internal fragment	243.11	N^5Q^6
217.14	Phe^1-Pro^2	a_2	217.12	P^2F^3
115.09	Val^8-Orn^9	b_1	115.09	O^9

Table SI-8 *Summary of fragment assignment of the product ions generated by CID of tyrocidine B_1` $[M+H]^+$*

m/z observed	Proposed ring opening	Proposed fragment type	m/z calculated	Sequence
1323.69	Phe^1-Pro^2	$[trcB_1`]^+$	1323.69	$P^2F^3W^4N^5Q^6Y^7V^8K^9L^{10}F^1$
1306.68	Phe^1-Pro^2	$trcB_1` -NH_3$	1306.68	$P^2F^3W^4N^5Q^6Y^7V^8K^9L^{10}F^1$
1295.72	Phe^1-Pro^2	$trcB_1` -CO$	1295.68	$P^2F^3W^4N^5Q^6Y^7V^8K^9L^{10}F^1$
1176.62	Phe^1-Pro^2	b_9	1176.62	$P^2F^3W^4N^5Q^6Y^7V^8K^9L^{10}$
1159.61	Phe^1-Pro^2	$b_9 -NH_3$	1159.61	$P^2F^3W^4N^5Q^6Y^7V^8K^9L^{10}$
1063.57	Phe^1-Pro^2	b_8	1063.54	$P^2F^3W^4N^5Q^6Y^7V^8K^9$
918.43	Phe^1-Pro^2	$b_7 -NH_3$	918.43	$P^2F^3W^4N^5Q^6Y^7V^8$
819.36	Phe^1-Pro^2	$b_6 -NH_3$	819.37	$P^2F^3W^4N^5Q^6Y^7$
673.32	Phe^1-Pro^2	b_5	673.31	$P^2F^3W^4N^5Q^6$
545.26	Phe^1-Pro^2	b_4	545.25	$P^2F^3W^4N^5$
431.21	Phe^1-Pro^2	b_3	431.21	$P^2F^3W^4$
406.18	any	Internal fragment	406.17	$N^5Q^6Y^7$
245.13	Phe^1-Pro^2	b_2	245.13	P^2F^3
243.14	any	Internal fragment	243.11	N^5Q^6
217.14	Phe^1-Pro^2	a_2	217.12	P^2F^3
159.10	any	Internal fragment -CO	159.08	W^4

Table SI-9 *Summary of fragment assignment of the product ions generated by CID of tryptocidine B $[M+H]^+$*

m/z observed	Proposed ring opening	Proposed fragment type	m/z calculated	Sequence
1332.68	Phe^1-Pro^2	$[tpcB]^+$	1332.69	$P^2W^3F^4N^5Q^6W^7V^8O^9L^{10}F^1$
1315.67	Phe^1-Pro^2	tpcB $-NH_3$	1315.68	$P^2W^3F^4N^5Q^6W^7V^8O^9L^{10}F^1$
1304.70	Phe^1-Pro^2	tpcB –CO	1304.68	$P^2W^3F^4N^5Q^6W^7V^8O^9L^{10}F^1$
1167.61	Phe^1-Pro^2	b_9 $-NH_3$	1168.61	$P^2W^3F^4N^5Q^6W^7V^8O^9L^{10}$
1072.54	Phe^1-Pro^2	b_8	1072.54	$P^2W^3F^4N^5Q^6W^7V^8O^9$
958.47	Phe^1-Pro^2	b_7	958.46	$P^2W^3F^4N^5Q^6W^7V^8$
859.39	Phe^1-Pro^2	b_6	859.39	$P^2W^3F^4N^5Q^6W^7$
788.38	Val^8-Orn^9	b_6	788.43	$O^9L^{10}F^1P^2W^3F^4$
673.32	Phe^1-Pro^2	b_5	673.32	$P^2W^3F^4N^5Q^6$
545.26	Phe^1-Pro^2	b_4	545.25	$P^2W^3F^4N^5$
528.26	Phe^1-Pro^2	b_4 $-NH_3$	528.24	$P^2W^3F^4N^5$
431.21	Phe^1-Pro^2	b_3	431.21	$P^2W^3F^4$
429.19	any	Internal fragment	429.19	$N^5Q^6W^7$
390.18	any	Internal fragment	390.18	$F^4N^5Q^6$
284.14	Phe^1-Pro^2	b_2	284.14	P^2W^3
256.15	Phe^1-Pro^2	a_2	256.13	P^2W^3
243.12	any	Internal fragment	243.11	N^5Q^6

Table SI-10 *Summary of fragment assignment of the product ions generated by CID of tryptocidine C $[M+H]^+$*

m/z observed	Proposed ring opening	Proposed fragment type	m/z calculated	Sequence
1371.70	Phe^1-Pro^2	$[tpcC]^+$	1371.70	$P^2W^3W^4N^5Q^6W^7V^8O^9L^{10}F^1$
1354.71	Phe^1-Pro^2	tpcC $-NH_3$	1354.69	$P^2W^3W^4N^5Q^6W^7V^8O^9L^{10}F^1$
1207.62	Phe^1-Pro^2	b_9 $-NH_3$	1207.62	$P^2W^3W^4N^5Q^6W^7V^8O^9L^{10}$
1111.56	Phe^1-Pro^2	b_8	1111.55	$P^2W^3W^4N^5Q^6W^7V^8O^9$
997.48	Phe^1-Pro^2	b_7	997.47	$P^2W^3W^4N^5Q^6W^7V^8$
881.39	Phe^1-Pro^2	b_6 $-NH_3$	881.39	$P^2W^3W^4N^5Q^6W^7$
712.33	Phe^1-Pro^2	b_5	712.32	$P^2W^3W^4N^5Q^6$
584.27	Phe^1-Pro^2	b_4	584.26	$P^2W^3W^4N^5$
470.22	Phe^1-Pro^2	b_3	470.22	$P^2W^3W^4$
429.20	any	Internal fragment	429.19	$N^5Q^6W^7$
284.15	Phe^1-Pro^2	b_2	284.14	P^2W^3
256.15	Phe^1-Pro^2	a_2	256.13	P^2W^3
243.10	any	Internal fragment	243.11	N^5Q^6

Chapter 3

Spectrophotometric investigation of tyrocidine structure

3.1 Introduction

In order to develop novel therapeutic agents or bio-preservatives based on antimicrobial peptides, insight regarding factors that modulate activity is imperative. The bioactivity of antimicrobial peptides, including that of the tyrocidines (Chapters 5-7), has been shown to be modulated by the peptide conformation [1-9] and self-assembly [3, 10-16]. A clearer understanding of the structure-function relationships, modulation of bioactivity and mode of action therefore requires investigation of the secondary structure and aggregation state/self-assembly of the tyrocidines. Due to the observed influence of peptide sequence on bioactivity (Chapters 5 and 7), the influence of the variable cationic residue (Orn^9 or Lys^9) and the variable aromatic dipeptide unit ($Trp^{3,4}$/$Phe^{3,4}$) on tyrocidine structure and aggregation state/self-assembly is of particular interest. Furthermore, as the bioactivity of antimicrobial peptides requires interaction with the target cell membrane [10, 17-20], changes in tyrocidine structure and/or aggregation state/self-assembly induced in a membrane-mimetic environment may advance the understanding of the structure-activity relationships and mode of action of the tyrocidines.

Circular dichroism spectroscopy, which exploits the sensitivity of the chiral properties of the peptide bond to secondary structural motifs, is an important tool for studying the secondary structure and solvent-induced conformational changes of peptides. Tyrocidine A has been shown to adopt an amphipathic type I β-turn/type II` β-turn/β-pleated sheet conformation, which is stabilised by four internal hydrogen bonds [21, 22]. Previous research by Laiken *et al.* (1969) indicated that the CD spectra of the tyrocidines resemble that of an α-helical structure rather than that of a typical β-sheet structure, exhibiting negative ellipticity minima at about 205 and 215 nm [23]. Although the far-UV CD spectra of peptides usually arise due to the backbone peptide bonds, aromatic amino acid side-chains may contribute significantly and have been shown to distort typical CD spectra [24-26]. As previously noted for the structurally related peptide gramicidin S, the uncharacteristic CD spectra of the tyrocidines may be

attributed to the combined contribution of β-sheet structure, β-turns and aromatic residues [6, 23, 27-29]. In addition to the influence of the aromatic amino acids, the CD spectra of the tyrocidines have been shown to be influenced by the aggregation state of the peptides, which has been shown to be highly dependent on peptide and solvent properties [23, 30-34]. In general, peptide self-assembly is influenced by peptide properties (conformation, hydrophobicity, amphipathicity and size of the hydrophobic and charged surface areas), the environment/solvent (polarity, ionic strength and presence of lipids) and the interactions involved (hydrophobic and electrostatic) [7, 35].

In addition to circular dichroism, fluorescence spectroscopy can be used to study peptide conformation, dynamics and intermolecular interactions by investigating changes in fluorescence emission maxima as well as fluorescence (quantum) yield. Intrinsic fluorophores of the tyrocidines include phenylalanine (Phe), tyrosine (Tyr) and tryptophan (Trp). The use of phenylalanine fluorescence is, however, limited to peptides that lack tryptophan and tyrosine residues due to its low extinction coefficient and short absorption (λ_{ex} = 260 nm) and emission (λ_{em} = 282 nm) wavelengths [36, 37]. The use of tyrosine, which is excited at 280 nm and exhibits an emission maximum at 303 nm, for studying peptide structure and intermolecular interactions is also limited due the relative insensitivity of the phenol group to solvent polarity [37, 38]. Furthermore, Tyr exhibits a lower extinction coefficient than Trp and its emission is thus usually overshadowed by Trp emission [37, 38]. Tryptophan is the most commonly used intrinsic fluorophore for studying peptide structure, dynamics and intermolecular interactions due to its large extinction coefficient and the high sensitivity of the indole group to the polarity/hydrophobicity of its local environment [36, 37, 39]. In an aqueous environment, the indole group of tryptophan exhibits an absorbance maximum at 295 nm and an emission maximum at 350 nm, while residues in a hydrophobic environment emit at shorter wavelengths [37]. Although fluorescence at wavelengths greater than 310 nm is usually due to Trp fluorescence, the ionised *p*-hydroxyphenyl moiety of Tyr (tyrosinate) has been shown to fluoresce between 315 and 350 nm [37, 38, 40]. Deprotonation of tyrosine in the native peptide will lead to ground-state tyrosinate, which is excited at both 280 and 295 nm [38, 40], whereas excitation at 280 nm leads to the formation of excited-state tyrosinate [37, 40]. Fluorescence (quantum) yields can be used to assess the relative exposure, orientation and/or local environment of the aromatic amino acids, which may allow deductions regarding

peptide conformation, intermolecular interactions and state of aggregation. The fluorescence yield of Trp, Tyr and tyrosinate is sensitive to the local environment due to various quenching mechanisms and resonance energy transfer (RET) [37-40]. Quenching of Trp and Tyr fluorescence may occur via a number of molecular interactions, including excited-state reactions, molecular rearrangements, ground-state complex formation and dynamic/collisional quenching [37]. Resonance energy transfer (RET) may occur if the emission spectrum of a fluorophore (donor) overlaps with the absorption spectrum of another molecule (acceptor) [37]. Due to the spectral overlap of Trp, Tyr, and tyrosinate, RET from Tyr to tyrosinate or Trp, and from tyrosinate to Trp is likely to occur [37]. Furthermore, Trp-to-Trp RET can be expected if some of the Trp residues exhibit blue-shifted emission [37]. Tyrosinate fluorescence yield is dependent on the degree of tyrosine deprotonation, which requires an acceptor that is in close enough proximity to allow optimal proton transfer, as well as its degree of motional freedom and solvent accessibility [38].

3.2 Materials

Analytical grade ethanol (>99.8%) was supplied by Merck (Darmstadt, Germany), 2,2,2-trifluoreoethanol (TFE) was supplied by Sigma (St. Louis, USA), and $CaCl_2$ was supplied by Saarchem (Krugersdorp, South Africa). Analytical grade water was prepared by filtering water from a reverse osmosis plant through a Millipore Milli-Q® water purification system (Milford, USA).

3.3 Methods

Analytical stock solutions (2.00 mg/mL) of the purified tyrocidines were prepared in ethanol:water (1:1, *v*/*v*), and diluted to 10 µM in water, 2,2,2-trifluoroethanol (TFE) or 75 mM $CaCl_2$ (final ethanol concentration was 0.5% *v*/*v*). Circular dichroism scans were obtained on a Chirascan CD spectrometer (Applied Photophysics, UK) using a 1.00 cm quartz cuvette. Three scans were collected between 200 and 250 nm with 0.1 nm steps. The spectra of the blank solutions were auto-subtracted. UV-absorbance spectra were collected simultaneously with the CD spectra. Fluorescence measurements of the same peptide solutions were performed on model RF-5301PC spectrofluorophotometer (Shimadzu, Japan). Emission spectra were recorded between 280 and 450 nm, 0.2 nm

steps, for excitation at 280 and 295 nm. Slit widths of 5nm were used for both excitation and emission, unless otherwise stated.

This study represents the first comprehensive spectrophotometric comparison of a natural tyrocidine library in terms of conformation and self-assembly in different solvents. The results presented in this chapter have important implications for tyrocidine bioactivity and should therefore be regarded in the context of the structure-activity relationships (QSAR studies) as discussed in Chapters 5-7.

3.4 Results and Discussion

Interpretation of the spectrophotometric results of the tyrocidines is complicated by both the variable aromatic residues and aggregation/self-assembly. The contribution of aromatic amino acids to the circular dichroism of proteins and peptides is often considered to be negligible due to the low abundance of these residues [37]. However, the tyrocidines have a high (40%) aromatic content, which implies that the contribution of these residues will be considerable, but different due to varying aromatic composition. Although the influence of varying aromatic residue composition may be negated by only comparing tyrocidines with identical aromatic content, differences in the orientation/exposure/local environment of such residues will also affect their contribution to CD spectra. In order to evaluate the contribution of aromatic amino acids to the CD spectra, the UV absorbance of the tyrocidines were compared. Comparison of the far-UV absorbance spectra of the tyrocidines indicated marked differences in absorbance of the tyrocidines from 210 and 230 nm. Although UV absorbance in this wavelength region represents the combined absorbance of the peptide bonds, phenylalanine, tyrosine and tryptophan, differences in the average absorbance between 210 and 230 nm ($A_{210\text{-}230}$) were assumed to be predominantly due to the aromatic amino acid side-chains. Although such differences in UV absorbance may be related to the influence of concentration, the ionic environment and pH, all the tyrocidines were treated in the same manner during purification and preparation and their concentration, ionic environment and pH were therefore assumed to be the same. The differences in UV absorbance were thus attributed to differences in the orientation/exposure/local environments of the aromatic amino acids. The orientation/exposure/local environment of the aromatic residues may be influenced by

conformational differences and/or differences in the manner of association/self-assembly and the size of the prevalent species.

Diffusion-ordered 2D NMR spectroscopy (DOSY), performed in collaboration with Prof Katalin Kövėr (University of Debrecen, Hungary), has indicated that TrcA, TrcC as well as gramicidin S form multimeric complexes of between 6 and 10 monomers in 50% (*v/v*) $D_2O/CNCD_3$ (Personal communication). Furthermore, as discussed in Chapter 2, TrcA and A_1 tend to form aggregates that cause changes in their HPLC profiles at concentrations > 200 μg/mL. Previous research regarding tyrocidine aggregation indicted that TrcB forms elongated aggregates in an aqueous environment [32]. In an aqueous environment, the tendency for self-assembly is, at least in part, dictated by properties of the peptide, such as primary structure, conformation, hydrophobicity, amphipathicity and size of the hydrophobic and charged surface areas [7, 35], and tyrocidine aggregation is highly dependent on the cyclic conformation and proper spatial alignment of the amino acid residues [30, 31]. Variation in self-assembly may be due to (1) steric factors as a result of differences in the size/available surface area of the polar/charged face of the peptide molecule; (2) differences in hydrophobicity or (3) differences in solvent systems. Self-assembly may therefore influence the CD spectra directly by leading to 'apparent' changes in backbone conformation due to differences in the manner of association/self-assembly and/or the size of the prevalent species, or by affecting orientation/exposure/local environment, and thus the contribution of the aromatic amino acids.

It is thus assumed in the discussion of the results that some aggregates/higher order self-assembly structures already exist in solution. The results of the spectroscopic investigation are discussed in two parts: spectroscopic investigation of tyrocidine structure in an aqueous environment (*Part 1*) and in trifluoroethanol (TFE), a membrane-mimetic environment (*Part 2*).

3.4.1 Results and Discussion: Part 1

3.4.1.1 Circular dichroism of the tyrocidines in an aqueous environment

The CD spectra of the tyrocidines in an aqueous environment exhibited two negative bands at approximately 205 and 216 nm, which may be attributed to β-turn and β-sheet structure, respectively [23, 27, 29]. The shape and ellipticities of these bands are,

however, influenced by the aggregation state of the peptides, as well as the aromatic amino acids [23, 24]. Previous investigators have used spectral shapes, characterised by the ratio of the negative ellipticity minima ($\theta_{205}/\theta_{216}$), as an indication of differences in backbone conformation [7, 26]. Although such ratios are expected to provide information regarding the backbone conformation of monomeric peptides, self-assembly to form higher-order structures are also expected to influence the spectral shape. As the tyrocidines have been shown to form multimeric complexes in an aqueous environment [30-32](this study), differences between the negative minima at 205 and 216 nm, as well as spectral shape, are most probably more related to different aggregation states (manner of association/self-assembly and the size of the prevalent species) than differences in peptide backbone conformation.

Comparison of the CD spectra of the Orn^9- and Lys^9-containing peptides (Figures 1 - 3) indicated marked differences in the ellipticity at 205 and 216 nm (Table 1). Orn^9-containing TrcC exhibited enhanced θ_{205} and θ_{216} relative to Lys^9-containing $TrcC_1$, whereas all the other Orn^9-containing tyrocidines (TrcB, B` and A) exhibited reduced $\theta_{205}$ and $\theta_{216}$ relative to their $Lys^9$-containing counterparts ($TrcB_1$, $B_1$` and A_1). These changes in θ_{205} and θ_{216} may be due to (1) changes in backbone conformation, (2) different contributions of the aromatic amino acids and/or (3) differences in aggregation state. Comparison of the spectral shapes indicated that the Orn^9- and Lys^9-containing peptides exhibit similar $\theta_{205}/\theta_{216}$, which suggests that the tyrocidines adopt similar backbone conformations/higher-order structure. However, the $\theta_{205}/\theta_{216}$ of tyrocidines containing a Phe^3 residue (TrcA, A_1, B', B_1') was slightly lower than those with a Trp^3 residue (TrcC, C_1, B, B_1), due to the $\theta_{205} > \theta_{216}$ of the Trp^3-containing tyrocidines, while those with a Phe^3 exhibited a $\theta_{205} < \theta_{216}$ (Table 1). These results may indicate that a larger population of the Phe^3 containing tyrocidines may have stable β-pleated sheets, possibly due higher order structures/aggregates, in an aqueous environment. This is supported by the Raman scattering, which indicates the presence of aggregates/higher order structures, observed for all the Phe^3 containing peptides (see discussion later) and the changes in HPLC profiles (discussed in Chapter 2).

Comparison of the average UV absorbance of the natural tyrocidines (Figures 1 - 3) indicated significant differences in $A_{210\text{-}230}$ of the Orn^9- and Lys^9-containing peptides (Table 1). Orn^9-containing TrcC exhibited greater $A_{210\text{-}230}$ than Lys^9-containing $TrcC_1$,

whereas all the other Orn^9-containing tyrocidines (TrcB, B` and A) exhibited lower $A_{210-230}$ than their $Lys^9$-containing counterparts ($TrcB_1$, $B_1$` and A_1). Such differences in $A_{210-230}$, which are indicative of differences in the orientation/exposure/local environments of the aromatic amino acids, imply that the change in θ_{216} may, at least in part, be due to different contributions by the aromatic residues. Although differences in the orientation/exposure/local environments of the aromatic amino acids may be due to conformational differences related to the Orn^9/Lys^9 content, such differences are more likely to be related to differences in the manner and/or extent of self-assembly of the tyrocidines in aqueous solution.

In addition to the influence of Orn^9/Lys^9 content, comparison of the far-UV absorbance and CD spectra of tyrocidines B, B`, $B_1$ and $B_1$` allowed evaluation of the influence of the variable aromatic dipeptide unit ($Trp^{3,4}$-D-$Phe^{3,4}$) on the structure and aggregation state of the tyrocidines in an aqueous environment. The CD spectra of TrcB and B_1 (Trp^3-D-Phe^4) exhibited greatly enhanced ellipticities at 205 and 216 nm, as well as significantly greater $\theta_{205}/\theta_{216}$ ratios, relative to TrcB` and $B_1$` (Phe^3-D-Trp^4), respectively (Table 1, Figure 2). Although these differences may be related to different backbone conformations, different aggregation states and contributions of the aromatic amino acids are more likely. Previous studies [41], as well as homology modelling (Chapter 4), have indicated that the aromatic residues of the dipeptide unit are located on opposite sides of the peptide structure. The relative positioning of the aromatic residues may lead to differences in the manner and/or extent of self-assembly as the spatial alignment of the amino acid residues influence tyrocidine aggregation/self-assembly [30, 31]. Comparison of the UV absorbance spectra indicated that the $A_{210-230}$ of TrcB and B_1 is significantly greater than that of TrcB` and $TrcB_1$` (Table 1, Figure 2), respectively, which suggests that the orientation/exposure/local environments of the aromatic amino acids are different. Such differences may be due the direct influence of the relative positioning of the aromatic residues and/or differences in the manner and/or extent of self-assembly. It should, however, be noted that reduced ellipticity and $A_{210-230}$ of TrcB` and $B_1$` may also be related to loss of peptide due to formation of large aggregates settling out of solution.

In addition to the negative ellipticity minima at 205 and 216 nm, an additional negative band was observed for tyrocidines C and C_1 (231 nm) and tyrocidines B` and

B_1` (225 nm). Laiken *et al.* (1969) previously attributed this band to the influence of Trp [23]. It is plausible to attribute this negative band to the influence of D-Trp$^4$, as tyrocidines C, $C_1$, B` and B_1` all contain this residue and tyrocidines that lack D-Trp^4 do not exhibit negative bands in this wavelength region. These bands may, however, also be due to red-shifted ellipticity of the β-sheets as a result of hydrogen bonding within the assembly.

Table 1 *Influence of the tyrocidine sequence on UV absorbance and CD spectra of the tyrocidines in an aqueous environment* (Ellipticities (θ) are given in degree.cm^2.dmol^{-1} ± SEM of three determinations)

	$A_{210-230}$	θ_{205}	θ_{216}	$\theta_{205}/\theta_{216}$
TrcC	0.269	-6.6 ± 0.22	-5.8 ± 0.11	1.1 ± 0.026
$TrcC_1$	0.249	-5.6 ± 0.054	-5.4 ± 0.098	1.0 ± 0.025
TrcB	0.159	-6.7 ± 0.17	-5.8 ± 0.070	1.2 ± 0.040
$TrcB_1$	0.213	-9.9 ± 0.087	-8.7 ± 0.35	1.2 ± 0.037
TrcB`	0.096	-3.0 ± 0.16	-3.5 ± 0.16	0.85 ± 0.048
$TrcB_1$`	0.165	-4.0 ± 0.046	-4.4 ± 0.046	0.92 ± 0.012
TrcA	0.130	-8.3 ± 0.11	-9.1 ± 0.18	0.92 ± 0.0077
$TrcA_1$	0.203	-12.2 ± 0.082	-12.9 ± 0.027	0.94 ± 0.077

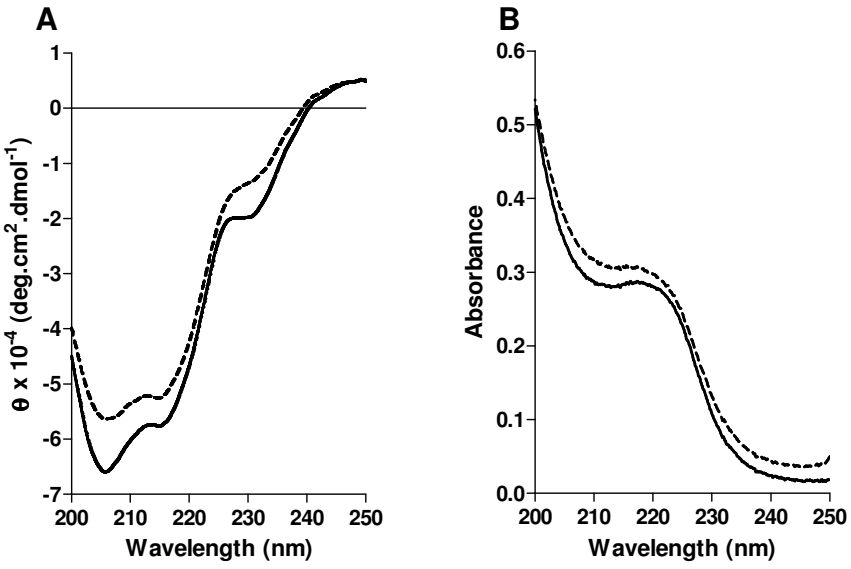

Figure 1 (A) *CD and* (B) *far-UV absorbance spectra of tyrocidines C and C_1 in an aqueous environment.* Spectra of the Orn^9-containing peptides are represented by solid lines; spectra of Lys^9-containing peptides are represented by dotted lines. Each CD spectrum is depicted by a Lowess fit line (20 point smoothing window) for an average of triplicate determinations. UV spectra are the average of triplicate determinations.

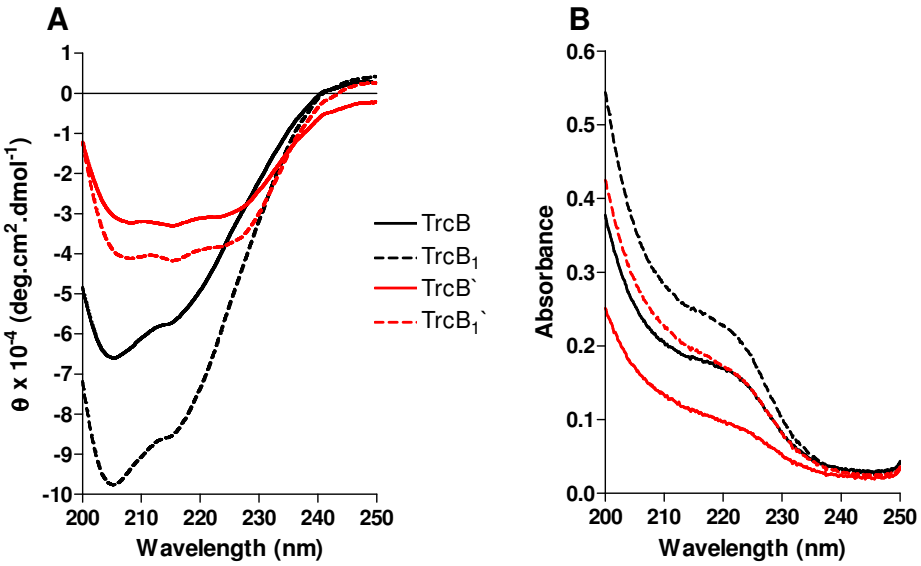

Figure 2 (A) *CD and* (B) *far-UV absorbance spectra of tyrocidines from the B-group in an aqueous environment.* Spectra of the Orn^{9}-containing peptides are represented by solid lines; spectra of Lys^{9}-containing peptides are represented by dotted lines. Spectra of tyrocidines B and B_1 (Trp^{3}-D-Phe^{4}) are indicated by black lines; spectra of tyrocidines B` and $B_1$` (Phe^{3}-D-Trp^{4}) are indicated by red lines. Each CD spectrum is depicted by a Lowess fit line (20 point smoothing window) for an average of triplicate determinations. UV spectra are the average of triplicate determinations.

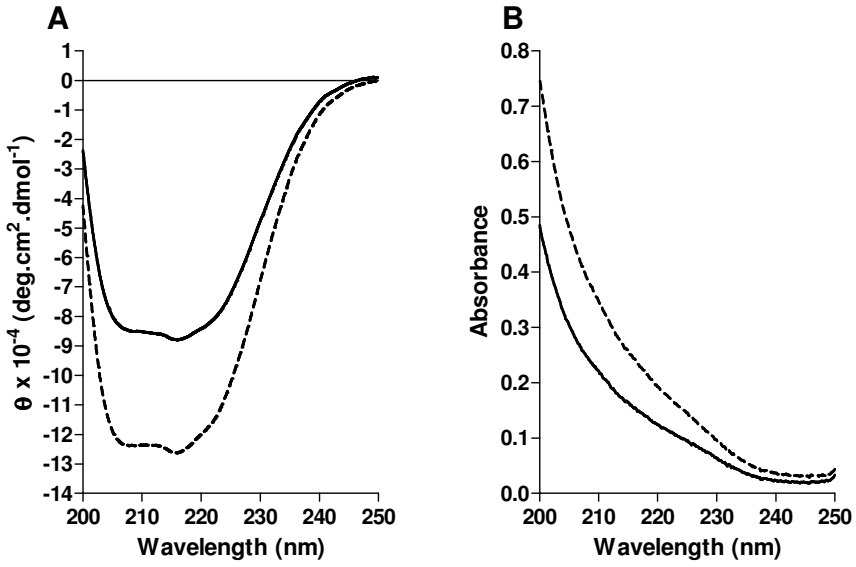

Figure 3 (A) *CD and* (B) *far-UV absorbance spectra of tyrocidines A and A_1 in an aqueous environment* Spectra of the Orn^{9}-containing peptides are represented by solid lines; spectra of Lys^{9}-containing peptides are represented by dotted lines. Each CD spectrum is depicted by a Lowess fit line (20 point smoothing window) for an average of triplicate determinations. UV spectra are the average of triplicate determinations.

3.4.1.2 Fluorescence spectrophotometry of the tyrocidines in an aqueous environment

Tryptophan-containing tyrocidines

Emission spectra for $\lambda_{ex\ 280}$ and $\lambda_{ex\ 295}$ of tyrocidines C, C_1, B and B_1 exhibited emission maxima at 350 nm, while tyrocidines B` and $B_1$` exhibited emission maxima at 345 nm. Fluorescence emission for $\lambda_{ex\ 280}$ represents the combined contribution of Tyr, ground-state tyrosinate, excited-state tyrosinate and Trp. Tyr emission (λ_{max} at 303 nm), however, is not observed due to the Trp emission dominating the spectra and/or due to energy transfer from the Tyr to the Trp residues and/or formation of tyrosinate. Trp is expected to be the predominant source of emission for $\lambda_{ex\ 295}$ as the contribution of ground-state tyrosinate is expected to be small or negligible. The additional peaks observed at 311 nm ($\lambda_{ex\ 280}$) and 330 nm ($\lambda_{ex\ 295}$) for TrcB` and $B_1$` are probably due to light (Raman) scattering as a result of increased quenching, suspended particulate, aggregation or self-assembly structures [37].

The influence of $Orn^9 \rightarrow Lys^9$ substitution on Trp fluorescence was evaluated by comparing the emission spectra of the Orn^9- and Lys^9-containing tyrocidines. The fluorescence emission spectra of tyrocidines C and C_1 (Trp^3-D-Trp^4) indicated a decrease in Trp emission (fluorescence yield) for Lys^9-containing TrcC_1 (Figure 4), whereas tyrocidines B and B_1 (Trp^3) and tyrocidines B` and $B_1$` (Trp^4) indicated an increase in Trp emission for the Lys^9-containing TrcB_1 and B_1` (Figure 5). Trp fluorescence yield is influenced by quenching, which may occur via ground-state complex formation, excited-state reactions and/or dynamic/collisional quenching [37]. Although excited-state electron transfer is likely to be the major quenching mechanism in peptides, ground-state interactions may become more significant if the indole moiety is surrounded by functional groups [39]. The aggregation state of the tyrocidines is therefore expected to have a significant influence on fluorescence emission and the Trp quenching may, at least in part, be due to ground-state complex formation due to self-assembly. Excited-state reactions that may contribute to the observed quenching of Trp fluorescence include excited-state electron transfer to the peptide backbone and the amide groups of Asn and Gln, and/or excited-state proton transfer from the ε-amino group of Lys and the phenol group of Tyr [37, 39]. As quenching is influenced by both proximity and orientation [37, 39], Orn^9/Lys^9 content may lead to different degrees of quenching by favouring different aggregation states. Different aggregation states may

also lead to differences in the solvent accessibility of the indole group, which will influence the degree of dynamic/collisional quenching by water molecules. Increased Trp quenching in the presence of Lys^9 (as seen for $TrcC_1$) may thus be due to increased solvent accessibility of the indole moiety of Trp_3 and/or Trp_4, enhanced excited-state proton transfer from the Lys^9 or Tyr^7 side chains and/or enhanced excited-state electron transfer to the Asn^5 or Gln^6 side chains. Increased Trp quenching in the presence of Orn^9 (as seen for TrcB and B`) may be due to increased solvent accessibility of the indole moiety of Trp, enhanced excited-state proton transfer from the Orn^9 or Tyr^7 side chains and/or enhanced excited-state electron transfer to the Asn^5 or Gln^6 side chains.

Comparison of the fluorescence emission spectra of tyrocidines B, B`, $B_1$ and $B_1$` (Figure 5) indicated that Trp^3 and Trp^4 exhibit different emission maxima, as well as different fluorescence yields (Table 2). Trp^3 (TrcB and B_1) exhibited emission maxima at 350 nm, whereas Trp^4 (TrcB` and $B_1$`) exhibited blue-shifted emission at 345 nm. Furthermore, Trp^3 (TrcB and B_1) exhibited greater fluorescence yield than Trp^4 (TrcB` and $B_1$`). These results may also be explained by peptide self-assembly in an aqueous environment. The blue-shifted emission of Trp^4 (TrcB` and $B_1$`) suggests that this residue is located in a more hydrophobic environment than Trp^3 (TrcB and B_1). Self-assembly may lead to reduced fluorescence yield of Trp^4 by ground-state complex formation within the assembly. Alternatively, self-assembly may increase the proximity of nearby quenchers such as the peptide backbone, the amide groups of Asn and Gln, the ε-amino group of lysine and/or the phenol group of Tyr.

Fluorescence difference spectra, which are obtained by subtracting the emission spectra for $\lambda_{ex\ 295}$ from the emission spectra for $\lambda_{ex\ 280}$, represent the contribution of Tyr energy transfer and tyrosinate to the emission for $\lambda_{ex\ 280}$ (Table 2; Figures 4 and 5). The relative contribution of Tyr/tyrosinate was found to be much greater than expected, which suggests that the Trp residues of the tyrocidines are quenched to a great extent and/or the fluorescence yield of Tyr/tyrosinate is enhanced by environmental factors. As discussed above, quenching of Trp fluorescence is expected to be enhanced by self-assembly due to ground-state complex formation and/or enhanced proximity to quenchers that favour excited-state reactions. Enhanced Tyr/tyrosinate fluorescence may also be related to self-assembly as Tyr/tyrosinate residues in a hydrophobic environment (decreased solvent accessibility) exhibit enhanced fluorescence yield [38,

40]. As seen for Trp fluorescence, the contribution of Tyr/tyrosinate to fluorescence emission of the Trp-containing tyrocidines is influenced by the Orn^9/Lys^9 content. The fluorescence emission spectra of TrcC versus C_1 exhibited a decrease in the contribution of Tyr energy transfer and/or tyrosinate emission for Lys^9-containing $TrcC_1$ (Figure 4), whereas tyrocidines B versus B_1 and TrcB` versus $B_1$` indicated an increase in the contribution of Tyr energy transfer and/or tyrosinate emission for the Lys^9-containing $TrcB_1$ and B_1` (Figure 5). As the efficiency/extent of resonance energy transfer (RET) between Tyr and Trp is dependent on the proximity of these side-chains [37], changes in the contribution of Tyr may be due to different aggregation states and/or changes in the orientation of the Trp and/or Tyr^7 side-chains due to Orn^9/Lys^9 content. Changes in the contribution of tyrosinate may be related to different degrees of tyrosinate formation and/or differences in the local environment of the Tyr^7 residue. Tyrosinate formation requires proton transfer from the excited- or ground-state phenolic moiety to an acceptor that is in close enough proximity to allow optimal proton transfer [38]. Lys residues are expected to be suitable proton acceptors for tyrosinate formation, while water, the amide groups of the peptide chain, Gln or Asn are not expected to promote protolysis [38, 40]. The Lys^9/Orn^9 amino-groups may thus affect tyrosinate formation directly due to different proton accepting abilities. Alternatively, the Orn^9/Lys^9 content may influence the motion and/or solvent accessibility of the phenolic moiety, as restricted motion and/or reduced solvent accessibility has been shown to enhance tyrosinate fluorescence (quantum) yield [38].

In addition to the influence of Orn^9/Lys^9 content, inversion of the dipeptide unit also influenced the contribution of Tyr energy transfer and/or tyrosinate emission. For the Orn^9-containing peptides, TrcB and B', decreased contribution of Tyr energy transfer and/or tyrosinate emission was observed for TrcB` (contains a Trp^4). In contrast, for the Lys^9-containing $TrcB_1$ and B_1', increased contribution of Tyr energy transfer and/or tyrosinate emission was observed for $TrcB_1$ (contains a Trp^3). Such differences are likely to be related to different aggregation states, which may lead to differences in the proximity of the Trp and Tyr residues, differences in formation of tyrosinate and/or differences in the solvent accessibility of tyrosinate.

Table 2 *Influence of tyrocidine sequence on fluorescence emission of the Trp-containing tyrocidines in an aqueous environment* (Fluorescence values are given in arbitrary units ± SEM of three determinations)

	$\lambda_{ex\ 280}$	$\lambda_{ex\ 295}$	Difference spectra
	$\lambda_{em\ max\ 350}$	$\lambda_{em\ max\ 350}$	$\lambda_{em\ max\ 350}$
TrcC	699 ± 16	280 ± 5.9	420 ± 12
$TrcC_1$	434 ± 30	192 ± 2.1	242 ± 28
TrcB	269 ± 8.8	117 ± 0.90	152 ± 7.9
$TrcB_1$	415 ± 2.7	170 ± 1.5	246 ± 4.0
TrcB`	181 ± 4.32[1]	54 ± 0.82[1]	127 ± 3.5[1]
$TrcB_1$`	381 ± 1.6[1]	111 ± 1.4[1]	271 ±1.3[1]

[1] The emission maxima of TrcB` and $B_1$` are blue-shifted to 345 nm.

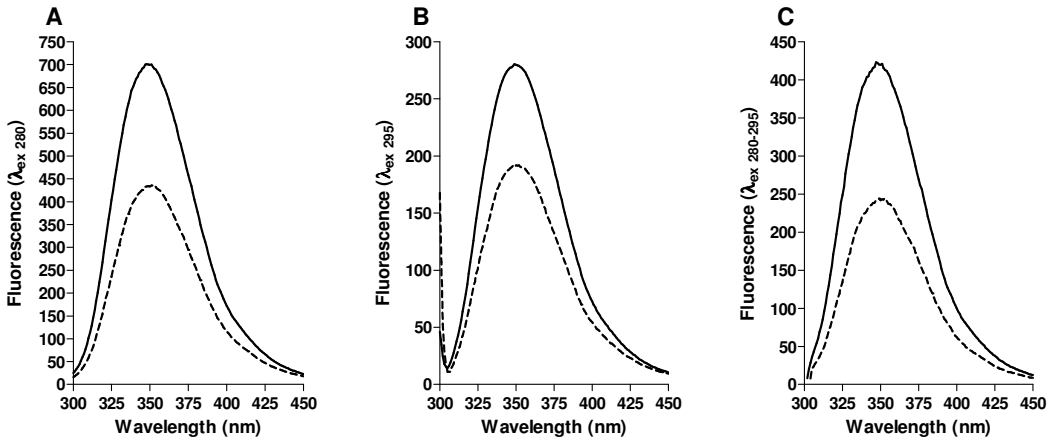

Figure 4 *Fluorescence emission spectra of the L-Trp-D-Trp-containing tyrocidines in an aqueous environment.* (A) Excitation at 280 nm represents the combined emission of Trp and Tyr; (B) excitation at 295 nm represents the emission of Trp; whereas the (C) difference spectra represent the contribution of Tyr and/or tyrosinate emission. Spectra (average of triplicate determinations) of the Orn^9-containing TrcC are represented by solid lines; spectra (average of triplicate determinations) of Lys^9-containing $TrcC_1$ are represented by dotted lines.

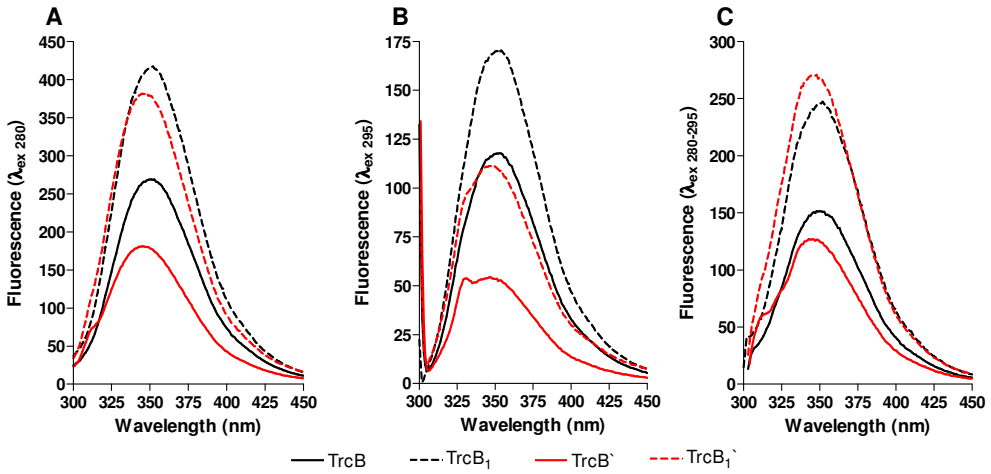

Figure 5 *Fluorescence emission spectra of the tyrocidines from the B-group, containing both Phe and Trp in the aromatic dipeptide moiety, in an aqueous environment.* (A) Excitation at 280 nm represents the combined emission of Trp and Tyr; (B) excitation at 295 nm represents the emission of Trp; whereas the (C) difference spectra represent the contribution of Tyr and/or tyrosinate emission. Spectra of the Orn^9-containing peptides are represented by solid lines; spectra of Lys^9-containing peptides are represented by dotted lines. Spectra (average of triplicate determinations) of tyrocidines B and B$_1$ (Trp^3-D-Phe^4) are indicated by black lines; spectra (average of triplicate determinations) of tyrocidines B` and B$_1$` (Phe^3-D-Trp^4) are indicated by red lines.

Tyrocidines that lack tryptophan residues

The emission spectra for $\lambda_{ex\ 280}$ for the TrcA and A$_1$ exhibited emission maxima at 305 nm, which may be attributed to Tyr fluorescence. Comparison of the fluorescence emission spectra indicated an increase in Tyr emission (fluorescence yield) for Lys^9- containing TrcA$_1$ (Table 3; Figure 6). As discussed above, such increased Tyr fluorescence yield may be due to differences in aggregation state leading to differences in the hydrophobicity of the local environment of the phenolic moiety, or differences in the proximity of the Tyr residues to quenching groups. In addition to Tyr fluorescence TrcA and TrcA$_1$ also exhibited a shoulder at 340 nm (for $\lambda_{ex\ 280}$), which may be attributed to the combined contribution of ground- and excited-state tyrosinate. Emission spectra for $\lambda_{ex\ 295}$ of tyrocidines A and A$_1$ exhibited emission maxima at about 350 nm, which may be attributed to ground-state tyrosinate fluorescence. The shoulders observed at 330 nm may be attributed to light (Raman) scattering [37], and are probably due to the presence of higher order structures. The contribution of excited-state tyrosinate could be determined from difference spectra (λ_{max} at 340 nm) (Table 3;

Figure 6). $TrcA_1$ exhibited greater tyrosinate emission than TrcA, which may be related to different degrees of tyrosinate formation and/or differences in the local environment. It is possible that the Lys^9 residue of $TrcA_1$ acts as a better proton acceptor for tyrosinate formation than the Orn^9 residue of TrcA. Alternatively, the Orn^9/Lys^9 content may influence the motion and/or solvent accessibility of the phenolic moiety, due to differences in aggregation state.

Table 3 *Influence of $Orn_9 \rightarrow Lys_9$ substitution on fluorescence emission of the Trp-lacking tyrocidines in an aqueous environment.* (Fluorescence values are given in arbitrary units ± SEM of three determinations)

	$\lambda_{ex\ 280}$		$\lambda_{ex\ 295}$	Difference spectra	
	$\lambda_{em\ max\ 305}$	$\lambda_{em\ max\ 340}$	$\lambda_{em\ max\ 350}$	$\lambda_{em\ max\ 305}$	$\lambda_{em\ max\ 340}$
TrcA	62 ± 2.1	53 ± 3.1	24 ± 1.2	60 ± 2.0	31 ± 2.3
$TrcA_1$	95 ± 1.5	75 ± 2.0	32 ± 0.38	92 ± 1.5	45 ± 1.3

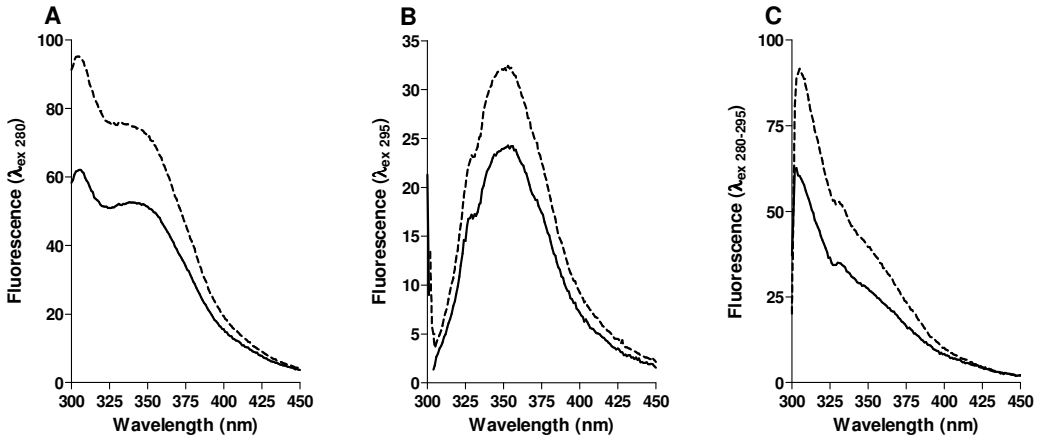

Figure 6 *Fluorescence emission spectra of tyrocidines A and A_1 in an aqueous environment* (A) Excitation at 280nm represents the combined emission of Tyr and tyrosinate; (B) excitation at 295 represents the emission of tyrosinate; whereas the (C) difference spectra represent the emission of Tyr. Spectra (average of triplicate determinations) of the Orn^9-containing peptides are represented by solid lines; spectra (average of triplicate determinations) of Lys^9-containing peptides are represented by dotted lines.

Summary and Conclusions: Part 1

With the assumption that aggregates/higher order self-assembly structures already exists in solution, differences in the negative ellipticities (θ_{205} and θ_{216}), UV absorbance and fluorescence of the Orn^9- and Lys^9-containing tyrocidines suggest that the variable

cationic residue influences the manner/extent of self-assembly of the tyrocidines, as well as the orientation/exposure/local environments of the aromatic amino acids, in an aqueous environment. Differences in the negative ellipticities (θ_{205} and θ_{216}), spectral shapes ($\theta_{205}/\theta_{216}$), UV absorbance and fluorescence of tyrocidines B, B`, $B_1$ and $B_1$` suggest that the relative positioning of the aromatic residues in the variable aromatic dipeptide moiety also influences the manner/extent of self-assembly of the tyrocidines, as well as the relative orientation/exposure/local environments of the aromatic amino acids, in an aqueous environment. Such differences may be explained by the segregation of the two residues in the aromatic dipeptide moiety on opposite faces of the molecule. The results also suggest that self-assembly is likely to involve shielding of the aromatic residue in position 4 from the aqueous environment (as indicated by the blue-shifted emission of Trp^4), while the aromatic residue in position 3 remains exposed to the polar solvent environment. Furthermore, the lower $\theta_{205}/\theta_{216}$ and increased Raman scattering exhibited by the Phe^3-containing tyrocidines suggest that these peptides may form more/larger higher-order structures that the Trp^3-containing tyrocidines.

3.4.2 Results and Discussion: Part 2

2,2,2-Trifluoroethanol has been shown to stabilise β-turn and β-sheet structures and is commonly used as a membrane-mimetic solvent as it induces peptide structures similar to those produced by membrane environments [6, 28, 42, 43]. As the bioactivity of antimicrobial peptides requires interaction with the target cell membrane [10, 17-20], insight regarding the mode of action may be gained by investigation of changes in tyrocidine structure/aggregation state induced by a membrane-mimetic environment. Furthermore, insight regarding the structure-activity relationships may be gained by evaluation of the influence of primary sequence on peptide structure/aggregation state in a membrane-mimetic environment.

3.4.2.1 Changes in tyrocidine structure/aggregation state induced by a membrane-mimetic environment

Inducibility of secondary structure and higher order structures was evaluated by comparing the UV absorbance and CD spectra of the tyrocidines in an aqueous and membrane-mimetic environment. Comparison of the CD spectra in a membrane-mimetic and aqueous environment (Table 4; Figures 7 - 9) indicated

significant differences in ellipticity and spectral shape. The negative ellipticity minima observed at 205 and 216 nm in an aqueous environment were slightly blue-shifted to 204 and 214 nm, respectively. This shift was accompanied by the loss of resolution of the 214 nm minima. Furthermore, with the exception of $TrcA_1$, TFE led to enhanced negative ellipticities, as well as a significant increase in the ratio of the ellipticity minima ($\theta_{204}/\theta_{214}$) (Table 4). The CD spectra of the structurally related gramicidin S (Figure 10) also exhibited significantly enhanced θ_{204} and θ_{214}, accompanied by a loss of resolution of the negative minima at 219 nm observed in an aqueous environment. The enhanced ellipticities may be due to increased association by intermolecular hydrogen bonding and/or increased intramolecular hydrogen bonding in a membrane-mimetic environment. The enhanced ellipticities and change in $\theta_{204}/\theta_{214}$ may be thus attributed to the induction of higher-order structures that differ from those formed in an aqueous environment in the manner of association, degree of hydrogen bonding and/or size of the prevalent species.

Differences between the CD spectra are also expected to be related to differing contributions of the aromatic amino acids due to changes in their orientation/exposure/local environment. This is supported by the observation that, with the exception of $TrcA_1$, the average UV absorbance ($A_{210\text{-}230}$) is significantly greater in TFE than in water. The differences in orientation/exposure/local environment of the aromatic residues are probably due to changes in aggregation state (both the manner of association and size of the prevalent species). The reduced UV absorbance and negative ellipticities observed for $TrcA_1$ may be related to its increased state of aggregation and settling of the larger aggregates out of solution.

Table 4 *Change in UV absorbance and CD spectra of the tyrocidines induced in a membrane-mimetic environment.* The average UV absorbance, negative ellipticities (θ_{204} and θ_{214}) and the ellipticity ratios ($\theta_{204}/\theta_{214}$) of the tyrocidines in TFE are given. The average UV absorbance, negative ellipticities (θ_{205} and θ_{216}) and the ellipticity ratios ($\theta_{205}/\theta_{216}$) of the tyrocidines in water are given in parentheses. (Ellipticities (θ) are given in degree.cm^2.dmol^{-1} ± SEM of three determinations)

	$A_{210-230}$	**θ_{204} (θ_{205})**	**θ_{214} (θ_{216})**	**$\theta_{204}/\theta_{214}$ ($\theta_{205}/\theta_{216}$)**
TrcC	0.571 (0.249)	-22.1 ± 0.5 (-6.6)	-12.7 ± 0.74 (-5.8)	1.7 ± 0.117 (1.1)
$TrcC_1$	0.465 (0.269)	-17.1 ± 0.36 (-5.6)	-10.2 ± 0.86 (-5.4)	1.7 ± 0.168 (1.0)
TrcB	0.261 (0.159)	-15.8 ± 0.38 (-6.7)	-10.5 ± 0.48 (-5.8)	1.5 ± 0.038 (1.2)
$TrcB_1$	0.448 (0.213)	-23.1 ± 1.4 (-9.9)	-15.5 ± 0.75 (-8.7)	1.5 ± 0.155 (1.2)
TrcB`	0.205 (0.096)	-10.8 ± 0.42 (-3.0)	-6.5 ± 0.85 (-3.5)	1.7 ± 0.167 (0.85)
$TrcB_1$`	0.252 (0.165)	-10.4 ± 0.44 (-4.0)	-6.3 ± 0.52 (-4.4)	1.7 ± 0.160 (0.92)
TrcA	0.172 (0.130)	-14.3 ± 0.48 (-8.3)	-12.8 ± 0.48 (-9.1)	1.1 ± 0.078 (0.92)
$TrcA_1$	0.188 (0.203)	-7.8 ± 0.47 (-12.2)	-9.1 ± 1.1 (-12.9)	0.86 ± 0.062 (0.94)
GS	0.115 (0.116)	-36.4 ± 0.98 (-12.0)	-25.7 ± 0.94 (-16.0) [1]	1.4 ± 0.083 (0.75)[1]

[1] Negative ellipticity minimum at 219 nm; ellipticity ratio $\theta_{205}/\theta_{219}$

The CD spectra in an aqueous and membrane-mimetic environment also exhibited significant differences between 220 and 240 nm. For tyrocidines C and C_1 (Trp_3-D-Trp_4), the negative band observed at 231 nm in water was either lost or blue-shifted to 225 nm, and the negative ellipticity of this band was significantly enhanced. TrcB and B_1 (Trp_3), which do not exhibit a negative band in this wavelength

region in water, exhibited a shoulder at 225 nm, while the negative band observed at 225 nm in water for TrcB` and $B_1$` (Trp_4) was significantly enhanced. The tryptophan-lacking tyrocidines A and A_1 exhibited an additional negative band at 222 nm, which corresponds to the shoulder seen in the UV absorbance spectra. These changes may be related to differing contributions of the aromatic amino acids due to re-orientation of and/or differences in exposure/local environment of the aromatic side-chains. However, these changes may also be related to β-sheet/stack formation and increased intermolecular hydrogen bonding as would be expected in self-assembling structures.

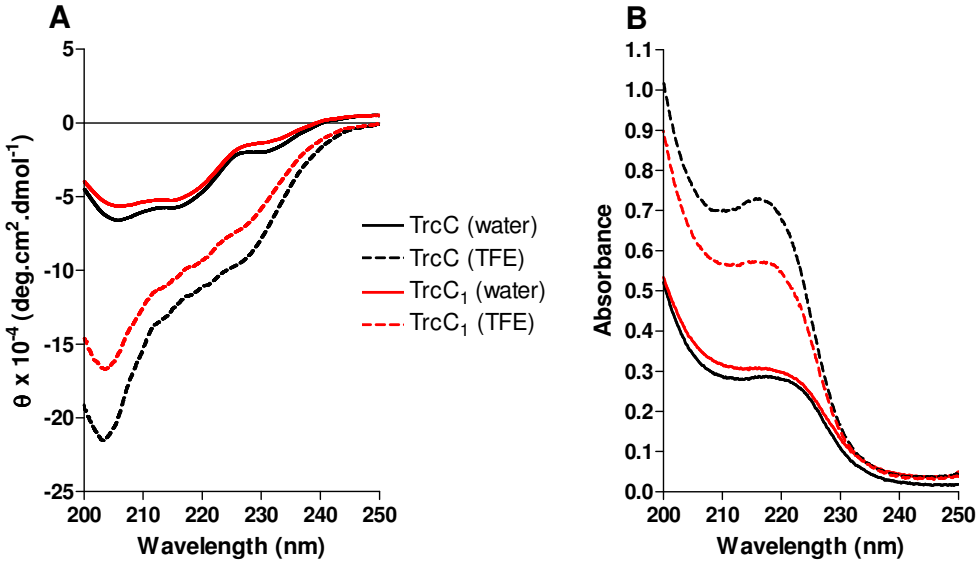

Figure 7 (A) *CD and* (B) *UV absorbance spectra of tryptophan-containing tyrocidines C and* C_1 *in an aqueous and membrane-mimetic environment.* Spectra in an aqueous environment (water) are represented by solid lines; spectra in TFE are represented by dotted lines. The spectra of TrcC are indicated in black; the spectra of $TrcC_1$ are indicated in red. Each CD spectrum is depicted by a Lowess fit line (20 point smoothing window) for an average of triplicate determinations. UV spectra are the average of triplicate determinations.

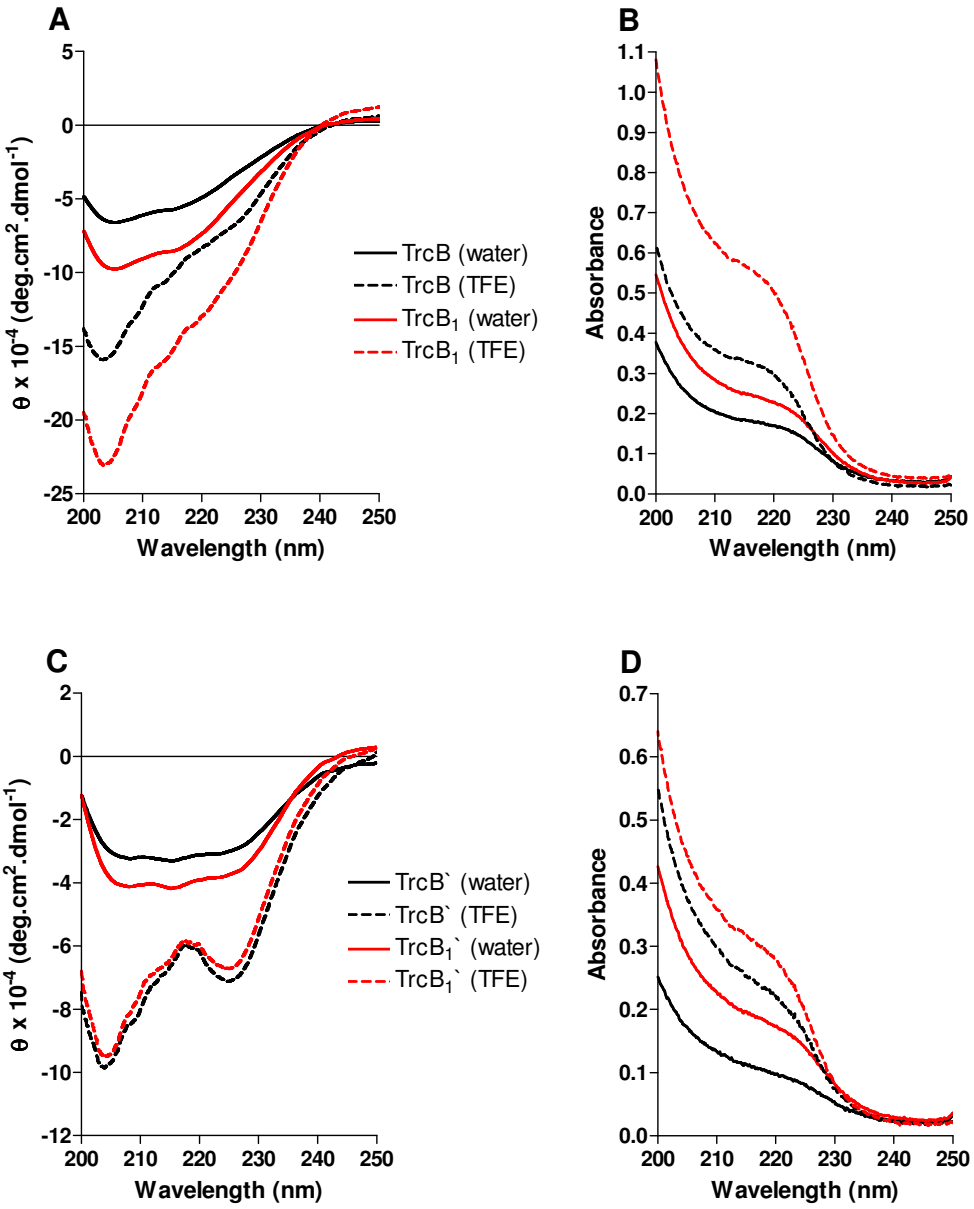

Figure 8 *CD and UV absorbance spectra of tryptophan-containing tyrocidines of the B-group in an aqueous and membrane-mimetic environment.* (A) CD and (B) UV absorbance spectra of TrcB and B_1; (C) CD and (D) UV absorbance spectra of TrcB` and $B_1$`. Spectra in an aqueous environment (water) are represented by solid lines; spectra in TFE are represented by dotted lines. The spectra of TrcB and B` are indicated in black; the spectra of $TrcB_1$ and $B_1$` are indicated in red. Each CD spectrum is depicted by a Lowess fit line (20 point smoothing window) for an average of triplicate determinations. UV spectra are the average of triplicate determinations.

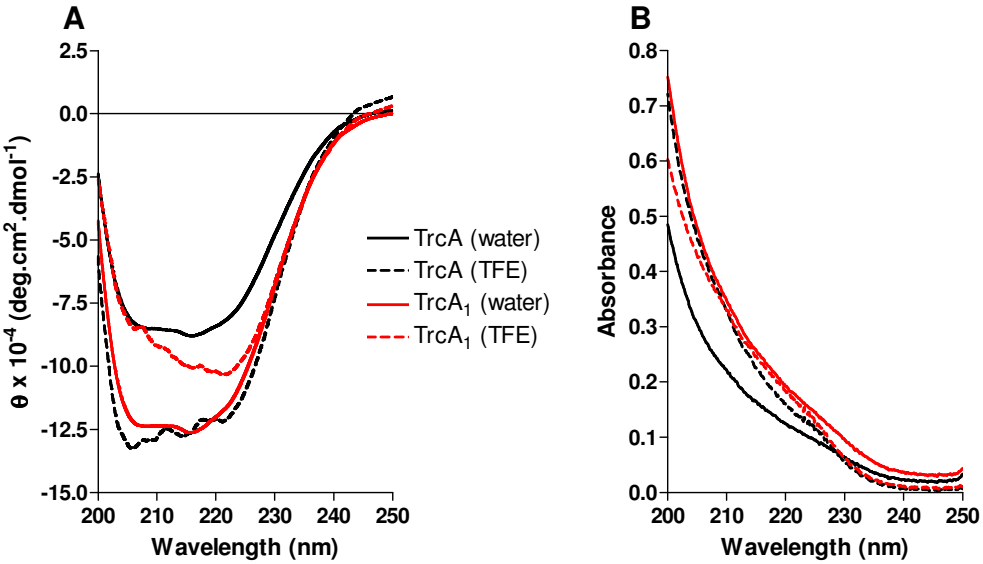

Figure 9 (A) *CD and* (B) *UV absorbance spectra of tryptophan-lacking tyrocidines A and A_1 in an aqueous and membrane-mimetic environment.* Spectra in an aqueous environment (water) are represented by solid lines; spectra in TFE are represented by dotted lines. The spectra of TrcA are indicated in black; the spectra of $TrcA_1$ are indicated in red. Each CD spectrum is depicted by a Lowess fit line (20 point smoothing window) for an average of triplicate determinations. UV spectra are the average of triplicate determinations.

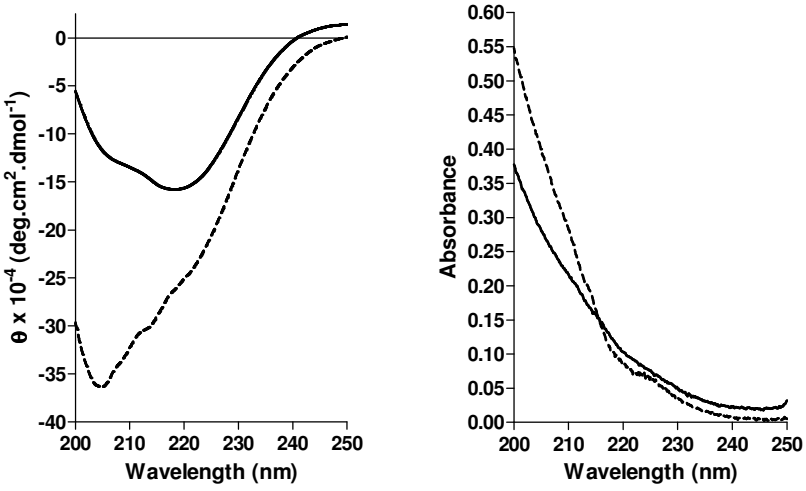

Figure 10 (A) *CD and* (B) *UV absorbance spectra of gramicidin S in an aqueous and membrane-mimetic environment.* Spectra in an aqueous environment are represented by solid lines; spectra in TFE are represented by dotted lines. Each CD spectrum is depicted by a Lowess fit line (20 point smoothing window) for an average of triplicate determinations. UV spectra are the average of triplicate determinations.

3.4.2.2 The influence of the variable amino acids on tyrocidine structure in a membrane-mimetic environment

Comparison of the CD spectra of the Orn^9- and Lys^9-containing tyrocidines indicated differences in θ_{204} and θ_{214}, but similar $\theta_{204}/\theta_{214}$ ratios. As seen in an aqueous environment, Orn^9-containing TrcC exhibited enhanced negative ellipticity relative to Lys^9-containing $TrcC_1$, while Orn^9-containing TrcB exhibited reduced negative ellipticity relative to Lys^9-containing $TrcB_1$ (Figures 7 and 8). These differences are probably related to the orientation/exposure/local environment of the aromatic amino acids as a result of differences in the aggregation state favoured by the Orn^9/Lys^9 content. In contrast, similar CD spectra were observed for tyrocidines B` and $B_1$` (Figure 8), which suggests that the cationic residue does not influence the aggregation state or orientation/exposure/local environment of the aromatic amino acids of these peptides in a membrane-mimetic environment. Differences between the CD spectra of TrcA and A_1 (Figure 9) may also be related to differences in aggregation state, although the generally reduced negative ellipticity of $TrcA_1$ may have been influenced by other factors, such as the settling out of larger self-assembled structures. Comparison of the CD spectra of tyrocidines B, B`, $B_1$ and $B_1$` in a membrane-mimetic environment indicated generally reduced negative ellipticity for tyrocidines B` and $B_1$`, as well as differences in $\theta_{204}/\theta_{214}$ (Figure 8). These differences are probably related to differences in the manner and/or extent of self-assembly due to the different relative positioning of the aromatic residues of the dipeptide unit. Furthermore, the Trp-containing tyrocidines (TrcC, C_1, B, B_1, B` and $B_1$`) exhibited $\theta_{204} > \theta_{214}$, and significantly greater $\theta_{204}/\theta_{214}$ ratios, than the Trp-lacking tyrocidines (TrcA and A_1), which may be indicative of greater hydrogen bonding and therefore more/larger higher-order structures.

Summary and Conclusions: Part 2

The results presented in Part 2 suggest that TFE induces significant changes in the self-assembly state, hydrogen bonding and the orientation/exposure/local environment of the aromatic amino acids. As peptide self-assembly is influenced by the environment/solvent, the manner of association of the tyrocidines, as well as the size of the predominant species, in TFE, which is considered a membrane environment mimic, is expected to differ from that in water. Furthermore, self-assembly of the tyrocidines in an aqueous environment is probably driven by hydrophobic interactions, whereas other interactions, such as hydrogen bonds, are expected to drive self-assembly in TFE,

as TFE disrupts the hydrophobic interactions involved in aggregation [7]. Visual observation indicated that tyrocidine C_1 (the least hydrophobic peptide) formed a small number of large, fibre-like structures just after addition to TFE, which dispersed after mixing. It was hypothesised that the other tyrocidines would also form such structures, albeit too small to be seen. β-sheet peptides are likely to form superstructures upon membrane interaction [10] and induction of large higher-order structures of the tyrocidines in the presence of TFE is supported by the enhanced negative ellipticities, which are indicative of intermolecular interaction (self-assembly) and structural stabilisation [7]. The enhanced negative ellipticity at around 204 nm and the fact that TFE facilitates hydrogen-bond formation [42, 43] suggests that the higher-order structures formed in the presence of TFE are stabilised by intermolecular hydrogen bonding. The manner in which peptide conformation, amphipathicity and available surface area will influence self-assembly in TFE is also expected to be different from that in water. In an aqueous environment, the hydrophobic regions of the peptides will associate in order to shield them from the polar solvent. In contrast, the hydrophobic portions of the peptide are expected to be exposed in TFE, with preferential shielding of the polar regions from the solvent. Differences in the contribution of the aromatic amino acids around 230 nm also suggest differences in the arrangements of peptide molecules within the higher-order structures, resulting in increased exposure of the aromatic residues. The enhanced negative ellipticity around 230 nm was most pronounced for tyrocidines B` and $B_1$`, which further supports the hypothesis of increased exposure of Trp^4 in TFE (Trp^4 is "buried" in water induced self-assembly). Unfortunately, due to the high Raman scattering and fluorescence quenching by TFE, fluorescence spectroscopy could not be applied to evaluate structural changes in a membrane environment.

An additional important observation is that the changes observed for the Trp-containing tyrocidines differ significantly from the changes seen for tyrocidines A and A_1. The Trp-containing tyrocidines exhibited greatly enhanced θ_{204} and less dramatically enhanced θ_{214}, which gives rise in the large increase in $\theta_{204}/\theta_{214}$. These results correlate strongly with the results for GS (Figure 10), which showed greatly enhanced negative ellipticity at 205 nm, less dramatically enhanced θ_{216}, and significantly increased $\theta_{205}/\theta_{216}$. The conformational changes of the Trp-containing tyrocidines upon membrane interaction may therefore be similar to that of GS. In contrast, the θ_{205} and θ_{216} of trcA are enhanced to more similar extents, leading to a less pronounced change in $\theta_{205}/\theta_{216}$.

$TrcA_1$ exhibited reduced θ_{205} and some reduction of θ_{216}, which may be related to the self-assembly state and/or precipitation. These results indicated that the conformational changes of the Trp-lacking tyrocidines upon target membrane interaction may differ significantly from that of the Trp-containing tyrocidines and GS.

3.5 Conclusions

Several deductions could be made from the CD, UV absorbance and fluorescence results. First, the variable cationic residue (Orn^9/Lys^9) and aromatic dipeptide unit ($Phe^{3,4}$/$Trp^{3,4}$) probably influences the manner and/or extent of tyrocidine self-assembly in an aqueous and membrane-mimetic environment. The results suggest that, in an aqueous environment, the Phe^3-containing tyrocidines exhibit greater self-assembly/β-sheet stability than the Trp^3-containing tyrocidines, while the Trp-containing tyrocidines exhibit greater self-assembly/ β-sheet stability than the Trp-lacking tyrocidines in a membrane-mimetic environment. Second, the manner and/or extent of self-assembly in an aqueous and membrane-mimetic environment differ, probably due to different driving forces for association. Last, the Trp-containing and Trp-lacking tyrocidines exhibit differences in the manner and/or extent of self-assembly induced by a membrane-mimetic environment.

The observed differences in self-assembly of the various tyrocidines may be due to the differences in physicochemical properties, such as amphipathicity, hydrophobicity and size (Chapter 4). Furthermore, differences in self-assembly of the various tyrocidines in aqueous solution and a membrane environment are likely to influence the bioactivity (Chapters 5 and 7), and possibly the mode of action (Chapters 6 and 7), of the tyrocidines.

3.6 References

[1] K.H. Lee, Development of short antimicrobial peptides derived from host defense peptides or by combinatorial libraries, Curr. Pharm. Des. 8 (2002) 795-813.

[2] W. Van 't Hof, E.C. Veerman, E.J. Helmerhorst, A.V. Amerongen, Antimicrobial peptides: properties and applicability, Biol. Chem. 382 (2001) 597-619.

[3] N.Y. Yount, A.S. Bayer, Y.Q. Xiong, M.R. Yeaman, Advances in antimicrobial peptide immunobiology, Biopolymers (Pept. Sci.) 84 (2006) 435–458.

[4] M. Stark, L.P. Liu, C.M. Deber, Cationic hydrophobic peptides with antimicrobial activity, Antimicrob. Agents Chemother. 46 (2002) 3585-3590.

[5] C. McInnes, L.H. Kondejewski, R.S. Hodges, B.D. Sykes, Development of the structural basis for antimicrobial and hemolytic activities of peptides based on gramicidin S and design of novel analogs using NMR spectroscopy, J. Biol. Chem. 275 (2000) 14287-14294.

[6] L.H. Kondejewski, D.L. Lee, M. Jelokhani-Niaraki, S.W. Farmer, R.E. Hancock, R.S. Hodges, Optimization of microbial specificity in cyclic peptides by modulation of hydrophobicity within a defined structural framework, J. Biol. Chem. 277 (2002) 67-74.

[7] M. Jelokhani-Niaraki, E.J. Prenner, L.H. Kondejewski, C.M. Kay, R.N. McElhaney, R.S. Hodges, Conformation and other biophysical properties of cyclic antimicrobial peptides in aqueous solutions, J. Pept. Res. 58 (2001) 293-306.

[8] M. Jelokhani-Niaraki, E.J. Prenner, C.M. Kay, R.N. McElhaney, R.S. Hodges, Conformation and interaction of the cyclic cationic antimicrobial peptides in lipid bilayers, J. Pept. Res. 60 (2002) 23-36.

[9] Y. Jin, J. Hammer, M. Pate, Y. Zhang, F. Zhu, E. Zmuda, J. Blazyk, Antimicrobial activities and structures of two linear cationic peptide families with various amphipathic B-sheet and a-helical potentials, Antimicrob. Agents Chemother. 49 (2005) 4957–4964.

[10] N.Y. Yount, M.R. Yeaman, Immunocontinuum: perspectives in antimicrobial peptide mechanisms of action and resistance, Protein Pept. Lett. 12 (2005) 49-67.

[11] P.M. Hwang, H.J. Vogel, Structure-function relationships of antimicrobial peptides, Cell Biol. 76 (1998) 235-246.

[12] Y. Shai, Mode of action of membrane active antimicrobial peptides, Biopolymers (Pept. Sci.) 66 (2002) 236-248.

[13] B. Bechinger, K. Lohner, Detergent-like actions of linear amphipathic cationic antimicrobial peptides, Biochim. Biophys. Acta 1758 (2006) 1529–1539.

[14] E. Guerrero, J.M. Saugar, K. Matsuzaki, L. Rivas, Role of positional hydrophobicity in the leishmanicidal activity of magainin 2, Antimicrob. Agents Chemother. 48 (2004) 2980-2986.

[15] E. Glukhov, M. Stark, L.L. Burrows, C.M. Deber, Basis for selectivity of cationic antimicrobial peptides for bacterial versus mammalian membranes, J. Biol. Chem. 280 (2005) 33960–33967.

[16] A. Scaloni, M. Dalla Serra, P. Amodeo, L. Mannina, R.M. Vitale, A.L. Segre, O. Cruciani, F. Lodovichetti, M.L. Greco, A. Fiore, M. Gallo, C. D'Ambrosio, M. Coraiola, G. Menestrina, A. Graniti, V. Fogliano, Structure, conformation and biological activity of a novel lipodepsipeptide from *Pseudomonas corrugata*: cormycin A, Biochem. J. 384 (2004) 25-36.

[17] D. Andreu, L. Rivas, Animal antimicrobial peptides: an overview, Biopolymers (Pept. Sci.) 47 (1998) 415-433.

[18] R.M. Epand, H.J. Vogel, Diversity of antimicrobial peptides and their mechanisms of action, Biochim. Biophys. Acta 1462 (1999) 11-28.

[19] R.E. Hancock, A. Rozek, Role of membranes in the activities of antimicrobial cationic peptides, FEMS Microbiol. Lett. 206 (2002) 143-149.

[20] K.A. Brogden, Antimicrobial peptides: pore formers or metabolic inhibitors in bacteria?, Nature Rev. Microbiol. 3 (2005) 238-250.

[21] W.A. Gibbons, C.F. Beyer, J. Dadok, R.F. Sprecher, H.R. Wyssbrod, Studies of individual amino acid residues of the decapeptide tyrocidine A by proton double-resonance difference spectroscopy in the correlation mode, Biochemistry 14 (1975) 420-429.

[22] M.C. Kuo, W.A. Gibbons, Nuclear Overhauser effect and cross-relaxation rate determinations of dihedral and transannular interproton distances in the decapeptide tyrocidine A, Biophys. J. 32 (1980) 807-836.

[23] S. Laiken, M. Printz, L.C. Craig, Circular dichroism of the tyrocidines and gramicidin S-A, J. Biol. Chem. 244 (1969) 4454-4457.

[24] C. Krittanai, W.C. Johnson, Correcting the circular dichroism spectra of peptides for contributions of absorbing side chains, Anal. Biochem. 253 (1997) 57-64.

[25] S.M. Kelly, T.J. Jess, N.C. Price, How to study proteins by circular dichroism, Biochim. Biophys. Acta 1751 (2005) 119-139.

[26] M. Jelokhani-Niaraki, R.S. Hodges, J.E. Meissner, U.E. Hassenstein, L. Wheaton, Interaction of gramicidin S and its aromatic amino-acid analog with phospholipid membranes, Biophys. J. 95 (2008) 3306-3321.

[27] L.H. Kondejewski, S.W. Farmer, D.S. Wishart, C.M. Kay, R.E. Hancock, R.S. Hodges, Modulation of structure and antibacterial and hemolytic activity by ring size in cyclic gramicidin S analogs, J. Biol. Chem. 271 (1996) 25261-25268.

[28] L.H. Kondejewski, M. Jelokhani-Niaraki, S.W. Farmer, B. Lix, C.M. Kay, B.D. Sykes, R.E. Hancock, R.S. Hodges, Dissociation of antimicrobial and hemolytic activities in cyclic peptide diastereomers by systematic alterations in amphipathicity, J. Biol. Chem. 274 (1999) 13181-13192.

[29] D.L. Lee, J.-P.S. Powers, K. Pflegerl, M.L. Vasil, R.E.W. Hancock, R.S. Hodges, Effects of single D-amino acid substitutions on disruption of β-sheet structure and hydrophobicity in cyclic 14-residue antimicrobial peptide analogs related to gramicidin S, J. Pept. Res. 63 (2004) 69-84.

[30] M.A. Ruttenberg, T.P. King, L.C. Craig, The use of the tyrocidines for the study of conformation and aggregation behavior, J. Am. Chem. Soc. 87 (1965) 4196-4198.

[31] M.A. Ruttenberg, T.P. King, L.C. Craig, The chemistry of tyrocidine. VII. Studies on association behavior and implications regarding conformation, Biochemistry 5 (1966) 2857-2863.

[32] H.H. Paradies, Aggregation of tyrocidine in aqueous solutions, Biochem. Biophys. Res. Commun. 88 (1979) 810-817.

[33] S.L. Laiken, M.P. Printz, L.C. Craig, Studies on the mode of self-assembly of tyrocidine B, Biochem. Biophys. Res. Commun. 43 (1971) 595-600.

[34] R.C. Williams, D.A. Yphantis, L.C. Craig, Noncovalent association of tyrocidine B, Biochemistry 11 (1972) 70-77.

[35] V.B. Naidoo, The supramolecular chemistry of novel synthetic biomacromolecular assemblies, Polymer science, vol. PhD, University of Stellenbosch, Stellenbosch, 2004.

[36] A. Chattopadhyay, H. Raghuraman, Application of fluorescence spectroscopy to membrane protein structure and dynamics, Curr. Sci. 87 (2004) 175-180.

[37] J.R. Lakowicz, Principles of fluorescence spectroscopy, 3 ed., Springer, New York, 2006.

[38] F.G. Prendergast, P.D. Hampton, B. Jones, Characteristics of tyrosinate fluorescence emission in alpha- and beta-Purothionins, Biochemistry 23 (1984) 6690-6697.

[39] Y. Chen, M.D. Barkley, Toward understanding tryptophan fluorescence in proteins, Biochemistry 37 (1998) 9976-9982.

[40] J.D.J. O'Niel, T. Hofmann, Tyrosine and tyrosinate fluorescence of pig intestinal Ca^{2+}-binding protein, Biochem. J. 243 (1987) 611-615.

[41] M.A. Marques, D.M. Citron, C.C. Wang, Development of tyrocidine A analogues with improved antibacterial activity, Bioorg. Med. Chem. (2007).

[42] Y. Chen, B. Liu, M.D. Barkley, Trifluoroethanol quenches indole fluorescence by excited-state proton transfer, J. Am. Chem. Soc. 117 (1995) 5608-5609.

[43] R. Rajan, P. Balaram, A model for the interaction of trifluoroethanol with proteins and peptides, Int. J. Peptide Protein Res. 48 (1996) 328-336.

Chapter 4

Homology modelling and physicochemical characterisation of the tyrocidines

4.1 Introduction

Physicochemical properties of antimicrobial peptides that influence their biological activity and selectivity include conformation, size, amphipathicity, hydrophobicity, and charge distribution [1-6]. In addition to these physicochemical properties, studies involving the activity of cyclic β-sheet antimicrobial peptides, such as gramicidin S [7-12] and tachyplesin [5], have revealed that the relative positioning of the basic residues and the maintenance of a critical balance in amphipathic character are essential for antimicrobial activity. In order to determine the role of tyrocidine structure in activity modulation and analyse the structure-activity (toxicity) relationships (QSA(T)R), the three-dimensional structure and physicochemical characteristics of the tyrocidines must be elucidated. Furthermore, self-assembly influences the bioactivity of antimicrobial peptides [3, 5, 13-18] and the tendency/ability of antimicrobial peptides to form aggregates/self-assemblies is related to their primary structure, conformation, general topology, amphipathicity and hydrophobicity [10, 16, 17, 19, 20]. As the primary sequence of the tyrocidines was shown to influence self-assembly in both aqueous and membrane-mimetic environments (Chapter 3), the relationship between tyrocidine self-assembly and physicochemical descriptors of hydrophobicity/amphipathicity and size are of particular interest. The physicochemical and self-assembly descriptors, as well as the correlations between them, described in this chapter are of particular significance to the structure-activity relationships discussed in Chapters 5-7.

4.2 Methods

4.2.1 Homology modelling of the tyrocidines and gramicidin S

A low energy model of TrcC, using 2D-NMR NOE constraints, was generated in a collaborative study with the group of Prof. Graham Jackson (University of Cape Town). Homology modelling using the low energy model of TrcC as starting structure of

gramicidin S (GS) and the five other major tyrocidines was done by M. Rautenbach using YASARA 9.10.5© software [21, 22]. TrcB' and $trcB_1$' was mutated from low energy structures of TrcA and $TrcA_1$, respectively. Mutated structures were subjected to a number of 200 fs YASARA molecular dynamic (MD) simulations at 298 K, followed by *in vacuo* energy minimisations using the NOVA force field [22]. Low energy structures were subjected to MD simulations for 400 fs at 333 K, followed by NOVA minimisation in order to test whether the structures have reached global minima. It was assumed that local or global energy minima had been reached once consecutive simulation runs, followed by energy minimisations yielded structures with similar energy minima and structures. Ten low energy structures (average RMSD<1) of each peptide were used to evaluate the secondary structure, intramolecular hydrogen bonding and physicochemical parameters, including solvent accessible volume (SAV) and solvent accessible surface area (SASA) with YASARA 9.10.5©.

4.2.2 Physicochemical characterisation

Basic physicochemical properties that describe hydrophobicity, amphipathicity, conformation and size were determined *in vitro* by analytical RP-HPLC analysis (Chapter 2), circular dichroism (CD) (Chapter 3), calculated using theoretical parameters and *in silico* using models from homology modelling. Theoretical molecular descriptors of hydrophobicity/amphipathicity included hydropathy, lipophilicity (L), and amphipathicity (Q/L). Theoretical hydropathy and lipophilicity were calculated as the sum of the hydropathy indices [23] and lipophilicity parameters (π_{FP}) [24, 25] of the constituent amino acids, respectively. Theoretical amphipathicity was calculated as the ratio of overall charge (Q) to overall lipophilicity (L). The theoretical molecular descriptors of size and charge included theoretical side-chain surface area (SCSA) and theoretical molecular volume, calculated as the sum of the side-chain surface areas and volumes of the constituent amino acids [24], respectively. The *in silico* conformational dependent parameters, calculated from the low energy structures of the tyrocidines using YASARA software, included solvent-accessible surface area (SASA) and solvent accessible volume (SAV). *In vitro* descriptors of conformation were calculated from CD parameters: $\theta_{205}/\theta_{216}$ in water ($\theta_{205}/\theta_{216,\ water}$); $\theta_{204}/\theta_{214}$ in TFE ($\theta_{204}/\theta_{214,\ TFE}$); and change in $\theta_{205}/\theta_{216}$ from water to TFE ($\Delta\ \theta_{205}/\theta_{216,\ water\rightarrow TFE}$). Correlations between the various physicochemical parameters were investigated by performing linear or exponential

regression analysis using GraphPad Prism® 4.00 (GraphPad Software, San Diego, USA).

4.3 Results and Discussion

4.3.1 Homology modelling of the tyrocidines and gramicidin S

A low energy model of TrcC, generated by using 2D-NMR NOE constraints (model courtesy of G. Jackson), was used as the basic structure for the homology modeling of GS and the tyrocidines. Validation of the homology modelling experiments in this study was done by M. Rautenbach who obtained exceptional correspondence of the GS structure (GS was mutated from a low energy TrcC model) to the known GS structure [8, 26-31] (Figure 1). GS adopts an anti-parallel β-sheet/β-turn structure with four hydrogen bonds which is amphipathic due to sequestration of the cationic Orn side chains and D-Phe rings on the hydrophilic face and the four hydrophobic Leu and Val side-chains on the non-polar face [8, 26-31]. The low energy structures of the GS homology model adopted the known antiparallel β-sheet structure composed of Val^{3}-Orn^{4}-Leu^{5} and Val^{8}-Orn^{9}-Leu^{10} and connected by two β-turns composed of D-Phe^{1}-Pro^{2} and D-Phe^{6}-Pro^{7}. The β-sheet in the GS validation model is also stabilised by the known four internal hydrogen bonds: Val^{3}-NH-O-Leu^{10}, Leu^{10}-NH-O-Val^{3}, Leu^{5}-NH-O-Val^{8}, and Val^{8}-NH-O-Leu^{5}. The low energy structures of GS also indicated that the hydrophobic Leu and Val side-chains are located on the non-polar face of the molecule, whereas the D-Phe and cationic Orn side-chains are located on the polar face, leading to a highly amphipathic structure. However, in addition to the backbone amide-carbonyl hydrogen bonds, some of the GS models showed hydrogen bonds between the δ-amide group of Orn^{4}-RNH-O-Pro^{2} and Orn^{9}-RNH-O-Phe^{1}, as well as different D-Phe and Orn rotamers [32] (results not shown).

Comparison of the low energy TrcC model with the GS structure showed good backbone homology, with two corresponding hydrogen bonds in the conserved VOLPF pentapeptide moiety (Figure 1). Previous research concerning TrcA structure indicated that this peptide adopts a type I β-turn/type II` β-turn/β-pleated sheet conformation in solution [33]. Six residues of the backbone ($Val^{8}$-$Orn^{9}$-$Leu^{10}$ and $Phe^{3}$-D-$Phe^{4}$-$Asn^{5}$) form an antiparallel β-pleated sheet structure, which is joined at one end by a type I β-turn composed of $Gln^{6}$-$Tyr^{7}$, and a type II` β-turn composed of D-Phe^{1}-Pro^{2} at the

other end [33, 34]. It has been proposed that the β-sheet moiety is stabilised by four internal hydrogen bonds, analogous to GS (Figure 1), that form between Phe^{3}-NH-O-Leu^{10}, Leu^{10}-NH-O-Phe^{3} and Val^{8}-NH-O-Asn^{5} and Asn^{5}-NH-O-Val^{8} [34]. All the tyrocidines modelled exhibited similar backbone conformations and the secondary structures and hydrogen-bonding observed for these low energy structures correspond to the proposed structures of Gibbons *et al.* (1975) [34] and Kuo *et al.* (1980) [33] (Figures 2 and 3).

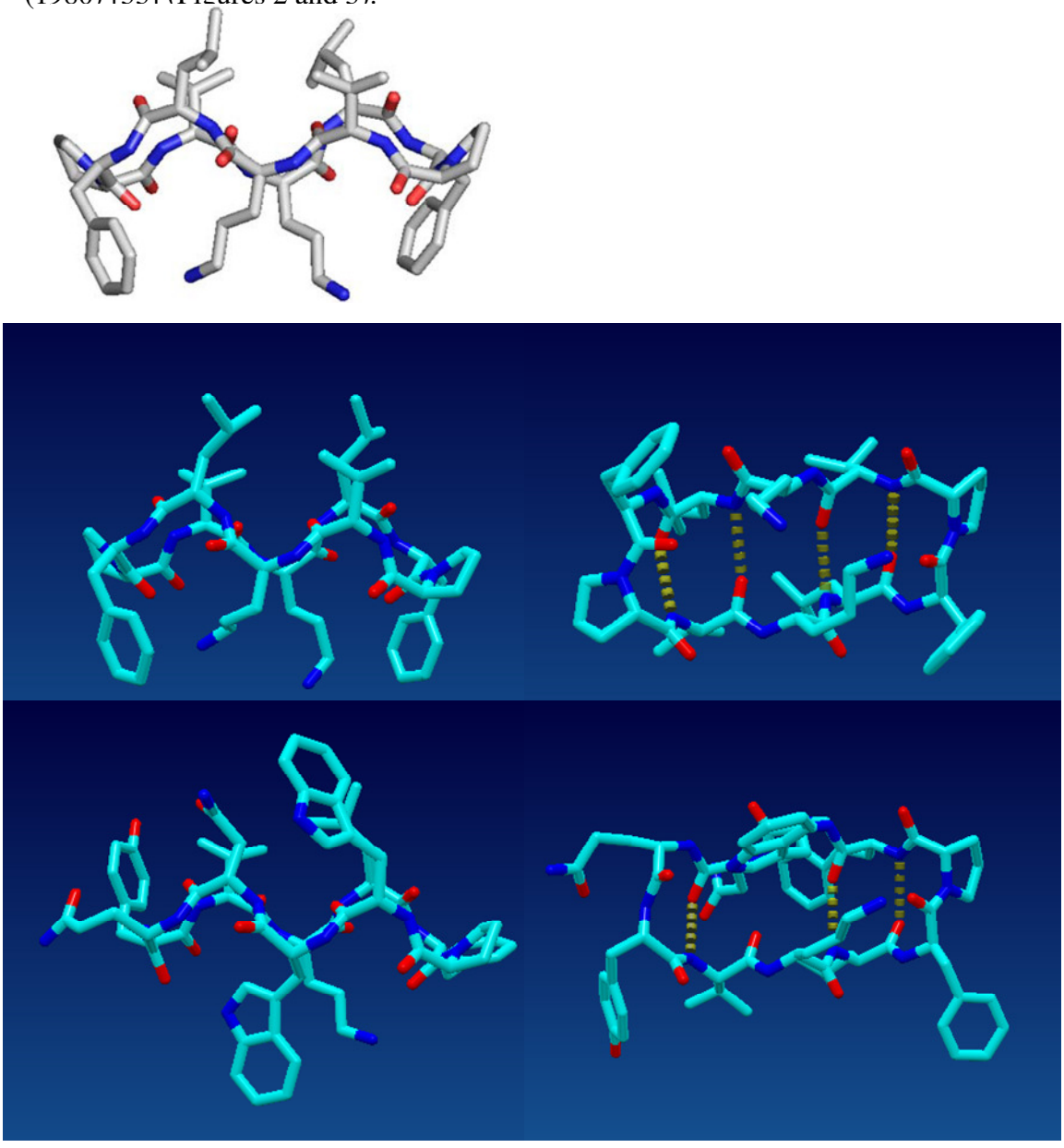

Figure 1 *Low energy molecular models of gramicidin S and tyrocidine C.* The known molecular structure of gramicidin S (top (clear) figure, from Jelokhani-Niaraki *et al.* (2008) [35], corresponds well with the molecular model obtained in this study (middle panel). The low energy model of TrcC (bottom panel) shows high backbone homology to the gramicidin S model. GS and TrcC models courtesy of M. Rautenbach.

Molecular dynamic (MD) simulations run on the TrcC structure showed the exceptional rigidity of the β-sheet backbone structure (Figure 2, data courtesy of M Rautenbach). The β-sheet is composed of Val^{8}-Orn^{9}-Leu^{10} and X^{3}-D-X^{4}-Asn^{5}, where X denotes Trp or Phe. The two strands of the β-sheet are joined by two β-turns composed Gln^{6}-Tyr^{7} and D-Phe^{1}-Pro^{2}. However, in contrast to the four hydrogen bonds that Gibbons *et al.* (1975) [34] predicted in Trc A, all the low energy tyrocidine structures only displayed three internal hydrogen bonds (Phe^{3}-NH-O-Leu^{10}, Leu^{10}-NH-O-Phe^{3} and Val^{8}-NH-O-Asn^{5}) stabilising the β-sheet structure. Only $TrcB_1$ exhibited the formation of Asn^{5}-NH-O-Val^{8} internal hydrogen bond (Figure 3). The Trc homology models also indicated that the Trp^{4} amino group of tyrocidines C, C_1, B` and $B_1$` participate in a hydrogen bond with the backbone carboxyl group of Gln^{6} (Figure 3). In contrast, the Trp^{3} amino-groups do not participate in any hydrogen bonds in the homology models.

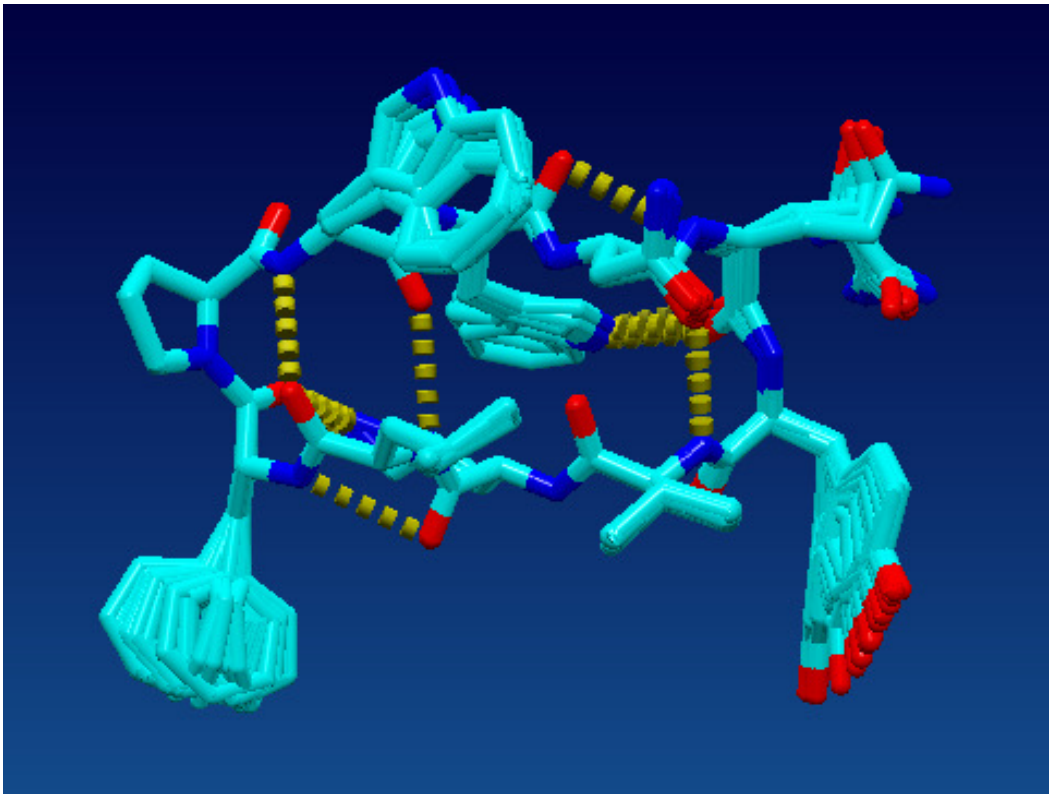

Figure 2 *Overlay of 30 low energy structures of TrcC to show the rigidity of the backbone structure.* The original NOE constrained TrcC structure was subjected to a number of 200 ps YASARA MD simulations at 298 K and minimised with the NOVA forcefield (data courtesy of M Rautenbach).

The homology modelling also indicated that, unlike GS, TrcC does not contain segregated hydrophobic and polar sides (Figures 1 and 2). Instead, an aromatic residue extends from each face of the peptide. An important observation is that the aromatic residues of the variable dipeptide unit extent to opposite sides of the tyrocidine structure, with residue 3 (Phe^3/Trp^3) extending to one side while residue 4 (Phe^4/Trp^4) and the cationic residue (Orn^9/Lys^9) extend toward the opposite side (Figure 3). Such segregation of the variable aromatic residues may have important implications for tyrocidine self-assembly and membrane interaction.

4.3.2 Physicochemical characterisation and correlation between the physicochemical properties of the tyrocidines

The *in vitro*, theoretical and *in silico* physicochemical properties of the tyrocidines that describe hydrophobicity, amphipathicity and size are summarised in Table 1. Investigation of correlations between the various physicochemical parameters may provide an indication of the accuracy of the theoretical descriptors, as well as the extent to which conformation and self-assembly influence the true parameters. In interpreting correlations between the physicochemical properties, it is important to consider the manner in which the parameters were determined as this will determine which peptide properties are taken into consideration.

RP-HPLC retention time, which is representative of apparent hydrophobicity/solution amphipathicity, is determined *in vitro* and the influence of conformation and self-assembly are thus inherently taken into consideration. In contrast, the theoretical descriptors of hydrophobicity/amphipathicity and size only consider the amino acid content, reflecting the combined contribution of the constituent amino acids without considering the influence of conformation or self-assembly.

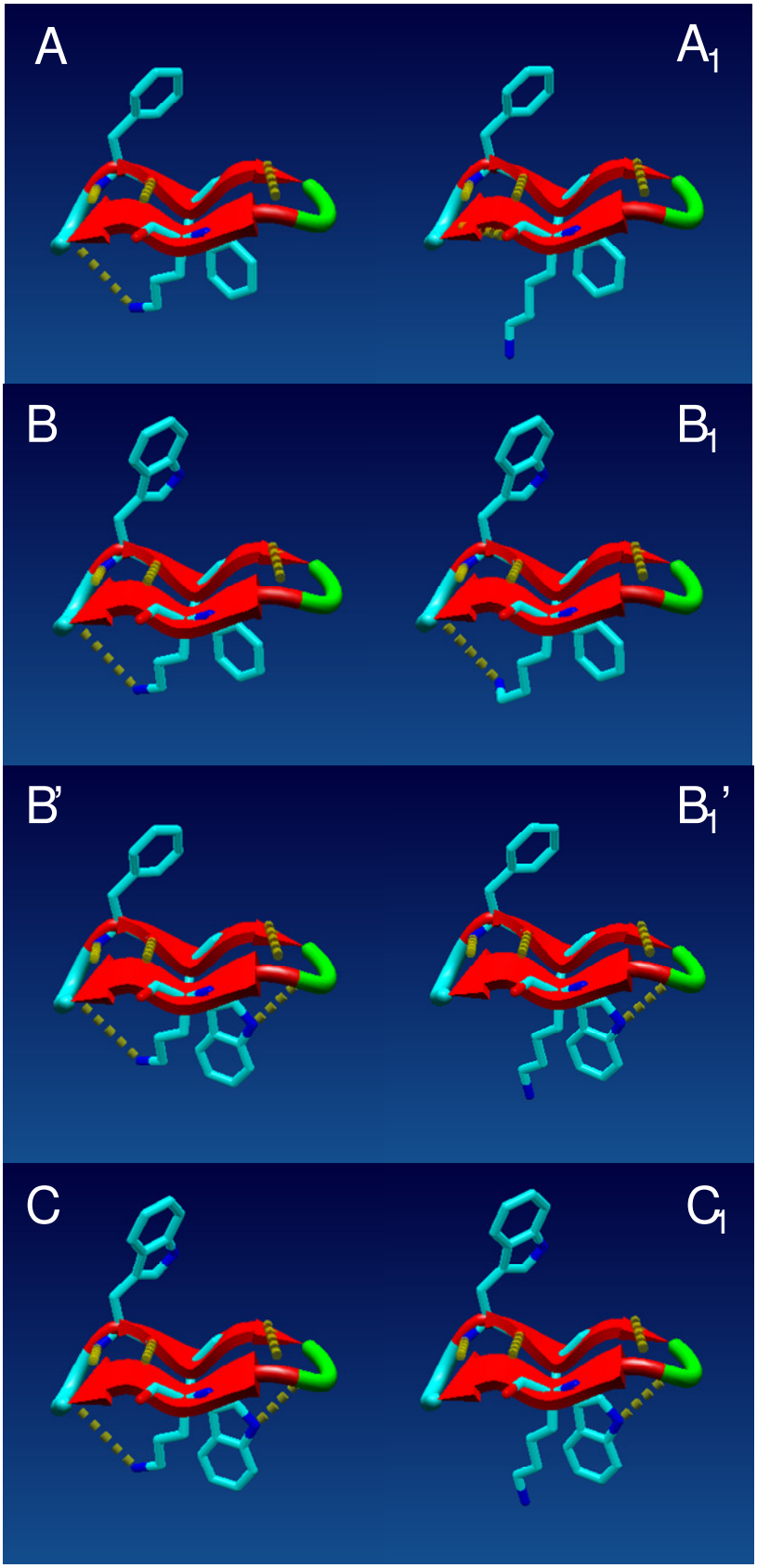

Figure 3 *Low energy molecular models of the tyrocidines showing the β-sheet structure as a ribbon and the side chains of the variable amino acids.* Low energy models of the six major tyrocidines are courtesy of M. Rautenbach

The *in silico* parameters determined from the homology models take the conformation of the peptides into consideration and should thus provide a more accurate estimate of available surface area/volume than the theoretical parameters. It should, however, be kept in mind that the modelling was done *in vacuo*, which influence the results as the peptides may assume different conformations in solution. Furthermore, the *in silico* parameters do not take self-assembly into account and could differ significantly from the "true" available surface area/volume of the tyrocidines in an aqueous solution.

All the physicochemical parameters of the tyrocidines and gramicidin S given in Table 1 were correlated with each other (*in vitro/in silico* with theoretical; *in vitro* with *in silico*, *in vitro* with *in vitro*). Only correlations with $R^2 > 0.80$ were considered for inclusion in this study.

Investigation of correlations between *in vitro* RP-HPLC retention time and theoretical hydropathy, lipophilicity and amphipathicity indicated that the tyrocidines may be categorised into two distinct groups based on their Lys^9/Orn^9 content. The results indicated linear relationships ($R^2 > 0.88$), but with a constant difference between curves representing the Lys^9-containing (tyrocidines A_1, B_1, B1` and $C_1$) and $Orn^9$-containing (tyrocidines A, B, B` and C) peptides (results not shown). RP-HPLC retention time and theoretical amphipathicity (Q/L) exhibited the best correlation with R^2-values of 0.92 and 0.98 for the Orn^9- and Lys^9-containing tyrocidines, respectively (Figure 4A). The required segregation of the Orn^9- and Lys^9-containing tyrocidines suggests that the conformations and/or self-assembly of the two groups are significantly different so as to influence their true solution amphipathicity to different extents. However, homology modelling indicated similar backbone conformations for the Orn^9- and Lys^9-containing tyrocidines (Figures 2 and 3).

Table 1 *Summary of the physicochemical parameters of the tyrocidines and gramicidin S* The theoretical molecular descriptors were calculated from the peptide sequences [36] and documented amino acid properties [23-25].

Parameter	**Type**	**TrcA**	**TrcA$_1$**	**TrcB**	**TrcB$_1$**	**TrcC**	**TrcC$_1$**	**TrcB'**	**TrcB$_1$'**	**GS**
HPLC R_T[1] (minutes)	*In vitro*	11.81	11.33	9.48	9.24	8.31	7.90	8.98	9.72	12.05
Hydropathy[2]	Theoretical	24.0	23.1	23.7	22.8	23.4	22.5	23.7	22.8	29.2
Lipophilicity[3]	Theoretical	9.55	8.16	10.01	8.62	10.47	9.08	10.01	8.62	11.66
Q/L[4]	Theoretical	0.105	0.123	0.100	0.116	0.096	0.110	0.100	0.116	0.172
Side-chain surface area[5] (SCSA, Å^2)	Theoretical	721.9	741.4	750.8	770.3	779.7	799.2	750.8	770.3	648.2
Molecular volume[6] (Å^3)	Theoretical	1582.2	1609.2	1620.1	1647.1	1658.0	1685.0	1620.1	1647.1	1501.8
Solvent accessible surface area[7] (SASA, Å^2)	*In silico*	1199	1208	1217	1231	1267	1269	1277	1253	1170
Solvent accessible volume[7] (SAV, Å^3)	*In silico*	2680	2715	2741	2777	2833	2854	2808	2801	2606
$\theta_{205}/\theta_{216}$ in water	*In vitro*	0.92	0.94	1.15	1.14	1.15	1.03	0.85	0.92	0.75
$\theta_{204}/\theta_{214}$ in TFE	*In vitro*	1.11	0.93	1.51	1.49	1.74	1.68	1.67	1.67	1.42
change in $\theta_{205}/\theta_{216}$ from water to TFE	*In vitro*	21.39	-1.21	31.52	30.28	52.10	63.83	95.85	82.02	89.10

[1] From analytical HPLC chromatograms of purified peptides (Chapter 2).
[2] Sum of hydropathy indices [23] of constituent amino acids.
[3] Sum of lipophilicity parameters (π_{FP}) [24, 25] of constituent amino acids.
[4] Theoretical amphipathicity expressed as ratio between overall charge (Q) and overall lipophilicity (L).
[5] Sum of side-chain surface areas [24] of constituent amino acids.
[6] Sum of residue volumes [24] of constituent amino acids; volume of Orn = volume of Lys – methylene (27Å^3)
[7] *In silico* determination from homology models (average of 10 low energy models).

One difference between the models of the Orn^9- and Lys^9-containing tyrocidines is the participation of the Orn δ-amino group in a backbone hydrogen bond in most of the low energy models, while only a few models indicated such participation of the Lys ε-amino group (Figure 3). It is thus most likely that the Orn^9/Lys^9 content of the tyrocidines influences the extent of self-assembly (size of self-assembly structures) and/or the orientation of the peptide molecules within the higher-order structures. The influence of conformation and/or self-assembly on solution amphipathicity is further illustrated by the different HPLC retention times of TrcB versus B' and $TrcB_1$ versus B_1' (Table 1). These peptides have identical amino acid compositions, varying only in sequence due to inversion of the aromatic dipeptide unit (Phe/Trp^3-D-Phe/D-Trp^4). Although homology modelling indicated similar backbone conformations, the aromatic side-chains of the dipeptide unit were shown to extend to opposite sides of the molecule (Figure 3). The relative positioning of the aromatic residues within the variable dipeptide unit may thus influence the solution amphipathicity (HPLC retention time) directly due to varying exposure of the aromatic residues, and/or indirectly due to differences in the extent or manner of self-assembly.

Investigation of correlations between theoretical and *in silico* molecular descriptors of size indicated a poor correlation ($R^2 = 0.52$) between theoretical side-chain surface area and *in silico* solvent-accessible surface area, which confirms that the influence of peptide conformation on available surface area is sequence-dependent. In contrast, a linear relationship ($R^2 = 0.82$) was observed between theoretical molecular volume and *in silico* solvent-accessible volume (Figure 4B), indicating that the peptide conformation influences the volume of the various tyrocidines in a similar manner/extent. The influence of conformation on accessible surface area and volume is further illustrated by the different solvent-accessible surface areas and solvent-accessible volumes of TrcB versus B' and $TrcB_1$ versus B_1' (Table 1), which may be attributed to the influence of the relative positioning/orientation of the aromatic residues of the variable dipeptide unit.

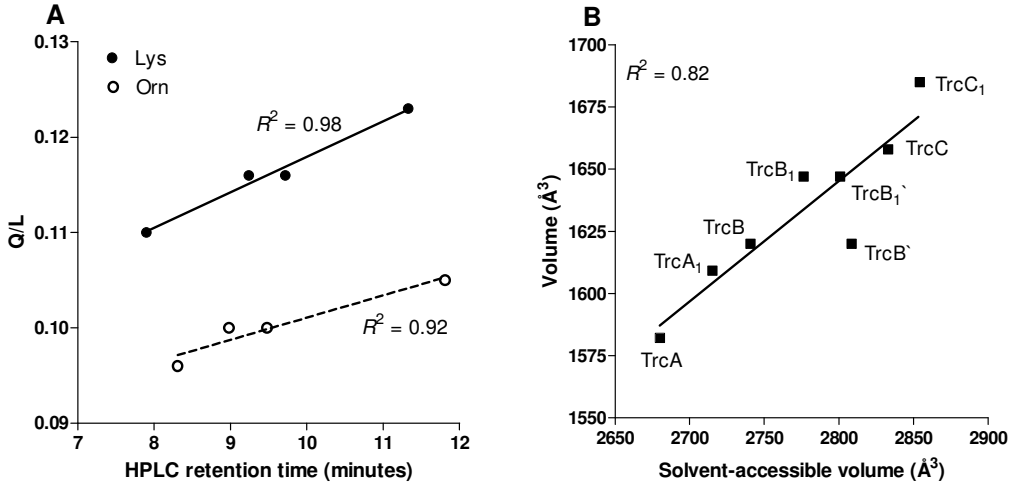

Figure 4 *Linear correlations between molecular descriptors of A. amphipathicity (HPLC R_T and theoretical Q/L) and B. size (theoretical volume and in silico determined solvent accessible volume).*

Inverse linear correlations were observed between HPLC retention time and *in silico* molecular descriptors of size (Figure 5), which, as previously noted by Rautenbach *et al.* (2007) [37], imply that larger peptides may have a weaker interaction with the C_{18} matrix. However, correlations between *in silico* solvent-accessible surface area and HPLC retention required segregation of the Phe^3- ($R^2 = 0.997$) and Trp^3- ($R^2 = 0.95$) containing tyrocidines. The required segregation based on Phe^3/Trp^3 content suggest that the solvent-accessible surface areas of the Phe^3- and Trp^3-containing tyrocidines may differ sufficiently so as to lead to differences in the size of the self-assembly structure in an aqueous solution and/or orientation of peptide molecules within the self-assembly structure. However, the extent and/or manner of self-assembly is less sensitive to differences in the solvent-accessible volume of the Phe^3- and Trp^3-containing tyrocidines as indicated by the linear correlation ($R^2 = 0.88$) observed when peptides are not segregated (Figure 5B).

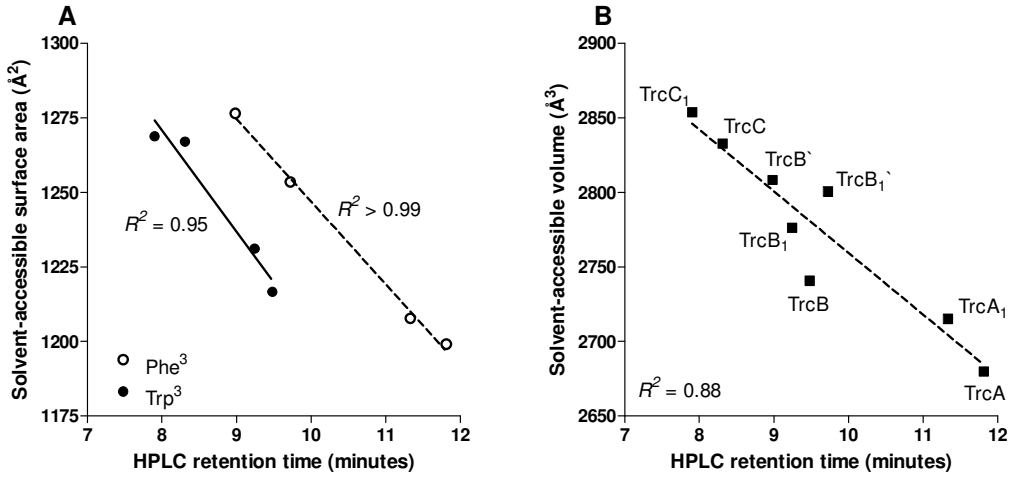

Figure 5 *Linear correlations between molecular descriptors of solution amphipathicity (HPLC retention time) and size A. solvent-accessible surface area and B. solvent-accessible volume).*

4.3.3 Correlation between the physicochemical and CD parameters of the tyrocidines

Circular dichroism ellipticity ratios were chosen as indicators of backbone conformation and self-assembly (different size assemblies and/or different orientation of molecules within the assembly) in an aqueous ($\theta_{205}/\theta_{216}$) and membrane-mimetic ($\theta_{204}/\theta_{214}$) environment. The change in ellipticity ratio from water to TFE ($\Delta\ \theta_{205}/\theta_{216,\ water \rightarrow TFE}$) was chosen as an indicator of induction of secondary structure and self-assembly in a membrane environment. As self-assembly is, at least in part, dictated by physicochemical characteristics of the tyrocidines, correlations between self-assembly and molecular descriptors of hydrophobicity/amphipathicity and size are expected.

No clear correlations were observed between HPLC retention time, solvent-accessible surface area, solvent-accessible volume and $\theta_{205}/\theta_{216}$ in an aqueous environment. However, the identity of residue 3 was found to be an important determinant of the $\theta_{205}/\theta_{216}$ in water, with the Trp^3-containing tyrocidines (TrcC, C_1, B and B_1) exhibiting greater $\theta_{205}/\theta_{216}$ (ranging between 1.0 and 1.2) in water than the Phe^3-containing tyrocidines (TrcA, A_1, B` and $B_1$`) (ranging between 0.85 and 0.94) (Table 1). As discussed in Chapter 3, greater $\theta_{205}/\theta_{216}$ in an aqueous environment is related to lower θ_{216}, which is indicative of reduced β-sheet structure. The greater $\theta_{205}/\theta_{216}$ of the Trp^3-containing tyrocidines may thus imply reduced self-assembly of the Trp^3-containing tyrocidines in an aqueous environment. Such differences in the

tendency for self-assembly of Trp^3- and Phe^3-containing tyrocidines may be related to the influence of differing solvent-accessible surface areas (refer to Figure 4).

A negative linear correlation was observed between $\theta_{204}/\theta_{214}$ in TFE and HPLC retention time ($R^2 = 0.81$) (Figure 6). As greater $\theta_{204}/\theta_{214}$ in TFE is generally associated with enhanced θ_{204}, which is indicative of increased hydrogen bonding and self-assembly (*refer to Chapter 3*), these results suggests that increased solution amphipathicity is associated with reduced β-sheet structure/self-assembly in TFE. Furthermore, the Trp-containing tyrocidines exhibited greater $\theta_{204}/\theta_{214}$ in TFE than the Trp-lacking tyrocidines (Figure 6). The greater $\theta_{204}/\theta_{214}$ of the Trp-containing tyrocidines may thus imply that the presence of Trp (irrespective of position) leads to enhanced β-sheet structure/self-assembly induction in TFE.

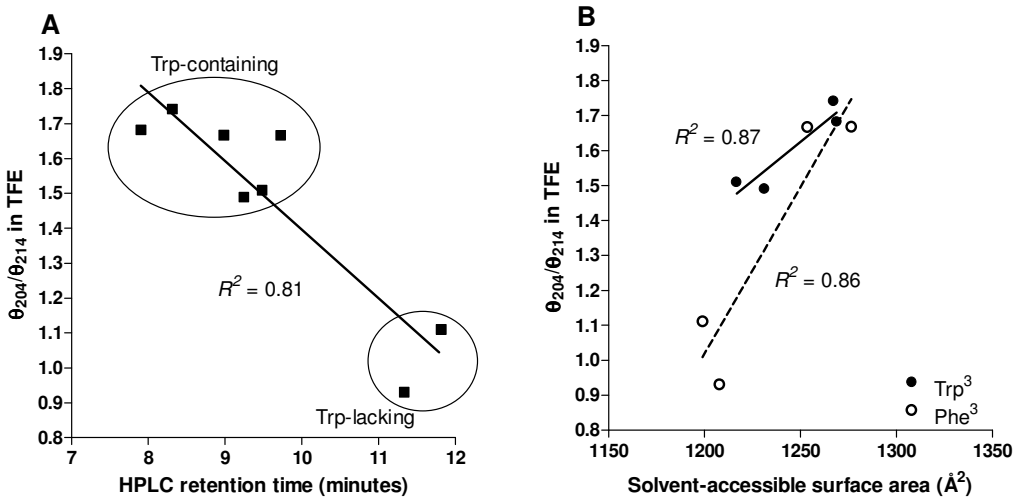

Figure 6 *Correlations between molecular descriptors of solution amphipathicity, size and conformation/self-assembly.* Ellipticity ratio $\theta_{204}/\theta_{214}$ in TFE versus (A) HPLC retention time and (B) *in silico* solvent-accessible surface area.

Positive linear correlations were observed between the $\theta_{204}/\theta_{214}$ in TFE and solvent-accessible surface area of the Phe^3- ($R^2 = 0.86$) and Trp^3- ($R^2 = 0.87$) containing tyrocidines. The required segregation of the Phe^3- and Trp^3-containing tyrocidines indicated that the identity (possibly due to its solvent-accessible surface area) of residue 3 is an important determinant of the tendency for self-assembly in TFE.

Linear correlations were also observed between the Trc changes in CD ellipticity ratio from water to TFE ($\Delta\ \theta_{205}/\theta_{216\ water \rightarrow TFE}$), HPLC retention time and solvent-accessible surface area when the peptides were segregated based on their Phe^3/Trp^3 content (Figure 7). Negative linear correlations were observed between $\Delta\ \theta_{205}/\theta_{216\ water \rightarrow TFE}$ and HPLC retention times of the Phe^3- ($R^2 = 0.87$) and Trp^3- ($R^2 = 0.97$) containing tyrocidines (Figure 7A), which implies that increased solution amphipathicity is associated with reduced inducibility of secondary structure/self-assembly.

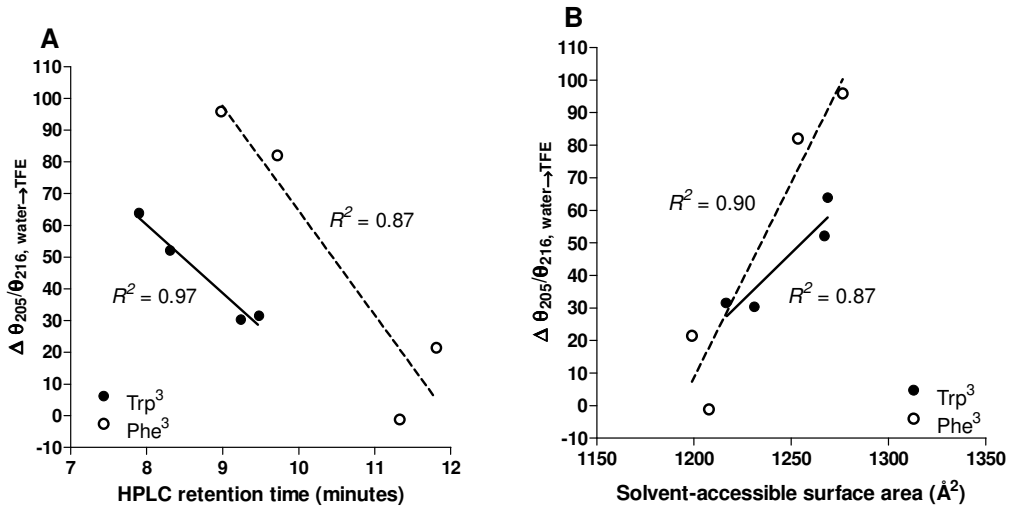

Figure 7 *Correlations between molecular descriptors and change in ellipticity ratio from water to TFE.* Change in ellipticity ratio $\theta_{205}/\theta_{216}$ from water to TFE versus (A) HPLC retention time, and (B) *in silico* solvent-accessible surface area.

Positive linear correlations were observed between $\Delta\ \theta_{205}/\theta_{216\ water \rightarrow TFE}$ and solvent-accessible surface areas of the Phe^3- ($R^2 = 0.90$) and Trp^3- ($R^2 = 0.87$) containing tyrocidines (Figure 7B), which implies that increased solvent-accessible surface area is associated with enhanced inducibility of secondary structure/self-assembly. The required segregation of the Phe^3- and Trp^3-containing tyrocidines indicated that the identity of residue 3 is an important determinant of inducibility of secondary structure/self-assembly in TFE. Furthermore, the identity of residue 4 was found to be an important determinant of inducibility of secondary structure/self-assembly, with the Trp^4-containing tyrocidines (TrcC, C_1, B and B_1) exhibiting greater change in $\theta_{205}/\theta_{216}$ than the Phe^4-containing tyrocidines (TrcA, A_1, B` and $B_1$`) (Table 1).

4.4 Conclusions

Correlations between *in vitro*, *in silico* and theoretical molecular descriptors indicated that the three-dimensional conformation, extent and/or manner of self-assembly of the tyrocidines influence both the true solution amphipathicity and available surface area/volume. The influence of the cationic residue on true solution amphipathicity, the sequence-dependence of solvent-accessible surface area and the influence of conformation on solvent-accessible surface area suggest that the theoretical descriptors do not provide an accurate reflection of the physicochemical character of the tyrocidines in solution. Although the theoretical molecular descriptors may be used to perform QSAR analyses, these results suggest that *in vitro* and *in silico* physicochemical parameters should be used as far as possible.

Correlations between *in vitro* solution amphipathicity (HPLC retention time) and *in silico* descriptors of size suggested that the solvent-accessible surface areas of the Phe^3- and Trp^3-containing tyrocidines may differ sufficiently so as to lead to differences in amphipathicity, the manner and/or extent of self-assembly. This hypothesis is supported by correlations observed between *in vitro* solution amphipathicity (HPLC retention time) and CD-derived descriptors of conformation/self-assembly in an aqueous environment, which suggested reduced self-assembly of the Trp^3-containing tyrocidines relative to Phe^3-containing tyrocidines. Correlations between *in vitro* solution amphipathicity, *in silico* solvent-accessible surface area and CD-derived descriptors of conformation/self-assembly in TFE (membrane-mimetic environment) suggested that decreased solution amphipathicity and greater solvent-accessible surface area is associated with enhanced β-sheet structure/self-assembly. Furthermore, the presence of Trp (irrespective of position) was found to be associated with enhanced β-sheet structure/self-assembly in TFE. Correlations between *in vitro* solution amphipathicity, *in silico* solvent-accessible surface area and CD-derived descriptors of inducibility of conformation/self-assembly suggested that decreased solution amphipathicity and greater solvent-accessible surface area is associated with enhanced inducibility of secondary structure/self-assembly. However, it may also indicate that increased solution amphipathicity may lead to an increased loss of peptide due to the formation of large structures in TFE. Furthermore, greater inducibility of secondary structure/self-assembly was seen for the Trp^4-containing tyrocidines (TrcC, C_1, B and

B_1) than the Phe^4-containing tyrocidines (TrcA, A_1, B` and $B_1$`). However, this result may also indicate that the Phe^4-containing tyrocidines may already be approaching maximal self-assembly in an aqueous solution, leading to lower observed inducibility of secondary structure/self-assembly in TFE.

Overall, the results illustrate the importance of the variable cationic residue and aromatic dipeptide unit in peptide conformation and/or self-assembly. The identity of residue 3 was found to be an important determinant of β-sheet structure/self-assembly in both an aqueous and membrane-mimetic environment, while the identity of both residues 3 and 4 are important determinants of inducibility of secondary structure/self-assembly.

4.5 References

[1] R.M. Epand, H.J. Vogel, Diversity of antimicrobial peptides and their mechanisms of action, Biochim. Biophys. Acta 1462 (1999) 11-28.

[2] W. Van 't Hof, E.C. Veerman, E.J. Helmerhorst, A.V. Amerongen, Antimicrobial peptides: properties and applicability, Biol. Chem. 382 (2001) 597-619.

[3] Y. Shai, From innate immunity to *de-novo* designed antimicrobial peptides, Curr. Pharm. Des. 8 (2002) 715-725.

[4] M. Jelokhani-Niaraki, E.J. Prenner, C.M. Kay, R.N. McElhaney, R.S. Hodges, Conformation and interaction of the cyclic cationic antimicrobial peptides in lipid bilayers, J. Pept. Res. 60 (2002) 23-36.

[5] N.Y. Yount, M.R. Yeaman, Immunocontinuum: perspectives in antimicrobial peptide mechanisms of action and resistance, Protein Pept. Lett. 12 (2005) 49-67.

[6] O. Toke, Antimicrobial peptides: new candidates in the fight against bacterial infections, Biopolymers (Pept. Sci.) 80 (2005) 717-735.

[7] E.J. Prenner, R.N. Lewis, K.C. Neuman, S.M. Gruner, L.H. Kondejewski, R.S. Hodges, R.N. McElhaney, Nonlamellar phases induced by the interaction of gramicidin S with lipid bilayers. A possible relationship to membrane-disrupting activity, Biochemistry 36 (1997) 7906-7916.

[8] E.J. Prenner, R.N. Lewis, R.N. McElhaney, The interaction of the antimicrobial peptide gramicidin S with lipid bilayer model and biological membranes, Biochim. Biophys. Acta 1462 (1999) 201-221.

[9] M. Jelokhani-Niaraki, L.H. Kondejewski, S.W. Farmer, R.E.W. Hancock, C.M. Kay, R.S. Hodges, Diastereoisomeric analogues of gramicidin S: structure, biological activity and interaction with lipid bilayers, Biochem. J. 349 (2000) 747-755.

[10] M. Jelokhani-Niaraki, E.J. Prenner, L.H. Kondejewski, C.M. Kay, R.N. McElhaney, R.S. Hodges, Conformation and other biophysical properties of cyclic antimicrobial peptides in aqueous solutions, J. Pept. Res. 58 (2001) 293-306.

[11] E.J. Prenner, R.N.A.H. Lewis, R.N. McElhaney, The interaction of the antimicrobial peptide gramicidin S with lipid bilayer model and biological membranes, Biochim. Biophys. Acta 1462 (1999) 201-221.

[12] E.J. Prenner, R.N.A.H. Lewis, K.C. Neuman, S.M. Gruner, L.H. Kondejewski, R.S. Hodges, R.N. McElhaney, Nonlamellar phases induced by the interaction of gramicidin S with lipid bilayers: a possible relationship to membrane-disrupting activity, Biochemistry and Cell Biology 36 (1997) 7906-7916.

[13] N.Y. Yount, A.S. Bayer, Y.Q. Xiong, M.R. Yeaman, Advances in antimicrobial peptide immunobiology, Biopolymers (Pept. Sci.) 84 (2006) 435–458.

[14] P.M. Hwang, H.J. Vogel, Structure-function relationships of antimicrobial peptides, Cell Biol. 76 (1998) 235-246.

[15] B. Bechinger, K. Lohner, Detergent-like actions of linear amphipathic cationic antimicrobial peptides, Biochim. Biophys. Acta 1758 (2006) 1529–1539.

[16] E. Guerrero, J.M. Saugar, K. Matsuzaki, L. Rivas, Role of positional hydrophobicity in the leishmanicidal activity of magainin 2, Antimicrob. Agents Chemother. 48 (2004) 2980-2986.

[17] A. Scaloni, M. Dalla Serra, P. Amodeo, L. Mannina, R.M. Vitale, A.L. Segre, O. Cruciani, F. Lodovichetti, M.L. Greco, A. Fiore, M. Gallo, C. D'Ambrosio, M. Coraiola, G. Menestrina, A. Graniti, V. Fogliano, Structure, conformation and biological activity of a novel lipodepsipeptide from *Pseudomonas corrugata*: cormycin A, Biochem. J. 384 (2004) 25-36.

[18] E. Glukhov, M. Stark, L.L. Burrows, C.M. Deber, Basis for selectivity of cationic antimicrobial peptides for bacterial versus mammalian membranes, J. Biol. Chem. 280 (2005) 33960–33967.

[19] V. Frecer, B. Ho, J.L. Ding, *De novo* design of potent antimicrobial peptides, Antimicrob. Agents Chemother. 48 (2004) 3349-3357.

[20] S. Rotem, I. Radzishevsky, A. Mor, Physicochemical properties that enhance discriminative antibacterial activity of short dermaseptin derivatives, Antimicrob. Agents Chemother. 50 (2006) 2666-2672.

[21] www.yasara.org.

[22] E. Krieger, G. Koraimann, G. Vriend, Increasing the precision of comparative models with YASARA NOVA - a self-parameterizing force field, Proteins 47 (2002) 393-402.

[23] A. Tossi, Sandri, L., Giangaspero, A., New consensus hydrophobicity scale extended to non-proteinogenic amino acids, in: E. Benedetti, Pedone,C. (Ed.), Proceedings of the 27th European Peptide Symposium, Sorrento, 2002.

[24] V. Frecer, QSAR analysis of antimicrobial and haemolytic effects of cyclic cationic antimicrobial peptides derived from protegrin-1, Bioorg. Med. Chem. 14 (2006) 6065-6074.

[25] J.L. Fauchere, V. Pliska, Hydrophobic parameters-Pi of amino-acid side-chains from the partitioning of N-acetyl-amino-acid amides, Eur. J. Med. Chem. 18 (1983) 369-375.

[26] G.F. Gause, M.G. Brazhnikova, Nature (London) 154 (1944).

[27] A.R. Battersby, L.C. Craig, J. Am. Chem. Soc. 73 (1951) 1887-1888.

[28] D.C. Hodgekin, B.M. Oughton, Biochem. J. 65 (1957) 752-756.

[29] A. Stern, W.A. Gibbons, L.C. Craig, Proc. Nat. Acad. Sci. 61 (1968) 643-741.

[30] I.D. Rae, H.A. Scherage, Biochem. Biophys. Res. Commun. 81 (1978) 481-485.

[31] L.H. Kondejewski, S.W. Farmer, D.S. Wishart, C.M. Kay, R.E. Hancock, R.S. Hodges, Modulation of structure and antibacterial and hemolytic activity by ring size in cyclic gramicidin S analogs, J. Biol. Chem. 271 (1996) 25261-25268.

[32] C. Jones, M.C. Kuo, W.A. Gibbons, Multiple solution conformations and internal rotations of the decapeptide gramicidin S, J. Biol. Chem. 254 (1979) 10307-10312.

[33] M.C. Kuo, W.A. Gibbons, Nuclear Overhauser effect and cross-relaxation rate determinations of dihedral and transannular interproton distances in the decapeptide tyrocidine A, Biophys. J. 32 (1980) 807-836.

[34] W.A. Gibbons, C.F. Beyer, J. Dadok, R.F. Sprecher, H.R. Wyssbrod, Studies of individual amino acid residues of the decapeptide tyrocidine A by proton double-resonance difference spectroscopy in the correlation mode, Biochemistry 14 (1975) 420-429.

[35] M. Jelokhani-Niaraki, R.S. Hodges, J.E. Meissner, U.E. Hassenstein, L. Wheaton, Interaction of gramicidin S and its aromatic amino-acid analog with phospholipid membranes, Biophys. J. 95 (2008) 3306-3321.

[36] X.-J. Tang, P. Thibault, R.K. Boyd, Characterisation of the tyrocidine and gramicidin fractions of the tyrothricin complex from *Bacillus brevis* using liquid chromatography and mass spectrometry, Int. J. Mass Spectrom. Ion Process. 122 (1992) 153-179.

[37] M. Rautenbach, N.M. Vlok, M. Stander, H.C. Hoppe, Inhibition of malaria parasite blood stages by tyrocidines, membrane-active cyclic peptide antibiotics from *Bacillus brevis*, Biochim. Biophys. Acta - Biomembranes 1768 (2007) 1488–1497.

Chapter 5

Anti-listerial activity and structure-activity relationships of the six major tyrocidines, cyclic decapeptides from *Bacillus aneurinolyticus*

This chapter has been published in *Bioorganic and Medicinal Chemistry*, Volume 17, June 2009, pages 5541-5548; first author B. M. Spathelf (all experimental work, data analysis, writing of article), co-author. M. Rautenbach (co-writer and editing, critical evaluation of study and data). The article, as published, is included as Chapter 5 of this thesis.

Bioorganic & Medicinal Chemistry 17 (2009) 5541–5548

Contents lists available at ScienceDirect

Bioorganic & Medicinal Chemistry

journal homepage: www.elsevier.com/locate/bmc

Anti-listerial activity and structure–activity relationships of the six major tyrocidines, cyclic decapeptides from *Bacillus aneurinolyticus*

Barbara M. Spathelf, Marina Rautenbach *

BIOPEP Peptide Group, Department of Biochemistry, University of Stellenbosch, Private Bag X1, Matieland 7602, South Africa

ARTICLE INFO

Article history:
Received 9 April 2009
Revised 8 June 2009
Accepted 14 June 2009
Available online 21 June 2009

Keywords:
Tyrocidines
Antibacterial activity
Listeria monocytogenes
QSAR

ABSTRACT

Six major tyrocidines, purified from the antibiotic tyrothricin complex produced by *Bacillus aneurinolyticus*, showed significant lytic and growth inhibitory activity towards the Gram+ bacteria, *Micrococcus luteus* and *Listeria monocytogenes,* but not against the Gram− bacterium, *Escherichia coli*. The isolated natural tyrocidines were in particular more active against the leucocin A (antimicrobial peptide) resistant strain, *L. monocytogenes* B73-MR1, than the sensitive *L. monocytogenes* B73 strain. Remarkably similar structure–activity trends toward the three Gram+ bacteria were found between growth inhibition and different physicochemical parameters (solution amphipathicity, theoretical lipophilicity, side-chain surface area and mass-over-charge ratio).

1. Introduction

The necessity for the development of a new class of antimicrobial agents is underlined by the rapid emergence of microbial resistance to classical antibiotics.[1] Over the past two decades, antimicrobial peptides have been considered as candidates for development of therapeutic agents and bio-preservatives.[1] The broad spectrum antimicrobial activity, selectivity, speed of action, and reduced likelihood of resistance development toward antimicrobial peptides implies that these compounds may serve as invaluable templates for the development of novel therapeutic agents.[1]

Almost 70 years ago Dubos and Hotchkiss[2] found potent antimicrobial activity in the fermentation broth of *Bacillus brevis*, now classified as *Bacillus aneurinolyticus.* This activity was due to a diverse group of antimicrobial peptides collectively known as the tyrothricin complex, which is composed of the basic, cyclic tyrocidines and neutral, linear gramicidins.[2,3] Tyrothricin was one of the first antibiotics in clinical use, albeit as topical antibiotic.[4] The primary structures of 28 tyrocidines and analogues have been determined,[3] and a study by Gibbons et al.[5] suggests that these cyclic decapeptides assume antiparallel β-pleated sheet structures. The tyrocidines contain one of the pentapeptide repeats of gramicidin S, Val-Orn-Leu-Pro-D-Phe. In some tyrocidines the Orn residue is substituted with Lys (Table 1, Fig. 1).[3] The other five residues in the tyrocidines differ only by conservative substitutions in the aromatic dipeptide unit.[3] In some of the minor tyrocidines the aliphatic residues in the gramicidin S pentapeptide, Val and Leu, are substituted by other aliphatic residues. In the tyrocidine-like peptides the invariable Tyr is substituted with Trp (tryptocidines) or Phe (denoted as phenicidines by our group).[3] The tyrocidines are known to possess broad spectrum antimicrobial activity toward Gram-positive and Gram-negative bacteria[6] and parasites, notably the malarial parasite *Plasmodium falciparum*.[7] Since the antibacterial studies early last century on the tyrocidine mixture, only a few follow up molecular and activity studies were conducted. These studies mostly involved investigation of the structure[3,5,8,9] and aggregation properties[9–11] of the tyrocidines, generation of synthetic analogue libraries,[12,13] and the antiplasmodial activity of the major tyrocidines.[7]

We decided to revisit the natural antimicrobial peptide library of tyrocidines and focused on the six major tyrocidines (Table 1) and their structure–activity relationships, with the food-borne pathogen, *Listeria monocytogenes*, as one of the bacterial targets. *L. monocytogenes* is the causative agent of listeriosis, a severe disease with high hospitalisation and case fatality rates.[14] As with many pathogenic microbes, the development of resistance of *L. monocytogenes* to antibiotics poses a major problem with the severity of listeriosis, in addition to the economic impact of big product recalls, necessitating the development of preventative measures to control the spread of *L. monocytogenes*.[14] Nisin, a bacteriocin produced by lactic acid bacteria, was the first antibiotic peptide to be approved as a bio-preservative for the control of food spoilage organisms, including *L. monocytogenes*.[15] Unfortunately, nisin-resistant *Listeria* strains have already been identified,[16] necessitating the development of alternative preservatives and treatments.

* Corresponding author. Tel.: +27 21 8085872/8; fax: +27 21 8085863.
E-mail address: mra@sun.ac.za (M. Rautenbach).

0968-0896/$ - see front matter © 2009 Elsevier Ltd. All rights reserved.
doi:10.1016/j.bmc.2009.06.029

Table 1
Summary of the purification and characterisation data of the eight tyrocidines in this study

Identity	Abbreviation	Sequence	HPLC t_R (min)	Monoisotopic Mr observed (expected)
Tyrocidine A	TrcA	*Cyclo*-(VQLfPFfNQY)	11.81	1269.64 (1269.70)
Tyrocidine A_1	$TrcA_1$	*Cyclo*-(VKLfPFfNQY)	11.33	1283.71 (1283.70)
Tyrocidine B	TrcB	*Cyclo*-(VQLfPWfNQY)	9.48	1308.66 (1308.70)
Tyrocidine B_1	$TrcB_1$	*Cyclo*-(VKLfPWfNQY)	9.24	1322.69 (1322.70)
Tyrocidine C	TrcC	*Cyclo*-(VQLfPWwNQY)	8.31	1347.67 (1347.70)
Tyrocidine C_1	$TrcC_1$	*Cyclo*-(VKLfPWwNQY)	7.90	1361.69 (1361.70)
Gramicidin S	GS	*Cyclo*-(VQLfPVQLfP)	12.05	1140.72 (1140.70)

The HPLC retention times of the six natural tyrocidines and two synthetic tyrocidines were obtained from analytical HPLCs of the purified tyrocidines; the observed monoisotopic weights were calculated from ESMS spectra of the purified peptides; the expected monoisotopic weights were calculated as the sum of the molecular weights of the constituent amino acids. The percentage purity of all the purified tyrocidines was >95%, as calculated from analytical HPLC analyses at 254 nm. Standard one letter abbreviations are used for the amino acid residues, except for ornithine that was denoted as O. D-residues are given in lower case letters. The underlined residues highlight the variable cationic residue and variable aromatic dipeptide unit.

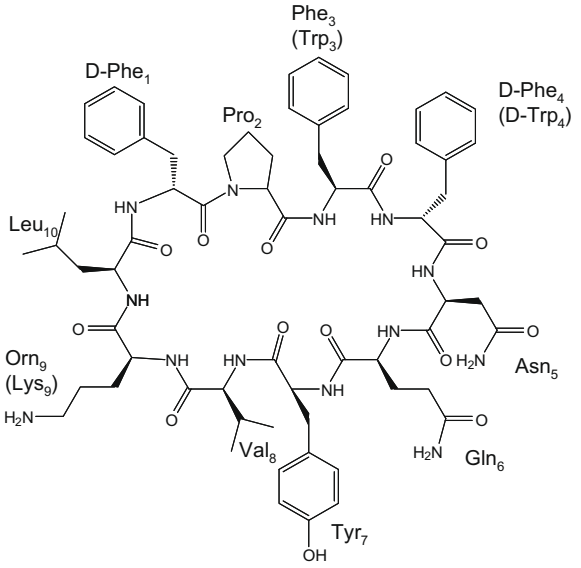

Figure 1. The primary structure of the cyclic depapeptide antibiotic, tyrocidine A. Standard three letter abbreviations are used for the amino acid residues, except for ornithine that was denoted as Orn. Amino acid abbreviations in brackets indicates the variable amino acid identities in the other tyrocidines (refer to Table 1 for detail). The numbering of the peptide chain is based on the biological synthesis sequence.

The tyrocidines may be promising templates for alternative treatments for various bacterial infections, especially as bio-preservatives or as 'last-resort' chemotherapeutic agents. In order to develop the tyrocidines into therapeutic agents or bio-preservatives, insight regarding their structure–activity relationships and mechanism of action is imperative. An understanding of the structure–function relationships may allow for the development of more efficacious molecules, improved selectivity and reduced toxicity, as well as provide insight regarding the mechanism of action and possible resistance. Therefore, the aims of this study were to purify the major tyrocidines found in the tyrothricin complex, determine the relative activities of the different tyrocidines toward Gram-positive bacteria, in particular *L. monocytogenes*, and Gram-negative bacteria, and quantify any correlation between the structural characteristics and the activities of these peptides.

2. Materials

The tyrothricin (from *B. aneurinolyticus*), gramicidin S, trifluoroacetic acid (TFA, >98%) and Corning Incorporated® cell culture cluster, non-pyrogenic polypropylene microtiter plates was supplied by Sigma (St. Louis, USA). The microtiter plates (Nunc™-Immuno Maxisorp) and culture dishes were supplied by AEC Amersham (Johannesburg, South Africa) and Lasec (Cape Town, South Africa), respectively. The diethyl ether, acetone, butan-1-ol, acetic acid, propan-2-ol, agar powder, NaCl and disodium EDTA were supplied by Saarchem (Krugersdorp, South Africa). Acetonitrile (ACN) (HPLC-grade, far UV cut-off) and was supplied by Romill Ltd (Cambridge, UK). Biolab Diagnostics (Midrand, South Africa) supplied the tryptone, yeast extract and tryptone soy broth (TSB), brain heart infusion broth (BHI) and BHI agar. Bovine milk casein and was supplied by Fluka Chemicals (Buchs, Switzerland). The Na_2HPO_4 and KH_2PO_4 and ethanol (>99.8%) were supplied by Merck (Darmstadt, Germany). Capital Enterprises (Hillcrest, South Africa) supplied the KCl. Waters-Millipore (Milford, USA) supplied the Nova-Pak® C_{18} (5 μm particle size, 60 Å pore size, 150 mm × 3.9 mm) reverse-phase analytical column and the Nova-Pak® C_{18} (6 μm particle size, 60 Å pore size, 7.8 mm × 300 mm) semi-preparative HPLC column. Analytical grade water was prepared by filtering water from a reverse osmosis plant through a Millipore Milli-Q® water purification system (Milford, USA).

3. Methods

3.1. Peptide purification and characterisation

The six major tyrocidines were isolated from commercially obtained tyrothricin. The crude fractionation was performed by organic extraction, as described by Hotchkiss and Dubos (1941),[2] with some modifications. Briefly, the tyrothricin in dry powder form was washed three times with equal volumes ether/acetone (1:1, *v/v*) and the insoluble fraction/precipitate containing the tyrocidines was collected by centrifugation and dried under vacuum. The tyrocidines in the tyrocidine fraction were subsequently purified by reverse-phase high performance liquid chromatography (RP-HPLC), according to the methods described by Rautenbach et al. (2007).[7] The collected fractions were subjected to analytical RP-HPLC,[7] time-of-flight electrospray mass spectrometry (TOF-ESMS), and tandem mass spectroscopy (MS–MS) in order to determine the degree of purity of each fraction and to identify the purified product. TOF-ESMS and MS–MS analyses were performed using a Waters Q-TOF Ultima mass spectrometer fitted with an electrospray ionisation source. For TOF-ESMS, 10 μL of each peptide sample (10 μg/mL in acetonitrile/water, 1:1, *v/v*) was injected into the ESMS and subjected to a capillary voltage of 3.5 kV. The source temperature and cone voltage was set at 100 °C and 35 V, respectively. The data was collected in positive mode by scanning the first mass analyser (MS_1) through m/z = 100–1999. MS–MS analyses were performed by injecting 30 μL of peptide sample (10 μg/mL in acetonitrile/water, 1:1, *v/v*) into the mass spectrometer and subjecting the selected molecular species to decomposition at a collision energy of 40 eV. Data was collected in MS_2 through m/z = 100−1999.

3.2. Culturing of bacteria

Micrococcus luteus NCTC 8340 and *Escherichia coli* HB101 were cultured, using normal sterile techniques, from freezer stocks on Luria broth agar (1 g tryptone, 0.5 g yeast extract, 1 g NaCl, 2 g agar in 100 mL water) at 37 °C for 48 and 24 h, respectively. Selected colonies were cultured overnight at 37 °C in Luria broth (10 g tryptone, 5 g yeast extract, 10 g NaCl in 1 L water) and TSB (30 g TSB in 1 L water), respectively. The overnight cultures were sub-cultured in TSB at 37 °C to an OD_{620} of 0.6. *L. monocytogenes* B73 and *L. monocytogenes* B73-MR1 were cultured from freezer stocks on BHI agar at 37 °C for 24 h. Selected colonies were cultured overnight at 37 °C in BHI broth (37 g in 1 L water). The overnight cultures were sub-cultured in BHI broth at 37 °C to an OD_{620} of 0.4 for use in lytic experiments and dose–response assays.

3.3. Lytic activity

Mid-log phase cultures (OD_{620} of 0.4) of *L. monocytogenes* B73 were diluted to OD_{620} of 0.2 ($\sim 6 \times 10^8$ CFUs). The cell suspension (90 μL) were pipetted into microtiter plates and 10 μL peptide solution was added. Plates were prepared as for the broth microdilution assays (see below) and peptides were made up to a known analytical concentration (approximately 10 μM) in ethanol/water (1:1, *v/v*). The growth (in absence of peptide) and reduction of optical density (in presence of peptide) of *L. monocytogenes* B73 was monitored over time at 595 nm using a Biorad microtiter plate reader. Percentage lysis was calculated according to Eq. 1:

$$\%\,\text{lysis} = 100 - \frac{100 \times (A_{595}\text{ of well} - \text{Average } A_{595}\text{ of background})}{\text{Average } A_{595}\text{ of growth wells} - \text{Average } A_{595}\text{ of background}} \quad (1)$$

The initial lytic rate (% lysis/min) was determined as the slope of the linear regression on % lysis versus time (up to 60 min), performed using GraphPad Prism® 3.01 and 4.00 (GraphPad Software, San Diego, USA).

3.4. Antibacterial activity determinations

The dose–responses of *E. coli*, *M. luteus* and *L. monocytogenes* toward the six purified tyrocidines were determined using broth microdilution assays.[17,18] The six purified tyrocidines were dissolved in ethanol:water (1:1, *v/v*) to concentrations of 2.00 mg/mL. Doubling dilution series (using ethanol:water (1:3, *v/v*) for *E. coli* and *M. luteus*; and growth medium for *L. monocytogenes*) were then constructed in polypropylene microtiter plates. Suspensions for the broth microdilution assays were prepared by diluting the sub-cultures in TSB (*E. coli* and *M. luteus*) or BHI broth (*L. monocytogenes*) to an OD_{620} of 0.2. The broth microdilution assays[17,18] were performed in 96-well microtiter plates that were sterilised with 70% isopropanol and blocked with sterile 0.5% casein in Dulbecco's phosphate buffered saline (PBS)[19] prior to use. After the addition of the peptides, the microtiter plates were incubated at 37 °C for 16 h, after which the light dispersion of each well was spectrophotometrically determined at 595 nm using a Biorad microtiter plate reader.

The light dispersion was used to calculate percentage growth inhibition (Eq. 2) as described by Rautenbach et al. (2006).[20]

$$\%\,\text{growth inhibition} = 100 - \frac{100 \times (A_{595}\text{ of well} - \text{Average } A_{595}\text{ of background})}{\text{Average } A_{595}\text{ of growth wells} - \text{Average } A_{595}\text{ of background}} \quad (2)$$

Dose–response curves were plotted using GraphPad Prism® 3.01 and 4.00 (GraphPad Software, San Diego, USA). The dose–response data was analysed by performing non-linear regression and sigmoidal curves (with variable slope and a constant difference of 100 between the top and bottom plateau) were fitted.[20] The sigmoidal curves were fitted according to Eq. 3:[20]

$$Y = \frac{\text{bottom} + (\text{top} - \text{bottom})}{1 + 10^{\log \text{IC}_{50} \times \text{Activity slope}}} \quad (3)$$

Top and bottom is defined as the percentage inhibition observed in the presence of high peptide concentrations and in the absence of peptide, respectively; $\log \text{IC}_{50}$ refers to the *x*-value denoting the response halfway between the top and bottom (represents the concentration of peptide required to induce 50% growth inhibition); and the activity slope, which is related to the Hill slope, defines the slope of the curve. IC_{max}, related to the maximum inhibitory concentration (MIC), was calculated from the *x*-values at the intercept between the slope and the top plateau, as described by Du Toit and Rautenbach (2000).[18]

3.5. QSAR analyses

The relationship between the antibacterial activity and different physicochemical properties of the six purified tyrocidines was analysed. The molecular properties that were considered include analytical HPLC retention time [this study], theoretical lipophilicity,[21,22] theoretical side-chain surface area[22] and mass-over-charge (*m/z*) ratio [this study]. The HPLC retention times of the six tyrocidines were obtained from the analytical HPLC chromatograms of the purified tyrocidines. The theoretical parameters, lipophilicity (π_{FP}),[21,22] and side-chain surface area (SCSA),[22] of each peptide was calculated as the sum of the parameters of all the constituent amino acids of the particular peptide. The *m/z* ratios were obtained from TOF-ESMS spectra (Fig. 1). The correlations between the molecular descriptors and the antibacterial activity of each peptide were analysed by performing non-linear regression and fitting a fourth order polynomial equation using GraphPad Prism® 3.01 and 4.00 (GraphPad Software, San Diego, USA). Optimal molecular descriptors were calculated by determining the minimum turning points of the fitted polynomial equations from the theoretical curve data.

4. Results and discussion

4.1. Purification and characterisation

The six major tyrocidines were successfully isolated and purified to >95% purity as determined with analytical HPLC analyses at 254 nm. The chemical purity and integrity, in terms of expected molecular mass, of the isolated tyrocidines was confirmed by TOF-ESMS (Table 1, Fig. 2). The primary sequence of each of the isolated tyrocidines was confirmed with MS–MS studies (results not shown). For more detail on the HPLC and ESMS analyses of the purified peptides refer to Supplementary data.

4.2. Lytic activity

The lytic effect of the crude tyrocidine mixture and the purified tyrocidines on cultures of *L. monocytogenes* B73 was investigated in order to verify previous studies.[6] Incubation of *L. monocytogenes* B73 with the crude tyrocidine mixture and purified tyrocidines led to total loss of light dispersion over approximately 2 h, which suggest a membrane-lytic mechanism of action. The initial lytic rates were found to be the similar (about 1.6% per minute) for the six tyrocidines and gramicidin S. The lysis half life was ±30 min and ±60% lysis was found after 60 min for the six tyrocidines (Table 2). Gramicidin S, however, differed from the tyrocidines in that the % lysis after an hour was significantly different

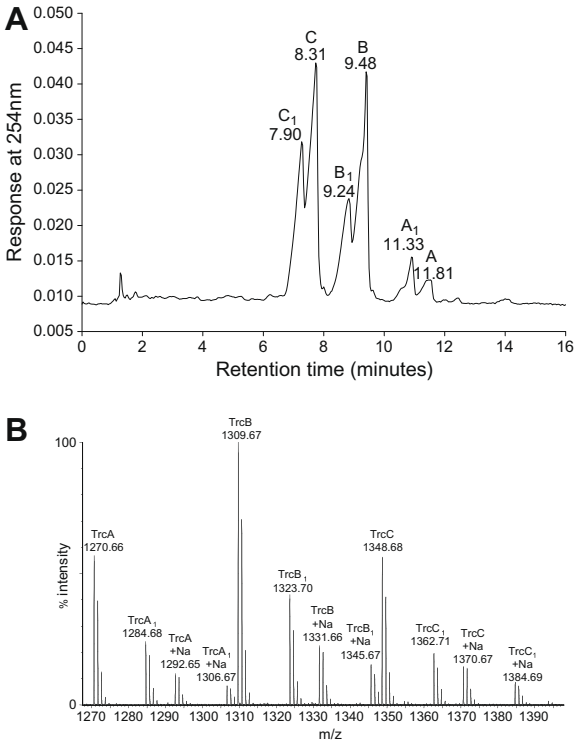

Figure 2. (A) A representative analytical HPLC chromatogram of the crude tyrocidine mixture on a C_{18} matrix. The HPLC retention times in minutes of the six major tyrocidines are given and unlabelled elution peaks represent the minor tyrocidines. (B) TOF-ESMS spectrum in positive mode of the crude tyrocidine mixture showing the isotope peaks and monoisotopic *m/z* ratios for the singly charged species ([M+H$^+$], in bold) and singly charged sodium adducts ([M+Na]$^+$) of the six major tyrocidines.

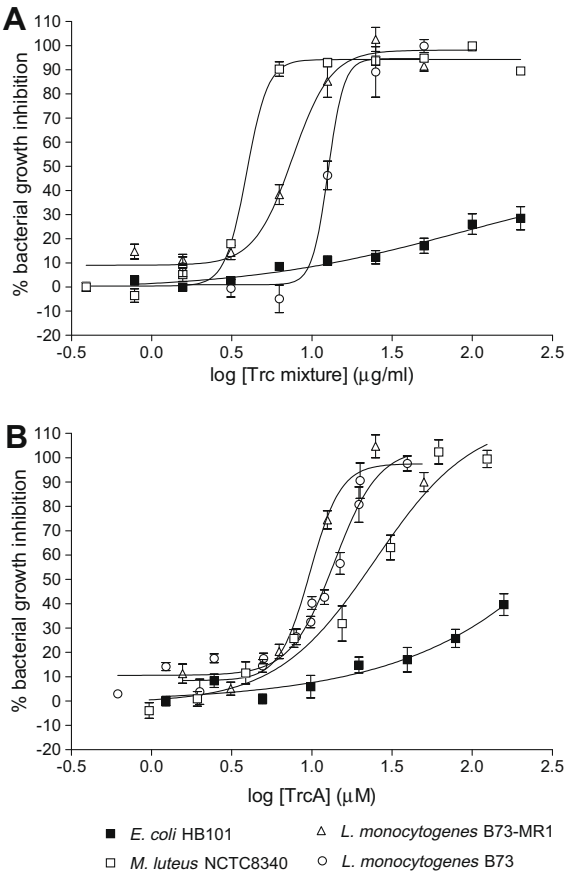

Figure 3. Representative dose–response curves of (A) crude tyrocidine mixture and (B) purified tyrocidine A toward the different bacterial strains. Each data point represents the mean of at least 3 biological repeats, with 3–5 technical repeats per assay ± standard error of the mean (SEM). The sigmoidal dose–response curves fitted the experimental data with R^2-values of >0.99.

Table 2
Summary of the lytic activity parameters determined for the eight tyrocidines toward *L. monocytogenes* B73

Peptide	% Lysis/min ± SEM (*n*)[a]	% Lysis at 60 min ± SEM (*n*)	Lysis half life – 95% confidence levels (min)
Trc mix	1.53 ± 0.038 (12)	67 ± 2.1 (10)	28.9–32.5
TrcA	1.62 ± 0.047 (12)	59 ± 1.7 (12)*	32.3–34.0
$TrcA_1$	1.47 ± 0.026 (6)	62 ± 0.77 (6)	32.2–34.5
TrcB	1.53 ± 0.062 (8)	64 ± 0.95 (8)	28.8–30.5
$TrcB_1$	1.68 ± 0.061 (7)	63 ± 1.5 (7)	29.6–31.7
TrcC	1.48 ± 0.067 (7)	66 ± 2.8 (7)	31.2–33.9
$TrcC_1$	1.55 ± 0.063 (7)	60 ± 2.0 (6)*	27.5–30.4
GS	1.61 ± 0.042 (9)	70 ± 1.9 (9)*	38.5–42.8

Lytic experiments were done with 12.5 μg/mL for the tyrocidine mixture and 10 μM for the purified tyrocidines and gramicidin S. Each value represents the mean of at least two biological repeats, with four technical repeats per assay ± SEM.

[a] R^2 values for the fits of all the linear regression lines are >0.99.

* Gramicidin S lysis is significantly different from TrcA ($P < 0.001$) and $TrcC_1$ ($P < 0.05$).

from some of the tyrocidines and that it also displayed a slightly longer lysis half life (Table 2).

4.3. Antibacterial activity

In order to investigate how the lytic activity of the tyrocidine mixture (tyrothricin with the gramicidins removed) and purified tyrocidines translated into antibacterial activity, we determined their ability to induce growth inhibition of *E. coli* and *M. luteus*, model Gram-negative and Gram-positive representatives, respectively. Toward *M. luteus*, tyrothricin and the tyrocidine mixture had IC_{50} values of 3.5 ± 0.49 μg/mL and 3.9 ± 0.04 μg/mL, respectively. Even at concentrations as high as 200 μg/mL for the tyrocidine mixture as well as the purified tyrocidines, 50% inhibition toward *E. coli* was not reached (Fig. 3). The observed selectivity of the tyrocidines may be a result of the differing cell walls of Gram-positive and Gram-negative bacteria.[23] We therefore focussed our studies of the purified tyrocidines on Gram-positive bacteria.

M. luteus, as well as two strains of pathogenic Gram-positive bacterium, *L. monocytogenes* B73 and B73-MR1, were sensitive to all the tyrocidines. A previous study conducted by Rautenbach et al. (2006)[20] indicated the necessity of at least two activity parameters to characterise dose-dependence and activity. We therefore chose IC_{50} (concentration that gives 50% growth inhibition) and IC_{max} (maximal inhibitory concentration, which is related to minimum inhibitory concentration or MIC)[18,20] for characterising the activity of the tyrocidines and identifying activity trends. When considering IC_{50} and IC_{max} values toward *M. luteus*, the activity sequences were ($TrcB_1$, TrcC, TrcB, $TrcC_1$) > TrcA > $TrcA_1$ and ($TrcB_1$, TrcC, TrcB) > $TrcC_1$ > (TrcA, $TrcA_1$), respectively (tyrocidines in parentheses gave statistically similar activities) (Table 3). When considering IC_{50} and IC_{max} values toward *L. monocytogenes* B73, the activity sequences were ($TrcB_1$, $TrcC_1$, TrcC, TrcB) > TrcA > $TrcA_1$ and TrcC > ($TrcB_1$, TrcB) > $TrcC_1$ > TrcA > $TrcA_1$, respectively (Table 3, Fig. 4). When considering IC_{50} toward *L. monocytogenes* B73-MR1, the activity sequence was ($TrcB_1$ > TrcC > $TrcC_1$ > TrcB > TrcA > $TrcA_1$), but only the most active ($TrcB_1$ and TrcC) and least active (TrcA and $TrcA_1$) tyrocidines differed statistically in their activities (Tables 3 and 4, Fig. 4). When considering IC_{max} values toward *L.*

Table 3
Summary of the antibacterial activity parameters of tyrothricin, the tyrocidine mixture, the eight purified tyrocidines and Gramicidin S toward three Gram-positive bacterial strains

Peptide	*M. luteus* NCTC 8340		*L. monocytogenes* B73		*L. monocytogenes* B73-MR1	
	IC_{50} ± SEM (n)	IC_{max} ± SEM (n)	IC_{50} ± SEM (n)	IC_{max} ± SEM (n)	IC_{50} ± SEM (n)	IC_{max} ± SEM (n)
Trt	3.5 ± 0.49 (3)	6.3 ± 0.10 (3)	12 ± 0.80 (3)	21 ± 0.10 (3)	9.7 ± 0.53 (3)	29 ± 0.68 (3)
Trc mix	3.9 ± 0.04 (3)	5.7 ± 0.11 (3)	13 ± 1.2 (6)	23 ± 0.63 (6)	7.9 ± 0.84 (3)	14 ± 0.30 (3)
TrcA	22 ± 0.19 (3)	70 ± 1.3 (3)	13 ± 0.49 (7)	25 ± 0.54 (7)	9.9 ± 0.36 (3)	16 ± 0.29 (3)
$TrcA_1$	26 ± 2.0 (4)	72 ± 2.4 (4)	18 ± 0.94 (3)	38 ± 1.0 (3)	10 ± 1.4 (3)	16 ± 0.32 (3)
TrcB	6.5 ± 0.07 (3)	9.9 ± 0.13 (3)	10 ± 0.46 (7)	15 ± 0.41 (7)	7.7 ± 0.59 (3)	12 ± 0.28 (3)
$TrcB_1$	4.2 ± 0.26 (5)	8.9 ± 0.13 (5)	8.1 ± 0.19 (3)	15 ± 0.47 (3)	6.7 ± 0.24 (3)	10 ± 0.21 (3)
TrcC	6.4 ± 0.59 (4)	9.0 ± 0.17 (4)	9.5 ± 0.73 (6)	13 ± 0.32 (6)	7.0 ± 0.25 (3)	11 ± 0.21 (3)
$TrcC_1$	7.3±0.96 (4)	15 ± 0.36 (4)	9.3 ± 0.25 (3)	22 ± 0.54 (3)	7.5 ± 0.43 (3)	16 ± 0.21 (3)
GS	6.7 ± 0.48 (10)	31 ± 0.46 (10)	6.6 ± 0.06 (4)	11 ± 0.20 (4)	3.9 ± 0.25 (3)	6.2 ± 0.078 (3)

The values of tyrothricin and tyrocidine mixture are given in μg/mL (top two rows) and those of the purified tyrocidines and gramicidin S are given in μM. Each value represents the mean of n biological repeats (number of repeats in brackets), with 3–5 technical repeats per assay ± SEM.

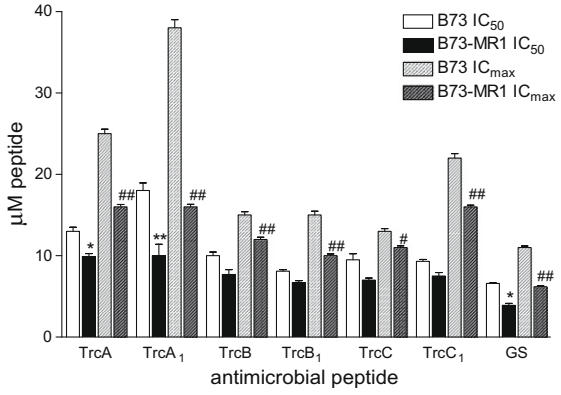

Figure 4. Comparison between the activity of the tyrocidines and gramicidin S towards the leucocin A-sensitive *L. monocytogenes* B73 and leucocin A resistant *L. monocytogenes* B73-MR1. Parameter data are given in Table 2. According to the Newman-Keuls multiple comparison test the IC_{50} values of only TrcA, $TrcA_1$ and GS were significantly different ($^{*}P > 0.01$; $^{**}P > 0.001$) and the IC_{max} values of all the peptides were significantly different ($^{\#}P > 0.05$; $^{\#\#}P > 0.001$).

monocytogenes B73-MR1, the activity sequence was $TrcB_1$ > TrcC > TrcB > ($TrcC_1$, TrcA, $TrcA_1$) (Table 3). Overall, the results showed that antimicrobial activity is modulated by properties of both the peptide and the target cell. Refer to Tables 3 and 4 for details on activity parameters and statistical analyses.

For each tyrocidine, the different target cells were found to have varying sensitivities. Only the activities toward the two listeria strains were compared as identical cell size and initial inoculate could be assumed. For all tested tyrocidines and gramicidin S, *L. monocytogenes* B73-MR1, a highly-resistant mutant of B73[23] was shown to be more sensitive than *L. monocytogenes* B73, a leucocin A-sensitive wild-type meat-isolate (Fig. 4).[24] In particular, a significantly lower ($P < 0.001$ for all peptides, with the exception of TrcC at $P < 0.05$) IC_{max} ('MIC') is necessary to inhibit the resistant strain (Fig. 4). The different activities toward the two listeria strains may be ascribed to different membrane structures. Resistance mechanisms associated with *L. monocytogenes* B73-MR1 include increased membrane fluidity[25] and increased positive charge of the cell wall and cell membrane.[26] In general, the presence of anionic phospholipids, a highly negative electrochemical gradient and the absence of cholesterol promote membrane–peptide interaction.[1,27] The increased fluidity and decreased anionicity of the cell wall and membrane of *L. monocytogenes* B73-MR1 would thus be expected to interfere with the hydrophobic and electrostatic interactions of cationic peptides.[25] The opposite was, however,

Table 4
Summary of the *P*-values from Newman-Keuls multiple comparison test on the bacterial growth inhibition parameters (Table 3)

	TrcA		$TrcA_1$		TrcB		$TrcB_1$		TrcC		$TrcC_1$	
	IC_{50}	IC_{max}	IC_{50}	IC_{max}	IC_{50}	IC_{max}	IC_{50}	IC_{max}	IC_{50}	IC_{max}	IC_{50}	IC_{max}
$TrcA_1$	0.01											
	0.001	0.001										
	ns	ns										
TrcB	0.001	0.001	0.001	0.001								
	0.001	0.001	0.001	0.001								
	ns	0.001	ns	0.001								
$TrcB_1$	0.001	0.001	0.001	0.001	ns	ns						
	0.001	0.001	0.001	0.001	ns	ns						
	0.05	0.001	0.05	0.001	ns	0.001						
TrcC	0.001	0.001	0.001	0.001	ns	ns	ns	ns				
	0.001	0.001	0.001	0.001	ns	0.01	ns	0.05				
	0.05	0.001	0.05	0.001	ns	0.05	ns	0.05				
$TrcC_1$	0.001	0.001	0.001	0.001	ns	0.01	ns	0.001	ns	0.001		
	0.01	0.001	0.001	0.001	ns	0.001	ns	0.001	ns	0.001		
	ns	ns	ns	ns	ns	0.001	ns	0.001	ns	0.001		
GS	0.001	0.001	0.001	0.001	ns	0.001	ns	0.001	ns	0.001	ns	0.001
	0.001	0.001	0.001	0.001	0.01	0.001	ns	0.001	0.01	0.01	0.05	0.001
	0.001	0.001	0.001	0.001	0.01	0.001	0.01	0.001	0.01	0.001	0.01	0.001

Accurate *P*-values are smaller than maximum value given in table. The ns denotes a *P*-value >0.5. In each cell, the top value represents the *P* value for *M. luteus*, the middle value *L. monocytogenes* B73 and the bottom value *L. monocytogenes* B73-MR1.

observed for the tyrocidines, with higher activity found toward *L. monocytogenes* B73-MR1. This may be related to the manner by which the tyrocidines associate with the target cell membrane and/or their mechanism of action. Although the precise mechanism of action of antimicrobial peptides is not fully understood, it is generally believed that these peptides are membrane-active.[28–36] This theory is supported by the physicochemical characteristics of antimicrobial peptides; the rapid, concentration-dependent action; and the observed toxicity toward higher eukaryotic cells.[35,37,38] We were able to show that the tyrocidines act, at least in part, via a membrane-lytic mechanism of action. The observation that the different tyrocidines exhibit similar lytic rates (% lysis/min) but different activities in terms of growth inhibition (IC_{max}), however, suggests that lysis is not the only factor leading to cell death/growth inhibition. The tyrocidines have also been shown to interfere with the glucose metabolism of Gram-positive bacteria,[6] and the reduced glucose consumption rate of *L. monocytogenes* B73-MR1[23,25] may render it more susceptible to the tyrocidines. The difference in activity toward the two listeria strains may thus also be related to metabolic differences.

4.4. QSAR analyses

Our results showed that all the tested tyrocidines exhibit similar lytic activity, but differed in their growth inhibition activity (Tables 2 and 3). The lytic results indicated that lytic activity is not highly dependent on the identity of the cationic residue or the identity of residues in the aromatic dipeptide unit. Investigation of growth inhibition, however, indicated that there are, unlike for lytic activity, marked differences between some IC_{50} and most IC_{max} values of the various tyrocidines (Tables 3 and 4). This suggests that the tyrocidines may have an alternative/additional mechanism of action or target and that there are structural prerequisites for such mechanism(s) of action and/or interaction with an alternative target(s).

To elucidate the role of structural parameters in modulating bacterial growth inhibition, we used the theoretical hydropathy, lipophilicity, side-chain surface area (SCSA), and mass-over-charge ratio (m/z) as well as HPLC retention time (t_R, reflecting solution amphipathicity) in the analyses of qualitative structure activity relationships (QSAR) (Table 5, Fig. 5). IC_{max} values were chosen as

Table 5
Summary of selected physicochemical parameters of the six major tyrocidines

Peptide	HPLC t_R (min)	Σ lipophilicity	Σ side-chain surface area (Å)	m/z
TrcA	11.81	9.55	721.9	1269.64
$TrcA_1$	11.33	8.16	741.4	1283.71
TrcB	9.48	10.01	750.8	1308.66
$TrcB_1$	9.24	8.62	770.3	1322.69
TrcC	8.31	10.47	779.7	1347.67
$TrcC_1$	7.90	9.08	799.2	1361.69
GS	12.05	11.66	648.2	1140.70

HPLC retention times and m/z values were obtained from the analytical HPLC chromatography and ESMS analysis of the purified tyrocidines, respectively. The theoretical hydropathies, lipophilicities and side-chain surface areas were calculated as the sum of all the hydropathy indices,[41] lipophilicity parameters (π_{FP}),[22] and side-chain surface areas,[22] respectively, of the constituent amino acids.

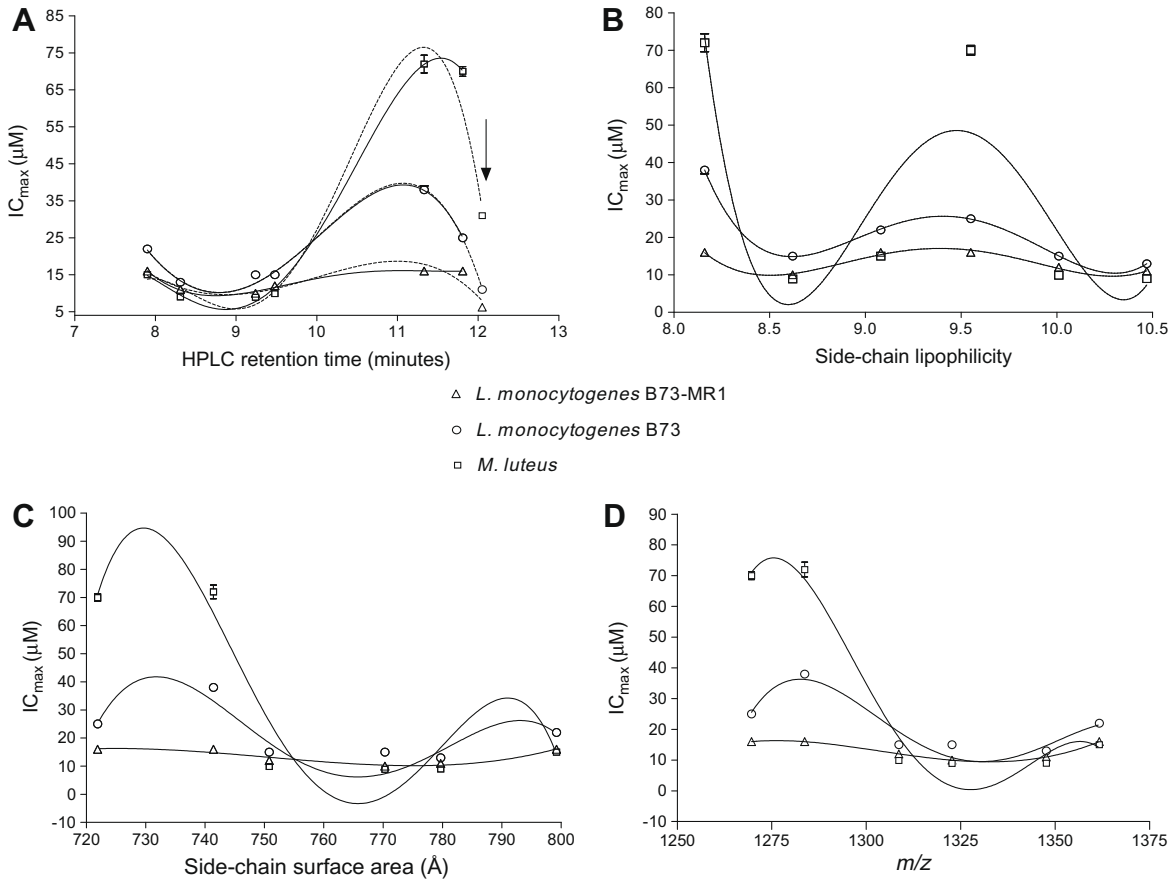

Figure 5. QSAR relationships of the six major tyrocidines showing curves fitted to fourth order polynomial equations (R^2-values are >0.93, refer to Table 6). Curves show the IC_{max} values versus (A) HPLC t_R on a C_{18} matrix (gramicidin S was included in the dataset as depicted by the arrow and curves shown with dotted lines), (B) theoretical total lipophilicity, (C) theoretical total side-chain surface area, and (D) mass-over-charge ratio (m/z). Each data point represents the mean of at least 3 biological repeats, with 3–5 technical repeats per assay ± SEM.

Table 6
Summary of the predicted optimal physicochemical parameters of the major natural tyrocidines for antibacterial growth inhibition, as determined from the fourth order polynomial QSAR trends in Figure 3

Parameter	*M. luteus* NCTC8340		*L. monocytogenes* B73		*L. monocytogenes* B73-MR1	
	Optimum	R^2	Optimum	R^2	Optimum	R^2
HPLC t_R	8.89 (>12.05)	0.999 (0.993)	8.75 (>12.05)	0.997 (0.998)	8.75 (>12.05)	0.996 (0.930)
Σ lipophilicity	8.57	0.948	8.62	>0.999	8.50	0.992
Σ side-chain surface area	781.5	0.931	782.5	0.920	775.0	0.971
m/z	1327.8	0.973	1330.6	0.906	1332.8	>0.999

The R^2 value is given for the fit of each fourth order polynomial curve used for determining the specific optimum. The values in brackets for the optimal HPLC t_R are those determined with gramicidin S as part of the dataset.

the activity parameter for the QSAR analyses as insufficient statistical differences between IC_{50} values were observed (Table 4). The lipophilicity and HPLC retention time were indicators of hydrophobic interaction and membrane activity (Fig. 5A and 4B), while SCSA and *m/z* were used as indicators of side-chain steric and charge factors that may influence target interaction (Fig. 5C and D).

Our correlation between antimicrobial activity, as reflected by the IC_{max} values ('MIC'), and the four structural parameters (Fig. 5) were quite different from those observed by Rautenbach et al.[7] with *P. falciparum* infected erythrocytes as tyrocidine target cells. Only fourth order polynomial equations could be fitted for all our datasets, however, remarkably similar trends were obtained from correlations between IC_{max} and solution amphipathicity (HPLC t_R), lipophilicity, *m/z* and SCSA for the three Gram-positive target cells (Fig. 5). The curve fits also allowed us to predict optimal structural parameters for the antibacterial activity of the natural tyrocidine library. Similar optima were predicted for all the target cells, indicating that the structural prerequisite for activity is independent of the Gram-positive bacterial strain (Table 6).

The best fourth order polynomial correlations and curve fits were found between IC_{max} and HPLC retention time (Table 6, Fig. 5A). This is most probably because the peptide conformation influences the hydropathy, lipophilicity and accessible surface area of the peptide, which will in turn influence the HPLC retention time and antibacterial activity, while the calculated theoretical parameters do not take the three-dimensional conformation of the peptide into consideration. Optimal HPLC retention time (solution amphipathicity) and *m/z* were predicted between that of tyrocidine B_1 and C, and tyrocidine B_1 exhibited optimal theoretical lipophilicity (Tables 5 and 6). When we included GS in the QSAR analysis of HPLC t_R versus IC_{max}, two optima became apparent. The one optimum still correlated with the t_R near $TrcB_1$ and C, whereas the second optimum corresponds to near the t_R of GS (Fig. 5A). The predicted optimal side-chain surface area corresponded with that of tyrocidine C (Tables 5 and 6).

In general, the optima, as expected, coincided with that of the two most active peptides in terms of growth inhibition, namely tyrocidine B_1 and C. In general, tyrocidine C exhibits optimal SCSA, while tyrocidine B_1 exhibits optimal lipophilicity, *m/z* and HPLC retention time. This suggests that TrcC may approach the optimal structural characteristics for target interaction, whereas $TrcB_1$ may have optimal amphipathicity for hydrophobic interaction and membrane insertion.

In order to explain our QSAR results we needed to make some assumptions. First, regardless of precise mechanism of action/molecular target, initial membrane association is essential. Second, the initial membrane association is governed primarily by electrostatic interactions, and is followed by membrane integration driven by hydrophobic interactions.[39,40] The tyrocidines carry the same charge with only small differences in *m/z* and should thus all have a similar propensity for initial association. However, there are two groups of tyrocidines, those with Lys and those with Orn as cationic residue. Lys and Orn differ in their side chain with only a CH_2 unit, but this small difference translates into different amino group pK_a's (pK_a = 10.54 and 10.76, respectively),[40] and different hydropathies (−9.9 and −9.0, respectively).[41] Also, it has been shown that Lys, with a butylene moiety in its side chain, 'snorkels' into the membrane,[7,42] which leads to a tighter membrane interaction than Orn. Our results, however, show that the Lys-containing tyrocidines are not necessarily more active.

The tyrocidines containing Trp (TrcC, $TrcC_1$, TrcB and $TrcB_1$) were found to be more active than the more hydrophobic Phe-containing (A and A_1) peptides. A 2–4-fold increase in activity was found between $TrcA/A_1$ with a Phe in position 3 and $TrcB/B_1$ with a Trp in position 3. A similar increase 2–4-fold increase in activity was found by Marques et al.[12] when Phe_3 in synthetic TrcA was replaced with a pentafluoro-Phe residue which is larger but more hydrophobic. Furthermore $TrcB_1$ (containing one Trp and one Phe), was found to be more active than $TrcC_1$ (containing two Trp residues), while TrcB and C have similar activities. Substituting D-Phe_4 to D-Trp_4 ($TrcB/B_1$ vs $TrcC/C_1$) had a minor influence on activity. These results indicated that the aromatic residue on position 3 has a major influence on activity. However, the two most active peptides, $TrcB_1$ and C differ from each other at two residues. $TrcB_1$ contains Lys and TrcC Orn as the cationic residue, while $TrcB_1$ contains D-Phe and TrcC D-Trp in the position 4 of aromatic dipeptide moiety.

The aromatic residues (Trp, Phe and Tyr), two of which are found in the variable aromatic dipeptide unit, have a considerable impact on the hydrophobicity of the tyrocidines and are expected to be responsible for/contribute to integration into the membrane. The efficacy with which the tyrocidines lead to cell death is determined, at least in part, by the efficiency of the initial membrane association and integration and/or translocation steps. As the Tyr residue is constant for all investigated tyrocidines, differences in efficacy of membrane integration may be contributed to the Trp and/or Phe residues of the dipeptide unit. The greater lipophilicity, indicative of the preference for the water–phospholipid interface, of the Phe residue suggests that peptides containing Phe rather than Trp will be more active if activity only depended on the membrane interaction. Phe was found to insert much deeper into the membrane than Trp.[43,44] However, previous research has shown that the size of the residue is important with larger (Trp) residues having good anchoring properties.[45] Despite Trp's shallow membrane insertion, the anchoring is probably due to the formation of hydrogen bonds via its NH-group with fatty-acyl carbonyl groups.[46] Overall, it is deduced that tyrocidines containing Lys and Phe may undergo tighter membrane association than tyrocidines containing Orn and Trp. However, it should be kept in mind that a stronger association with the cell membrane does not necessarily lead to greater activity as the mechanism of cell death and/or molecular target also plays a role. This result therefore suggests that there is an optimal amphipathicity, in which Phe and/or Lys is required for tighter binding, but Trp and/or Orn modulates this binding, possibly by reduction of peptide trapping and allowing for the most efficient membrane integration and self-assembly into

active lytic complexes and/or translocation to an internal target. The tyrocidines have been shown to interfere with glucose metabolism[6] as well as inhibition of RNA synthesis of *B. brevis*.[47] The tyrocidines may thus also interact with a molecular target, such as DNA or RNA precursors. Marques et al.[12] came to a similar conclusion, namely that there is a fine amphipathic balance that must be maintained in order for their synthetic TrcA analogues to remain active.

5. Conclusions

Investigation of the antibacterial activity of the tyrocidines indicated that activity is (1) strain-specific and thus dependent on properties of the target cell; and (2) dependent on peptide structure. The greater sensitivity of *L. monocytogenes* B73-MR1 relative to *L. monocytogenes* B73 towards the tyrocidines and gramicidin S may be related to differences in membrane structure and/or metabolic differences.

Although the natural library of tyrocidines that we analysed is too small to draw firm conclusions on the QSAR of the tyrocidines, we were able to determine a number of prerequisites for activity towards Gram-positive bacteria. First, we found that the more polar tyrocidines (B and C groups) were more active than the more hydrophobic A group. Second, the more active B and C groups contained at least one Trp residue, with position 3 being more sensitive, which may point to the importance of this aromatic residue in their activity. Third, there was no direct indication for a preference for either Lys of Orn in the tyrocidine activity. However, an optimal *m/z* of between 1333 and 1340 was observed, which indicated activity was dependent on both charge and overall size.

Although the bacterial growth inhibition of the tyrocidines displayed a dependency on primary structure, pertaining primarily to the aromatic dipeptide moiety, investigation of the lytic activity indicated that lysis is independent of the specific tyrocidine structure. This suggests that the tyrocidines, apart from their membranolytic activity, may have a second target/mechanism of action. The observed structural prerequisites for bacterial growth inhibition are thus probably related to the ability of the different tyrocidines to reach another target, associate with, or influence an alternative internal (such as RNA or DNA)[47] or membrane bound target (such as autolysins[6,48]or phosholipases[49]) and not only their ability to induce overt membrane lysis.

Research concerning the tyrocidines may play an important role in future combating of infections caused by treatment-resistant food-borne bacteria. The development of novel therapeutic agents or bio-preservatives based on the tyrocidines, however, requires consideration of several safety considerations and technical difficulties. These include selectivity, toxicity and sensitivity to physiologically relevant ionic strength, pH and serum conditions. Further research regarding the basis of selectivity, the role of specific amino acid residues in bacterial growth inhibition and elucidation of mechanism of action may allow for the development of more efficacious molecules, improved selectivity and reduced toxicity. Furthermore, investigation of the role of environmental conditions, such as changes in ionic strength and pH, on antilisterial activity may provide valuable information for development of bio-preservatives.

Acknowledgements

This study was funded by the BIOPEP peptide fund and the South African Malaria Initiative. The authors wish to thank Dr. Marietjie Stander (University of Stellenbosch, LCMS Central analytical facility) for the mass spectrometry of the tyrocidines.

Supplementary data

Supplementary data associated with this article can be found, in the online version, at doi:10.1016/j.bmc.2009.06.029.

References and notes

1. Hancock, R. E.; Lehrer, R. *Trends Biotechnol.* **1998**, *16*, 82.
2. Hotchkiss, R. D.; Dubos, R. J. *J. Biol. Chem.* **1941**, 155.
3. Tang, X.-J.; Thibault, P.; Boyd, R. K. *Int. J. Mass Spectrom. Ion Processes* **1992**, *122*, 153.
4. Van Epps, H. L. *J. Exp. Med.* **2006**, *203*, 259.
5. Gibbons, W. A.; Beyer, C. F.; Dadok, J.; Sprecher, R. F.; Wyssbrod, H. R. *Biochemistry* **1975**, *14*, 420.
6. Dubos, R. J. *J. Exp. Med.* **1939**, *70*, 1.
7. Rautenbach, M.; Vlok, N. M.; Stander, M.; Hoppe, H. C. *Biochim. Biophys. Acta—Biomembr.* **2007**, *1768*, 1488.
8. Kuo, M. C.; Gibbons, W. A. *Biophys. J.* **1980**, *32*, 807.
9. Laiken, S.; Printz, M.; Craig, L. C. *J. Biol. Chem.* **1969**, *244*, 4454.
10. Hasko Paradies, H. *Biochem. Biophys. Res. Commun.* **1979**, *88*, 810.
11. Laiken, S. L.; Printz, M. P.; Craig, L. C. *Biochem. Biophys. Res. Commun.* **1971**, *43*, 595.
12. Marques, M. A.; Citron, D. M.; Wang, C. C. *Bioorg. Med. Chem.* **2007**.
13. Qin, C.; Zhong, X.; Bu, X.; Ng, N. L. J.; Guo, Z. *J. Med. Chem.* **2003**, *46*, 4830.
14. Gandhi, M.; Chikindas, M. L. *Int. J. Food Microbiol.* **2007**, *113*, 1.
15. Holzapfel, W. H.; Geisen, R.; Schillinger, U. *Int. J. Food Microbiol.* **1995**, *24*, 343.
16. Ming, X. T.; Daeschel, M. A. *J. Food Prot.* **1993**, *56*, 944.
17. Lehrer, R. I.; Rosenman, M.; Harwig, S. S. S. L.; Jackson, R.; Eisenhauer, P. *J. Immunol. Methods* **1991**, *137*, 167.
18. du Toit, E. A.; Rautenbach, M. *J. Microbiol. Methods* **2000**, *42*, 159.
19. Dulbecco, R.; Vogt, M. *J. Exp. Med.* **1954**, *98*, 67.
20. Rautenbach, M.; Gerstner, G. D.; Vlok, N. M.; Kulenkampff, J.; Westerhoff, H. V. *Anal. Biochem.* **2006**, *350*, 81.
21. Fauchere, J. L.; Pliska, V. *Eur. J. Med. Chem.* **1983**, *18*, 369.
22. Frecer, V. *Bioorg. Med. Chem.* **2006**, *14*, 6065.
23. Ramnath, M.; Beukes, M.; Tamura, K.; Hastings, J. W. *Appl. Environ. Microbiol.* **2000**, *66*, 3098.
24. Dykes, G. A.; Hastings, J. W. *Lett. Appl. Microbiol.* **1998**, *26*, 5.
25. Vadyvaloo, V.; Arous, S.; Gravesen, A.; Hechard, Y.; Chauhan-Haubrock, R.; Hastings, J. W.; Rautenbach, M. *Microbiology* **2004**, *150*, 3025.
26. Vadyvaloo, V.; Hastings, J. W.; van der Merwe, M. J.; Rautenbach, M. *Appl. Environ. Microbiol.* **2002**, *68*, 5223.
27. Prenner, E. J.; Lewis, R. N.; Neuman, K. C.; Gruner, S. M.; Kondejewski, L. H.; Hodges, R. S.; McElhaney, R. N. *Biochemistry* **1997**, *36*, 7906.
28. Sitaram, N.; Nagaraj, R. *Biochim. Biophys. Acta* **1999**, *1462*, 29.
29. Lehrer, R. I.; Barton, A.; Daher, K. A.; Harwig, S. S. S. L.; Ganz, T.; Selsted, M. E. *J. Clin. Invest.* **1989**, *84*, 553.
30. Ganz, T.; Lehrer, R. I. *Curr. Opin. Immunol.* **1998**, *10*, 41.
31. Heller, W. T.; Waring, A. J.; Lehrer, R. I.; Huang, H. W. *Biochemistry* **1998**, *37*, 17331.
32. Giacometti, A.; Cirioni, O.; Greganti, G.; Quarta, M.; Scalise, G. *Antimicrob. Agents Chemother.* **1998**, *42*, 3320.
33. Zasloff, M.; Martin, B.; Chen, H.-C. *Proc. Natl. Acad. Sci.* **1988**, *85*, 910.
34. Shai, Y. *Biopolymers (Pept. Sci.)* **2002**, *66*, 236.
35. Van't Hof, W.; Veerman, E. C.; Helmerhorst, E. J.; Amerongen, A. V. *Biol. Chem.* **2001**, *382*, 597.
36. Rotem, S.; Radzishevsky, I.; Mor, A. *Antimicrob. Agents Chemother.* **2006**, *50*, 2666.
37. Kondejewski, L. H.; Lee, D. L.; Jelokhani-Niaraki, M.; Farmer, S. W.; Hancock, R. E.; Hodges, R. S. *J. Biol. Chem.* **2002**, *277*, 67.
38. Huang, H. W. *Biochemistry* **2000**, *39*, 8347.
39. Yount, N. Y.; Yeaman, M. R. *Protein Pept. Lett.* **2005**, *12*, 49.
40. Dawson, R. M.; Elliot, D. C.; Elliot, W. H.; Jones, K. M. In *Data for Biochemical Research*, 3rd ed.; Claridon Press: Oxford, 1986; pp 22–24.
41. Tossi, A.; Sandri, L.; Giangaspero. In *Peptides 2002: Proceedings of the 27th European peptide symposium*; Benedetti, E.; Pedone, C., Eds.; Edizioni Ziino: Napolo, 2002; pp 461–417.
42. Segrest, J. P.; De Loof, H.; Dohlmann, J. G.; Brouillette, C. G.; Anantharamaiah, G. M. *Proteins: Struct., Funct., Genet.* **1990**, *8*, 103.
43. Kelkar, D. A.; Chattopadhyay, A. *J. Biosci.* **2006**, *31*, 297.
44. Wymore, T.; Wong, T. C. *Biophys. J.* **1999**, *76*, 1199.
45. Strom, M. B.; Haug, B. E.; Rekdal, O.; Skar, M. L.; Stensen, W.; Svendsen, J. S. *Biochem. Cell Biol.* **2002**, *80*, 65.
46. Norman, K. E.; Nymeyer, H. *Biophys. J.* **2006**, *91*, 2046.
47. Danders, W.; Marahiel, M. A.; Krause, M.; Kosui, N.; Kato, T.; Izumiya, N.; Kleinkauf, H. *Antimicrob. Agents Chemother.* **1982**, *22*, 785.
48. Gálvez, A.; Valdivia, E.; Martínez-Bueno, M.; Maqueda, M. *J. Appl. Microbiol.* **1990**, *9*, 406.
49. Latoud, C.; Peypoux, F.; Michel, G. *J. Antibiot.* **1988**, *40*, 1588.

Addendum (Chapter 5)

Correlations between tyrocidine self-assembly and antilisterial activity

Background

Following publication of the antilisterial activity and structure activity-relationships of the six major tyrocidines (Chapter 5), indicators of peptide conformation and self-assembly were derived from circular dichroism data (Chapter 3). Peptide self-assembly is expected to influence antibacterial activity by modulating membrane interaction. β-sheet peptides, such as the tyrocidines, are likely to undergo superstructure organisation upon membrane interaction [1], and such multimer formation has been suggested to play a key role in the cytolytic activity of β-sheet peptides [2-6]. However, self-assembly in aqueous solution is expected to impact membrane interaction and reduce antibacterial activity [5-8]. Insight regarding the structure-activity relationships and mode of action of the tyrocidines may thus be gained by investigating correlations between self-assembly and antilisterial activity.

Correlations between tyrocidine self-assembly and antilisterial activity

Circular dichroism (CD)-derived parameters, negative ellipticity minima ratios in water ($\theta_{205}/\theta_{216,\ water}$) and TFE ($\theta_{204}/\theta_{214,\ TFE}$), were chosen as indicators of conformation and self-assembly in an aqueous and membrane environment, respectively (*Refer to Chapters 3 and 4 for more detail*). Correlations between antibacterial activity toward *L. monocytogenes* B73 and CD-derived parameters (Table 1) were investigated in order to determine the role of tyrocidine self-assembly in the modulation of antibacterial activity.

Table 1 *Summary of antilisterial activity and selected CD-derived parameters of self-assembly of the purified tyrocidines*The identity of the variable amino acid residues in positions 3, 4 and 9 are given, with Phe = F; Trp = W; Lys = K; and Orn = O, and D-amino acids indicated by lower case letters.

Peptide	**Antilisterial activity (μM)[1]**		**Variable residue identity**	**$\theta_{205}/\theta_{216}$ in water[2]**	**$\theta_{204}/\theta_{214}$ in TFE[2]**
	IC_{50}	IC_{max}			
TrcA	13 ± 0.49	25 ± 0.54	F^3f^4-O^9	0.92 ± 0.0077	1.11 ± 0.078
$TrcA_1$	18 ± 0.94	38 ± 1.0	F^3f^4-K^9	0.94 ± 0.077	0.93 ± 0.062
TrcB	10 ± 0.46	15 ± 0.41	W^3f^4-O^9	1.15 ± 0.040	1.51 ± 0.038
$TrcB_1$	8.1 ± 0.19	15 ± 0.47	W^3f^4-K^9	1.14 ± 0.037	1.49 ± 0.155
TrcC	9.5 ± 0.73	13 ± 0.32	W^3w^4-O^9	1.15 ± 0.026	1.74 ± 0.117
$TrcC_1$	9.3 ± 0.25	22 ± 0.54	W^3w^4-K^9	1.03 0 ± 0.025	1.68 ± 0.168

[1] Refer to Chapter 5
[2] Refer to Chapter 3

Strong exponential correlations were observed between antilisterial activity and the CD-derived parameters of self-assembly. For all the tyrocidines, an increase in antilisterial activity (against *L. monocytogenes* B73) correlated exponentially with an increase of the ellipticity ratio $\theta_{204}/\theta_{214}$ in the membrane-mimetic TFE (Figure 1). It is important to note that, although the IC_{50} values are not all statistically different (*refer to Chapter 5* [9]), they follow the same trend as the statistically different IC_{max} values. In a membrane environment, the Trp-containing tyrocidines (TrcC, C_1, B and B_1) exhibit greater β-sheet structure/self-assembly than the Trp-lacking tyrocidines (TrcA and A_1) (*Refer to Chapter 3*). As discussed in Chapter 5 [9], the Trp-containing tyrocidines (TrcC, C_1, B and B_1) exhibited greater antilisterial activity than the Trp-lacking tyrocidines (TrcA and A_1). Activity as characterised by IC_{50} and IC_{max} therefore correlated with the ability to self-assemble in membrane environments and are probably related to the lytic activity of the tyrocidines towards *L. monocytogenes*.

As discussed in Chapter 3, the Phe^3-containing tyrocidines (TrcA and A_1) probably form more/larger higher-order structures (β-sheet formation) than the Trp^3-containing tyrocidines (TrcC, C_1, B and B_1) in an aqueous environment. Such self-assembly in an aqueous environment corresponds to the observed antilisterial activity as the Phe^3-containing tyrocidines A and A_1 were found to be significantly less active than the Trp^3-containing tyrocidines C, C_1, B and B_1 [9] (Chapter 5). These results indicate that

enhanced self-assembly in aqueous solution leads to reduced antilisterial activity, probably due to reduced efficiency of membrane interaction and/or integration. However, as discussed in Chapter 5 [9], the six major tyrocidines exhibited similar lytic activities, which suggests that the correlation between enhanced self-assembly within a membrane-environment and enhanced antilisterial activity may be related to the manner in which/the extent to which the peptides translocate to the cytoplasm or cause membrane leakage, rather than the induction of overt lysis. It should also be kept in mind that the methodology used to characterise membrane lysis is only accurate/sensitive enough to indicated overt/extreme lysis and would not provide an indication of the ability of the tyrocidines to induce membrane leakage.

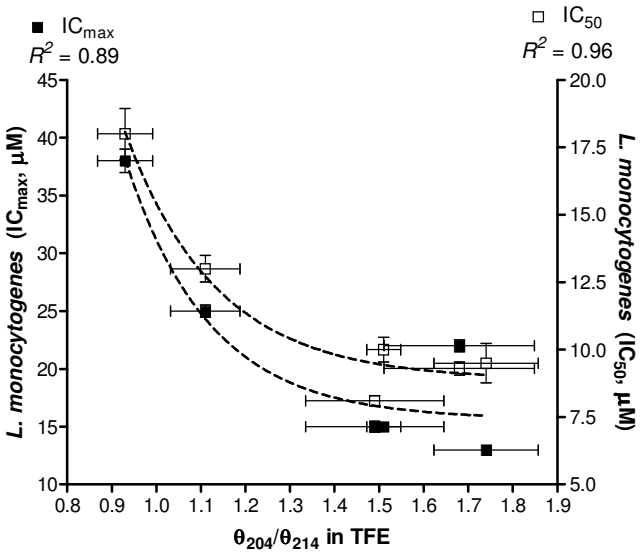

Figure 1 *Correlations between antilisterial activity (IC_{max} and IC_{50}) and the CD-derived descriptor of self-assembly in a membrane-mimetic environment ($\theta_{204}/\theta_{214}$ in TFE).* Each data point represents the mean of at least three determinations ± standard error of the mean (SEM).

Conclusion

Enhanced self-assembly in aqueous solution was found to be associated with reduced antilisterial activity, which suggests that premature self-assembly reduces target membrane interaction, integration and/or translocation to reach a cytoplasmic target. Enhanced self-assembly in a membrane environment was found to be associated with enhanced antilisterial activity, which suggests that self-assembly into active lytic

complexes within the target cell membrane and/or complexes than can traverse this barrier may be critical for the antilisterial activity of the tyrocidines.

References

[1] N.Y. Yount, M.R. Yeaman, Immunocontinuum: perspectives in antimicrobial peptide mechanisms of action and resistance, Protein Pept. Lett. 12 (2005) 49-67.

[2] P.M. Hwang, H.J. Vogel, Structure-function relationships of antimicrobial peptides, Cell Biol. 76 (1998) 235-246.

[3] V. Frecer, B. Ho, J.L. Ding, *De novo* design of potent antimicrobial peptides, Antimicrob. Agents Chemother. 48 (2004) 3349-3357.

[4] E. Glukhov, M. Stark, L.L. Burrows, C.M. Deber, Basis for selectivity of cationic antimicrobial peptides for bacterial versus mammalian membranes, J. Biol. Chem. 280 (2005) 33960–33967.

[5] A. Scaloni, M. Dalla Serra, P. Amodeo, L. Mannina, R.M. Vitale, A.L. Segre, O. Cruciani, F. Lodovichetti, M.L. Greco, A. Fiore, M. Gallo, C. D'Ambrosio, M. Coraiola, G. Menestrina, A. Graniti, V. Fogliano, Structure, conformation and biological activity of a novel lipodepsipeptide from *Pseudomonas corrugata*: cormycin A, Biochem. J. 384 (2004) 25-36.

[6] T. Rydlo, S. Rotem, A. Mor, Antibacterial properties of dermaseptin S4 derivatives under extreme incubation conditions, Antimicrob. Agents Chemother. 50 (2006) 490–497.

[7] Y. Shai, Mode of action of membrane active antimicrobial peptides, Biopolymers (Pept. Sci.) 66 (2002) 236-248.

[8] B. Bechinger, K. Lohner, Detergent-like actions of linear amphipathic cationic antimicrobial peptides, Biochim. Biophys. Acta 1758 (2006) 1529–1539.

[9] B.M. Spathelf, M. Rautenbach, Anti-listerial activity and structure–activity relationships of the six major tyrocidines, cyclic decapeptides from *Bacillus aneurinolyticus*, Bioorg. Med. Chem. 17 (2009) 5541-5548.

Chapter 6

A non-lytic mode of action towards *Listeria monocytogenes* depends on the complexation of the natural tyrocidines with Ca^{2+}

6.1 Introduction

Listeriosis, a severe disease with high hospitalisation and case fatality rates, is caused by *Listeria monocytogenes*, a food-borne pathogen that has drawn the interest of food manufacturers and government bodies [1-3]. Since the isolation of the first multi-resistant stain of *L. monocytogenes* in 1988 [4] numerous strains of *L. monocytogenes* exhibiting resistance to antimicrobial agents [5-8] and disinfectants [9-11] have been reported, which necessitates the development of new preservatives. Naturally occurring preservatives, such as small organic biomolecules and membrane or cell wall perturbing proteins and peptides have been receiving mounting interest from the food industry [2, 12, 13]. The broad spectrum antibacterial activity, speed of action and reduced likelihood of resistance development toward antimicrobial peptides suggest that these compounds may be useful as bio-preservatives [14]. Nisin and pediocin, bacteriocins produced by lactic acid bacteria (LAB), have been shown to effectively inhibit *L. monocytogenes* growth in various food products and are currently accepted for use as food preservatives [2, 13, 15-18]. Unfortunately, *L. monocytogenes* strains that exhibit resistance toward nisin and pediocin have been reported [2, 18-20]. In addition to the challenge of resistance-development, control of *L. monocytogenes* in food is complicated by its high temperature, salt and pH tolerance [1, 21, 22]. The ability of *L. monocytogenes* to grow under high salt conditions pose a significant problem for the application of antimicrobial peptides as bio-preservatives since the activity of most antimicrobial peptides is reduced by the presence of cations such as Na^{+}, Mg^{2+} and Ca^{2+} [23-27]. Divalent cations, especially Ca^{2+}, lead to a dramatic reduction in antibacterial activity of various antimicrobial peptides, including nisin and pediosin [16, 24-29]. The inhibition of antimicrobial peptide activity by cations may be due to either increased aggregation induced by cations [24, 30], which would decrease the number of “active”

peptide, or inhibition of membrane-binding, probably by shielding electrostatic interaction between the peptide and the target membrane [16, 24, 31]. The tyrocidines, a group of cyclic antimicrobial peptides produced by *Bacillus aneurinolyticus*, have been shown to possess significant antibacterial activity toward *L. monocytogenes* [32]. Furthermore, the tyrocidines were found to possess enhanced antilisterial activity toward *L. monocytogenes* B73-MR1, a leucocin A (a pediocin-like bacteriocin) resistant strain [32, 33], relative to the leucocin A-sensitive *L. monocytogenes* B73 [32, 34], which suggests that the tyrocidines may be useful bio-preservatives. Investigation of the influence of cations on the antilisterial activity of the tyrocidines may thus provide valuable information for development of the tyrocidines for use as bio-preservatives.

6.2 Materials

Tyrothricin (commercial extract from *B. aneurinolyticus*), gramicidin S, trifluoroacetic acid (TFA, >98%), trifluoroethanol (TFE), Corning Incorporated® cell culture cluster, non-pyrogenic polypropylene 96-well microtiter plates, bisbenzimide and propridium iodide was supplied by Sigma (St. Louis, USA). The microtiter plates (Nunc™-Immuno Maxisorp) and culture dishes were supplied by AEC Amersham (Johannesburg, South Africa) and Lasec (Cape Town, South Africa), respectively. The CellTiter-Blue™ Cell Viability Assay kit was supplied by Promega (Madison, USA). The diethyl ether, acetone, butan-1-ol, acetic acid, propan-2-ol, agar powder and NaCl were supplied by Saarchem (Krugersdorp, South Africa). Acetonitrile (ACN) (HPLC-grade, far UV cut-off) and was supplied by Romill Ltd. (Cambridge, UK). Biolab Diagnostics (Midrand, South Africa) supplied the brain heart infusion broth (BHI) and BHI agar. Bovine milk casein and was supplied by Fluka Chemicals (Buchs, Switzerland). The Na_2HPO_4 and KH_2PO_4 and ethanol (>99.8%) were supplied by Merck (Darmstadt, Germany). Capital Enterprises (Hillcrest, South Africa) supplied the KCl. Analytical grade water was prepared by filtering water from a reverse osmosis plant through a Millipore Milli-Q® water purification system (Milford, USA).

6.3 Methods

6.3.1 Peptide preparation

Peptides were isolated from commercially obtained tyrothricin and purified by semi-preparative reverse-phase high-performance liquid chromatography (RP-HPLC), as previously described by Rautenbach *et al.* (2007) [35] and Spathelf and Rautenbach (2009) [32]. Stock solutions of the purified peptides of 2.00 mg/mL were analytically prepared in ethanol:water (1:1, *v*/*v*). For dose-response experiments, the stock solution was diluted to 500 µg/mL in the appropriate solvent (water or salt solution) and used to construct a doubling dilution series in polypropylene 96 multi-well plates using the same solvent. For the single-concentration experiments, the stock solution was analytically diluted to 125 µg/mL or 0.100 mM in the appropriate solvent.

6.3.2 Culturing of bacteria

L. monocytogenes B73 was cultured, using normal sterile techniques, from freezer stocks on BHI agar at 37°C for 24 hours. Selected colonies were cultured overnight at 37°C in BHI broth (37 g in 1L water) or BHI broth supplemented with 7.5 mM $CaCl_2$. The overnight cultures were sub-cultured in standard BHI broth or BHI broth supplemented with 7.5 mM $CaCl_2$ at 37°C to an OD_{620} of 0.4 for use in activity determinations, dose-response assays and live-cell fluorescent microscopy.

6.3.3 Cell viability assays

Suspensions for the cell viability assays were prepared by diluting the mid-log phase cultures (OD_{620} of 0.4) of *L. monocytogenes* B73 in standard BHI broth or BHI broth supplemented with 7.5 mM $CaCl_2$ to an OD_{620} of 0.20 (determined as 6.7×10^8 CFU/mL). The cell viability assays were performed in 96-well microtiter plates that were sterilised with 70% isopropanol and blocked with sterile 0.5% casein in Dulbecco's phosphate buffered saline (PBS) [36] prior to use. A 90 µL of cell suspension was added to the microtiter plates, followed by 10 µL of peptide solution. After the addition of the peptides, the microtiter plates were incubated at 37°C for 2 or 16 hours, after which 10 µL of the CellTiter-Blue™ reagent was added to each well and incubated for a further hour. Cell viability was determined using the CellTiter-Blue™ Cell Viability Assay in which resazurin (blue, absorption maximum at 605nm) is

reduced to resofurin (pink, absorption maximum at 573nm) in actively respiring cells [37]. The light absorption of each well was spectrophotometrically determined at 490 and 595 nm using a Biorad microtiter plate reader and percentage inhibition calculated according to equation 1:

$$\%\ inhibition\ = 100 - \frac{100 \times (A_{490/595}\ of\ well - Average\ A_{490/595}\ of\ background\ )}{Average\ A_{490/595}\ of\ growth\ \ wells - Average\ A_{490/595}\ of\ background} \quad (1)$$

6.3.4 Cell survival assays

Cell suspensions (OD_{620} of 0.20, $6.7x10^8$ CFU/mL) were prepared as for the cell viability assays. A 10 µL of the diluted peptide solution was added to 90 µL of cell suspension and incubated at 37ºC for 2 and 16 hours. Culture samples were subsequently diluted in sterile PBS, plated onto BHI agar plates and incubated at 37ºC for 24 hours after which colony forming units (CFU) were counted. Cell survival was calculated as the percentage of CFUs relative to the growth control.

6.3.5 Data analysis

Dose-response curves were plotted using GraphPad Prism® 3.01 and 4.00 (GraphPad Software, San Diego, USA). The dose-response data was analysed by performing nonlinear regression and sigmoidal curves (with variable slope and a constant difference of 100 between the top and bottom plateau) were fitted according to Rautenbach et al. (2006) [38]. IC_{50} is defined as the concentration of peptide required to induce 50% inhibition; and the activity slope, which is related to the Hill slope, defines the slope of the curve [38]. IC_{max}, related to the maximum inhibitory concentration (MIC), was calculated from the x-values at the intercept between the slope and the top plateau, as described by Du Toit and Rautenbach (2000) [39]. IC_{min}, the minimum inhibitory concentration, was calculated from the x-values at the intercept between the slope and the bottom plateau. IC_F-values were calculated according to equations 1-4 from Rautenbach et al. (2006) [38].

$$IC_F = IC_{max}/IC_{min} \quad (1)$$

$$IC_F = (IC_{50}/IC_{min})^2 \quad (2)$$

$$IC_F = (IC_{max}/IC_{50})^2 \quad (3)$$

$$IC_F = 0.25 \times (IC_{50}/IC_{min} + IC_{max}/IC_{50})^2 \quad (4)$$

All four equations were used to calculate an average IC_F in order to minimize the overall error by considering the whole dose-response curve. For single concentration experiments and CFU, percentage inhibition/survival and the standard error of the mean was determined using GraphPad Prism® 4.00 (GraphPad Software, San Diego, USA).

6.3.6 Fluorescent microscopy

Mid-log phase cultures (OD_{620} of 0.4) of *L. monocytogenes* B73 was washed in sterile NaCl (0.9% *m/v*) and resuspended to an OD_{620} of 0.20 in sterile NaCl (0.9% *m/v*). For each sample, 200 µL cell suspension was incubated with 2 µL bisbenzamide (a membrane permeable DNA chelator) and 2 µL propridium iodide (a membrane impermeable DNA chelator) at room temperature for 15 minutes. 10 µL of peptide solution was added to 90 µL of the stained cells (final peptide concentration of 6.25 µg/mL). Image acquisition was performed on an Olympus Cell^R system attached to an IX 81 Inverted fluorescence microscope equipped with an F-view-II cooled CCD camera (Soft Imaging Systems). Using a Xenon-Arc burner (Olympus Biosystems GMBH) as light source, images were acquired using the 360 nm and 472 nm excitation filters. Emission data was collected using a UBG triple-bandpass emission filter cube (Chroma). Images were acquired using an Olympus Plan Apo N60x/1.4 Oil objective. The degree of membrane leakage/lysis was deduced from the fluorescent signal of the membrane impermeable propridium iodide.

6.3.7 Circular dichroism and fluorescence spectroscopy

Analytical stock solutions (2.00 mg/mL) of the purified tyrocidines were prepared in ethanol:water (1:1, *v/v*), and diluted to 10 µM in water, 2,2,2-trifluoroethanol (TFE), 75 mM $CaCl_2$ or 75 mM $MgCl_2$ (final ethanol concentration was 0.5% *v/v*) for the circular dichroism, UV absorbance and fluorescence analyses. Circular dichroism scans were obtained on a Chirascan CD spectrometer (Applied Photophysics, UK) using a 1.00 cm quartz cuvette. Three scans were collected between 200 and 250 nm with 0.1 nm steps. UV-absorbance spectra were collected simultaneously with the CD spectra. Fluorescence measurements of the same peptide solutions were performed on a model RF-5301PC spectrofluorophotometer (Shimadzu, Japan). Emission spectra were

recorded between 280 and 450 nm, 0.2 nm steps, for excitation at 280 and 295 nm. Slit widths of 5 nm were used for both excitation and emission.

6.3.8 Mass spectrometry

Complexation between the tyrocidines and various cations was investigated by diluting the stock solution of tyrocidine complex to 12.5 μg/mL in 1.0 mM NaCl, KCl, $MgCl_2$ or $CaCl_2$. For investigation of complexation between the purified tyrocidines and divalent cations (Ca^{2+} and Mg^{2+}) by mass spectrometry, the purified tyrocidine stock solutions were diluted to 10 μM in various $CaCl_2$ or $MgCl_2$ concentrations. Time-of-flight electrospray mass spectrometry (TOF-ESMS) analyses were performed using a Waters Q-TOF Ultima mass spectrometer fitted with an electrospray ionisation source. Ten μL of each peptide sample was injected into the ESMS and subjected to a capillary voltage of 3.5 kV. The source temperature and cone voltage was set at 100 ºC and 35 V, respectively. The data was collected in positive mode by scanning the first mass analyser (MS_1) through m/z = 100–1999.

6.4 Results and Discussion

6.4.1 Influence of growth medium composition and cations on antilisterial activity

The influence of growth medium on the reduction of cell viability by the tyrocidine complex, tyrocidine A (TrcA), tyrocidine B (TrcB) and tyrocidine C (TrcC), and gramicidin S toward L. monocytogenes B73 was investigated by pre-incubating the peptides in BHI growth medium. Reduction of cell viability by TrcA and TrcB was increased by 70 % and 120 %, respectively, upon pre-incubation in BHI growth medium (Table1), which indicates that the tyrocidines are sensitive to solvent composition. The activity of the tyrocidine mixture and TrcC was, however, not significantly increased (Table1), which indicates that the various tyrocidines have different sensitivities to BHI growth medium.

Table 1 Influence of solvent conditions on reduction of cell viability after 3 hours. The inhibition of cell viability was induced by 12.5 μg/mL (tyrocidine mixture) or 10 μM (purified peptides) peptide diluted in water, BHI growth medium or salt solutions. The antilisterial activity is expressed relative to activity of peptides diluted in water.

	Fold change in activity				
Modifier/solvent	**Trc mix**	**Trc A**	**Trc B**	**Trc C**	**GS**
Water	1.0 ± 0.049	1.0 ± 0.040	1.0 ± 0.020	1.0 ± 0.015	1.0 ± 0.035
BHI medium	1.2 ± 0.034	1.7 ±0.076***	2.2 ± 0.096***	1.4 ± 0.077	1.02 ± 0.11
7.5mM NaCl	1.0 ± 0.053	0.92 ± 0.076	0.93 ± 0.034	0.87 ± 0.080	ND
15.0mM NaCl	1.1 ± 0.064	0.90 ± 0.061	0.91 ± 0.046	0.86 ± 0.078	ND
7.5mM KCl	1.0 ± 0.045	0.78 ± 0.089	0.91 ± 0.021	0.84 ± 0.054	ND
15.0mM KCl	1.1 ± 0.053	0.89 ± 0.090	0.98 ± 0.055	0.85 ± 0.053	ND
7.5mM $MgCl_2$	1.0 ± 0.050	1.0 ± 0.043	0.91 ± 0.048	0.93 ± 0.0.58	ND
15.0mM $MgCl_2$	1.1 ± 0.053	1.0 ± 0.073	0.92 ± 0.055	0.98 ± 0.056	ND
7.5mM $CaCl_2$	1.6 ± 0.021***	1.8 ± 0.20***	1.4 ± 0.030***	1.3 ± 0.042*	1.0 ± 0.084
15.0mM $CaCl_2$	1.4 ± 0.048***	1.6 ± 0.13***	1.3 ± 0.039***	1.0 ± 0.053	1.0 ± 0.039

Fold change in inhibition of peptide with water as solvent ± standard error of the mean (N≥3);
* P<0.05; ** P<0.01; *** P<0.001

Components in the growth medium that may affect the activity of cationic membrane active peptides include metal cations (such as Na^+, K^+, Mg^{2+} and Ca^{2+}), phosphate, amino acids, peptides, proteins, lipids and carbohydrates. The influence of the major biological alkali and earth metal cations on activity (reduction of cell viability) was determined by pre-incubating the natural tyrocidine complex, purified natural tyrocidines A, B and C, and gramicidin S in NaCl, KCl, $MgCl_2$ and $CaCl_2$ solutions. The results indicated that only $CaCl_2$ influenced the activity of the tyrocidines, whereas the other cations investigated (Na^+, K^+ and Mg^{2+}) did not significantly affect their inhibitory activity (Table 1). As seen for the influence of BHI growth medium, the different tyrocidines exhibit different sensitivities to $CaCl_2$. TrcA displayed the greatest increase in activity and was found to be more sensitive than TrcB, with the activity of TrcC the least sensitive (Table 1). The observation that the tyrocidines are relatively salt-insensitive and that $CaCl_2$ increased activity indicates that calcium plays a major role in the modulation of tyrocidine anti-listerial activity. Furthermore, the activity of gramicidin S was not influenced by the presence of $CaCl_2$ (Table 1), which suggest that

the $CaCl_2$-induced increase in tyrocidine activity involves a process specific to the tyrocidines and not non-specific cell sensitisation.

6.4.2 Investigation of tyrocidine-cation complexation by mass spectrometry

Complex formation between the tyrocidines and the major biological alkali and earth metal cations (Na^+, K^+, Mg^{2+} and Ca^{2+}) was investigated by TOF-ESMS. The degree of complex formation was deduced by monitoring the reduction of singly charged free peptide ions ($[M+H]^+$). In general, the addition of cations was shown to reduce the detection/availability of free peptide ions (Figure 1), which may be a result of precipitation ("salting-out"), peptide-cation complexation or masking of the peptide ion by the chloride counterion. Different cations led to varying degrees of free peptide ion loss, suggesting that the tyrocidines have different affinities for different types of cations. Addition of divalent cations (magnesium or calcium) led to a greater loss of free peptide ions (approximately 80%) than the addition of monovalent cations (sodium or potassium), which may suggest that the tyrocidines have a greater affinity for divalent cations. However, the higher chloride ion concentration may also lead to this result. When the detection of free peptide in the presence of the monovalent cations is considered it is clear that the tyrocidine affinity for Na^+ is greater than K^+. Comparing the divalent ions, lower free peptide signal was detected for Ca^{2+} suggesting a higher affinity than for Mg^{2+}. In addition to each tyrocidine having different affinities for the various cations, the tyrocidines exhibit varying affinities for each cation, which suggests that peptide structure influences cation complexation. The six major tyrocidines exhibited similar affinities for sodium. In general, greater affinity for monovalent potassium is associated with greater HPLC retention time (solution amphipathicity/apparent hydrophobicity) and lower side-chain surface areas (results not shown). In contrast, greater affinity for divalent cations is associated with shorter HPLC retention time (solution amphipathicity/apparent hydrophobicity) and larger side-chain surface areas (results not shown).

Complexation between the purified tyrocidines and divalent cations (Ca^{2+} and Mg^{2+}) was further investigated by mass spectrometry. The degree of complex formation was deduced by monitoring the signal intensity of the cation adducts ($[M+Ca]^{2+}$ or $[M+Mg]^{2+}$) in the presence of various $CaCl_2$ or $MgCl_2$ concentrations and used to

calculate the apparent maximal Ca^{2+} or Mg^{2+} binding (maximal/plateau MS signal of complex, S_{max}) of the six major tyrocidines (Figure 2).

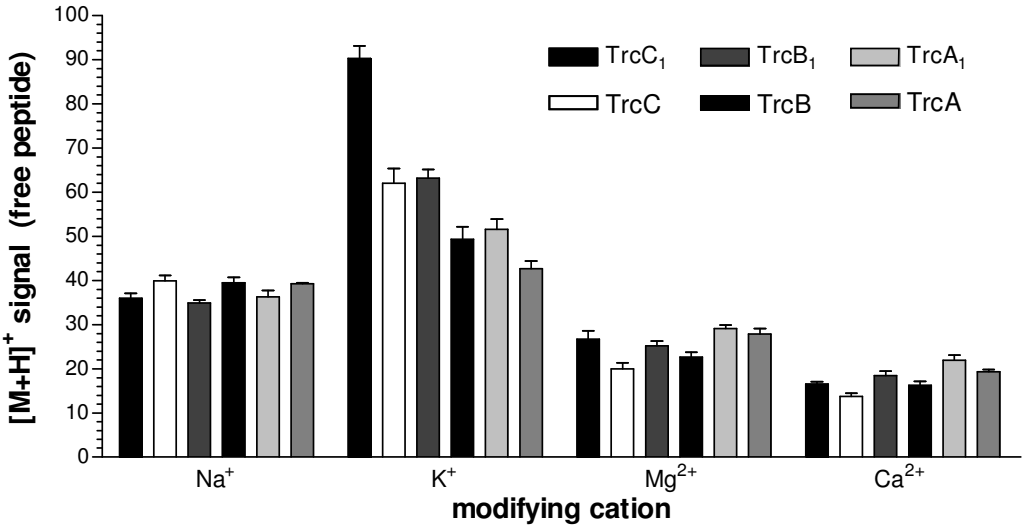

Figure 1 *Tyrocidine-cation complexation as determined by TOF-ESMS.* TOF-ESMS *s*ignal of singly charged free peptide ions ($[M+H]^+$) relative to ethanol:water (1:1, *v/v*) of tyrocidines in the tyrocidine complex prepared in solutions containing different chloride salts at 1 mM. The average of triplicate determinations with the standard error of the mean is shown.

The apparent maximal calcium binding of the tyrocidines was found to be related to their solution amphipathicity, as illustrated by the linear correlation ($R^2 = 0.82$) between S_{max} for Ca^{2+} and HPLC retention time (Figure 3A), and suggests that increased amphipathicity allows for increased Ca^{2+}-complexation. As increased amphipathicity is also expected to be associated with increased self-assembly in an aqueous environment, the increased apparent Ca^{2+}-complexation may be related to incorporation of Ca^{2+} within the assembly. Some correlation was also observed between S_{max} for Mg^{2+} and HPLC retention time, but required segregation of the Lys^9 and Orn^9 containing tyrocidines (Figure 3B). These correlations indicate that increased amphipathicity also allows for increased Mg^{2+}-complexation, possibly due to incorporation of Mg^{2+} with higher-order structures. However, the required segregation of the Lys^9- and Orn^9-containing tyrocidines, and the significantly lower S_{max} for Mg^{2+} of the Lys^9-containing tyrocidines, indicate that the manner of Mg^{2+}-complexation differs for these two groups, possibly due to differences in self-assembly (*Discussed in Chapter 3*).

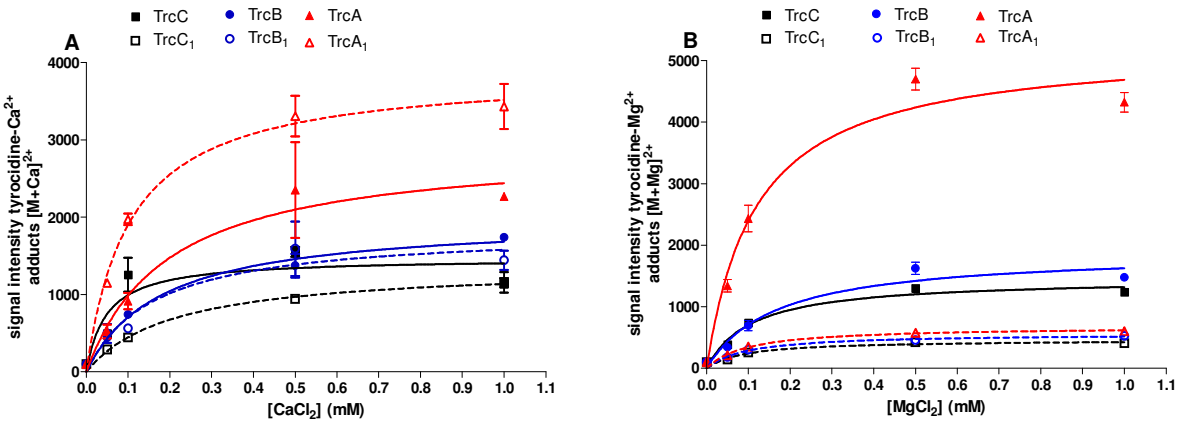

Figure 2 *Apparent (A) Ca^{2+}-tyrocidine and (B) Mg^{2+}-tyrocidine complexation as determined by TOF-ESMS.* TOF-ESMS signal of tyrocidine-Ca^{2+} or -Mg^{2+} adducts ($[M+Ca]^{2+}$ or $[M+Mg]^{2+}$) relative to ethanol:water (1:1, *v/v*) of the purified major tyrocidines prepared in solutions of varying $CaCl_2$ or $MgCl_2$ concentrations. Each data point represents the average of triplicate determinations ± SEM.

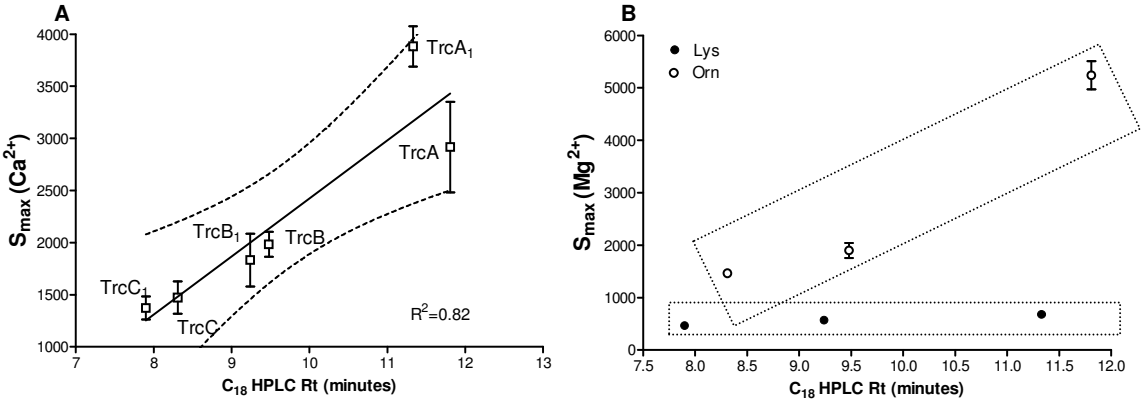

Figure 3 *Correlation between the apparent maximal (A) Ca^{2+} or (B) Mg^{2+} binding (S_{max}) and HPLC retention time of the tyrocidines.* Each data point represents the average of triplicate determinations ± SEM. The dashed lines in A indicates the 95% confidence interval and the boxes in B shows the two tyrocidine groupings.

As tyrocidine-Ca^{2+} complexation and/or induction of higher-order structures influences the antilisterial activity and mode of action, correlations between S_{max} for Ca^{2+} and antilisterial activity may provide insight regarding the structure-activity relationships and mode of action. With the exception of $TrcC_1$, a strong linear correlation ($R^2 = 0.95$) was observed between the S_{max} for Ca^{2+} and antilisterial activity of the tyrocidines (Figure 4), which suggest that increased calcium binding leads to reduced antilisterial

activity. However, $TrcC_1$ does not follow the same trend. $TrcC_1$ exhibited the lowest S_{max} for Ca^{2+} and reduced activity, which strongly suggest that an optimal amount of Ca^{2+}-complexation is required for antilisterial activity. The loss of activity associated with increased Ca^{2+}-binding may be related to increased self-assembly within solution leading to loss of peptide due to precipitation, whereas the reduced activity of $TrcC_1$ associated with low Ca^{2+}-complexation indicates that a certain amount of Ca^{2+}-binding is required for antilisterial activity. No clear correlations were observed between the antilisterial activity and S_{max} for Mg^{2+}, which suggests that Mg^{2+}-complexation is not a direct determinant of antilisterial activity. However, increased Mg^{2+}-complexation may compete with Ca^{2+}-complexation, indirectly influencing tyrocidine activity. These results suggests that the correlation between antilisterial activity and S_{max} for Ca^{2+} may be unique to this divalent cation, which corresponds to the earlier observations that only Ca^{2+} influences antilisterial activity (Table 1).

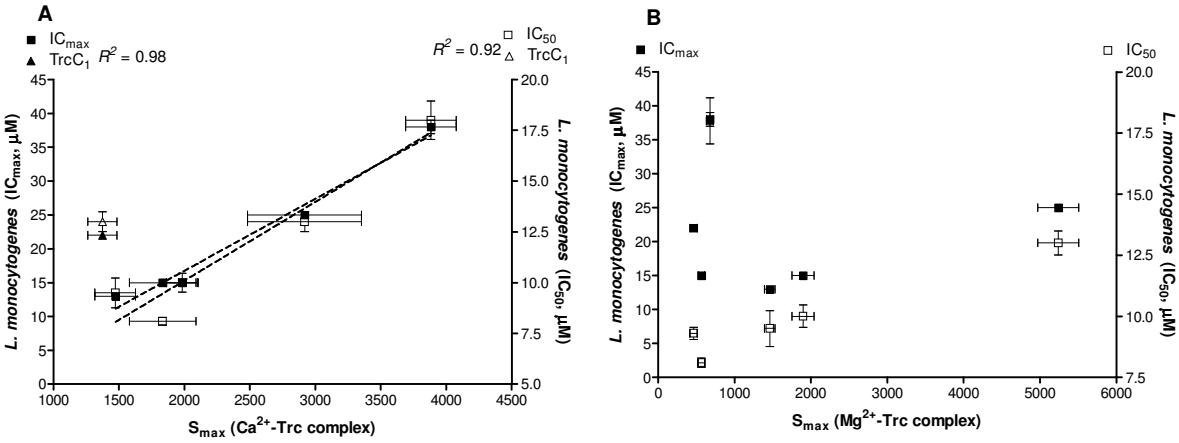

Figure 4 *Correlation between the apparent maximal divalent cation (Ca^{2+} in A and Mg^{2+} in B) binding (S_{max}) and antilisterial activity (IC_{max} and IC_{50}) of the tyrocidines.* Each data point represents the average of at least three determinations ± SEM.

6.4.3 Influence of divalent cations on the conformation/self-assembly of tyrocidines A, B and C

Circular dichroism (CD) spectroscopy was used to investigate the influence of calcium, magnesium and trifluoroethanol (TFE) on tyrocidine conformation and/or self-assembly. As discussed in Chapter 3, the CD spectra of tyrocidines A, B and C in an aqueous environment exhibit negative ellipticity minima at 205 (θ_{205}) and

216 (θ_{216}) nm. Although such CD spectra are reminiscent of an α-helical structure, previous research has indicated that these negative ellipticities are due to type II` β-turn (205 nm) and β-sheet (216 nm) structure [40-44]. It should, however, be noted that the shape and intensity of the minima are influenced by the aromatic amino acids, which are known to distort CD spectra, as well as the aggregation state of the peptide [44-46].

In the presence of Ca^{2+}, the CD spectra of the Trp-containing tyrocidines B (Trp^3-D-Phe^4) and C (Trp^3-D-Trp^4) exhibited enhanced θ_{205} and θ_{216} (Figures 5A and B). The CD spectra of TrcB in the presence of Mg^{2+} also exhibited negative ellipticity minima at 205 and 216 nm, but with decreased intensity relative to water (Figure 5B). In contrast to the CD spectra of the Trp-containing tyrocidines, the CD spectra of tyrocidine A (Phe^3-D-Phe^4) in the presence of Ca^{2+} exhibited slightly red-shifted θ_{216} minima at 218 nm, and generally reduced ellipticity (Figure 5C). These changes in negative ellipticity may be due to changes in backbone conformation, changes in the relative contribution of the aromatic amino acids and/or differences in self-assembly. Previous research indicated that the TrcB forms elongated aggregates in a salt-free environment [47], whereas micelle-like association leads to the formation of spherical aggregates in the presence of NaCl [48, 49]. The manner of self-assembly, the size of the formed aggregate/self-assembled structure and/or the relative orientation of the peptide molecules within the induced structure may affect CD spectra directly or indirectly due to the influence on the orientation/exposure/local environment of the aromatic amino acids. The reduced ellipticity of TrcA in the presence of Ca^{2+} may be related to loss of peptide due to settling out of higher-order structures.

The CD spectra of TrcB and TrcC in TFE exhibited slightly blue shifted negative ellipticity minima with increased intensity at 204 nm and 214 nm, although the resolution of the latter was lost (Figure 5A and B). The CD spectra of TrcA in TFE also exhibited slightly blue shifted negative ellipticity minima with increased intensity at 204 nm and 214 nm, as well as an additional negative band around 222 nm (Figure 5C). These changes in ellipticity may be attributed to the induction of significant changes in the self-assembly state, hydrogen bonding and the orientation/exposure/local environment of the aromatic amino acids. (*Refer to Chapter 3*). If it is assumed that the CD spectra in TFE represent self-assembled structures that may be found in membranes,

then the spectrum in $CaCl_2$ represents self-assembled structures that are different from those in TFE (Figures 5A-C).

Fluorescence spectroscopy was used to further investigate the influence of Ca^{2+} and Mg^{2+} on the conformation/self-assembly. For TrcB and TrcC, photoselective excitation of Trp fluorescence (λ_{ex} = 295 nm) indicated emission maxima at 350 nm in water and 75 mM $CaCl_2$, with greatly increased Trp fluorescence observed in the presence of Ca^{2+} (Figures 5D and E). These results suggest that the presence of Ca^{2+} leads to significant changes in the conformation/self-assembly of TrcB and C, which influence the exposure/local environment/quenching of the Trp residue(s). The fluorescence spectra of TrcB in 75 mM $MgCl_2$ also exhibited increased Trp fluorescence, however, Ca^{2+} led to a 2.0 fold increase in Trp fluorescence yield, whereas Mg^{2+} only led to a 1.1 fold increase in Trp fluorescence yield. For TrcA, excitation of Tyr fluorescence (λ_{ex} = 280 nm) indicated emission maxima at 305 and 340 nm in water (Figure 5F), which may be attributed to Tyr and tyrosinate fluorescence [50-52], respectively (*Refer to Chapter 3*). The presence of Ca^{2+} led to greatly increased Tyr fluorescence yield, but a loss of tyrosinate fluorescence yield (Figure 5F). These results suggest that the presence of Ca^{2+} leads to significant conformational changes of TrcA that influence the exposure/local environment/quenching of the Tyr residue and prevents tyrosinate formation.

The CD and fluorescence spectroscopy results therefore indicate that Ca^{2+} induce distinct changes in the conformation/self-assembly of the tyrocidines, which supports the hypothesis that peptide-calcium complexes/aggregates represent the active form of the peptide. Further, comparison of the spectra of TrcB (Figures 5B and E) clearly shows that Ca^{2+} had a significantly greater influence than Mg^{2+}, which explains the observation that Mg^{2+} does not induce similar changes in antilisterial activity. This result was confirmed by NMR titration studies on TrcC that suggested that an increase in Ca^{2+} causes a change in the TrcC structure while increasing Mg^{2+} does not have an effect on the Trc structure (personal communication, K. Köver).

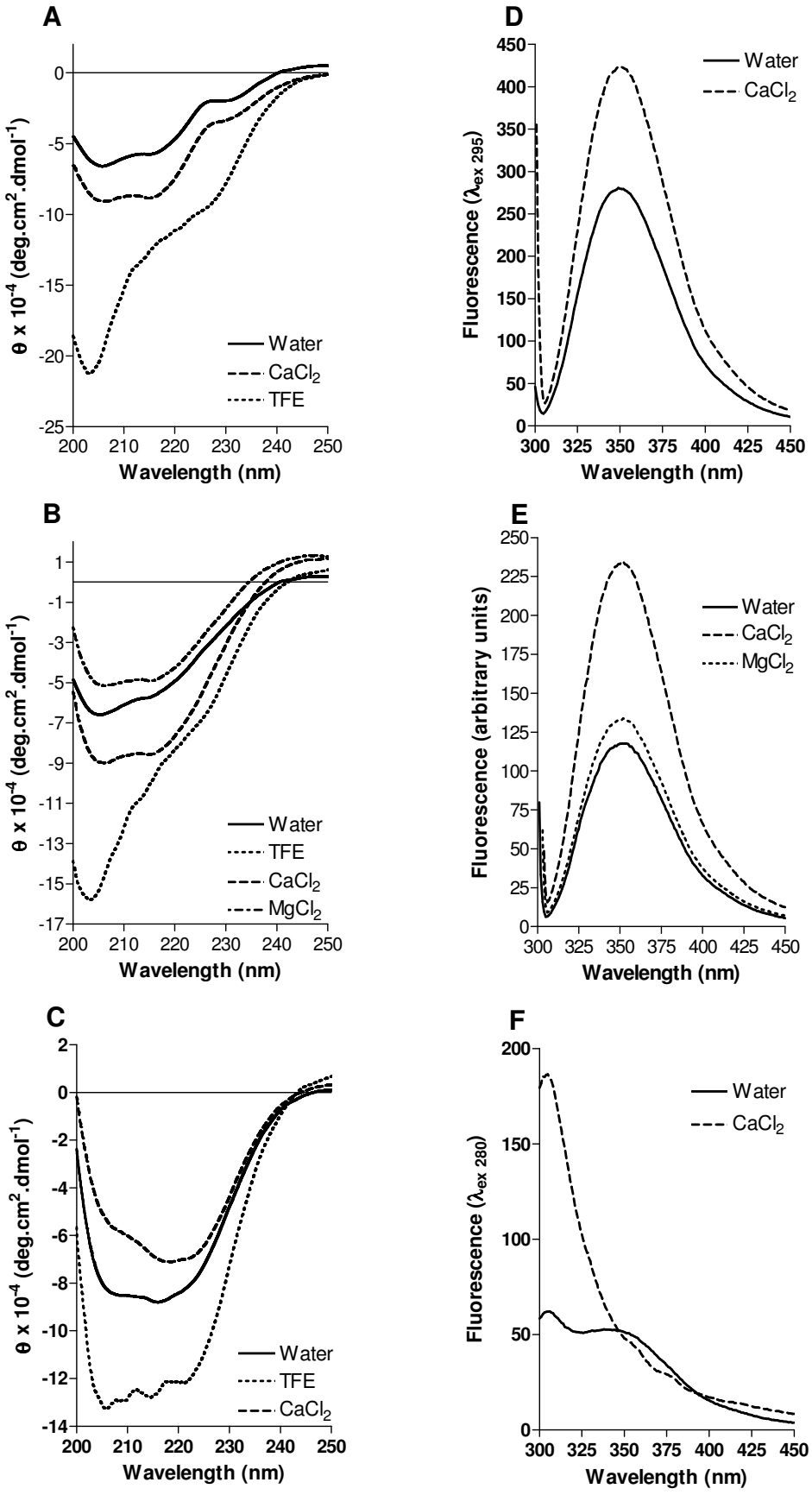

Figure 5 *Influence of solution composition/identity on the CD spectra* ***A****. TrcC,* ***B.*** *TrcB and* ***C.*** *TrcA and fluorescence emission spectra of* ***D****.TrcC,* ***E****. TrcB and* ***F****. TrcA.* Each CD spectrum is depicted by a Lowess fit line (20 point smoothing window) for an average of triplicate determinations.

6.4.4 Influence of calcium on antilisterial activity of the tyrocidines

The optimal calcium concentration for increased activity of the tyrocidine mixture was found to be at least 7.5mM $CaCl_2$ (Figure 6). The undiluted tyrocidine mixture in 37.5 mM $CaCl_2$ (before 10 fold dilution in the assay) became visibly opaque, but a major loss of activity only occurred at 30

0 mM $CaCl_2$ (Figure 6). This loss of activity is due to visible precipitation (salting out) of the tyrocidine mixture in the undiluted stock. When 75 mM $CaCl_2$ (7.5 mM in assay) was added to the peptide solutions, the activity of the tyrocidine complex, as well as the three purified tyrocidines were significantly increased (Table 1, Figure 6).

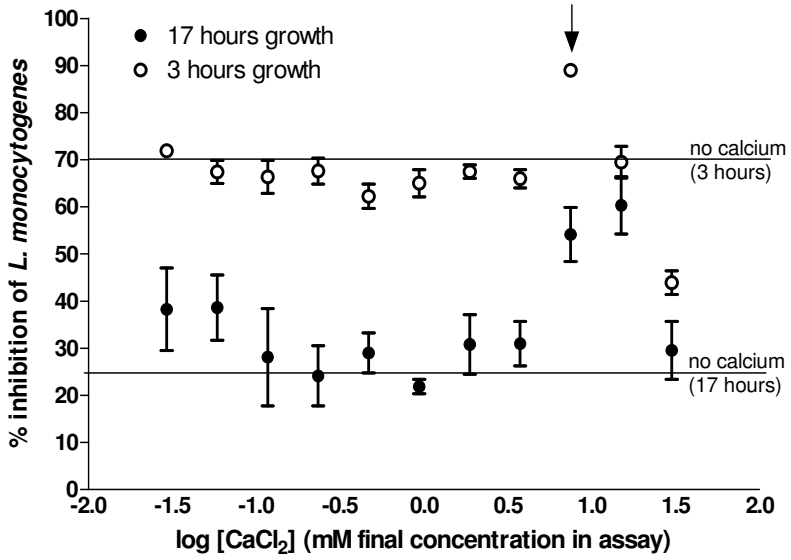

Figure 6 *Effect of calcium concentration on the antilisterial activity of the tyrocidine mixture.* The reduction of cell viability after 3 hours and 17 hours by 12.5 μg/mL tyrocidine mixture diluted in different calcium concentrations was determined. The arrows indicate maximal activity, which was observed at 7.5 mM $CaCl_2$. Each data point represents the mean of quadruplicate repeats, with ± standard error of the mean (SEM).

As discussed above, the increased activity induced by 7.5 mM $CaCl_2$ may be due to complexation between calcium and the tyrocidines inducing a more active conformation or formation of active complexes/higher-order structures. Alternatively, the increased activity in the presence of calcium may be due to increased calcium in the bacterial cell wall or membrane, which may serve as docking sites for the tyrocidines. In order to determine the mode in which calcium modulates antilisterial activity of the tyrocidines, the tyrocidine complex and TrcB were diluted in 75 mM $CaCl_2$ (10× concentrate),

allowing pre-complexation before exposure to growth media and bacteria, and tested toward *L. monocytogenes* cultured in standard BHI growth medium. The second hypothesis was tested by culturing *L. monocytogenes* in BHI growth medium supplemented with 7.5 mM $CaCl_2$, which would allow the influence of calcium-bacteria interaction on activity to be evaluated. It was assumed that bacteria grown in the presence of calcium would have a greater amount of calcium in their cell wall and membrane, possibly providing more binding sites for the tyrocidines. TrcB was chosen to evaluate this aspect as it is more sensitive to solvent composition than TrcC (refer to Table 1) and more active toward *L. monocytogenes* B73 than tyrocidine A [32]. The antilisterial activity of the tyrocidine complex and tyrocidine B was assessed by measurement of cell viability (cell reducing potential) and cell survival (CFU determination) after 2 to 3 hours (short-term effect) and 16 to 17 hours (long-term effect) of exposure and culturing (Figure 7).

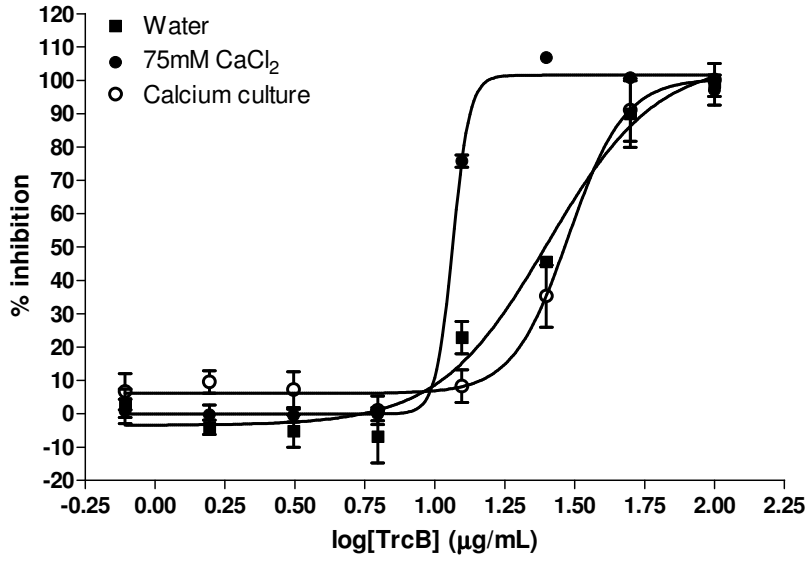

Figure 7 *Representative dose–response curves of TrcB toward L. monocytogenes.* TrcB was either diluted in 75 mM $CaCl_2$ (7.5 mM in assay) or water, or diluted in water and exposed to 7.5 mM $CaCl_2$ in the bacterial culture. Each data point represents the mean of quadruplicate repeats ± SEM. The sigmoidal dose–response curves fitted the experimental data with R^2-values of >0.99.

Investigation of the short term antilisterial activity indicated that both $CaCl_2$ in the peptide solvent and in culturing medium of *L. monocytogenes* B73 led to an increase in activity, as reflected by significantly lower IC_{50}-values and reduced cell survival (Table

2). With 75 mM $CaCl_2$ as peptide solvent (7.5 mM in assay), the reduction of cell viability by the tyrocidine complex and TrcB increased with 2.6 and 1.9 fold, respectively, while cell survival was reduced by 40 and 67%, respectively. The reduction of cell viability by the tyrocidine complex and TrcB toward *L. monocytogenes* B73 cultured in BHI growth medium supplemented with calcium increased with 3.4 and 3.1 fold, respectively, while cell survival was reduced by 24% and 45%, respectively. In contrast, with the longer exposure and culturing (16-17 hours) only 75 mM $CaCl_2$ in the tyrocidine solvent led to an increase in tyrocidine activity (Table 2). The reduction of cell viability by the tyrocidine complex and TrcB increased with 1.5 and 2.3 fold, respectively, while cell survival was reduced by 38 and 25%, respectively.

Table 2 *Effect of peptide solvent on the antilisterial activity of the tyrocidine mixture and tyrocidine B.* The antilisterial activity of the tyrocidine mixture and tyrocidine B (diluted in either water or 75 mM $CaCl_2$) toward *L. monocytogenes* B73 (cultured in either standard BHI growth medium or BHI growth medium supplemented with $CaCl_2$) reflected by inhibition of cell viability, was characterised in terms of IC_{50}, given in µg/mL. Percentage cell survival after incubation with 6.25 µg/mL peptide, is given in terms of CFUs.

	IC_{50} ± SEM (µg/mL)		**% Cell survival ± SEM**	
	3 hours	**17 hours**	**2 hours**	**16 hours**
Trc mix				
Water	7.1 ± 1.2	25 ± 0.40	40 ± 4.4	50 ± 6.0
7.5 mM $CaCl_2$	2.7 ± 0.42*	13 ± 0.0033***	0.010 ± 0.010***	12 ± 8.0*
Calcium culture	2.1 ± 0.30*	28 ± 0.31***,†††	16 ± 2.1**,†	52 ± 10†
TrcB				
Water	13 ± 1.1	25 ± 1.0	72 ± 2.5	56 ± 1.0
7.5 mM $CaCl_2$	6.8 ± 0.25**	11 ± 0.27**	5.3 ± 0.20***	31 ± 4.8*
Calcium culture	4.2 ± 0.077***	30 ± 3.7††	27 ± 2.5**,†	62 ± 10††

P-values were determined with Tukey's multiple comparison test. For statistical difference of activity parameters from parameters for bacteria cultured in standard medium with water used as peptide solvent: *, $P < 0.05$; **, $P < 0.01$, ***, $P < 0.001$ ($N \geq 3$). For statistical difference of activity parameter from parameters for bacteria cultured in standard medium with 75 mM $CaCl_2$ used as peptide solvent: †, $P < 0.05$; ††, $P < 0.01$, †††, $P < 0.001$ ($N \geq 3$).

The discrepancy between the results of short and long term activity toward *L. monocytogenes* cultured in calcium-supplemented growth media suggests that a concomitant tyrocidine challenge leads to reversible cell stress and/or damage.

Fluorescence microscopy with propridium iodide as membrane permeability indicator showed that the calcium exposed cultures exhibit greater intrinsic cell permeability/death (results not shown). The observed increase in short-term activity toward *L. monocytogenes* cultured in calcium-supplemented growth media may thus be attributed to cell damage, which leads to decreased redox potential, but translates to a bacteriostatic and not a bacteriocidal effect. The reduced cell survival seen under these conditions after two hours may be due to loss of damaged but viable cells during dilution of the cultures in PBS before plating-out. Overall, our results indicate that the increased bacteriocidal activity requires peptide-calcium pre-incubation which may lead to the formation of complexes (see discussion on the spectrophotometric analysis of TrcB). The different Ca^{2+}-sensitivities of the various tyrocidines may be due to differences in peptide-calcium interaction and/or different propensities for aggregation. Differences in peptide-calcium complexation and/or aggregation may be related to structural differences of the tyrocidines.

6.4.5 Influence of calcium on the mode of action of the tyrocidines

Previous research has suggested that the antilisterial activity of the tyrocidines may involve a membranolytic as well as an additional/alternative mechanism of action [32]. Two activity parameters related to peptide mechanism of action were determined, namely inhibition concentration factor (IC_F), which describes the increase in peptide concentration between minimum and maximum inhibition and the activity slope (A_S), which is related to the Hill coefficient [38]. Furthermore, live-cell fluorescent microscopy with propridium iodide as permeability indicator was used to assess the microscopic influence of the different solvents and culturing conditions on the lytic activity of TrcB.

In addition to changes in antilisterial activity (as described by IC_{50}), changes in activity parameters indicative of mechanism of action (as indicated by IC_F and A_S) were induced by the use of 75 mM $CaCl_2$ as peptide solvent (7.5 mM in assay). When water was used as peptide solvent, the tyrocidine mixture and TrcB both exhibit IC_{50}s of 25 µg/mL; IC_Fs of 3.2 and 4.1, respectively; and A_S of 3.6 and 4.7, respectively, toward *L. monocytogenes* B73 cultured in standard BHI growth medium (Table 3). The high A_S (>1) suggests that, under these conditions, the peptides self-assemble into active lytic

complexes [38]. This is supported by the results of live-cell fluorescent microscopy, which indicated that TrcB (with water as solvent) induced membrane lysis/leakage of *L. monocytogenes* cultured in standard BHI growth medium, with an apparent lytic rate of 8.6 fluorescent units/min ($R^2 = 0.99$) (Figures 8 and 9). The activity of the tyrocidine complex and TrcB toward *L. monocytogenes* B73 cultured in calcium-supplemented growth medium exhibited similar IC_Fs (2.6 and 3.4, respectively) and A_Ss (4.7 and 3.6, respectively) as toward bacteria cultured in standard growth medium (Table 3). Furthermore, tyrocidine induced lysis/leakage of *L. monocytogenes* cultured in the presence of calcium had an apparent lytic rate of 7.3 fluorescent units/min ($R^2 = 0.99$) which is equivalent to that induced toward *L. monocytogenes* cultured in standard BHI growth medium (Figures 8 and 9).

Table 3 *Effect of peptide solvent on the antilisterial activity after 17 hours growth in the tyrocidine mixture and TrcB.* The antilisterial activity of the tyrocidine mixture and TrcB (diluted in either water or 75 mM $CaCl_2$) toward *L. monocytogenes* B73 (cultured in either standard BHI growth medium or BHI growth medium supplemented with $CaCl_2$) was characterised in terms of IC_{min}, IC_{max}, IC_{50}, IC_F and A_S.

	IC_{min}[1]	**IC_{50}**	**IC_{max}[2]**	**IC_F[3] ± SEM**	**A_S ± SEM**
Trc mix					
Water	14 (14)	25	45 (45)	3.2 ± 0.0041	3.6±0.76
75 mM $CaCl_2$	12 (11)	13***	15 (14)	1.2 ± 0.024***	18±1.6***
Calcium culture	20 (15)	28***,†††	52 (38)	2.6 ± 0.32††	4.7±1.2†††
TrcB					
Water	12 (13)	25	49 (52)	4.1 ± 0.076	2.8±0.35
75 mM $CaCl_2$	10 (8.8)	11**	14 (12)	1.3 ± 0.092***	15±0.32***
Calcium culture	19 (15)	30††	62 (48)	3.4 ± 0.35†††	3.6±1.6†††

[1] From dose-response curves, values in parentheses calculated as $IC_{min} = IC_{50}/\sqrt{IC_F}$; $IC_F = (IC_{max}/IC_{50})^2$
[2] From dose-response curves, values in parentheses calculated as $IC_{max} = IC_{min} \times IC_F$; $IC_F = (IC_{50}/IC_{min})^2$
[3] Average of IC_Fs calculated according to equations (2)-(5)
P-values were determined with Tukey's multiple comparison test. For statistical difference of activity parameters from parameters for bacteria cultured in standard medium with water used as peptide solvent: *, $P < 0.05$; **, $P < 0.01$, ***, $P < 0.001$ ($N \geq 3$). For statistical difference of activity parameter from parameters for bacteria cultured in standard medium with 75 mM $CaCl_2$ used as peptide solvent: †, $P < 0.05$; ††, $P < 0.01$, †††, $P < 0.001$ ($N \geq 3$).

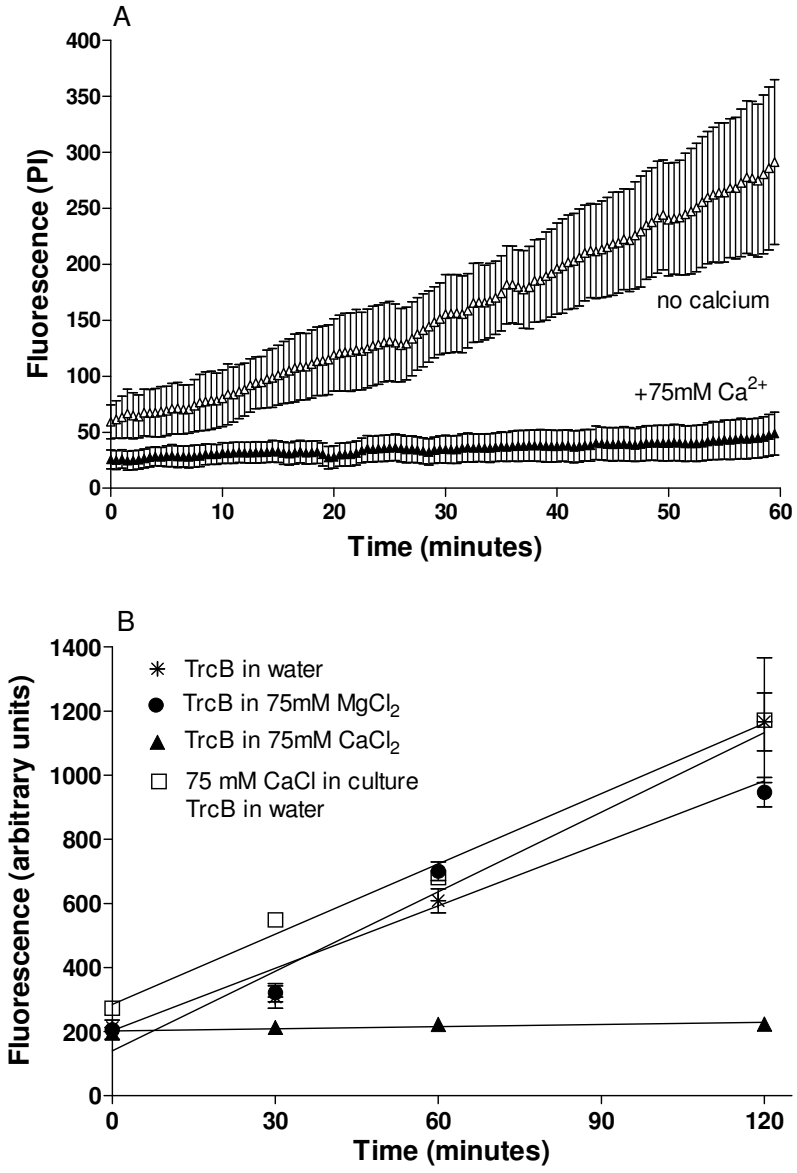

Figure 8 The influence of divalent cations on TrcB-induced leakage of propridium iodide into *L. monocytogenes* B73. **A.** A real time monitoring of propridium iodide fluorescence in the presence of 6.25 µg/mL TrcB either diluted in water or 75 mM $CaCl_2$ (7.5 mM in assay); **B.** The lytic activity of 6.25 µg/mL TrcB (diluted in water, 75 mM $MgCl_2$ or 75 mM $CaCl_2$; 7.5 mM in assay) toward *L. monocytogenes* B73 (cultured in either standard BHI growth medium or BHI growth medium supplemented with $CaCl_2$) was evaluated at different time points by fluorescence microscopy, using propridium iodide. The increase in fluorescent signal of propridium iodide is indicative of increased membrane leakage/lysis.

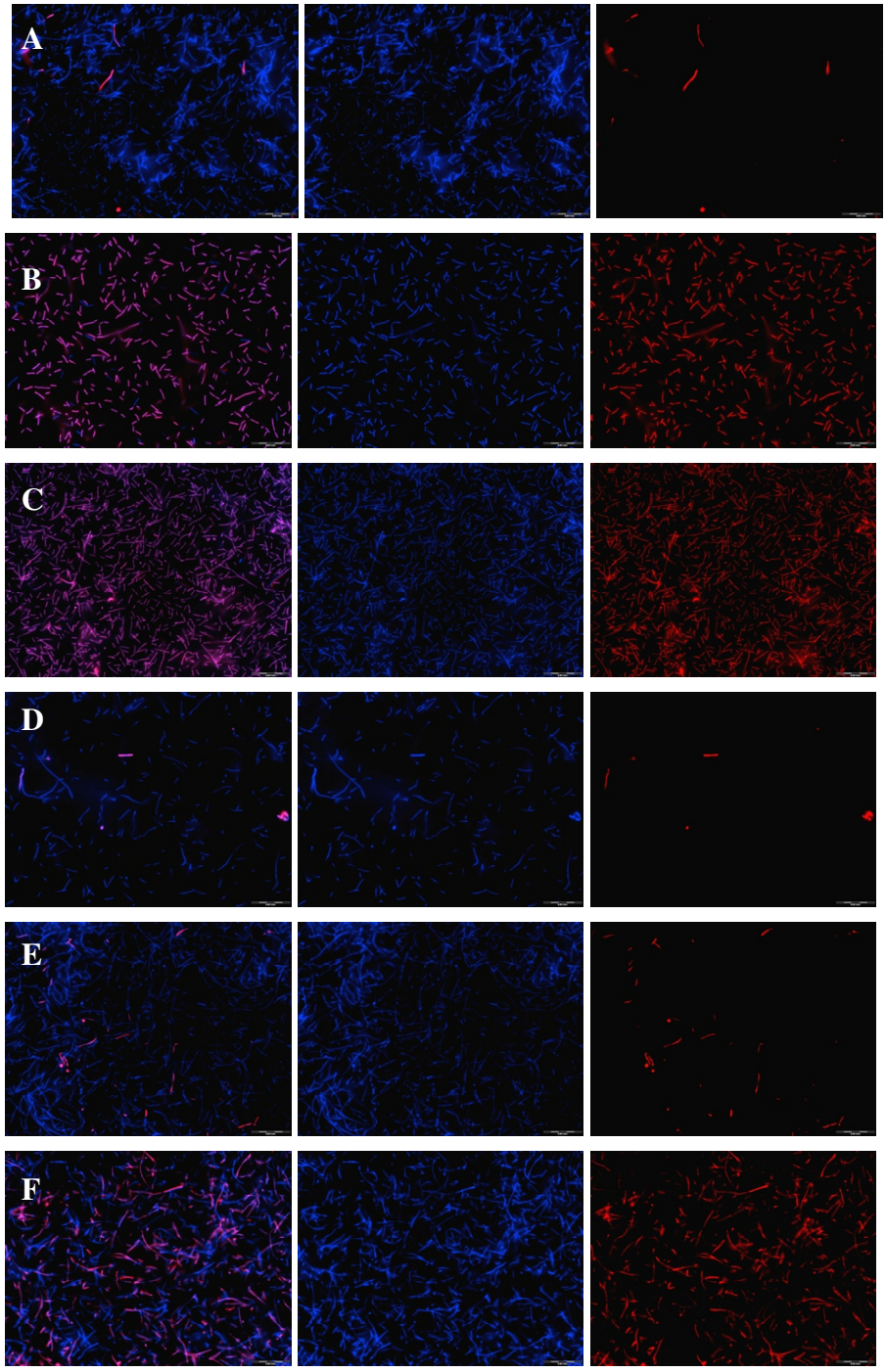

Figure 9 Fluorescent microscopy of *L. monocytogenes* using propridium iodide and bisbenzimide to assess the influence of TrcB, in the presence and absence of divalent cations, on cell integrity. Bisbenzimide (membrane permeable DNA marker) fluorescence (blue) indicates all *L. monocytogenes* cells, whereas propridium iodide (membrane impermeable DNA marker) fluorescence (red) indicates *L. monocytogenes* cells with compromised membrane integrity. The left hand panels show the overlay of bisbenzimide and propridium iodide fluorescence; the middle panels the bisbenzimide fluorescence and the right hand panels the propridium iodide fluorescence. **A**: Untreated *L. monocytogenes* cultured in standard BHI growth medium; **B**: *L. monocytogenes* cultured in standard BHI growth medium and treated with 6.25 µg/mL TrcB diluted in water; **C**: *L. monocytogenes* cultured in standard BHI growth medium and treated with 6.25 µg/mL TrcB diluted in 75 mM $MgCl_2$ (7.5 mM in assay); **D**: *L. monocytogenes* cultured in standard BHI growth medium and treated with 6.25 µg/mL TrcB diluted in 75 mM $CaCl_2$ (7.5 mM in assay); **E**: Untreated *L. monocytogenes* cultured in calcium-supplemented BHI growth medium; **F**: *L. monocytogenes* cultured in calcium-supplemented BHI growth medium and treated with 6.25 µg/mL TrcB diluted in water.

When 75 mM $CaCl_2$ was used as peptide solvent (7.5 mM in assay), the tyrocidine complex and TrcB exhibit lower IC_Fs (1.2 and 1.3, respectively) and significantly higher A_S (18 and 15, respectively) toward *L. monocytogenes* B73 cultured in standard BHI growth medium (Table 3). The low IC_Fs and very high A_Ss are indicative of either antimicrobial peptide self-assembly into active lytic complexes (as seen with water as peptide solvent) or a lethal cellular event at a threshold concentration [38]. Fluorescence microscopy results indicated a complete absence of lytic activity when 75 mM $CaCl_2$ was used as peptide solvent (Figures 8 and 9), which strongly suggests that these conditions lead to a non-lytic lethal cellular event. The specificity of the influence of calcium on the modulation of tyrocidine mode of action is supported by the observation that the use of 75 mM $MgCl_2$ as peptide solvent did not significantly influence the membrane lysis/leakage by TrcB (Figures 8 and 9), exhibiting an apparent lytic rate of 6.7 fluorescent units/min (R^2 = 0.95). These results indicate that, in addition to improving antilisterial activity, peptide-calcium pre-complexation and/or induction of active complexes/higher-order structures changes the mechanism of action of the tyrocidines from a predominantly lytic to non-lytic mechanism of action.

6.5 Conclusions

The activities of tyrocidines were found to be highly sensitive to solvent composition in terms of solubility, aggregation/self-assembly and complexation with cations, however, they showed relatively good salt tolerance. The observed sensitivity is highly dependent on peptide structure and probably purity. Furthermore, the solvent composition leads to changes in both activity (characterised by IC_{50}) and mechanism of action (reflected by IC_F and A_S). When considering the activity toward *L. monocytogenes* B73 cultured in standard BHI growth medium, the results suggest that when the tyrocidines are dissolved and diluted in water, they self-assemble to form active, bactericidal lytic complexes. As with most lytic antimicrobial peptides, the self-assembly of the tyrocidines probably occurs within the membrane, disrupting membrane integrity when a certain critical peptide concentration is reached. However, a novel result from this study indicated that calcium plays an important role in the antilisterial activity and mode of action of the tyrocidines. Correlations between apparent Ca^{2+}-complexation and antilisterial activity of the tyrocidines further supported the hypothesis that Ca^{2+}-complexation is an important modulator of tyrocidine antilisterial activity. The

spectrophotometric investigation indicated that Ca^{2+} has a significant influence on the self-assembly of the tyrocidines and that such self-assembly is distinct, possibly in terms of size and/or the relative orientation of the peptide molecules with the assembly, from assemblies formed in a salt-free environment, and a membrane environment. We were able to show that calcium-peptide interaction is important in activity modulation, whereas calcium-bacteria interaction does not influence the long term activity or mode of action. When peptides are pre-incubated in 75 mM $CaCl_2$, they form active complexes/higher-order structures, which lead to a non-lytic bacteriocidal cellular event. Pre-incubation of the tyrocidines in 75 mM $CaCl_2$ therefore not only increases the specific antilisterial activity of the tyrocidines, but also changes the mechanism of action of the tyrocidines from a predominantly lytic to an alternative/intracellular mode of action. Our results also strongly indicate that a novel antimicrobial peptide target may exist in *L. monocytogenes.*

6.6 References

[1] M. Gandhi, M.L. Chikindas, *Listeria*: A foodborne pathogen that knows how to survive, Int. J. Food. Microbiol. 113 (2007) 1-15.

[2] J. Cleveland, T.J. Montville, I.F. Nes, M.L. Chikindas, Bacteriocins: safe, natural antimicrobials for food preservation, Int. J. Food Microbiol. 71 (2001) 1-20.

[3] J.M. Farber, P.I. Peterkin, *Listeria monocytogenes*, a food-borne pathogen, Microbiol. Rev. 55 (1991) 476-511.

[4] C. Poyart-Salmeron, C. Carlier, P. Trieu-Cuot, P. Courvalin, A.-L. Courtieu, Transferable plasmid-mediated antibiotic resistance in *Listeria monocytogenes* The Lancet 335 (1990) 1422-1426

[5] E. Charpentier, G. Gerbaud, C. Jacquet, J. Rocourt, P. Courvalin, Incidence of antibiotic resistance in *Listeria* species, J. Infect. Dis. 172 (1995) 277–281.

[6] E. Charpentier, P. Courvalin, Antibiotic Resistance in *Listeria* spp., Antimicrob. Agents Chemother. 43 (1999) 2103–2108.

[7] M.A. Prazak, E.A. Murano, I. Mercado, G.R. Acuff, Antimicrobial resistance of *Listeria monocytogenes* isolated from various cabbage farms and packing sheds in Texas, J. Food Prot. 65 (2002) 1796-1799.

[8] C. Mauro, P. Domenico, D.O. Vincenzo, V. Alberto, I. Adriana, Antimicrobial susceptibility of *Listeria monocytogenes* isolated from food and food-processing environment, Ann. Fac. Medic. Vet. di Parma XXVII (2007) 157-164.

[9] L. Mereghetti, R. Quentin, N. Marquet-van der Mee, A. Audurier, Low sensitivity of *Listeria monocytogenes* to quaternary ammonium compounds, Appl. Environ. Microbiol. 66 (2000) 5083–5086.

[10] J. Lunden, T. Autio, A. Markkula, S. Hellstrom, H. Korkeala, Adaptive and cross-adaptive responses of persistent and non-persistent *Listeria monocytogenes* strains to disinfectants, Int. J. Food Microbiol. 82 (2003) 265–272.

[11] N. Romanova, S. Favrin, M.W. Griffiths, Sensitivity of *Listeria monocytogenes* to sanitizers used in the meat processing industry, Appl. Environ. Microbiol. 68 (2002) 6405–6409.

[12] J.K. Branen, P.M. Davidson, Enhancement of nisin, lysozyme, and monolaurin antimicrobial activities by ethylenediaminetetraacetic acid and lactoferrin, Int. J. Food Microbiol. 90 (2004) 63– 74.

[13] S. Brul, P. Coote, Preservative agents in foods: Mode of action and microbial resistance mechanisms, Int. J. Food Microbiol. 50 (1999) 1-17.

[14] R.E. Hancock, R. Lehrer, Cationic peptides: a new source of antibiotics, Trends Biotechnol. 16 (1998) 82-88.

[15] N. Benkerroum, W.E. Sandine, Inhibitory action of nisin against *Listeria monocytogenes*, J. Dairy Sci. 71 (1988) 3237-3245.

[16] T.J. Montville, Y. Chen, Mechanistic action of pediocin and nisin: recent progress and unresolved questions, Appl. Microbiol. Biotechnol. 50 (1998) 511-519.

[17] I.F. Nes, H. Holo, Class II antimicrobial peptides from lactic acid bacteria, Biopolymers (Pept. Sci.) 55 (2000) 50-61.

[18] A. Gravesen, B. Kallipolitis, K. Holmstrøm, P.E. Høiby, M. Ramnath, S. Knøchel, *pbp2229*-Mediated nisin resistance mechanism in *Listeria monocytogenes* confers cross-protection to class IIa bacteriocins and affects virulence gene expression, Appl. Environ. Microbiol. 70 (2004) 1669–1679.

[19] X.T. Ming, M.A. Daeschel, Nisin resistance of foodborne bacteria and the specific resistance responses of *Listeria monocytogenes* Scott A, J. Food Prot. 56 (1993) 944-948.

[20] E.A. Davies, M.R. Adams, Resistance of *Listeria monocytogenes* to the bacteriocin nisin, Int. J. Food Microbiol. 21 (1994) 341-347.

[21] E. Parente, M.A. Giglio, A. Ricciardi, F. Clementi, The combined effect of nisin, leucocin F10, pH, NaCl and EDTA on the survival of *Listeria monocytogenes* in broth, Int. J. Food Microbiol. 40 (1998) 65-75.

[22] L.J. Pearson, E.H. Marth, *Listeria monocytogenes* - Threat to a safe food supply: A review, J. Dairy Sci. 73 (1990) 912-928.

[23] R. Bals, M.J. Goldman, J.M. Wilson, Mouse beta-Defensin 1 is a salt-sensitive antimicrobial peptide present in epithelia of the lung and urogenital tract, Infect. Immun. 66 (1998) 1225-1232.

[24] S. Cociancich, A. Ghazi, C. Hetru, J.A. Hoffmann, L. Letellier, Insect defensin, an inducible antibacterial peptide, forms voltage-dependent channels in *Micrococcus luteus*, J. Biol. Chem. 268 (1993) 19239-19245.

[25] R.I. Lehrer, T. Ganz, D. Szklarek, M.E. Selsted, Modulation of the *in vitro* candidacidal activity of human neutrophil defensins by target cell metabolism and divalent cations, J. Clin. Invest. 81 (1988) 1829-1835.

[26] W.F. Broekaert, F.R.G. Terras, B.P.A. Cammue, R.W. Osborn, Plant defensins: Novel antimicrobial peptides as components of the host defense system, Plant Physiol. 108 (1995) 1353-1358.

[27] D.M.E. Bowdish, D.J. Davidson, Y.E. Lau, K. Lee, M.G. Scott, R.E.W. Hancock, Impact of LL-37 on anti-infective immunity, J. Leukoc. Biol. 77 (2005) 451-459.

[28] K. Yamauchi, K. Tomita, T.J. Giehl, R.T. Ellison, Antibacterial activity of lactoferrin and a pepsin-derived lactoferrin peptide fragment, Infect. Immun. 61 (1993) 719-728.

[29] B. Skerlavaj, D. Romeo, R. Gennaro, Rapid membrane permeabilization and inhibition of vital functions of Gram-negative bacteria by bactenecins, Infect. Immun. 58 (1990).

[30] R. Urrutia, R.A. Cruciani, J.L. Barker, B. Kachar, Spontaneous polymerization of the antibiotic peptide magainin 2, FEBS Lett. 247 (1989) 17-21.

[31] T. Rydlo, S. Rotem, A. Mor, Antibacterial properties of dermaseptin S4 derivatives under extreme incubation conditions, Antimicrob. Agents Chemother. 50 (2006) 490–497.

[32] B.M. Spathelf, M. Rautenbach, Anti-listerial activity and structure–activity relationships of the six major tyrocidines, cyclic decapeptides from *Bacillus aneurinolyticus*, Bioorg. Med. Chem. 17 (2009) 5541-5548.

[33] M. Ramnath, M. Beukes, K. Tamura, J.W. Hastings, Absence of a putative mannose-specific phosphotransferase system enzyme IIAB component in a leucocin A-resistant strain of *Listeria monocytogenes*, as shown by two-dimensional sodium dodecyl sulfate-polyacrylamide gel electrophoresis, Appl. Environ. Microbiol. 66 (2000) 3098–3101

[34] G.A. Dykes, J.W. Hastings, Fitness costs associated with class IIa bacteriocin resistance in *Listeria monocytogenes* B73, Lett. Appl. Microbiol. 26 (1998) 5-8.

[35] M. Rautenbach, N.M. Vlok, M. Stander, H.C. Hoppe, Inhibition of malaria parasite blood stages by tyrocidines, membrane-active cyclic peptide antibiotics from *Bacillus brevis*, Biochim. Biophys. Acta - Biomembranes 1768 (2007) 1488–1497.

[36] R. Dulbecco, M. Vogt, Plaque formation and isolation of pure lines with poliomyelitis viruses, J. Exp. Med. 99 (1954) 167-182.

[37] Promega, Technical Bulletin No. 317 CellTiter-Blue™ Cell Viability Assay, 2002.

[38] M. Rautenbach, G.D. Gerstner, N.M. Vlok, J. Kulenkampff, H.V. Westerhoff, Analyses of dose-response curves to compare the antimicrobial activity of model cationic alpha-helical peptides highlights the necessity for a minimum of two activity parameters, Anal. Biochem. 350 (2006) 81-90.

[39] E.A. du Toit, M. Rautenbach, A sensitive standardised micro-gel well diffusion assay for the determination of antimicrobial activity, J. Microbiol. Methods 42 (2000) 159-165.

[40] L.H. Kondejewski, S.W. Farmer, D.S. Wishart, C.M. Kay, R.E. Hancock, R.S. Hodges, Modulation of structure and antibacterial and hemolytic activity by ring size in cyclic gramicidin S analogs, J. Biol. Chem. 271 (1996) 25261-25268.

[41] L.H. Kondejewski, M. Jelokhani-Niaraki, S.W. Farmer, B. Lix, C.M. Kay, B.D. Sykes, R.E. Hancock, R.S. Hodges, Dissociation of antimicrobial and hemolytic activities in cyclic peptide diastereomers by systematic alterations in amphipathicity, J. Biol. Chem. 274 (1999) 13181-13192.

[42] L.H. Kondejewski, D.L. Lee, M. Jelokhani-Niaraki, S.W. Farmer, R.E. Hancock, R.S. Hodges, Optimization of microbial specificity in cyclic peptides by modulation of hydrophobicity within a defined structural framework, J. Biol. Chem. 277 (2002) 67-74.

[43] D.L. Lee, J.-P.S. Powers, K. Pflegerl, M.L. Vasil, R.E.W. Hancock, R.S. Hodges, Effects of single D-amino acid substitutions on disruption of β-sheet structure and hydrophobicity in cyclic 14-residue antimicrobial peptide analogs related to gramicidin S, J. Pept. Res. 63 (2004) 69-84.

[44] S. Laiken, M. Printz, L.C. Craig, Circular dichroism of the tyrocidines and gramicidin S-A, J. Biol. Chem. 244 (1969) 4454-4457.

[45] S.M. Kelly, T.J. Jess, N.C. Price, How to study proteins by circular dichroism, Biochim. Biophys. Acta 1751 (2005) 119-139.

[46] C. Krittanai, W.C. Johnson, Correcting the circular dichroism spectra of peptides for contributions of absorbing side chains, Anal. Biochem. 253 (1997) 57-64.

[47] H.H. Paradies, Aggregation of tyrocidine in aqueous solutions, Biochem. Biophys. Res. Commun. 88 (1979) 810-817.

[48] S.L. Laiken, M.P. Printz, L.C. Craig, Studies on the mode of self-assembly of tyrocidine B, Biochem. Biophys. Res. Commun. 43 (1971) 595-600.

[49] R.C. Williams, D.A. Yphantis, L.C. Craig, Noncovalent association of tyrocidine B, Biochemistry 11 (1972) 70-77.

[50] F.G. Prendergast, P.D. Hampton, B. Jones, Characteristics of tyrosinate fluorescence emission in alpha- and beta-Purothionins, Biochemistry 23 (1984) 6690-6697.

[51] J.D.J. O'Niel, T. Hofmann, Tyrosine and tyrosinate fluorescence of pig intestinal Ca^{2+}-binding protein, Biochem. J. 243 (1987) 611-615.

[52] J.R. Lakowicz, Principles of fluorescence spectroscopy, 3 ed., Springer, New York, 2006.

Chapter 7

Antiplasmodial activity and structure-activity relationships of the tyrocidines

7.1 Introduction

Malaria is one of the principal causes of morbidity and mortality worldwide, with nearly 250 million cases and one million deaths reported annually [1]. The majority of these fatal cases are caused by *Plasmodium falciparum*, the most virulent species [2, 3]. The prevalence of drug-resistant *P. falciparum* species [3, 4] necessitates the development of new antimalarial compounds. Various antimicrobial peptides have been shown to possess selective antimalarial activity. The modification of the host erythrocyte membrane by the infecting parasite may render it vulnerable to selective recognition and perturbation by membrane-active compounds, such as membrane active antibiotics, antimicrobial peptides and polymers. Membrane active polyene antibiotics, such as amphotericin B and nystatin [5], linear antimicrobial peptides, such as mellitin, magainin 2, cecropin B and cecropin-mellitin analogues [6, 7], dermaseptin S4 [8-10] and the cyclic antimicrobial peptide gramicidin S [11] have been shown to selectively lyse *P. falciparum* infected erythrocytes. However, antimicrobial peptides with alternative/internal targets have also been identified. Aminoacyl analogues of dermaseptin S4 inhibit *P. falciparum* by crossing several membranes to reach the intracellular parasite target [8-10]. A linear antimicrobial peptide representing the cationic core region of the lymphocytic effector protein NK-lysin, NK-2, exerts its antiplasmodial activity by permeabilising and transversing the erythrocyte membrane as well as the parasitophorous vacuole membrane to reach the intracellular parasite [12]. A small library of microheterogeneous cyclohexadepsipeptides has also been shown to inhibit the intraerythrocytic growth of *P. falciparum*, without lysis of erythrocytes [13].

Rautenbach *et al.* (2007) [11] previously reported selective inhibition of *P. falciparum* 3D7 blood stages by the tyrocidines, a group of membrane active cyclic decapeptide antibiotics from *Bacillus aneurinolytcus*. Unlike the lytic mechanism of the analogous gramicidin S, the antiplasmodial activity of the tyrocidines was found to involve a

non-lytic mechanism of action focussed on the trophozoite developmental stage [11]. The reported selective antiplasmodial activity of the tyrocidines suggests that they may be promising compounds for the development of new antimalarial drugs. However, the tyrocidines also exhibit haemolytic activity and toxicity toward certain human cell lines *in vitro* [11, 14]. In order to develop therapeutic agents based on the tyrocidines, insight regarding their structure-activity-toxicity relationships, formulation determinants of activity and mechanism of action is imperative.

As described in Chapter 2, the six major tyrocidines (tyrocidines A, A_1, B, B_1, C and C_1) and two minor tyrocidines (tyrocidines B` and $B_1$`) were successfully purified. A further two minor natural tyrocidines (TpcB and TpcC) were partially purified. (*Refer to Chapter 2 for more detail.*) The antiplasmodial and haemolytic activities of these purified peptides were investigated and correlated with selected physicochemical descriptors of hydrophobicity/amphipathicity, size and structure (*Chapter 4*) in order to gain insight regarding the structural features of the peptides that modulate activity. In addition to hydrophobicity/amphipathicity and size, peptide self-assembly in solution may influence antiplasmodial activity and insight regarding the structure-activity relationships and mode of action of the tyrocidines may thus be gained by investigating correlations between self-assembly and antiplasmodial activity. Furthermore, the bioactivity of antimicrobial peptides requires interaction with the target cell membrane [15-19] and correlations between changes in tyrocidine structure/aggregation state induced by a membrane-mimetic environment may thus advance our understanding of tyrocidine structure-activity relationships and mode of action. In addition to the role of peptide properties, the physiological salt and serum components, such as albumin, may influence the antiplasmodial activity of the tyrocidines [15, 20]. The observation that Ca^{2+} has significant influence on the antilisterial activity of the tyrocidines (Chapter 6) motivates investigation of the influence of divalent cations on antiplasmodial activity.

7.2 Materials

Tyrothricin (commercial extract from *B. aneurinolyticus*), gramicidin S, trifluoroacetic acid (TFA, >98%), Corning Incorporated® cell culture cluster, non-pyrogenic polypropylene 96-well microtiter plates, Malstat™ reagent and bisbenzimide and propridium iodide was supplied by Sigma (St. Louis, USA). The diethyl ether, acetone, butan-1-ol, acetic acid, and propan-2-ol were supplied by Saarchem (Krugersdorp,

South Africa). Acetonitrile (ACN) (HPLC-grade, far UV cut-off) and was supplied by Romill Ltd. (Cambridge, UK). Ethanol (>99.8%) was supplied by Merck (Darmstadt, Germany). Albumax II and RPMI-1640 were supplied by Scientific Group (Auckland, New Zealand). Analytical grade water was prepared by filtering water from a reverse osmosis plant through a Millipore Milli-Q® 58 water purification system (Milford, USA).

7.3 Methods

7.3.1 Peptide preparation

Peptides were isolated from commercially obtained tyrothricin and purified by semi-preparative reverse-phase high-performance liquid chromatography (RP-HPLC) (Chapter 2), as previously described by Rautenbach *et al.* (2007) [11] and Spathelf and Rautenbach (2009) [21].

Stock solutions of the purified peptides were prepared by dissolving the analytically weighed peptides in ethanol:water (1:1, *v/v*) to concentrations of 2.00 mg/mL. Stock solutions were diluted 1:1 in water to give peptide solutions of 1.00 mg/mL, which were subsequently used to construct quadrupling dilution series. The dilution series were constructed in polypropylene microtiter plates using supplemented RPMI-1640 culture medium (*sans* albumax II), used for *P. falciparum* culturing. The stock solutions and dilution series were prepared shortly before (<30min) before each assay. For investigation of the influence of peptide solvent, the peptide stock solutions (2.00 mg/mL, ethanol:water, 1:1 *v/v*) were diluted to 0.200 μM in RPMI-1640 culture medium (*sans* albumax II), 0.5% (w/v) albumax II or 10 mM $CaCl_2$.

7.3.2 Antiplasmodial and haemolytic activity determination

P. falciparum (D10 strain) was cultured under an atmosphere of 3% CO_2, 4% O_2 and 93% N_2 in RPMI-1640 medium supplemented with 50 mM glucose, 0.65 mM hypoxanthine, 25 mM HEPES, 0.2% (w/v) $NaHCO_3$, 0.048 mg/mL gentamicin, 0.5% (w/v) albumax II and 2–4% (v/v) human O^+ or A^+ erythrocytes. Prior to each assay, a 2% parasitemia and 2% haematocrit suspension was prepared by mixing culture-derived parasitised erythrocytes with fresh culture medium and erythrocytes. Dose-response assays were performed in sterile microtiter plates by adding 10 μL of the peptide

dilution series to 90 µL of the parasite suspension. For determination of total growth and total haemolysis, 10 µL culture medium and 10 µL 250 µg/mL saponin, respectively, was added to the parasite suspension. The microtiter plates were incubated at 37 °C for 48 h, after which 10 µL of the supernatant was removed and diluted 1:9 in water. The released haemoglobin in the supernatant was spectrophotometrically determined from their absorbance at 405 nm. The parasite viability in each well of the experimental microtiter plate was determined from the residual lactate dehydrogenase activity [22] after freeze-thawing. Briefly, 20 µL of lysate was removed from each well and added to 100 µL Malstat reagent, 10 µL nitroblue tetrazolium and 10 µL diaphorase, incubated at room temperature for 20 minutes and the absorbance at 600 nm measured.

7.3.3 Analysis of dose-response data

The percentage growth inhibition and haemolysis was calculated according to equations 1 [23] and 2, respectively.

$$\%\ growth\ \ inhibition\ \ = 100 - \frac{100 \times (A_{600}\ of\ well - Average\ \ A_{600}\ of\ background\ )}{Average\ \ A_{600}\ of\ growth\ \ \ wells - Average\ \ A_{600}\ of\ background} \quad (1)$$

$$\%\ haemolysis\ \ = 100 \times \frac{(A_{405}\ of\ well - Average\ \ A_{405}\ of\ background\ )}{Average\ \ A_{405}\ of\ haemolysis\ \ \ wells - Average\ \ A_{405}\ of\ background} \quad (2)$$

Dose-response curves were plotted using GraphPad Prism® 4.00 (GraphPad Software, San Diego, USA). The dose-response data was analysed by performing nonlinear regression and sigmoidal curves (with variable slope and a constant difference of 100 between the top and bottom plateau) were fitted according to Rautenbach *et al.* (2006) [23].

7.3.4 QSAR analyses

The relationship between the antiplasmodial activity, apparent selectivity and molecular descriptors of amphipathicity/hydrophobicity, size, conformation and self-assembly of the tyrocidines was analysed. The HPLC retention times of the tyrocidines were obtained from the analytical HPLC chromatograms of the purified tyrocidines. Theoretical side-chain surface area (SCSA) and volume was calculated as the sum of the SCSA and volumes [24] of the constituent amino acids. Solvent-accessible surface

area and volume was determined from low energy models from homology modelling (Chapter 4). Descriptors of conformation and self-assembly were calculated from circular dichroism parameters (Chapters 3 and 4). The correlations between the molecular descriptors, antiplasmodial activity and selectivity were analysed by performing a linear/exponential regression using GraphPad Prism® 4.00 (GraphPad Software, San Diego, USA).

7.3.5 Fluorescence microscopy

For each sample, 10 µL of peptide solution (0.4 µM, final peptide concentration of 40 nM) was added to 90 µL of parasite suspension (2% parasitemia, 4% hematocrit) and incubated for 24 hours. The samples were stained with 1 µL bisbenzamide (a membrane permeable DNA chelator) and 1 µL propridium iodide (a membrane impermeable DNA chelator) at room temperature for 15 minutes. For lytic controls, 90 µL of parasite suspension was treated with gramicidin S (final peptide concentration of 20 µM) fo 10 minutes. Image acquisition was performed on an Olympus Cell^{R} system attached to an IX 81 Inverted fluorescence microscope equipped with an F-view-II cooled CCD camera (Soft Imaging Systems). Using a Xenon-Arc burner (Olympus Biosystems GMBH) as light source, images were acquired using the 360 nm and 472 nm excitation filters. Emission data was collected using a UBG triple-bandpass emission filter cube (Chroma). Images were acquired using an Olympus Plan Apo N60x/1.4 Oil objective. The degree of membrane leakage/lysis was deduced from the fluorescent signal of the membrane impermeable propridium iodide.

7.3.6 Mass spectrometry

For investigation of complexation between the tyrocidines and Ca^{2+} by mass spectrometry, stock solutions of the purified tyrocidines were diluted to 10 µM in various $CaCl_2$ concentrations. Time-of-flight electrospray mass spectrometry (TOF-ESMS) analyses were performed using a Waters Q-TOF Ultima mass spectrometer fitted with an electrospray ionisation source. 10 µL of each peptide sample was injected into the ESMS and subjected to a capillary voltage of 3.5 kV. The source temperature and cone voltage was set at 100ºC and 35 V, respectively. The data was collected in positive mode by scanning the first mass analyser (MS_1) through m/z = 100–1999. Binding curves were plotted using GraphPad Prism® 4.00 (GraphPad Software, San Diego, USA) and analysed by performing nonlinear regression and the

curves were fitted according to $Y = S_{max}*X/(K_d+X)$, where S_{max} represents the apparent maximal calcium binding (S_{max}) of the tyrocidines.

7.4 Results and Discussion

7.4.1 Antiplasmodial and haemolytic activity

The activities of the purified tyrocidines and gramicidin S were determined toward normal and *P. falciparum* D10-infected human erythrocytes (Table 1). The antiplasmodial and haemolytic activities were characterised in terms IC_{50} or HC_{50} (concentration that gives 50% inhibition or haemolysis) [23]. The observed IC_{50}- and HC_{50}-values (Table 1) were highly comparable to those reported by Rautenbach *et al.* (2007) [11], in which antiplasmodial activity of the six major natural tyrocidines towards the *P. falciparum* 3D7 strain was determined. This study indicated that the major tyrocidines were slightly less active toward *P. falciparum* D10 than toward *P. falciparum* 3D7, which is most probably due to small differences in cultures and assay.

All the tyrocidines exhibited antiplasmodial activity in the nanomolar range (4.4 – 490 nM), and were found to be significantly more active than GS (Table 1). Tyrocidine A was found to be the most active (IC_{50} = 4.4 nM), whereas tyrocidine C_1 was the least active (IC_{50} = 490 nM). The minor tyrocidines B` ($IC_{50}$ = 420 nM) and $B_1$` (IC_{50} = 440 nM) were less active than the major tyrocidines B (IC_{50} = 110 nM) and B_1 (IC_{50} = 260 nM). TpcB(+TrcA) at 59 % purity and TpcC (+unknown) at 73 % purity exhibited low IC_{50}-values of 60 ng/mL and 100 ng/mL, respectively. These two tyrocidines could, however, not be sufficiently purified and were therefore not included in the analyses of the structure-activity relationships. The relatively high activity of TpcB and TpcC may be due to the activity of the contaminant(s) or synergistic activity.

The six major tyrocidines exhibited haemolytic activities toward normal human erythrocytes with HC_{50}-values ranging between 3.1 and 6.1 μM, which is greater than the haemolytic activity of GS (Table 1). For the major tyrocidines, the Lys^9-containing peptides were found to be slightly more haemolytic than their Orn^9-containing analogues (Table 1), possibly due to tighter association of Lys with cell membrane than Orn [11, 25]. The minor tyrocidines B` and $B_1$` (HC_{50} = 9.0 μM) were less haemolytic

than the major tyrocidines B (HC_{50} = 6.1 μM) and B_1 (HC_{50} = 4.9 μM), with HC_{50}-values similar to that of GS (Table 1). TpcB and TpcC exhibited HC_{50}-values of 4.9 μg/mL and 9.8 μg/mL, respectively.

All the natural tyrocidines, with the exception of $TrcC_1$, were found to be significantly more selective for infected erythrocytes than GS (Table 1). Tyrocidine A exhibited the highest selectivity index (SI = 1100), whereas tyrocidine C_1 had the lowest SI (9.5) (Table 1).

Table 1 *Summary of the antiplasmodial and haemolytic activity parameters of the tyrocidines in this study. For comparison the IC_{50} values of the major tyrocidines towards P. falciparum 3D7 from the study of Rautenbach et al. (2007) are given in parentheses.* IC_{50}-values are given in nM (the tyrocidine mixture, TpcB and TpcC given in ng/mL). Haemolytic activity was characterised in terms of HC_{50}, given in μM (the tyrocidine mixture, Tpc B and Tpc C given in μg/mL). The apparent selectivity index (SI) was calculated as HC_{50}/IC_{50}. Each value represent the mean of at least 3 biological repeats, with 3-5 technical repeats per assay ± standard error of the mean (SEM). Values are given to two significant digits.

	***P. falciparum* D10**	**Human erythrocytes**	**HC_{50}/IC_{50}**
Peptide	**IC_{50} ± SEM**	**HC_{50} ± SEM**	**SI ± SEM**
Trc mixture	410 ± 44	4.4 ± 0.059	11 ± 1.3
Trc A	4.4 ± 0.16 (0.58)	4.7 ± 0.33 (4.5)	1100 ± 68
Trc A_1	36 ± 2.5 (4.4)	3.1 ± 0.38 (4.1)	82 ± 10
Trc B	110 ± 8.1 (61)	6.1 ± 0.37 (2.6)	55 ± 5.9
Trc B_1	260 ±13 (310)	4.9 ± 0.89 (8.6)	20 ± 3.9
Trc C	370 ± 27 (290)	5.5 ± 0.47 (3.2)	15 ± 0.86
Trc C_1	490 ± 6.0 (460)	4.6 ± 0.25 (5.4)	9.5 ± 0.43
Trc B’	420 ± 28	9.0 ± 0.65	21 ± 0.55
Trc B_1’	440 ± 35	9.0 ± 0.091	19 ± 0.38
Tpc B + TrcA	60 ± 10	4.9 ± 0.51	81 ± 20
Tpc C + unk	100 ± 16	9.8 ± 0.72	98 ± 9.6
GS	1700 ± 160 (1300)	10 ± 0.14 (11)	6.6 ± 0.70

7.4.2 Structure-activity-selectivity relationships of the tyrocidines

In order to identify structural features of the tyrocidines associated with antiplasmodial activity and selectivity, correlations between activity (IC_{50}), apparent selectivity (HC_{50}/IC_{50}) and various physicochemical parameters (Table 2) of the eight purified tyrocidines were investigated. Previous research by Rautenbach *et al.* (2007) indicated strong correlations between the antiplasmodial activity, apparent selectivity, apparent hydrophobicity and theoretical side-chain surface area of the six major natural tyrocidines [11]. For this investigation RP-HPLC retention time was chosen as an indicator of solution amphipathicity/apparent hydrophobicity [11, 21]. As HPLC retention time is determined *in vitro*, the three-dimensional conformation and self-assembly are inherently taken into account (*Refer to Chapter 4 for more detail*). *In silico* solvent-accessible surface area (SASA) and *in silico* solvent-accessible volume (SAV) were chosen as indicators of peptide size. The theoretical parameters were omitted from this study as they only consider the amino acid composition, without taking the three-dimensional conformation or self-assembly into account. The *in silico* parameters are conformation-dependent, but also do not consider the influence of self-assembly.

In order to determine the role of tyrocidine self-assembly in the modulation of antiplasmodial activity and selectivity, correlations between activity (IC_{50}), apparent selectivity (HC_{50}/IC_{50}) and circular dichroism (CD)-derived indicators of peptide conformation and self-assembly (Table 2) were investigated. Negative ellipticity minima in water ($\theta_{205}/\theta_{216,\ water}$) and TFE ($\theta_{204}/\theta_{214,\ TFE}$) were chosen as indicators of conformation and self-assembly in an aqueous and membrane-like environment, respectively. Changes in negative ellipticity minima from water to TFE ($\Delta\theta_{205}/\theta_{216,\ water\rightarrow TFE}$) were chosen as indicators of inducibility of secondary structure/self-assembly upon membrane interaction. (*Refer to Chapters 3 and 4 for more detail*).

Table 2 *Summary of selected physicochemical parameters of the purified tyrocidines* The identity of the variable amino acid residues in positions 3, 4 and 9 are given, with Phe = F; Trp = W; Lys = K; and Orn = O, and D-amino acids indicated by lower case letters.

Peptide	Variable residue identity	HPLC R_T[1] (min)	SASA[2] (Å^2)	SAV[2] (Å^3)	$\theta_{205}/\theta_{216}$ in water[3]	$\theta_{204}/\theta_{214}$ in TFE[3]	$\Delta\theta_{205}/\theta_{216}$, water→TFE[3]
Trc A	F^3f^4-O^9	11.81	1199	2680	0.92	1.11	21.4
Trc A_1	F^3f^4-K^9	11.33	1207	2715	0.94	0.93	-1.21
Trc B	W^3f^4-O^9	9.48	1216	2740	1.15	1.51	31.5
Trc B_1	W^3f^4-K^9	9.24	1231	2776	1.14	1.49	30.3
Trc C	W^3w^4-O^9	8.31	1267	2833	1.15	1.74	52.1
Trc C_1	W^3w^4-K^9	7.90	1268	2854	1.03	1.68	63.8
Trc B`	F^3w^4-O^9	8.98	1276	2808	0.85	1.67	95.9
Trc B_1`	F^3w^4-K^9	9.72	1253	2800	0.92	1.67	82.0

[1] HPLC retention times were obtained from the analytical HPLC chromatograms of the purified tyrocidines.
[2] Obtained from analysis of the low energy structures from homology modelling.
[3] The ratios of the ellipticity minima were calculated from CD spectra of the tyrocidines.

7.4.3 Structure-activity relationships of the tyrocidines

A linear correlation was observed between antiplasmodial activity (*P. falciparum* D10 strain) and HPLC retention time ($R^2 = 0.89$) of the six major tyrocidines (Figure 1), which corresponds very well to previous research by Rautenbach *et al.* (2007) [11]. However, the two minor natural tyrocidines (TrcB` and Trc$B_1$`) do not follow the same trend (Figure 1), which may be due to the influence of three-dimensional conformation, self-assembly and/or individual amino acid identity. Good linear correlations were observed between the antiplasmodial activity and *in silico* solvent-accessible surface area ($R^2 = 0.91$) and volume ($R^2 = 0.91$) of all eight tyrocidines (Figure 1). The modulation of antiplasmodial activity by solution amphipathicity, peptide size and the individual variable residues may be related to a direct influence on initial association with the erythrocyte membrane; integration into the erythrocyte membrane leading to haemolysis and/or membrane leakage; translocation to the intracellular parasite and association/integration with parasite membrane(s) leading to membrane leakage and lysis and/or interaction with parasite molecular target leading to growth inhibition (halting of parasite development in the late trophozoite stage).

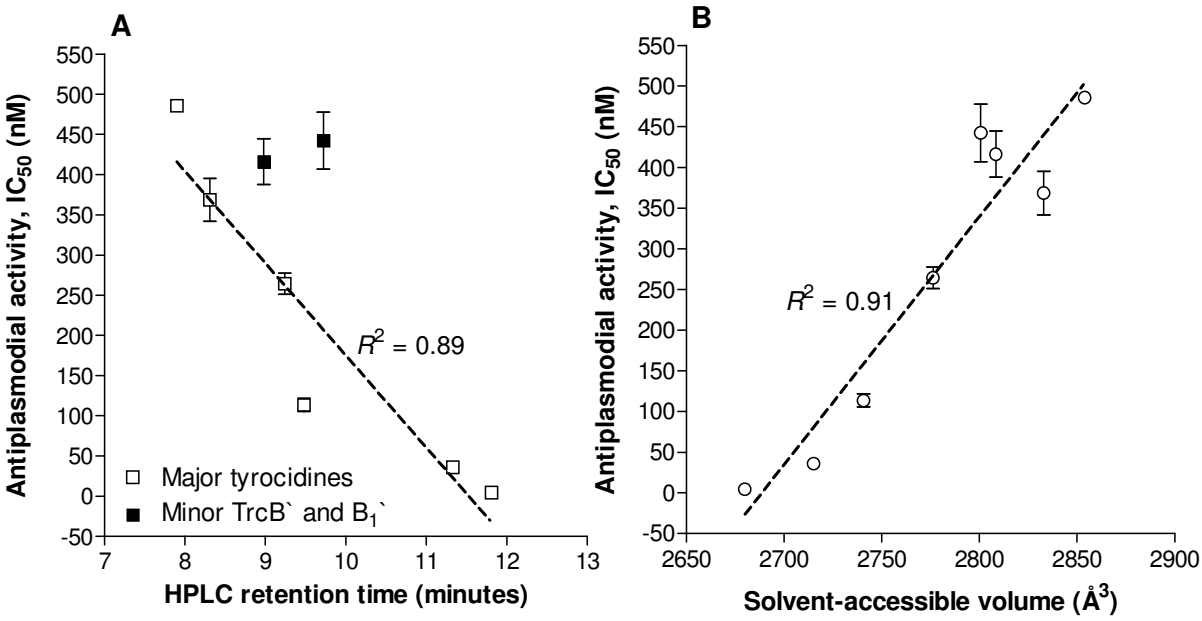

Figure 1 *Correlation between the tyrocidine antiplasmodial activity and molecular descriptors of A. solution amphipathicity (HPLC R_T) and B. size (solvent-accessible volume).* In A filled squares represent the six major tyrocidines, and clear squares represent the minor tyrocidines B` and $B_1$` (excluded from linear regression). Each data point represents the mean of at least 3 biological repeats, with 3-5 technical repeats per assay ± SEM.

Irrespective of mechanism of action (MOA), initial target membrane interaction is expected to be a central determinant of peptide activity. As initial membrane association is expected to be driven by electrostatic interaction and the cationic charge of the tyrocidines is carried by the Lys^9 or Orn^9 residue, these residues probably play an important role in initial membrane association. Lys has been found to interact more strongly with cell membrane than Orn [25], and such tighter association of Lys may improve lysis, but concurrently decrease the ability to translocate and reach an alternative internal target, thus decreasing activity. This hypothesis is supported by Lys^9-containing tyrocidines exhibiting greater haemolytic activity, but reduced antiplasmodial activity and selectivity, relative to their Orn^9-containing analogues (Table 1). Initial membrane association is followed by membrane integration driven by hydrophobic interactions [19, 26], possibly mediated by the aromatic residues in the variable dipeptide unit. In general, substitution of the Phe residues with Trp residues ($Phe^3 \rightarrow Trp^3$ and D-$Phe^4 \rightarrow$D-Trp^4) was found to lead to decreased antiplasmodial activity, which may be related to decreased amphipathicity, increased size, shallower membrane insertion and/or better membrane anchoring properties of Trp relative to Phe [27-29]. However, the influence of Phe→Trp substitution on antiplasmodial activity

was found to be sequence-dependent. For tyrocidines containing D-Phe^4, Phe^3→Trp^3 substitution leads to decreased activity (TrcA is 25 times more active than TrcB; TrcA$_1$ is 7 times more active than TrcB$_1$). However, for tyrocidines containing D-Trp$_4$, Phe$_3$→Trp$_3$ substitution does not influence activity. For tyrocidines containing Phe^3, D-Phe^4→D-Trp^4 substitution led to decreased antiplasmodial activity (TrcA is 95 times more active than TrcB`; TrcA$_1$ is 12 times more active than TrcB$_1$`). For tyrocidines containing Trp^3, Trp^3-D-Phe^4→ Trp^3-D-Trp^4 substitution also led to decreased antiplasmodial activity, but to a lesser extent (TrcB is 3 times more active than TrcC; TrcB$_1$ is 2 times more active than TrcC$_1$). These results emphasise the importance of position 4, which should ideally be D-Phe^4, in antiplasmodial activity.

Although solution amphipathicity and peptide size may directly modulate activity by influencing the productivity of membrane interaction, the observation that the minor tyrocidines B` and B$_1$` do not follow the same trends and that the influence of Phe→Trp substitution is sequence-dependent suggest that alternative/additional factors are involved. We hypothesised that solution amphipathicity and peptide size indirectly modulates membrane interaction by influencing the manner and/or extent of peptide self-assembly. Although no clear correlations were observed between antiplasmodial activity and self-assembly in an aqueous environment, the major Phe^3-containing tyrocidines (TrcA and A$_1$) exhibit greater antiplasmodial activity than the Trp^3-containing tyrocidines (TrcC, C$_1$, B and B$_1$) (Table 1). As discussed in Chapter 4, the Phe^3-containing tyrocidines exhibit enhanced β-sheet/self-assembly relative to Trp^3-containing tyrocidines in aqueous solution, which suggest that enhanced β-sheet/self-assembly in an aqueous environment leads to increased antiplasmodial activity. The same does, however, not apply for the minor Phe^3-containing tyrocidines (TrcB` and B$_1$`), which exhibit enhanced self-assembly in water, but reduced activity. This result again indicates the importance of D-Phe^4 in antiplasmodial activity.

Good exponential correlations were observed between antiplasmodial activity and $\theta_{204}/\theta_{214,\,TFE}$ of the Orn^9- ($R^2 = 0.84$) and Lys^9- ($R^2 > 0.99$) containing tyrocidines (Figure 2A), which suggest that the extent and/or manner of tyrocidine self-assembly in a membrane environment is a major determinant of antiplasmodial activity, with enhanced β-sheet/self-assembly in a membrane environment related to reduced activity. Furthermore, the Trp-containing tyrocidines (C and B groups) were less active than the Phe-containing tyrocidines (A group) (Table 1). As discussed in Chapter 4, decreased

solution amphipathicity, greater solvent-accessible surface area and the presence of a Trp residue (irrespective of position) is associated with enhanced β-sheet structure/self-assembly in a membrane environment. In addition to self-assembly in a membrane environment, enhanced inducibility of secondary structure/self-assembly upon membrane interaction ($\Delta\theta_{205}/\theta_{216,\ water\rightarrow TFE}$), was generally associated with reduced antiplasmodial activity (Figure 2B). The Trp^4-containing tyrocidines (TrcC, C_1, B` and $B_1$`) were less active than the Phe^4-containing tyrocidines (TrcA, A_1, B and B_1), following a sigmoidal relationship between ($\Delta\theta_{205}/\theta_{216,\ water\rightarrow TFE}$) and antiplasmodial activity.

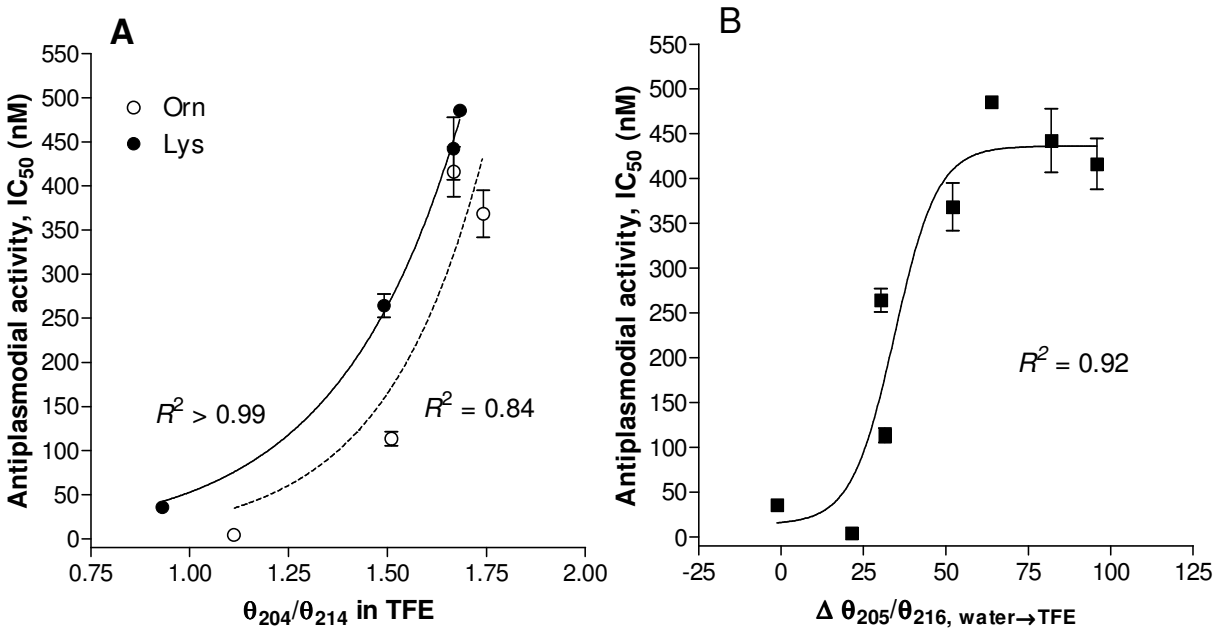

Figure 2 *Correlation between the tyrocidine antiplasmodial activity and CD-derived descriptors of A. self-assembly in a membrane environment ($\theta_{204}/\theta_{214,\ TFE}$) and B. inducibility of self-assembly upon membrane interaction ($\Delta\ \theta_{205}/\theta_{216,\ water\rightarrow TFE}$).* Each data point represents the mean of at least 3 biological repeats, with 3-5 technical repeats per assay ± SEM.

As discussed in Chapter 4, inducibility of β-sheet structure/self-assembly upon membrane interaction is associated with decreased solution amphipathicity, greater solvent-accessible surface area, and Trp^4-containing tyrocidines (TrcC, C_1, B` and $B_1$`) exhibit enhanced inducibility of β-sheet structure/self-assembly relative to Phe^4-containing tyrocidines (TrcA, A_1, B and B_1). The results therefore suggest that the reduced antiplasmodial activity associated with decreased solution amphipathicity and increased size may be an indirect result of the enhanced self-assembly in a membrane environment/inducibility of self-assembly upon membrane interaction leading to a

membrane associated MOA. The sigmoidal trend may also indicate a switch in MOA between a pure non-membrane associated MOA for TrcA and A_1, a mixed MOA for TrcB and B_1 (slope of curve) and a pure membrane associated MOA for TrcC, C_1, B` and $B_1$` (Figure 2B).

7.4.4 Structure-selectivity relationships of the tyrocidines

Excellent exponential correlations were observed between apparent selectivity for infected erythrocytes and *in silico* solvent-accessible surface area ($R^2 = 0.95$, results not shown) and *in silico* solvent-accessible volume ($R^2 = 0.98$) (Figure 3A), indicating that solution amphipathicity and peptide size are major determinants of selectivity, which corresponds to previous research by Rautenbach *et al.* (2007) [11]. However, correlation between apparent selectivity and HPLC retention time required segregation of the Orn^9- ($R^2 = 0.99$) and Lys^9- ($R^2 = 0.94$) containing tyrocidines, suggesting that the identity of the cationic residue in position 9 may have an important influence on selectivity (Figure 3B).

As discussed for antiplasmodial activity, increased solution amphipathicity and decreased peptide size may increase selectivity (1) directly by modulating the productivity of membrane interaction and/or (2) indirectly by modulating the manner and/or extent of peptide self-assembly. Good exponential correlations were observed between apparent selectivity for infected erythrocytes and $\theta_{204}/\theta_{214,\,TFE}$ of the Orn^9- ($R^2 > 0.99$) and Lys^9- ($R^2 = 0.91$) containing tyrocidines (Figure 4).

These results suggest that the extent and/manner of tyrocidine self-assembly in a membrane environment is a major determinant of selectivity, with enhanced β-sheet/self-assembly in a membrane environment related to reduced selectivity. The required segregation of the Orn^9- and Lys^9-containing tyrocidines is probably related to the influence of these cationic residues on the extent of self-assembly (size of self-assembly structures) and/or the orientation of the peptide molecules within the higher-order structures (*Discussed in Chapter 4*).

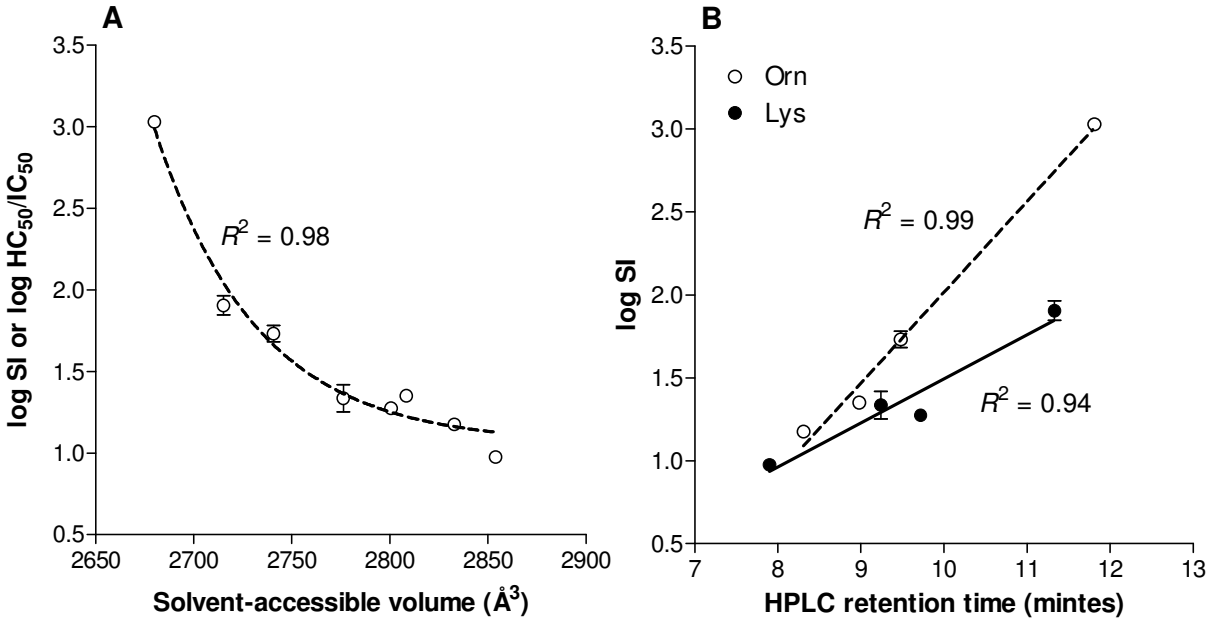

Figure 3 *Exponential correlation between apparent selectivity (SI) for P. falciparum-infected erythrocytes and molecular descriptors of A. size (*in silico *solvent-accessible volume) and B. solution amphipathicity (HPLC R_T) of the tyrocidines.* Each data point represents the mean of at least 3 biological repeats, with 3-5 technical repeats per assay ± SEM.

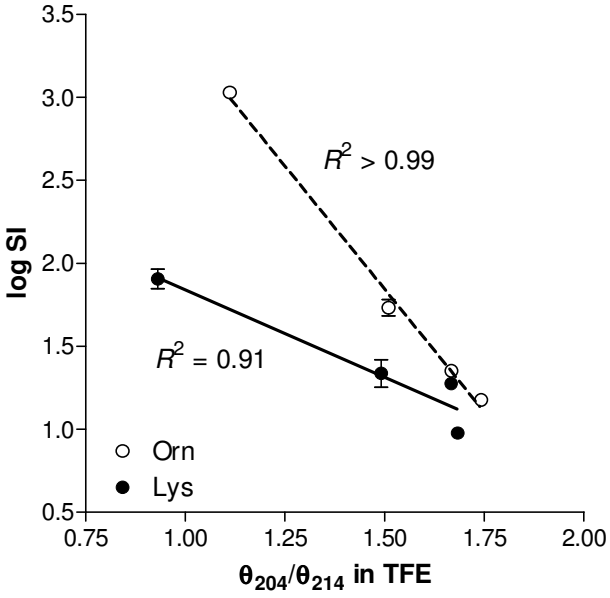

Figure 4 *Correlation between apparent selectivity for P. falciparum-infected erythrocytes and CD-derived descriptors of self-assembly in a membrane environment ($\theta_{204}/\theta_{214,\ TFE}$) of the tyrocidines.* Each data point represents the mean of at least 3 biological repeats, with 3-5 technical repeats per assay ± SEM.

Overall, these results indicate a central role for self-assembly in antiplasmodial activity and selectivity, and suggest that the structural requirements of activity and selectivity are, at least in part, related to the propensity for self-assembly in different environments. Tyrocidines with a higher propensity for self-assembly in an aqueous environment were in general more active and selective, while the inverse was observed for membrane associated self-assembly.

7.4.5 Modulation of antiplasmodial activity by solvent conditions/formulation

From the above correlations it is clear that the activity of the tyrocidines is very sensitive in terms of self-assembly and the formulation/solvent environment, such as ionic strength and the presence of serum proteins such as albumin [15], of the tyrocidines may therefore have a major influence on their activity.

7.4.5.1 Tyrocidine-Ca^{2+} complexation and antiplasmodial activity

The antibacterial activity of the tyrocidines was found to be relatively salt-insensitive, but calcium was found to play a major role in antilisterial activity modulation (Chapter 6). Investigation of the influence of calcium on the antiplasmodial activity of tyrocidine A (the most active antiplasmodial peptide) indicated that 1.0 mM $CaCl_2$ led to a 50% decrease in the activity of tyrocidine A. The observed loss of activity may be related to the precipitation of the TrcA-Ca^{2+} complexes. For antilisterial activity, a peptide-to calcium ratio of 1:750 (10 μM peptide:7.5 mM $CaCl_2$) led to optimal activity. Peptide-to-calcium ratios greater than 1:3000 led to reduced antilisterial activity, attributed to precipitation of active tyrocidine-Ca^{2+} complexes (refer to Chapter 6). The high peptide-to-calcium ratio (1:68 750; 20 ng/mL:1.375 mM $CaCl_2$) may therefore have lead to precipitation of TrcA-Ca^{2+} complexes and loss of antiplasmodial activity. However, the role of Ca^{2+} in the antiplasmodial activity of the tyrocidines cannot be fully ruled out as the RPMI culture medium contains approximately 375 μM $CaCl_2$ (15 ppm as determined with elemental analysis) leading to the an 1:18750 ratio at 20 ng/mL tyrocidine. As normal parasite development, as well as erythrocyte invasion by *P. falciparum* merozoites, is highly dependent on extracellular and intraparasitic Ca^{2+} [30-37], the influence of lower calcium concentrations could not be investigated.

The apparent maximal Ca^{2+} binding (maximal/plateau MS signal of complex, S_{max}) of the six major tyrocidines was calculated from TOF-ESMS data (Figure 5A). In Chapter 6, a linear correlation ($R^2 = 0.82$) was reported between the S_{max} for Ca^{2+} and HPLC retention time, which indicates that tyrocidine-Ca^{2+} complexation is related to solution amphipathicity. This correlation may also imply that greater self-assembly in aqueous solution (as seen for TrcA and A_1, refer to Chapter 3) allows for greater Ca^{2+} binding, possibly due to incorporation of Ca^{2+} in higher-order structures.

A strong exponential correlation ($R^2 = 0.96$) was observed between apparent maximal Ca^{2+} binding (S_{max}) and antiplasmodial activity (Figure 5B), which supports the hypothesis that Ca^{2+}-tyrocidine complexation plays an important role in antiplasmodial activity. The results indicate that increased S_{max} is associated with increased antiplasmodial activity, which may be related to induction of active conformations/higher-order structures by increased Ca^{2+}-complexation. Tyrocidine-Ca^{2+} complexation may interfere with calcium homeostasis, which is required for normal development of the parasite.

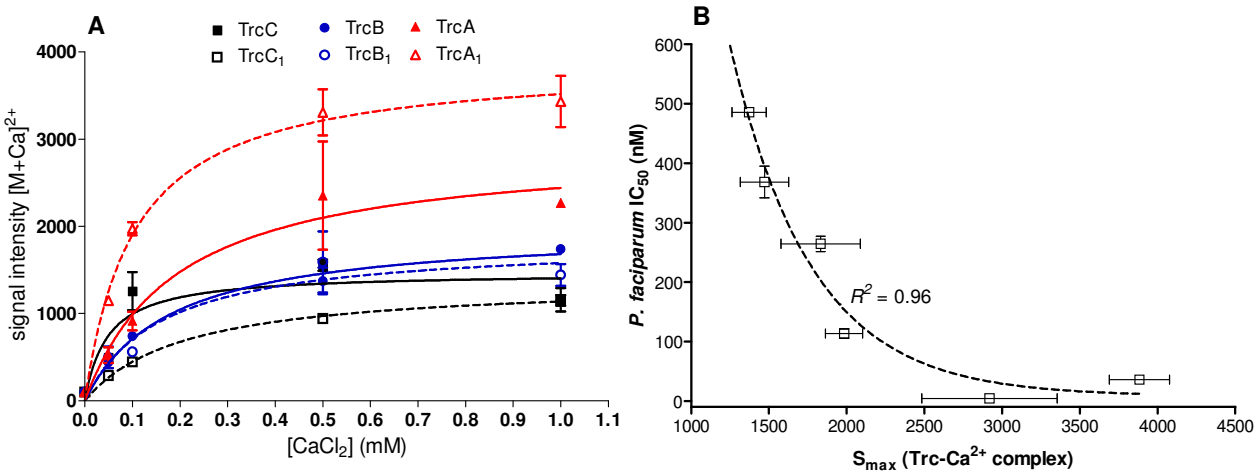

Figure 5 *A. Apparent tyrocidine-Ca^{2+} complexation as determined by TOF-ESMS and B. Correlation between apparent maximal Ca^{2+} binding (S_{max}) and the antiplasmodial activity (IC_{50}) of the six major tyrocidines.* Data points are the mean of at least three determinations ± SEM.

7.4.5.2 The influence of serum albumin on antiplasmodial activity

The potential influence of albumin on the antiplasmodial activity of the tyrocidines was evaluated diluting the peptides in RPMI culture medium or albumax II (human serum albumin preparation used as serum substitute). Albumax II did not influence the activity of tyrocidines A and A_1, but led to a significant loss in activity of tyrocidines B, B_1, C, C_1 and gramicidin S (Figure 6). The loss of gramicidin S activity, which acts mostly via a lytic mode of action [11], suggests that the presence of/binding to albumin reduces its specific lytic activity. The observed loss of activity of tyrocidines B, B_1, C and C_1, with B_1 the least affected of this group, may be related to the loss of lytic activity due to binding to albumin. In contrast, the more active peptides, tyrocidines A and A_1, did not exhibit reduced activity in the presence of albumin, which suggests that either these peptides do not associate with albumin or their mode of action is not influenced by such interaction.

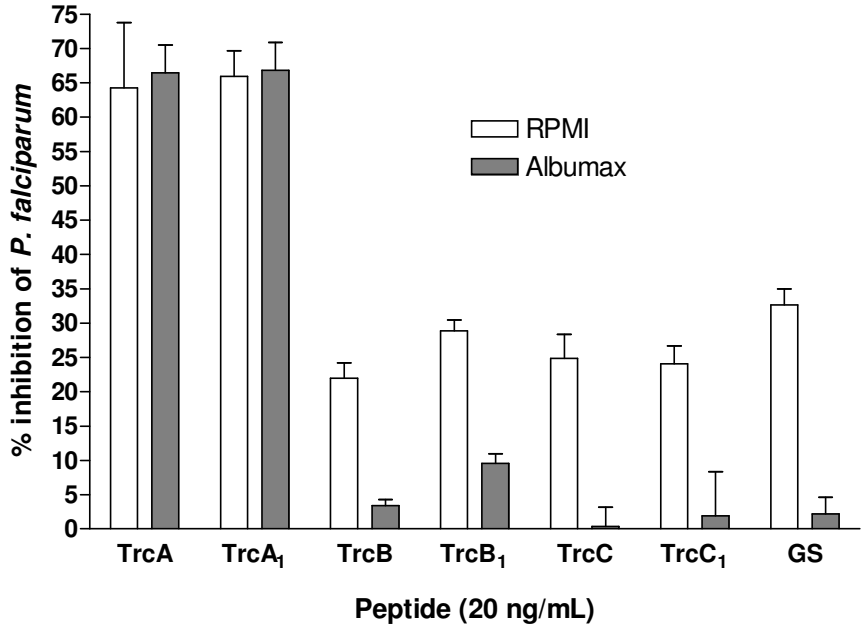

Figure 6 *Influence of pre-incubation conditions on the antiplasmodial activity of the tyrocidines.* The bars indicate inhibition of *P. falciparum* (% inhibition ± SEM, $n = 5$) by 20 ng/mL purified tyrocidine with RPMI culture medium (clear bars) or albumax II (grey bars) as peptide per-incubation solvent.

Results from fluorescent microscopy (see discussion below), as well as previous research, indicated that TrcA does not induce overt lysis, but rather acts via an alternative mode of action, halting parasite development in the late trophozoite stage [11]. Such an alternative mode appears to be unaffected by association with albumin.

7.4.6 Influence of tyrocidine A on membrane integrity

The previous study by Rautenbach *et al.* (2007) [11] indicated that the tyrocidines act by a non-lytic mode of action. In order to investigate this observation further, the influence of tyrocidine A on membrane integrity was visualised by live cell fluorescent microscopy. Bisbenzimide, a membrane permeable DNA marker, was used to visualise all *P. falciparum* nuclei, whereas propridium iodide, a membrane impermeable DNA marker, was used to identify nuclei of *P. falciparum* cells with compromised membrane integrity. As expected, the control cultures only exhibited bismenzamide fluorescence, especially in the vicinity of the hemozoin crystal (Figure 7A), indicating that membrane integrity is not compromised. The TrcA-treated *P. falciparum*-infected erythrocytes also did not exhibit propridium iodide fluorescence, indicating that TrcA does not compromise parasite membrane integrity within a 24 hour period, which corresponds to previous research by Rautenbach *et al*. (2007) [11]. Only cultures lysed with 20 μM gramicidin S indicated propridium iodide fluorescence (Figure 7C) in correspondence with previous results by Rautenbach *et al.* (2007) [11].

As seen for the control cultures, the bismenzamide fluorescence of the TrcA-treated cultures was found localised around the hemozoin crystal (Figure 7B). However, the hemozoin crystals of the treated cultures were generally found to be smaller, and in some cases unobservable (Figure 7B), than those of the control cultures. These results correspond to previous research, which found delayed growth (smaller trophozoites) in TrcA-treated cultures [11].

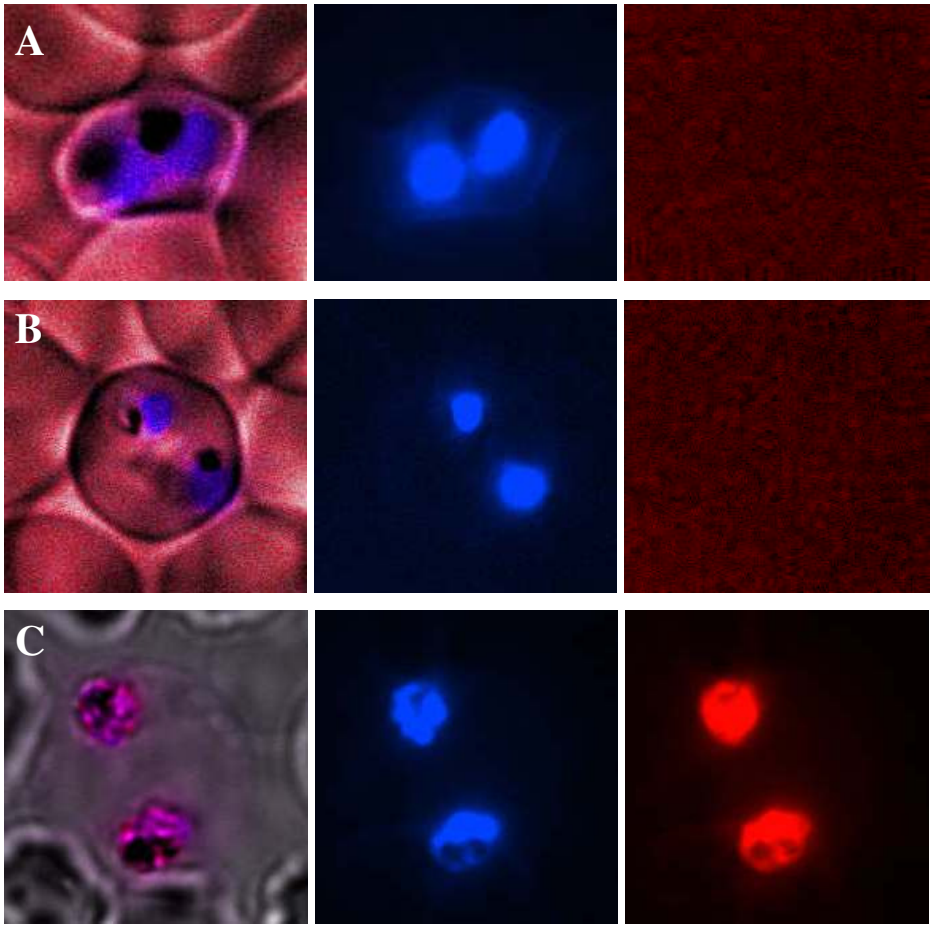

Figure 7 *Fluorescence and light microscopy of P. falciparum-infected erythrocytes incubated with propridium iodide and bismenzamide.* Bisbenzimide (membrane permeable DNA marker) fluorescence (blue) indicates all *P. falciparum* nuclei, whereas propridium iodide (membrane impermeable DNA marker) fluorescence (red) indicates nuclei of *P. falciparum* cells with compromised membrane integrity. In **A**: untreated *P. falciparum*-infected erythrocytes after 24 hours, **B**: *P. falciparum*-infected erythrocytes treated with 40 nM TrcA for 24 hours, and **C**: *P. falciparum*-infected erythrocytes treated with 20 μM gramicidin S for 10 minutes. The left hand panels show the overlay of bisbenzimide fluorescence (blue), propridium iodide fluorescence (red) and light (transmission) microscopy; the middlle panels show bisbenzimide fluorescence, and the right hand panels show propridium iodide fluorescence.

7.5 Conclusions

As was observed for antilisterial activity (Chapters 5 and 6), the antiplasmodial activity of the tyrocidines was found to be sensitive to solution composition and peptide identity, in particular the aromatic dipeptide unit identity. The manner in which different pre-incubation solutions modulate antiplasmodial activity is possibly related to self-assembly/aggregation. The QSAR analyses indicated a central role for tyrocidine self-assembly in antiplasmodial activity and selectivity, with reduced propensity for self-assembly in a membrane environment associated with enhanced antiplasmodial activity. Furthermore, the observed structural requirements (increased solution amphipathicity, reduced peptide size) for enhanced activity and selectivity are probably, at least in part, related to the propensity for self-assembly.

A non-lytic antiplasmodial MOA was confirmed for TrcA with live cell fluorescence microscopy and correlates with the Ca^{2+}- associated non-lytic antilisterial activity of the tyrocidines. Correlation between activity and Ca^{2+} binding also indicates that Ca^{2+} may play a role in the tyrocidine antiplasmodial activity, possibly due to interference of tyrocidine with Ca^{2+}-homeostasis. Previous research has shown that, although lysis may contribute to tyrocidine activity, the antiplasmodial activity of the tyrocidines does not depend on overt lysis, but rather inhibition of parasite development [11]. The loss of activity of lytic GS and tyrocidines B, B_1, C and C_1 in the presence of albumin strongly indicated that these tyrocidines share a lytic MOA with GS. The anti-plasmodium activity of the most active peptides, TrcA and A_1, were unaffected by albumin and indicates an alternative MOA. This result correlates with our finding that there is a sigmoidal trend between SI (selectivity towards *P. falciparum*) and the propensity of the tyrocidine to self-assemble in a membrane environment. As with this trend, the influence of albumin also points to a switch in MOA between a pure non-membrane associated MOA to a lytic MOA that is sequence dependent. As the lytic action of the tyrocidines have been associated with the VO(K)LFP pentapeptide unit, [11], the generally lower activity of the Lys^9-containng tyrocidines, relative to their Orn^9 counterparts may be ascribed to differences in initial membrane association leading to different propensities for membrane integration and induction of lysis. On the other hand, the variable pentapeptide unit (F/W)(f/w)NQY may allow for the alternative, non-lytic mechanism of action [11], with particular emphasis on the sequence and identity of the aromatic dipeptide unit. The importance of the aromatic amino acid sequence within

the dipeptide unit is illustrated by the reduced antiplasmodial activity of tyrocidines B` and $B_1$` (Phe^3-D-Trp^4) relative to tyrocidines B and B_1 (Trp^3-D-Phe^4). Optimal antiplasmodial activity was found to be mediated by Phe^3-D-Phe^4 (TrcA and A_1). Incorporation of a Trp residue in either position 3 or 4 led to reduced activity, which may be related to enhanced self-assembly in a membrane environment. Position 4 was, however, found to be significantly more sensitive to Phe→Trp substitution, which suggests that D-Phe^4 plays an important role in antiplasmodial activity. As D-residues are scarce, D-Phe^4 may be involved in interaction with a stereospecific target.

7.6 References

[1] World Health Organisation malaria report 2008 (www.who.int/malaria).

[2] E.L. Korenromp, Malaria incidence estimates at country level for the year 2004–proposed estimates and draft report, Geneva, Roll Back Malaria, World Health Organization, 2004.

[3] C. Guinovart, M.M. Navia, M. Tanner, P.L. Alonso, Malaria: burden of disease, Curr. Mol. Med. 6 (2006) 137-140.

[4] L.J. Bruce-Chwatt, Chemoprophylaxis of malaria in Africa: the spent 'magic bullet', Br. Med. J. 285 (1982) 674–676.

[5] U.I.M. Wiehart, M. Rautenbach, H.C. Hoppe, Selective lysis of erythrocytes infected with the trophozoite stage of *Plasmodium falciparum* by polyene macrolide antibiotics, Biochem. Pharm. 71 (2006) 779-790

[6] H.G. Boman, D. Wade, I.A. Boman, B. Wahlin, R.B. Merrifield, Antibacterial and antimalarial properties of peptides that are cecropinA-melittin hybrids, FEBS Lett. 259 (1989) 103-106.

[7] D. Wade, A. Boman, B. Wahlin, C.M. Drain, D. Andreu, H.G. Boman, R.B. Merrifeld, All-D amino acid-containing channel-forming antibiotic peptides, Proc. Natl. Acad. Sci. USA 87 (1990) 4761-4765.

[8] M. Krugliak, R. Feder, V.Y. Zolotarev, L. Gaidukov, A. Dagan, H. Ginsburg, A. Mor, Antimalarial activities of dermaseptin S4 derivatives, Antimicrob. Agents Chemother. 44 (2000) 2442-2451.

[9] A. Dagan, L. Efron, L. Gaidukov, A. Mor, H. Ginsburg, *In vitro* antiplasmodium effects of dermaseptin S4 derivatives, Antimicrob. Agents Chemother. 46 (2002) 1059-1066.

[10] L. Efron, A. Dagan, L. Gaidukov, H. Ginsburg, A. Mor, Direct interaction of dermaseptin S4 aminoheptanoyl derivative with intraerythrocytic malaria parasite leading to increased specific antiparasitic activity in culture J. Biol. Chem. 277 (2002) 24067-24072.

[11] M. Rautenbach, N.M. Vlok, M. Stander, H.C. Hoppe, Inhibition of malaria parasite blood stages by tyrocidines, membrane-active cyclic peptide antibiotics from *Bacillus brevis*, Biochim. Biophys. Acta - Biomembranes 1768 (2007) 1488–1497.

[12] C. Gelhaus, T. Jacobs, J. Andrä, M. Leippe, The antimicrobial peptide NK-2, the core region of mammalian NK-lysin, kills intraerythrocytic *Plasmodium falciparum*, Antimicrob. Agents Chemother. 52 (2008) 1713-1720.

[13] V. Sabareesh, R.S. Ranganayaki, S. Raghothama, M.P. Bopanna, H. Balaram, M.C. Srinivasan, P. Balaram, Identification and characterization of a library of microheterogeneous cyclohexadepsipeptides from the fungus Isaria, J. Nat. Prod. 70 (2007) 715-729.

[14] R.J. Dubos, R.D. Hotchkiss, The production of bactericidal substances by aerobic sporulating bacilli, J. Exp. Med. 73 (1941) 629-640.

[15] D. Andreu, L. Rivas, Animal antimicrobial peptides: an overview, Biopolymers (Pept. Sci.) 47 (1998) 415-433.

[16] R.M. Epand, H.J. Vogel, Diversity of antimicrobial peptides and their mechanisms of action, Biochim. Biophys. Acta 1462 (1999) 11-28.

[17] R.E. Hancock, A. Rozek, Role of membranes in the activities of antimicrobial cationic peptides, FEMS Microbiol. Lett. 206 (2002) 143-149.

[18] K.A. Brogden, Antimicrobial peptides: pore formers or metabolic inhibitors in bacteria?, Nature Rev. Microbiol. 3 (2005) 238-250.

[19] N.Y. Yount, M.R. Yeaman, Immunocontinuum: perspectives in antimicrobial peptide mechanisms of action and resistance, Protein Pept. Lett. 12 (2005) 49-67.

[20] A.K. Marr, W.J. Gooderham, R.E.W. Hancock, Antibacterial peptides for therapeutic use: obstacles and realistic outlook, Curr. Opin. Pharmacol. 6 (2006) 468-472.

[21] B.M. Spathelf, M. Rautenbach, Anti-listerial activity and structure–activity relationships of the six major tyrocidines, cyclic decapeptides from *Bacillus aneurinolyticus*, Bioorg. Med. Chem. 17 (2009) 5541-5548.

[22] M.T. Makler, D.J. Hinrichs, Measurement of the lactate dehydrogenase activity of *Plasmodium falciparum* as an assessment of parasitemia, Am. J. Trop. Med. Hyg. 48 (1993) 205-210.

[23] M. Rautenbach, G.D. Gerstner, N.M. Vlok, J. Kulenkampff, H.V. Westerhoff, Analyses of dose-response curves to compare the antimicrobial activity of model cationic alpha-helical peptides highlights the necessity for a minimum of two activity parameters, Anal. Biochem. 350 (2006) 81-90.

[24] V. Frecer, QSAR analysis of antimicrobial and haemolytic effects of cyclic cationic antimicrobial peptides derived from protegrin-1, Bioorg. Med. Chem. 14 (2006) 6065-6074.

[25] J.P. Segrest, H. De Loof, J.G. Dohlmann, C.G. Brouillette, G.M. Anantharamaiah, Amphipathic helix motif: classes and properties, Proteins: Struct., Funct., Genet. 8 (1990) 103-117.

[26] R.M. Dawson, D.C. Elliot, W.H. Elliot, K.M. Jones, Data for biochemical research, 3 ed., Claridon Press, Oxford, 1986.

[27] D.A. Kelkar, A. Chattopadhyay, Membrane interfacial localization of aromatic amino acids and membrane protein function, J. Biosci. 31 (2006) 297-302.

[28] T. Wymore, T.C. Wong, Molecular dynamics study of substance P peptides in a biphasic membrane mimic, Biophys. J. 76 (1999) 1199-1212.

[29] M.B. Strom, B.E. Haug, O. Rekdal, M.L. Skar, W. Stensen, J.S. Svendsen, Important structural features of 15-residue lactoferricin derivatives and methods for improvement of antimicrobial activity, Biochem. Cell Biol. 80 (2002) 65-74.

[30] R. Docampo, S.N.J. Moreno, The role of Ca^{2+} in the process of cell invasion by intracellular parasites, Parasitology Today 12 (1996) 61-65.

[31] M. Wasserman, J.P. Vernot, P.M. Mendoza, Role of calcium and erythrocyte cytoskeleton phosphorylation in the invasion of *Plasmodium falciparum* Parasitology Research 76 (1990).

[32] T. Tiffert, H.M. Staines, J.C. Ellory, V.L. Lew, Functional state of the plasma membrane Ca^{2+} pump in *Plasmodium falciparum*-infected human red blood cells, J. Physiol. 525 (2000) 125-134.

[33] P. Rohrbach, O. Friedrich, J. Hentschel, H. Plattner, R.H.A. Fink, M. Lanzer, Quantitative calcium measurements in subcellular compartments of *Plasmodium falciparum*-infected erythrocytes, J. Biol. Chem. 280 (2005) 27960–27969.

[34] C.R.S. Garcia, Calcium homeostasis and signaling in the blood-stage malaria parasite, Parasitology Today 15 (1999) 488-491.

[35] G.A. Biagini, P.G. Bray, D.G. Spiller, M.R.H. White, S.A. Ward, The digestive food vacuole of the malaria parasite is a dynamic intracellular Ca^{2+} store, J. Biol. Chem. 278 (2003) 27910–27915.

[36] M. Wasserman, C. Alarcón, P.M. Mendoza, Effects of Ca^{++} depletion on the asexual cell cycle of *Plasmodium falciparum*, Am. J. Trop. Med. Hyg. 31 (1982) 711-717.

[37] M.L. Caldas, M. Wasserman, Cytochemical localisation of calcium ATPase activity during the erythrocytic cell cycle of *Plasmodium falciparum*, Int. J. Parasitol. 31 (2001).

Chapter 8

Conclusions and recommendations for future studies

This study represents the first detailed investigation of the self-assembly, bioactivity and structure-activity relationships of the purified natural tyrocidines produced by *Bacillus aneurinolyticus*. Investigation of the structure-activity relationships and modulation of tyrocidine bioactivity was motivated by their possible application as novel therapeutic agents and bio-preservatives. The objectives of this study included purification of tyrocidines from the natural tyrothricin complex of *B. aneurinolyticus*; investigation of conformation, physicochemical character and self-assembly of the purified tyrocidines; investigation of the antibacterial, antiplasmodial, and haemolytic activity and selectivity; elucidation of the structure-activity-selectivity relationships; and evaluation of modulation of bioactivity by environmental conditions.

The complexity of tyrocidine chemistry and biochemistry became apparent during the purification process and initial bioactivity determinations, which indicated that the tyrocidines are extremely sensitive to solution composition and handling. Such sensitivity was found to be a result of their tendency for self-assembly. The spectrophotometric investigation of the tyrocidines was also complicated by their tendency for self-assembly, as well as their high aromatic content.

This study is the first reported study in which eight tyrocidines were successfully purified to >95% purity from the natural tyrothricin complex (Chapter 2), which allowed investigation of the physicochemical character, conformation, self-assembly and bioactivity (Chapters 3-7).

8.1 Experimental conclusions

8.1.1 Structural investigation

Spectrophotometric analyses of the tyrocidines indicated that the manner and/or extent of tyrocidine self-assembly are highly dependent on peptide identity and solvent

composition (Chapter 3). This observation corresponds to previous research, which indicated that the tyrocidines undergo extensive, stable aggregation/self-assembly in aqueous solution [1-6], and that such self-assembly is highly dependent on amino acid sequence, conformation and proper spatial orientation of the amino acid residues [1, 2, 6] and sensitive to solvent composition [3, 5]. The results of this study indicated that the variable cationic residue (Orn^9/Lys^9) and the variable aromatic dipeptide moiety ($Phe^{3,4}$/$Trp^{3,4}$) have a significant influence on the manner/extent of tyrocidine self-assembly, as well as the orientation/exposure/local environments of the aromatic amino acids. Such differences in self-assembly are likely to influence the bioactivity, and possibly the mode of action, of the tyrocidines. The manner in which the variable residues modulate self-assembly may be related to differences in molecular properties, such as hydrophobicity, amphipathicity, available surface area, and/or the spatial orientation of the amino acid side-chains. In an aqueous environment, the Phe^3-containing tyrocidines (TrcA, A_1, B` and $B_1$`) exhibited greater self-assembly/β-sheet stability than the Trp^3-containing tyrocidines (TrcC, C_1, B and B_1), and such differences in self-assembly were shown to be related to differences in the solvent-accessible surface areas of the Phe^3- and Trp^3-containing tyrocidines. Furthermore, we concluded that the relative positioning of the aromatic residues within the dipeptide moiety influences the manner/extent of self-assembly of the tyrocidines, which may be explained by the segregation of the two residues in the aromatic dipeptide moiety on opposite faces of the molecule. The results also suggested that self-assembly in an aqueous environment involves shielding of the aromatic residue in position 4 from the solvent, while the aromatic residue in position 3 remains exposed. In a membrane-mimetic environment, the Trp-containing tyrocidines (B and C group) exhibit greater self-assembly/β-sheet stability than the Trp-lacking tyrocidines (TrcA and A_1), indicating that the presence of Trp (irrespective of position) is associated with enhanced β-sheet structure/self-assembly. Furthermore, decreased solution amphipathicity and greater solvent-accessible surface area were shown to be associated with enhanced β-sheet structure/self-assembly, in a membrane-mimetic environment. The results also suggested that the arrangement of peptide molecules within the higher-order structures in an aqueous and membrane-mimetic environment differ, with increased exposure of residue 4, which was “buried” in water-induced self-assembly, in a membrane-mimetic environment.

The differences in the manner of association of the tyrocidines/arrangement of peptide molecules within the higher-order structures in an aqueous and membrane-mimetic environment may be attributed to differing driving forces for association. Previous research suggested that tyrocidine aggregation/self-assembly in an aqueous environment is mediated by hydrophobic side-chain interactions [1-3, 5], and self-assembly in an aqueous environment will thus involve association of the hydrophobic regions of the peptides in order to shield them from the polar solvent. In contrast, self-assembly in membrane-mimetic environment is expected to be mediated by other forces, and the results suggested that higher-order structures formed in the presence of TFE are probably stabilised by intermolecular hydrogen bonding. Self-assemblies in a membrane-mimetic environment will preferentially shield the polar regions from the hydrophobic solvent, while exposing the hydrophobic portions. The results also indicated that the structure of the predominant self-assembled species formed in a membrane-mimetic environment differ from, and are probably larger than, the higher-order structures formed in aqueous solution, which indicates that β-sheet peptides are likely to form superstructures upon membrane interaction [7].

Due to the limited amount of available peptide and the lack of ^{13}C enriched tyrocidines, nuclear magnetic resonance (NMR) spectroscopy could not be employed in this study for complete determination of the three-dimensional structure of the tyrocidines. Furthermore, NMR structure determination of the tyrocidines is complicated by their propensity for self-assembly. We therefore used a molecular model of tyrocidine C, modelled using NMR constraints for homology modelling, which indicated that the eight investigated tyrocidines adopt similar β-sheet backbone conformations (Chapter 4). However, unlike gramicidin S, the tyrocidines do not exhibit segregated hydrophobic and polar faces. Instead, an aromatic residue extends from each face of the peptide. Also, in contrast to previous predictions suggesting that the D-Phe^1 and Orn^9 side-chains extend from the same face [8], our modelling results correspond well to a previous report by Marques *et al.* (2007) [9]. The aromatic residues of the variable dipeptide unit were shown to extent to opposite sides of the tyrocidine structure, with residue 3 (Phe^3/Trp^3) extending to one side while residue 4 (Phe^4/Trp^4) and the cationic residue (Orn^9/Lys^9) extend toward the opposite side. Such segregation of the variable aromatic residues may have important implications for tyrocidine self-assembly and membrane interaction.

8.1.2 Bioactivity and selectivity

The antibacterial activity of the tyrocidines was found to be (1) strain-specific and thus dependent on properties of the target cell; (2) dependent on peptide identity/structure; and (3) sensitive to environmental/solvent conditions. The tyrocidines were found to be selective for Gram-positive bacteria, which may be attributed to differing cell walls of Gram-positive and Gram-negative bacteria. Due to the lack of activity toward Gram-negative bacteria under our assay conditions, this study focussed on the activity of the tyrocidines toward Gram-positive bacteria. Further evidence for the influence of target cell properties was gained from the observation that *L. monocytogenes* B73-MR1 is more sensitive to the tyrocidines than *L. monocytogenes* B73, which may be related to differences in membrane structure and/or metabolic differences [10-12] (Chapter 5). In addition to the role of the target cell, antibacterial growth inhibition induced by the tyrocidines was found to be dependent on peptide structure. QSAR analyses allowed prediction of optimal physicochemical parameters for antibacterial activity of the natural tyrocidine library (Chapter 5). In general, TrcC exhibited optimal side-chain surface area, while $TrcB_1$ exhibited optimal solution amphipathicity (HPLC R_T). Although these optimal physicochemical characteristics may be directly related to target cell membrane interaction/integration/translocation or interaction with alternative targets, such structural requirements may also be related to the propensity for tyrocidine self-assembly, as peptide self-assembly may impact membrane interaction, cytolytic activity and/or transport across biological barriers [7, 13-19]. We found that the Trp-containing tyrocidines (B and C groups) were more active towards Gram-positive bacteria than the Trp-lacking tyrocidines (A group). The reduced antibacterial activity seen for TrcA and A_1 was found to be associated with enhanced self-assembly in aqueous solution, which suggests that premature self-assembly reduces target membrane interaction, integration and/or translocation to reach a cytoplasmic target. The greater antilisterial activity of the Trp-containing tyrocidines C, C_1, B and B_1 corresponds to enhanced self-assembly in a membrane environment, which suggests that self-assembly into active bactericidal lytic complexes within the target cell membrane may be critical for the antilisterial activity of the tyrocidines.

In addition to the roles of the target cell and peptide structure/self-assembly in antibacterial activity modulation, a novel result from this study indicated that

tyrocidine-Ca^{2+} complexation plays an important role in the antilisterial activity and mode of action of the tyrocidines (Chapter 6). Spectrophotometric investigation indicated that Ca^{2+} has a significant influence on the self-assembly of the tyrocidines and that such self-assembly is distinct, possibly in terms of size and/or the relative orientation of the peptide molecules with the assembly, from assemblies formed in a salt-free environment and a membrane environment. Such formation of higher-order structures leads to a non-lytic bacteriocidal cellular event. Tyrocidine-Ca^{2+} complexation and the concomitant induction of higher-order structures therefore not only increase the antilisterial activity of the tyrocidines, but also change the mechanism of action of the tyrocidines from a predominantly lytic to an alternative/intracellular mode of action.

As was observed for antilisterial activity, the antiplasmodial activity of the tyrocidines was found to be sensitive to peptide identity and solvent composition and the QSAR analyses indicated a central role for tyrocidine self-assembly in antiplasmodial activity and selectivity (Chapter 7). However, contrasting structural and self-assembly requirements were observed for antilisterial and antiplasmodial activity. While enhanced self-assembly in a membrane-environment was shown to be associated with improved antilisterial activity, reduced propensity for self-assembly in a membrane environment associated with enhanced antiplasmodial activity. This study confirmed a non-lytic antiplasmodial mode of action (MOA) for TrcA, supporting the observation that, although lysis may contribute to tyrocidine activity, the antiplasmodial activity of the tyrocidines involves inhibition of parasite development and not overt membrane lysis [20]. Correlations between self-assembly and antiplasmodial activity, as well as observations regarding the influence of serum albumin, strongly indicated that the Trp-containing tyrocidines share a lytic MOA with gramicidin S, whereas the most active peptides, TrcA and A_1, act via an alternative MOA. The influence of albumin suggested a sequence-dependent switch in MOA between a pure non-membrane associated MOA to a lytic MOA. As seen for antilisterial activity, an alternative non-lytic mode of action may also be related to tyrocidine-Ca^{2+} complexation, as indicated by the correlation between enhanced Ca^{2+} binding and antiplasmodial activity. The (F/W)(f/w)NQY may allow for the alternative, non-lytic mechanism of action [20], with particular emphasis on the sequence and identity of the aromatic dipeptide unit. Optimal antiplasmodial activity was found to be mediated by Phe^3-D-Phe^4 (TrcA and A_1) and

incorporation of a Trp residue in either position 3 or 4 led to reduced activity, which may be related to enhanced self-assembly in a membrane environment. Position 4 was, however, found to be significantly more sensitive to Phe→Trp substitution, which suggests that D-Phe^4 plays an important role in antiplasmodial activity, possibly by interacting with alternative, stereospecific target.

8.2 Hypotheses

This study indicated contrasting structural and self-assembly requirements for antilisterial and antiplasmodial activity, which may be related to the different target cell *types* – bacterium or parasite – or target cell *locations* – extracellular or intracellular. If the effects of peptide self-assembly are due to the *localisation* of the pathogen, differences may be ascribed to the mechanism of peptide uptake and delivery to the (molecular) target. Higher-order structures may translocate to the cytoplasm (possibly via endocytosis) to reach an internal target more effectively than monomers/low-order structures, which may become trapped by interacting too strongly with the cell membrane. Furthermore, peptides that form larger assemblies (eg more hydrophobic peptides) may be delivered to an internal target in higher concentrations. A preliminary investigation, in which the tyrocidine complex was formulated in Pheroid^{TM} vesicles (in collaboration with A. Fourie, University of the North West), lipid based carriers that promote transfer across membranes, indicated that antiplasmodial activity was enhanced by >100%. This result strongly suggests that antiplasmodial activity requires the peptides to transverse the erythrocyte and parasite membranes, indicating that the tyrocidines may have an internal target. In the event that the effects of peptide self-assembly are modulated by target cell *type*, differences may be ascribed to different membrane compositions or different mechanisms of action. The influence of peptide organisation on activity is expected to be related to the type and/or efficacy of membrane interaction. The different responses of antibacterial and antiplasmodial activity may thus be related to different membrane types/compositions, which may have a preference for different peptide aggregation states. Alternatively, different organisms may require different interaction efficacies due to different mechanisms of action/target sites.

The results presented in this thesis suggest that the antilisterial and antiplasmodial activity of the tyrocidines is likely to be mediated, at least in part, by a non-

membranolytic mode of action. As the tyrocidines have been shown to inhibit RNA synthesis by binding to DNA [21-23], such a non-lytic mode of action may be related to tyrocidine-DNA interaction. Previous research has suggested that, at low concentrations, tyrocidine-DNA interaction involves intercalation of the aromatic side-chains between DNA bases, leading to unwinding of superhelical DNA [22]. At higher peptide concentrations, interaction between DNA and tyrocidine aggregates induces DNA packaging, and therefore inhibition of transcription [22]. The role of tyrocidine self-assembly in activity modulation may thus be related to the influence on DNA packaging. The role of Ca^{2+} in tyrocidine antilisterial activity may also be related to a DNA-associated mechanism of action, as the higher-order tyrocidine structures induced upon Ca^{2+} may favour tyrocidine-DNA interaction. The observation that antiplasmodial activity is associated with enhanced self-assembly of the tyrocidines in solution, as well as enhanced Ca^{2+} binding (TrcA and A_1), suggests that the same may apply for the antiplasmodial activity of the tyrocidines.

In addition to the possible DNA-related mode of tyrocidine action, the role of Ca^{2+} in tyrocidine activity suggests that the antilisterial and antiplasmodial activity of the tyrocidines may be due to disruption of Ca^{2+} homeostasis. As most cell types rely on calcium signalling to regulate cell function, interference with Ca^{2+} homeostasis may led to lethal disruption of normal cell functions. The vital importance of both intracellular and extracellular calcium for plasmodium invasion of erythrocytes and the normal development of the parasite have been widely documented [24-32], and interference with Ca^{2+} homeostasis is expected to disrupt normal parasite development and prevent re-invasion of erythrocytes. Disruption of Ca^{2+} homeostasis by the tyrocidines may thus contribute to their antiplasmodial activity, which has been shown to involve inhibition of parasite development [20].

8.3 Recommendations for future studies

This study only investigated tyrocidine activity toward *L. monocytogenes* in culture. *L. monocytogenes* is, however, an intracellular pathogen, which infects the mammalian cell by phagocytosis and, once released from the membrane-bound vacuole, starts to multiply [33]. A preliminary investigation into the activity of TrcC and TrcA towards intracellular *Mycobacterium tuberculosis* indicated selective low μM activity (IC_{50}< 1.25 μM). The possibility that the tyrocidines may be active toward intracellular

L. monocytogenes, potentially by a mechanism related to antiplasmodial/ antimycobacterial activity, should be investigated. Conversely, the activity of the tyrocidines toward *L. monocytogenes* in culture suggests that they may be active toward extracellular blood-borne parasites. This possibility should be investigated by determining the activity of the tyrocidines toward, for example, *Trypanasoma brucei*. Furthermore, investigation of the nature of the effect of peptide self-assembly on activity toward intracellular *L. monocytogenes, M. tuberculosis* and extracellular *T. brucei* may allow us to determine whether the effect of peptide self-assembly is related to target cell location or type.

Information regarding the interaction of peptides/peptide complexes with the target cell membrane may contribute to understanding the manner by which self-assembly influences activity. The ability of different self-assembly states of the tyrocidines to induce cell lysis or to translocate to the target cell cytoplasm may be investigated using model membrane systems composed of different phospholipids. The processes involved in tyrocidine/tyrocidine complex uptake and delivery may be further be elucidated by investigating the role of endocytosis and phagocytosis in the uptake of the tyrocidines in *P. falciparum* and intracellular *L. monocytogenes*, respectively.

In order to gain a better understanding of tyrocidine mode of action, the contribution of membrane interaction, self-assembly in membranes and lysis to their antimicrobial activity needs to be determined. The ability of the different tyrocidines to interact with membranes, self-assemble and induce cell lysis and/leakage can be evaluated by making use of model membrane systems. Unfortunately, our access to a fluorometer and circular dichroism spectrometer was limited and the available infrastructure did not allow such investigations using liposomes. In addition to providing information regarding the contribution of membrane activity to mechanism of action, selectivity between anionic and neutral liposomes, representative of bacterial and eukaryotic cell membranes respectively, will provide insight regarding the role of target cell properties in activity modulation. Gaining a better understanding of the manner in which the target cell modulates activity may provide valuable insight regarding the structure-activity relationships and mode of action of these peptides, as well as the foundation for optimising tyrocidine selectivity.

In order to evaluate the hypotheses regarding the mechanism(s) of action, investigation of the influence of the tyrocidines on DNA structure and gene expression of *Listeria* and *Plasmodium* may be investigated by DNA footprinting and microarray gene expression studies. Further, the possible influence of the tyrocidines on Ca^{2+} homeostasis and/or distribution within the target cells may be investigated by fluorescence microscopy using Ca^{2+} indicators.

Furthermore, the influence of the target cell and the central role of self-assembly in tyrocidine bioactivity motivates further research regarding the manner of tyrocidine-tyrocidine association in both aqueous and membrane environments. Analytical techniques, such as Fourier transform infrared spectroscopy and nuclear magnetic resonance, can be applied to elucidate these molecular interactions. Also, tyrocidine C_1 formed fibre-like structures in TFE, and microscopic/physical properties of such macromolecular structures may be investigated by scanning electron microscopy.

Shortly prior to submission of this manuscript, our collaborator, Prof. Graham Jackson (University of Cape Town) provided us with a dimer model of TrcC, stabilised by four intermolecular hydrogen bonds formed between the backbone carbonyl- and amino-groups of Orn^9 and D-Trp^4 (Figure 1). Comparison of the Yasara refined low energy dimer model with the monomer, indicated that the TrcC dimer has substantially lower potential energy than the TrcC monomer. This finding may explain the propensity for self-assembly and role of the variable cationic and aromatic residues in self-assembly. Further insight regarding possible dimer and higher order structure formation of the tyrocidines may thus shed light on the role of the variable residues in self-assembly and bioactivity.

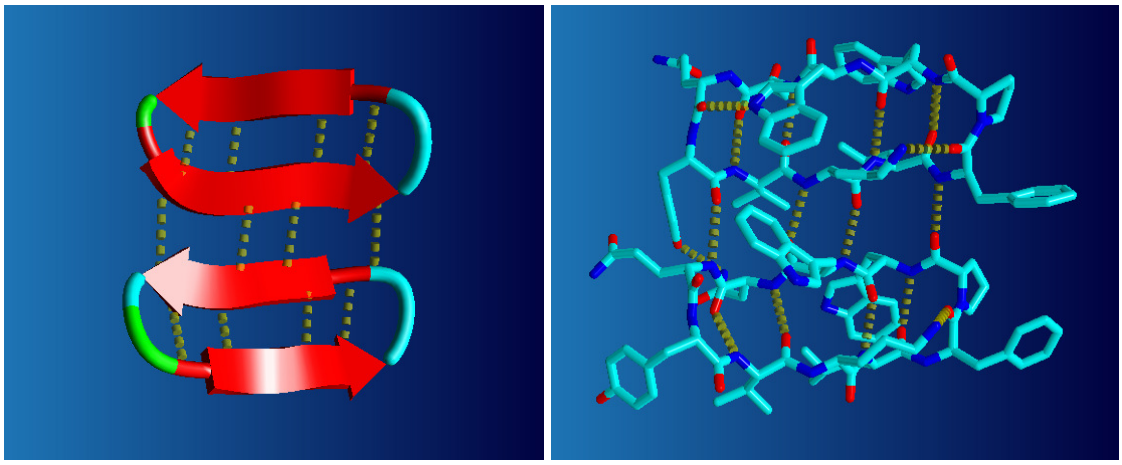

Figure 1 *Model of tyrocidine C dimer refined by Yasara 9.10.5©;* original model courtesy of Prof Graham Jackson (University of Cape Town).

8.4 Preliminary results pertaining to potential application as a bio-preservative

L. monocytogenes has drawn the interest of food manufacturers and government bodies due to food-borne outbreaks [34], with milk and milk products being particularly susceptible to contamination by *L. monocytogenes* [34-37]. As discussed in Chapter 5, the tyrocidines have been shown to possess significant antibacterial activity toward *L. monocytogenes* [38], as well as enhanced antilisterial activity toward *L. monocytogenes* B73-MR1, a leucocin A (a pediocin-like bacteriocin) resistant strain [38, 39], relative to the leucocin A-sensitive *L. monocytogenes* B73 [38, 40]. Furthermore, although the activity of most antimicrobial peptides (including nisin and pediosin) is reduced by the presence of cations such as Na^+, Mg^{2+} and Ca^{2+} [41-48], the tyrocidines were found to be reasonably salt-tolerant. These results suggest that the tyrocidines may be useful bio-preservatives. However, activity of antimicrobial agents may be influenced by additional food components, such as fat and protein [49] and the antilisterial activity of nisin has been shown to decrease in milk, largely due to the milk fat content [50]. Preliminary investigation indicated that *L. monocytogenes* growth in milk may be successfully inhibited by the presence of 100 µg/mL tyrocidine complex (Figure 2), which prompts further investigation.

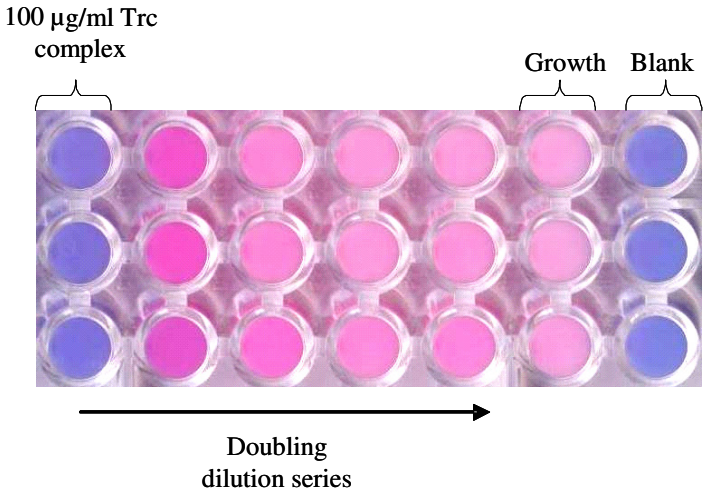

Figure 2 *Protective influence of the tyrocidine complex.* Blue wells indicate the absence of viable cells, while pink wells indicate the presence of viable *L. monocytogenes*. A doubling dilution series of the tyrocidine complex was added to store-bought skim milk (highest concentration = 0.10 mg/mL), followed by inoculation with *L. monocytogenes* B73 ($6.7x10^7$ CFU/mL). The inoculated plate was left at room temperature for two days, after which viability of *L. monocytogenes* was assessed using the CellTiter-Blue™ Cell Viability Assay.

8.5 Last word

Overall, it may be hypothesised that tyrocidine activity and mode of action is modulated by a critical play-off between self-assembly, cation-complexation and membrane-interaction. As these modulators of activity are highly dependent on tyrocidine sequence/structure, the wide variety of tyrocidines found in the natural complex may allow for optimal interaction with and activity toward a variety of microbes.

Research concerning the tyrocidines may play an important role in future combating of the spread of treatment-resistant food-borne bacteria, as well as treatment-resistant infections. However, as a consequence of their toxicity and the expense of synthesis of non-toxic alternatives they may find their primary applicability as bio-preservatives and for the treatment of serious bacterial and plasmodium infections that are resistant to conventional antibiotics.

8.6 References

[1] M.A. Ruttenberg, T.P. King, L.C. Craig, The use of the tyrocidines for the study of conformation and aggregation behavior, J. Am. Chem. Soc. 87 (1965) 4196-4198.

[2] M.A. Ruttenberg, T.P. King, L.C. Craig, The chemistry of tyrocidine. VII. Studies on association behavior and implications regarding conformation, Biochemistry 5 (1966) 2857-2863.

[3] S. Laiken, M. Printz, L.C. Craig, Circular dichroism of the tyrocidines and gramicidin S-A, J. Biol. Chem. 244 (1969) 4454-4457.

[4] S.L. Laiken, M.P. Printz, L.C. Craig, Studies on the mode of self-assembly of tyrocidine B, Biochem. Biophys. Res. Commun. 43 (1971) 595-600.

[5] H.H. Paradies, Aggregation of tyrocidine in aqueous solutions, Biochem. Biophys. Res. Commun. 88 (1979) 810-817.

[6] R.C. Williams, D.A. Yphantis, L.C. Craig, Noncovalent association of tyrocidine B, Biochemistry 11 (1972) 70-77.

[7] N.Y. Yount, M.R. Yeaman, Immunocontinuum: perspectives in antimicrobial peptide mechanisms of action and resistance, Protein Pept. Lett. 12 (2005) 49-67.

[8] W.A. Gibbons, C.F. Beyer, J. Dadok, R.F. Sprecher, H.R. Wyssbrod, Studies of individual amino acid residues of the decapeptide tyrocidine A by proton double-resonance difference spectroscopy in the correlation mode, Biochemistry 14 (1975) 420-429.

[9] M.A. Marques, D.M. Citron, C.C. Wang, Development of tyrocidine A analogues with improved antibacterial activity, Bioorg. Med. Chem. (2007).

[10] V. Vadyvaloo, J.W. Hastings, M.J. van der Merwe, M. Rautenbach, Membranes of class IIa bacteriocin-resistant *Listeria monocytogenes* cells contain increased levels of desaturated and short-acyl-chain phosphatidylglycerols, Appl. Environ. Microbiol. 68 (2002) 5223–5230.

[11] V. Vadyvaloo, J.L. Snoep, J.W. Hastings, M. Rautenbach, Physiological implications of class IIa bacteriocin resistance in *Listeria monocytogenes* strains, Microbiol 150 (2004) 335–340.

[12] V. Vadyvaloo, S. Arous, A. Gravesen, Y. Hechard, R. Chauhan-Haubrock, J.W. Hastings, M. Rautenbach, Cell-surface alterations in class IIa bacteriocin resistant *Listeria monocytogenes* strains, Microbiol. 150 (2004) 3025–3033.

[13] Y. Shai, Mode of action of membrane active antimicrobial peptides, Biopolymers (Pept. Sci.) 66 (2002) 236-248.

[14] B. Bechinger, K. Lohner, Detergent-like actions of linear amphipathic cationic antimicrobial peptides, Biochim. Biophys. Acta 1758 (2006) 1529–1539.

[15] E. Guerrero, J.M. Saugar, K. Matsuzaki, L. Rivas, Role of positional hydrophobicity in the leishmanicidal activity of magainin 2, Antimicrob. Agents Chemother. 48 (2004) 2980-2986.

[16] A. Scaloni, M. Dalla Serra, P. Amodeo, L. Mannina, R.M. Vitale, A.L. Segre, O. Cruciani, F. Lodovichetti, M.L. Greco, A. Fiore, M. Gallo, C. D'Ambrosio, M. Coraiola, G. Menestrina, A. Graniti, V. Fogliano, Structure, conformation and biological activity of a novel lipodepsipeptide from *Pseudomonas corrugata*: cormycin A, Biochem. J. 384 (2004) 25-36.

[17] E. Glukhov, M. Stark, L.L. Burrows, C.M. Deber, Basis for selectivity of cationic antimicrobial peptides for bacterial versus mammalian membranes, J. Biol. Chem. 280 (2005) 33960–33967.

[18] T. Rydlo, S. Rotem, A. Mor, Antibacterial properties of dermaseptin S4 derivatives under extreme incubation conditions, Antimicrob. Agents Chemother. 50 (2006) 490–497.

[19] P.M. Hwang, H.J. Vogel, Structure-function relationships of antimicrobial peptides, Cell Biol. 76 (1998) 235-246.

[20] M. Rautenbach, N.M. Vlok, M. Stander, H.C. Hoppe, Inhibition of malaria parasite blood stages by tyrocidines, membrane-active cyclic peptide antibiotics from *Bacillus brevis*, Biochim. Biophys. Acta - Biomembranes 1768 (2007) 1488–1497.

[21] W. Danders, M.A. Marahiel, M. Krause, N. Kosui, T. Kato, N. Izumiya, H. Kleinkauf, Antibacterial action of gramicidin S and tyrocidines in relation to active transport, in vitro transcription, and spore outgrowth, Antimicrob. Agents Chemother. 22 (1982) 785-790.

[22] A. Bohg, H. Ristow, DNA-supercoiling is affected in vitro by the peptide antibiotics tyrocidine and gramicidin, Eur. J. Biochem. 160 (1986) 587-591.

[23] A. Bohg, H. Ristow, Tyrocidine-induced modulation of the DNA conformation in *Bacillus brevis*, Eur. J. Biochem. 170 (1987) 253-258.

[24] M. Wasserman, C. Alarcón, P.M. Mendoza, Effects of Ca^{++} depletion on the asexual cell cycle of *Plasmodium falciparum*, Am. J. Trop. Med. Hyg. 31 (1982) 711-717.

[25] M. Wasserman, J.P. Vernot, P.M. Mendoza, Role of calcium and erythrocyte cytoskeleton phosphorylation in the invasion of *Plasmodium falciparum* Parasitology Research 76 (1990).

[26] R. Docampo, S.N.J. Moreno, The role of Ca^{2+} in the process of cell invasion by intracellular parasites, Parasitology Today 12 (1996) 61-65.

[27] C.D. Doerig, Signal transduction in malaria parasites, Parasitology Today 13 (1997) 307-313.

[28] C.R.S. Garcia, Calcium homeostasis and signaling in the blood-stage malaria parasite, Parasitology Today 15 (1999) 488-491.

[29] T. Tiffert, H.M. Staines, J.C. Ellory, V.L. Lew, Functional state of the plasma membrane Ca^{2+} pump in *Plasmodium falciparum*-infected human red blood cells, J. Physiol. 525 (2000) 125-134.

[30] M.L. Caldas, M. Wasserman, Cytochemical localisation of calcium ATPase activity during the erythrocytic cell cycle of *Plasmodium falciparum*, Int. J. Parasitol. 31 (2001).

[31] G.A. Biagini, P.G. Bray, D.G. Spiller, M.R.H. White, S.A. Ward, The digestive food vacuole of the malaria parasite is a dynamic intracellular Ca^{2+} store, J. Biol. Chem. 278 (2003) 27910–27915.

[32] P. Rohrbach, O. Friedrich, J. Hentschel, H. Plattner, R.H.A. Fink, M. Lanzer, Quantitative calcium measurements in subcellular compartments of *Plasmodium falciparum*-infected erythrocytes, J. Biol. Chem. 280 (2005) 27960–27969.

[33] M. Gandhi, M.L. Chikindas, *Listeria*: A foodborne pathogen that knows how to survive, Int. J. Food. Microbiol. 113 (2007) 1-15.

[34] J.M. Farber, P.I. Peterkin, *Listeria monocytogenes*, a food-borne pathogen, Microbiol. Rev. 55 (1991) 476-511.

[35] M. Sanaa, B. Pourel, J.L. Menard, F. Serieys, Risk factors associated with contamination of raw milk by *Listeria monocytogenes* in dairy farms, J. Dairy Sci. 76 (1993) 2891-2898.

[36] N. Benkerroum, W.E. Sandine, Inhibitory action of nisin against *Listeria monocytogenes*, J. Dairy Sci. 71 (1988) 3237-3245.

[37] S.J. Walker, J.G. Archer, J.G. Bank, Growth of *Listeria monocytogenes* at refrigeration temperatures, J. Appl. Bacteriol. 68 (1990) 157-162.

[38] B.M. Spathelf, M. Rautenbach, Anti-listerial activity and structure–activity relationships of the six major tyrocidines, cyclic decapeptides from *Bacillus aneurinolyticus*, Bioorg. Med. Chem. 17 (2009) 5541-5548.

[39] M. Ramnath, M. Beukes, K. Tamura, J.W. Hastings, Absence of a putative mannose-specific phosphotransferase system enzyme IIAB component in a leucocin A-resistant strain of *Listeria monocytogenes*, as shown by two-dimensional sodium dodecyl sulfate-polyacrylamide gel electrophoresis, Appl. Environ. Microbiol. 66 (2000) 3098–3101

[40] G.A. Dykes, J.W. Hastings, Fitness costs associated with class IIa bacteriocin resistance in *Listeria monocytogenes* B73, Lett. Appl. Microbiol. 26 (1998) 5-8.

[41] R. Bals, M.J. Goldman, J.M. Wilson, Mouse beta-Defensin 1 is a salt-sensitive antimicrobial peptide present in epithelia of the lung and urogenital tract, Infect. Immun. 66 (1998) 1225-1232.

[42] S. Cociancich, A. Ghazi, C. Hetru, J.A. Hoffmann, L. Letellier, Insect defensin, an inducible antibacterial peptide, forms voltage-dependent channels in *Micrococcus luteus*, J. Biol. Chem. 268 (1993) 19239-19245.

[43] R.I. Lehrer, T. Ganz, D. Szklarek, M.E. Selsted, Modulation of the *in vitro* candidacidal activity of human neutrophil defensins by target cell metabolism and divalent cations, J. Clin. Invest. 81 (1988) 1829-1835.

[44] W.F. Broekaert, F.R.G. Terras, B.P.A. Cammue, R.W. Osborn, Plant defensins: Novel antimicrobial peptides as components of the host defense system, Plant Physiol. 108 (1995) 1353-1358.

[45] D.M.E. Bowdish, D.J. Davidson, Y.E. Lau, K. Lee, M.G. Scott, R.E.W. Hancock, Impact of LL-37 on anti-infective immunity, J. Leukoc. Biol. 77 (2005) 451-459.

[46] K. Yamauchi, K. Tomita, T.J. Giehl, R.T. Ellison, Antibacterial activity of lactoferrin and a pepsin-derived lactoferrin peptide fragment, Infect. Immun. 61 (1993) 719-728.

[47] B. Skerlavaj, D. Romeo, R. Gennaro, Rapid membrane permeabilization and inhibition of vital functions of Gram-negative bacteria by bactenecins, Infect. Immun. 58 (1990).

[48] T.J. Montville, Y. Chen, Mechanistic action of pediocin and nisin: recent progress and unresolved questions, Appl. Microbiol. Biotechnol. 50 (1998) 511-519.

[49] J.K. Branen, P.M. Davidson, Enhancement of nisin, lysozyme, and monolaurin antimicrobial activities by ethylenediaminetetraacetic acid and lactoferrin, Int. J. Food Microbiol. 90 (2004) 63– 74.

[50] D. Jung, F.W. Bodyfelt, M.A. Daeschel, Influence of fat and emulsifiers on the efficacy of nisin in inhibiting *Listeria monocytogenes* in fluid milk, J. Dairy Sci. 75 (1992) 387-393.